

Novel insights in the congenital long QT-3 syndrome

Citation for published version (APA):

Wehrens, X. H. T. (2002). *Novel insights in the congenital long QT-3 syndrome*. [Doctoral Thesis, Maastricht University]. Universiteit Maastricht. <https://doi.org/10.26481/dis.20020322xw>

Document status and date:

Published: 01/01/2002

DOI:

[10.26481/dis.20020322xw](https://doi.org/10.26481/dis.20020322xw)

Document Version:

Publisher's PDF, also known as Version of record

Please check the document version of this publication:

- A submitted manuscript is the version of the article upon submission and before peer-review. There can be important differences between the submitted version and the official published version of record. People interested in the research are advised to contact the author for the final version of the publication, or visit the DOI to the publisher's website.
- The final author version and the galley proof are versions of the publication after peer review.
- The final published version features the final layout of the paper including the volume, issue and page numbers.

[Link to publication](#)

General rights

Copyright and moral rights for the publications made accessible in the public portal are retained by the authors and/or other copyright owners and it is a condition of accessing publications that users recognise and abide by the legal requirements associated with these rights.

- Users may download and print one copy of any publication from the public portal for the purpose of private study or research.
- You may not further distribute the material or use it for any profit-making activity or commercial gain
- You may freely distribute the URL identifying the publication in the public portal.

If the publication is distributed under the terms of Article 25fa of the Dutch Copyright Act, indicated by the "Taverne" license above, please follow below link for the End User Agreement:

www.umlib.nl/taverne-license

Take down policy

If you believe that this document breaches copyright please contact us at:

repository@maastrichtuniversity.nl

providing details and we will investigate your claim.

Novel Insights in the Congenital Long QT-3 Syndrome

© XANDER H.T. WEHRENS MD, MAASTRICHT 2002

All rights reserved. No part of this book may be translated or reproduced in any form by photo, photoprint, microfilm or any other means without written permission from the publisher.

ISBN 90-9015-470-1

DESIGN AND LAYOUT

Maas & van den Homberg designers, Maastricht

PRINTING AGENCY

Scorpio Offset bv

Novel Insights in the Congenital Long QT-3 Syndrome

PROEFSCHRIFT

ter verkrijging van de graad van doctor
aan de Universiteit Maastricht
op gezag van Rector Magnificus
Prof. Dr. A.C. Nieuwenhuijzen Kruseman,
volgens het besluit van het College van Decanen,
in het openbaar te verdedigen
op vrijdag 22 maart 2002 om 16.00 uur

door

Xander Hennie Theo Wehrens
geboren te Heerlen

PROMOTORES

Prof. dr. H.J.J. Wellens

Prof. dr. R.S. Kass (*Columbia University, New York*)

CO-PROMOTORES

Dr. P.A. Doevendans

Dr. M.A. Vos

BEOORDELINGSCOMMISSIE / ASSESSMENT COMMITTEE

Prof. dr. H.A.J. Struijker Boudier (*voorzitter*)

Prof. dr. E. Carmeliet (*Katholieke Universiteit Leuven, België*)

Prof. dr. H.J.G.M. Crijns

Prof. dr. J.P.M. Geraedts

Prof. dr. A.A.M. Wilde (*Universiteit van Amsterdam*)

Financial support by the Netherlands Heart Foundation for the publication of this thesis is gratefully acknowledged.

ADDITIONAL FINANCIAL SUPPORT WAS GRANTED BY:

3M Pharma Nederland BV, ASTA Medica BV, Astra Zeneca BV, Bayer Nederland BV, Bristol-Myers Squibb BV, Dr. Saal van Zwanenbergstichting, Guidant BV, Medtronic - Bakken Research Center BV, Merck Sharp & Dohme BV, Novartis Pharma BV, Pfizer BV, Rescar Foundation Maastricht, Roche Nederland BV, Sanofi-Synthélabo BV, St. Jude Medical Nederland BV, Wijnand M. Pon Stichting, Yamanouchi Pharma BV.

'Sei allem Abschied voran, als wäre er hinter
dir, wie der Winter, der eben geht.
Denn unter Wintern is einer so endlos Winter,
dab, überwinternd, dein Heiz überhaupt übersteht.'

Rainer Maria Rilke, Sonette an Orpheus, 2/XIII (1922)

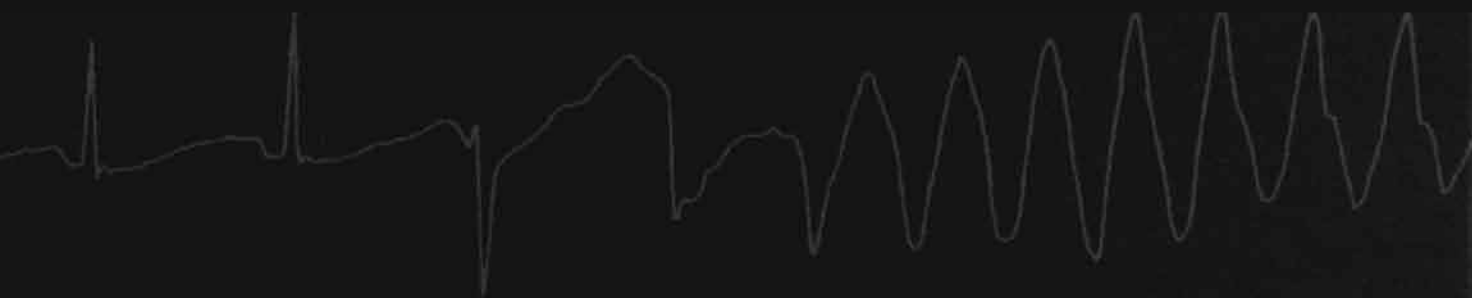
To my parents

Contents

CHAPTER 1	Clinical Aspects of the Congenital Long-QT Syndrome	9
CHAPTER 2	The Cardiac Sodium Channel	39
CHAPTER 3	Arrhythmogenic Mechanism of the D1790G Mutation of the Human Heart Na ⁺ Channel α -Subunit	73
CHAPTER 4	Molecular Pharmacology of the Sodium Channel Mutation D1790G Linked to the Long-QT Syndrome	91
CHAPTER 5	Novel Arrhythmogenic Mechanism Revealed by a Long-QT Syndrome Mutation in the Cardiac Na ⁺ Channel	105
CHAPTER 6	Heterozygous SCN5A Mutation in the Domain I-II Linker causes Long-QT Syndrome with 2:1 Atrioventricular Block	121
CHAPTER 7	General Discussion	139
	Summary	161
	Samenvatting	165
	Summarium	168
	Acknowledgments	169
	Curriculum Vitae	171
	Index	175

Chapter 1

Clinical Aspects of the Congenital Long-QT Syndrome



Based on:

WEHRENS XHT, Vos MA, Doevendans PA, Wellens HJJ.
Novel Insights in the Congenital Long-QT Syndrome.
Ann Internal Med 2002, *in press*.

Abstract

PURPOSE. To review new insights in the genetics and cellular electrophysiology, as well as the current understanding of the clinical diagnosis and treatment of the congenital long-QT syndrome.

DATA SOURCES. Personal databases of the authors and a search of the PubMed database from 1966 to 2001.

STUDY SELECTION. Experimental and clinical studies on the congenital long-QT syndrome.

DATA EXTRACTION. From peer-reviewed studies, data were manually extracted, classified, and summarized.

DATA SYNTHESIS. The congenital long-QT syndrome is characterized by abnormally prolonged ventricular repolarization, which predisposes patients to syncope, ventricular arrhythmias and sudden cardiac death. The recent discovery that mutations in genes encoding ion channels are responsible for the manifestation of this disease has improved our understanding of the cellular origin of this condition. Long-QT syndrome may result from inherited defects in cardiac K^+ and Na^+ channels, which both result in prolongation of the ventricular action potential. The diagnosis is based on electrocardiographic and clinical criteria. In addition, genetic screening of symptomatic patients or asymptomatic family members may identify patients at risk for life-threatening ventricular arrhythmias. Beta-blocking agents are the mainstay in the treatment. In addition, certain patients may benefit from a pacemaker or implantable cardioverter-defibrillator. Recent studies suggest that in the near future, genotype-specific treatment will become a novel approach to the congenital long-QT syndrome.

CONCLUSIONS. The congenital long-QT syndrome is a potentially life-threatening condition caused by mutations in genes encoding cardiac ion channels. The mechanisms responsible for these conditions are being increasingly better understood, and will guide genotype-specific therapy in the near future.

Introduction

Over the past decade, the discovery of mutations in genes encoding ion channels (1) has helped to better understand the mechanism of the congenital long-QT syndrome, an inherited disease characterized by prolonged ventricular repolarization and a propensity for life-threatening ventricular tachyarrhythmias resulting in syncope and sudden death (2). Current estimates suggest that 1 in 10,000 persons are gene carriers, and that long-QT syndrome causes 3000-4000 sudden deaths in children and young adults each year in the US only (3). The two major clinical syndromes that have been characterized on the basis of the genetic transmission pattern are a more common autosomal-dominant form (Romano-Ward syndrome) with a pure cardiac phenotype (4,5) and a rarer autosomal-recessive form (Jervell and Lange-Nielsen syndrome) characterized by the association with congenital neuronal deafness (6). Long-QT syndrome, occurring secondary to electrolyte disturbances or drug-therapy, is called acquired long-QT syndrome (7).

As a consequence of the genetic information, it became clear that what has been classified under the unifying name of the long-QT syndrome, actually represents a variety of different diseases caused by ion channel mutations, all producing alterations in ionic currents, leading to the same end result: prolonged ventricular repolarization (8). In addition, the first ion channel gene mutations and polymorphisms that predispose people to drug-provoked QT-interval prolongation and ventricular arrhythmias have been identified (9,10).

In this review, we A) classify the forms of congenital long-QT syndrome; B) discuss the proposed explanations of the cellular electrophysiology of the syndrome; C) review the clinical characteristics; and D) discuss the identification and management of patients with congenital long-QT syndrome, including novel approaches such as genotype-specific therapies.

Historical Remarks on the Congenital Long-QT Syndrome

The first report of the long-QT syndrome probably dates back to 1856. Meissner related the case of a girl, pupil at the Leipzig School of the Deaf, who collapsed and died while publicly admonished by the Director for a misdemeanor (151). One of her siblings had previously died suddenly after a terrible fright and another after a violent fit of rage (151). In 1901, before the electrocardiogram was widely available, Morquio reported a large Uruguayan family in which several siblings repetitively collapsed and died at a young age (152).

Latham and Munro described in 1937 a family with consanguineous marriage, in which all five children suffered from congenital deafness in association with spells that were interpreted as epileptic spells. One of these children died unexpectedly (153). In 1953, Herrlin and Möller reported the case of a congenitally deaf boy with frequent episodes of syncope, and described, for the first time, the electrocardiographic (ECG) features of the long-QT syndrome: a prolonged QT-interval, abnormal T waves in the precordial leads, and bradycardia (154).

The case report by Drs. Jervell and Lange-Nielssen, who described the association of congenital deafness with typical ECG abnormalities, in conjunction with fainting attacks and a propensity to sudden death, fully recognized the clinical picture and possible relevance of the disease (6). Soon thereafter, Drs. Romano (4,155), and Ward (5) described independently that fainting attacks and inherited QT-interval prolongation also occurred in the absence of neuronal deafness. The Romano-Ward syndrome (RWS) is now known as the long-QT syndrome with an autosomal-dominant mode of inheritance, although a recessive variant has also been reported recently (19). The Jervell Lange-Nielssen syndrome (JLN), on the other hand, inherits in an autosomal-recessive way (6,156-160). The concomitant neuronal deafness may not always be complete (158), and may be inherited separately from the cardiac defect in certain families (161).

Methods

We searched the PubMed database for literature on the congenital long-QT syndrome, focusing on advances in the four specified areas (A-D). From peer-reviewed studies, data were manually extracted, classified, and summarized.

A. Genetics of the Congenital Long-QT Syndrome

Genetic linkage mapping of the autosomal-dominant Romano-Ward syndrome has so far identified loci on six chromosomes (LQT-1 to LQT-6) (11-17). The autosomal-recessive variant (Jervell Lange-Nielssen syndrome) arises in individuals who inherit abnormal *KCNQ1* (= *KvLQT1*) or *KCNE1* (= *minK*) alleles from both parents (LQT-1, LQT-5). The abnormal gene can be the same (usually in consanguineous families) or different (so-called compound heterozygosity) (18). Parents of subjects with Jervell Lange-Nielssen syndrome are heterozygous for long-QT syndrome mutations, but are usually (but not always) asymptomatic (19). Most long-QT syndrome genes encode K^+ channels, with the exception of the LQT-3 gene (*SCN5A*) that encodes the cardiac Na^+ channel (current indicated by I_{Na}) (20).

Mutations in either the α -subunit encoded by *KCNQ1* (LQT-1) or the β -subunit encoded by *KCNE1* (LQT-5) can cause defects in the I_{Ks} current. Similarly, mutations in the LQT-2 (*KCNH2* = *HERG*) and LQT-6 (*KCNH2* = *MiRP1*) genes encoding the α - and β -subunit of the rapidly activating delayed rectifier K^+ channel I_{Kr} , respectively, may cause long-QT syndrome (17).

B. Functional Consequences of Long-QT Syndrome Mutations

The channels carrying the I_{Ks} and I_{Kr} potassium currents are multimeric (15,16); alleles from both parents are thought to contribute to the channel complexes (21). Using

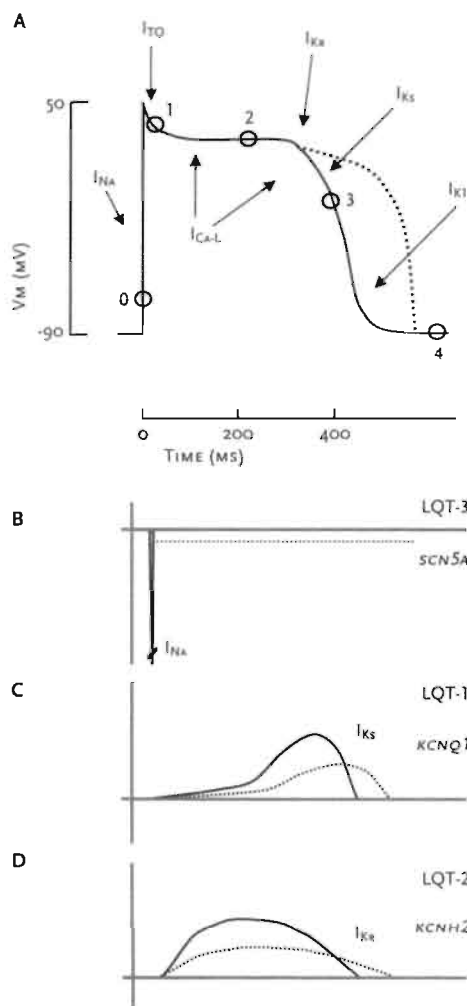
FIGURE 1.1

(A) The ventricular action potential is initiated by current flow through cardiac Na^+ channels (depolarization, phase 0). Early repolarization (1) is caused by the K^+ current I_{TO} . The action potential plateau phase (2) is maintained by $I_{\text{Ca,L}}$, I_{Kr} and I_{Ks} currents, and late repolarization (3) is caused by current flow through I_{Ks} and I_{K1} channels. The dotted line represents action potential prolongation as can be observed in the congenital long-QT syndrome.

(B) In case of LQT-3, most mutations in the *SCN5A* gene cause a small non-inactivating sodium current that remains active during the action potential plateau phase (dotted) and provides an additional depolarizing current, which prolongs repolarization.

(C) The *KCNQ1* gene encodes the slowly activating delayed rectifier K^+ channel which conducts the I_{Ks} current. In case of LQT-1, reduced I_{Ks} activity leads to action potential prolongation.

(D) The *KCNH2* gene encodes the rapidly activating delayed rectifier K^+ channel which conducts the I_{Kr} current. In LQT-2, a reduction of I_{Kr} causes prolongation of the repolarization phase (dotted line).



prolong repolarization and hence underlie the phenotype in carriers of these *SCN5A* mutations (8,28). However, this gain-of-function persistent Na^+ current is not observed in all *SCN5A* mutations (29), which implies that heterogeneity in arrhythmogenic mechanisms exists among Na^+ channel-related long-QT syndrome.

heterologous expression systems like *Xenopus* oocytes or mammalian cell lines, mutations in *KCNQ1*, *KCNE1*, *KCNH2*, or *KCNE2* expressed alone or in combination with wild-type alleles, typically exhibit a 'loss of function' (FIGURE 1.1). The total current carried by the defective potassium channel complexes is impaired by reduced gating, modified channel kinetics, or non-expression at the plasma membrane level by deficient transport from the endoplasmic reticulum. Because potassium channels are tetrameric proteins, there is also the potential for the presence of a single (or more) mutant subunit in a tetramer to disrupt the function of the remaining wildtype subunits (so-called dominant-negative effect) (22-25). Mutations in the cardiac Na^+ channels linked to LQT-3 generally promote additional Na^+ channel activity during the plateau phase of the action potential leading to an extra component of inward current (26,27). This additional inward current would be expected to

C. Clinical Characteristics

The International Long-QT Syndrome Registry was started in 1979 to study prospectively epidemiological and genetic characteristics (30-33). In (symptomatic) probands, 50% had experienced a first cardiac event by the age of 12 years, and by the age of 40 years this had increased to almost 90% (33). Multivariate analysis identified as independent risk factors for syncope or sudden cardiac death: congenital deafness, history of syncope, female gender, documented torsades de pointes or ventricular fibrillation, age at first episode and the long-QT syndrome gene affected (31-35). The QTc duration was independently associated with the risk of syncope or sudden death during follow-up (33). These results

ECG findings ⁽¹⁾	Points
a. QTc ⁽²⁾	
$\geq 480 \text{ ms}^{1/2}$	3
460-480 $\text{ms}^{1/2}$	2
450-460 $\text{ms}^{1/2}$ (in males)	1
b. Torsades de pointes ⁽³⁾	2
c. T wave alternans	1
d. Notched T wave in 3 leads	1
e. Low heart rate for age ⁽⁴⁾	0.5
Clinical history	
a. Syncope	
With stress	2
Without stress	1
b. Congenital deafness	0.5
Family history ⁽⁵⁾	
a. Family members with 'definite' long-QT syndrome ⁽⁶⁾	1
b. Unexplained sudden cardiac death < 30 yr among immediate family members	0.5

TABLE 1.1

Diagnostic criteria for the long-QT syndrome.

⁽¹⁾ In the absence of medication or disorders known to affect these electrocardiographic features;

⁽²⁾ QT calculated with Bazett's formula ($QTc = QT / \sqrt{RR}$); ⁽³⁾ No points if patient is taking drugs to favor QT prolongation; ⁽⁴⁾ Resting heart rate below second percentile for age (45); ⁽⁵⁾ The same family member can not be counted in A and B; ⁽⁶⁾ 'Definite' long-QT syndrome is defined as long-QT syndrome score of ≥ 4 . SCORING: ≥ 1 point, low probability of long-QT syndrome; 2-3 points, intermediate probability.

Adapted from: Schwartz PJ et al. 1993 (46).

are in line with the finding that QT-interval prolongation in an apparently healthy population (36,37) correlates to an increased risk of mortality. The question whether the QTc variability over time correlates with mortality remains to be resolved (38).

The Influence of Age and Gender

Since the QT-interval duration is shorter in adult males than females (39-44), a diagnosis of QT prolongation could be made relatively more often in adult females. However, after the introduction of the 1993 diagnostic criteria for long-QT syndrome (TABLE 1.1), that define sex specific criteria for QT duration, such bias leading to a female predominance is less likely. Nevertheless, a female predominance is consistently reported in clinical studies (32,33,43). In males, the risk of first cardiac events is typically higher in childhood, and decreases after puberty, probably due to a regression of QTc duration (40,42,43,47,48).

The Influence of Pregnancy

Probands with the hereditary long-QT syndrome are at significant risk for cardiac events during the postpartum interval, nearly 10% of the probands in the study by Rashba et al. (49) experienced their first cardiac event during the postpartum interval. The most important factors contributing to this risk may be related to an increase in sympathetic activity (2,50), or to increased levels of estrogen and progesterone that directly or indirectly influence the number and function of mutant ion channel proteins (51,52). Treatment with β -blockers can reduce the risk for cardiac events (49).

D. Identification and Management of Long-QT Syndrome Patients

Sudden death or a history of unexplained syncope in a child or young adult can bring the patient or family member under the clinician's attention. After informing the patient, an ECG should be recorded, and a detailed family history for syncope and sudden cardiac death should be taken. Many mutation carriers are asymptomatic despite the fact that they display electrocardiographic characteristics of long-QT syndrome. Another group consists of individuals that have been identified as mutation carriers without symptoms or ECG features (21), or they only intermittently display ECG signs. We recommend genetic

analysis or referral to a specialized combined genetic-cardiology out-patient clinic for all of these patients, as the study of long-QT mutations may aid to better understand the pathophysiology of the disease, and may help to develop mutation-specific therapies in the near future (53). In addition, there is a group of patients that carries ion channel mutations or polymorphisms, predisposing them to drug-induced long-QT syndrome (9). The following four paragraphs will discuss identification and management of these subgroups of long-QT syndrome patients.

1. Patients with Symptoms of Congenital Long-QT Syndrome

Symptoms

Vertigo, syncopal attacks, cardiac arrest, and unexplained sudden cardiac death among immediate family members, or family members with definite long-QT syndrome point to inheritance of an affected gene. Neurally mediated syncope and epileptic seizures are the most common differential diagnoses (54). A careful history of symptoms and signs can often clarify this diagnostic dilemma. Sudden cardiac death during sleep should also raise suspicion of the long-QT syndrome, particularly the LQT-3 phenotype (55).

	LQT-1	LQT-2	LQT-3
Gene mutated	KCNQ1 (=KvLQT1)	KCNH2 (=HERG)	SCN5A
Current affected	I _{Ks}	I _{Kr}	I _{Na}
Estimated prevalence (%)	42	45	8
Events occurring with exercise or emotional stress (%)	97	51	39
Exercise related trigger	+++	+	+
Other triggers	Diving	Loud noise	Sleep/rest
Events before age 10 (%)	40	16	2
Events before age 40 (%)	63	46	18
Median age 1 st event (yr)	9	12	16
Mean QTc interval (ms ^{1/2})	490 ± 43	495 ± 43	510 ± 48
QT shortening with exercise	< normal	normal	> normal
Efficacy β-blockade to prevent events	+++	++	+
Efficacy mexiletine to shorten QT	-	+	+++

Adapted from: Wilde AA et al. (58). Clinical data derived from Zareba et al. 1998 (34).

TABLE 1.2
Clinical characteristics in common genotypes of congenital long-QT syndrome.

The clinical course of the long-QT syndrome is importantly influenced by the gene affected (34). By age of 15, almost 60% of LQT-1 patients have had a cardiac event (syncope, cardiac arrest, or sudden cardiac death), compared to less than 10% in LQT-3 patients (34,35). The number of cardiac events that occurred till the age of 40 years was also higher among LQT-1 (63%) or LQT-2 subjects (46%) compared to LQT-3 (18%). In contrast, the likelihood of death during a cardiac event was much higher among LQT-3 (20%) compared to LQT-1 and LQT-2 (4%) (36) (TABLE 1.2). Due to the low number of patients, no data are available yet for LQT-4, LQT-5 and LQT-6 patients.



Example of torsades de pointes tachyarrhythmia.

Triggers for Syncopal Events

Episodes of sudden loss of consciousness are almost always due to TORSADES DE POINTES ARRHYTHMIAS in long-QT patients (57). Torsades de pointes can be defined as a polymorphic ventricular arrhythmia showing a peculiar electrocardiographic pattern characterized by a continuous twisting of the QRS axis around an imaginary baseline (58). An important characteristic of torsades de pointes is its potential for self-termination or deterioration into ventricular fibrillation. This explains why affected patients often survive several syncopal attacks before succumbing to a lethal one.

Recently, it has become evident that triggers for arrhythmic episodes and syncope are also dependent on the specific long-QT syndrome gene affected (TABLE 1.2) (35,59-61).

In I_{Ks} -related long-QT syndrome (LQT-1), exercise- and stress-related events dominate the clinical picture (48,59,62,63), which is related to activation of the I_{Ks} current by adrenergic stimulation (64). Diving and swimming, as triggers, are almost exclusive for LQT-1 patients (35,60). Patients with LQT-3-associated Na^+ channel mutations are at particularly high risk at rest or asleep because their QT-interval is prolonged excessively at slow heart rates (63,65). This clear distinction between LQT-1 and LQT-3 with respect to exercise-related triggers does not hold for LQT-2 patients, who tend to display events both at rest and during exercise (59). However, events provoked by auditory stimuli such as an alarm clock or telephone ringing almost exclusively occur in LQT-2 patients (35,59,60,66,67). No data are available yet for LQT-4, LQT-5 and LQT-6 patients.

Treatment Options for Symptomatic Patients

Symptomatic individuals require treatment (32,33,68). It is important to inform patients and their parents well about the importance of compliance, as noncompliance exposes patients to increased risk of cardiac events. This often requires frequent counseling of young patients to motivate them to continue to take their medication while they are

asymptomatic. Based on the observations that physical and emotional stress are important triggers for cardiac events in long-QT syndrome (type 1 and 2) patients (35,59,61), non-medical treatment should also include life-style advice and information on certain drugs that should be avoided because of their potential to prolong QT-intervals. Competitive sports should be generally discouraged, but recreational sports that do not cause sudden increases in heart rate are usually tolerated well. Finally, patients are instructed how to respond to excessive electrolyte loss, e.g. during diarrhea or excessive perspiring. Patients are advised to take drinks that contain minerals such as potassium.

BETA-BLOCKER THERAPY

Administration of β -blocking drugs is very effective in preventing ventricular arrhythmias in the long-QT syndrome, although the response is genotype-dependent (5,69-72).

The 10-year mortality rates among symptomatic patients dropped from approximately 50% when not treated to below 5% after long-QT syndrome patients were routinely put on β -adrenergic receptor blocking therapy (32,33). A recent retrospective study by Moss et al. (68) among 869 long-QT syndrome patients revealed a significant reduction in the rate of cardiac events in both probands and affected family members after initiation of beta-blocking therapy. In patients with aborted cardiac arrest before β -blocker therapy, the probability of aborted cardiac arrest or sudden death was 6.6% when using β -blockers (68). In patients with recurrent cardiac symptoms or aborted cardiac arrest, β -blocker therapy might not be completely effective in preventing sudden cardiac death, and implantable cardioverter defibrillator (ICD) therapy is warranted for these high-risk patients. An important criticism to this study is the retrospective nature without evidence that patients continued to take their β -blockers. After it became clear that the long-QT syndrome is caused by ion channel mutations and probably not by IMBALANCE OF THE CARDIAC AUTONOMOUS NERVOUS SYSTEM, the rationale for performing left cardiac denervation has become less obvious.

CARDIAC PACING

As the onset of torsades de pointes arrhythmias in long-QT syndrome patients has been associated with bradycardia or pauses during sinus rhythm (73-75), permanent cardiac pacing has been recommended as an adjuvant to β -blocker therapy in patients who also have bradycardia or atrioventricular conduction disturbances (76-81), or in carriers of *SCN5A* mutations who usually have slow heart rates (82,83). In addition, cardiac pacing can be an important adjuvant therapy in those patients in whom β -blocking drugs and left

The Sympathetic Imbalance Theory

In the seventies and eighties, two opposing hypotheses existed concerning the pathogenetic mechanisms in the congenital long-QT syndrome (LQTS). The 'sympathetic imbalance' theory (2,50,162) and the hypothesis of a 'primary myocardial membrane defect' (74,75,163) were put forward.

The first hypothesis considered a critical role of the autonomic nervous system in the pathogenesis of LQTS on the basis of clinical observations (162,164) and experimental results (50,165). Basically, QT prolongation and T wave alternation could be induced by either left stellate ganglion stimulation or blockade of the right stellate ganglion. These observations suggested that LQTS might have a congenital imbalance between the right and left sympathetic innervation with left dominance (50,162). Using ¹²³I-metaiodobenzylguanidine (MIBG) single-photon emission tomography (SPECT) scintigraphy (166,167), some studies demonstrated impaired regional sympathetic innervation in LQTS patients. In contrast, using ¹¹C-hydroxyephedrine (HED) positron emission tomography (PET), others showed a normal cardiac sympathetic innervation in LQTS patients (168). Although it is now generally believed that an abnormal distribution of cardiac sympathetic nerves is not a common mechanism in congenital LQTS, it cannot be excluded that the observed MIBG defects might have been regions of enhanced sympathetic activity according to (A) the hypothesis of hyperactivity of left sympathetic nerves (165), and (B) echocardiographic observations of an increased rate of thickening in the posterior wall, possibly related to increased sympathetic activity in this region (169).

Based upon the assumed pathogenesis of the disease, therapy with β -blockers and surgical left sympathetic denervation was performed (164). The rationale of left cardiac sympathetic denervation was to shorten the QT-interval (107), and to protect against ventricular arrhythmias (170). In a world-wide report on 85 patients with left cardiac sympathetic denervation, Schwartz and colleagues reported a decrease in the number of patients with cardiac events, and in the number of cardiac events per patient (171). Although a low five-year mortality rate of 6% was reported, the study was not designed to allow a conclusive analysis of a possible beneficial effect on mortality. Because few other groups were able to reproduce these findings, left sympathectomy is not a commonly used treatment option anymore for drug-refractory patients. Combination therapy of β -blockers with a pacemaker, or alternatively, an implantable cardioverter defibrillator are often preferred nowadays (87).

stellate ganglionectomy have proven inefficacious, even if bradycardia or conduction disturbances are not present (84). Cardiac pacing should be aimed at preventing (A) bradycardia, by using a relatively high lower rate limit (≥ 80 beats/min), and (B) pauses, by using pause-prevention pacing algorithms such as rate-smoothing. Applications of cardiac pacing were reviewed by Viskin (82).

IMPLANTABLE CARDIOVERTER DEFIBRILLATORS

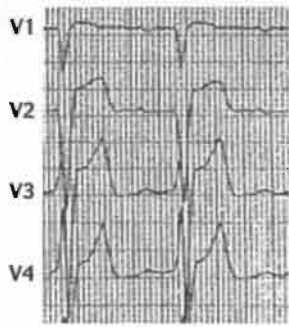
Implantable cardioverter defibrillators are increasingly being used in an attempt to prevent sudden cardiac death (85,86). Aborted sudden cardiac death and recurrent symptoms while on combined β -blocker and pacemaker therapy are the most frequent indications for ICD implantation (85-87). Since the ICD does not alter the underlying substrate leading to arrhythmias, it is recommended to initiate or continue β -adrenergic blockade therapy (88).

TOWARDS A GENOTYPE-SPECIFIC THERAPY OF SYMPTOMATIC LONG-QT PATIENTS

The emerging sense that gene-specific therapy might be feasible for some forms of long-QT syndrome has recently been supported by clinical and experimental studies. One of the first attempts studies showed that LQT-3 patients shorten their QT-interval more in response to a Na^+ channel blocker (mexiletine) compared to LQT-1 and LQT-2 patients (89). As most LQT-1 patients experience syncopal events during exercise, competitive sports should be avoided. As diving and swimming are particularly strong triggers for cardiac events in LQT-1 patients, it should be strongly discouraged (35,60,90). LQT-2 patients should be advised to remove sources of loud noise from their direct environment (such as telephone and alarm clocks).

Patients with LQT-1 and LQT-2 genotypes typically benefit from β -blocker therapy (35,68). Because the amplitude of I_{K_r} increases when extracellular potassium concentrations are increased (91,92), attempts have been undertaken to increase K^+ levels in LQT-2 patients by means of intravenous potassium infusion or administration of the diuretic spironolacton (93). Indeed, QT-intervals have been shown to shorten significantly in LQT-2 (94) but also LQT-1 (95) patients. Potassium supplementation is, however, hindered by difficulties in achieving sufficiently high K^+ concentrations with chronic oral therapy (96). On the other hand, nicorandil, a K^+ channel opener, has been shown to normalize repolarization abnormalities induced by epinephrine infusion in LQT-1 patients (97).

A beneficial effect of β -blocker therapy has not been demonstrated for LQT-3 patients (35,68). Since LQT-3 patients are at higher risk at slow heart rates, they may benefit from pacemaker therapy. Several clinical and experimental studies suggest a



Typical ECG of a patient with Brugada syndrome, showing right precordial ST-segment elevation.

beneficial effect of Na⁺ channel blockers such as lidocaine/ mexiletine (89,98,99), tocainide (98), or flecainide (83) in LQT-3 patients, although long-term follow-up data are not available yet. It should be noted, however, that flecainide may cause ECG changes reminiscent of the Brugada-syndrome (familial idiopathic ventricular fibrillation) in a significant number of LQT-3 patients (100). The BRUGADA SYNDROME is characterized by right bundle branch block and ST-segment elevation in the right precordial leads on the ECG, and may lead to ventricular fibrillation and sudden cardiac death (101). The impact of the flecainide-induced changes, which might suggest the introduction of a different arrhythmogenic substrate, is currently unknown. A further therapeutic differentiation on the basis of the specific mutations in the affected gene can be expected in the near future.

2. Patients Without Symptoms but With Electrocardiographic Characteristics Suggestive of Long-QT Syndrome

Some individuals are not identified on the basis of their symptoms, but because of typical electrocardiographic features suggestive of long-QT syndrome. The principal diagnostic hallmark of the long-QT syndrome is lengthening of the QT-interval on the 12-lead ECG. As the QTc value is often not sufficiently long to make or exclude the diagnosis in borderline cases, an elaborate point scoring system that goes beyond QTc duration was developed by Schwartz et al. (46) (TABLE 1.1).

QT Prolongation

QT-interval prolongation is usually most easily identified in lead II, V1, V3, or V5, but all 12 leads should be examined to identify the longest QT-interval (104-106). Despite ongoing criticism, Bazett's correction formula ($QTc = QT / \sqrt{RR}$) for heart rate continues to be useful (39,46,102,103). The 'cut-off value' commonly used was a QTc interval ≥ 440 ms, but more recent genotype-phenotype correlations indicated >460 ms to be more appropriate (35,48). Indeed, 40% of LQT-1 and LQT-2 mutation carriers show QTc values (410-470 ms) that overlap with non-carriers (34, 43). In this QTc range, phenotypic diagnosis from the ECG becomes imprecise and genetic studies may be helpful in diagnosing long-QT syndrome. When $QTc \geq 460$ ms is used, the positive predictive accuracy for long-QT syndrome is 96% in women and 91% in men; almost 100% positive predictive accuracy for long-QT syndrome can be achieved at $QTc \geq 470$ ms in males and $QTc \geq 480$ ms in females (50). Finally, QTc intervals tend to be longer in LQT-3 patients than LQT-1 and LQT-2 carriers (34,35,43).

QT-interval Dispersion

The second ECG characteristic is QT-interval dispersion, which can be measured as a lead-to-lead variability in QT-intervals (105-107). It is debated whether this phenomenon reflects regional differences in ventricular repolarization times (108,109). In normal individuals, the difference between maximal and minimal QT-intervals measured on the standard resting ECG has been reported to vary between 48 ± 18 msec (102) and 54 ± 27 msec (102). In patients with the congenital long-QT syndrome, however, regional dispersion of ventricular repolarization times has been reported to vary from $93 (\pm 39)$ to $185 (\pm 26)$ msec (105,106,110,111). In long-QT syndrome patients, QT dispersion has been suggested to correlate with the risk for ventricular arrhythmias (105,112), whereas a reduction in dispersion of the QT-interval could be used as a marker of therapeutic efficacy (107).

T Wave Morphology

In long-QT syndrome patients, not only the duration of repolarization is altered (QT-interval), but also its morphology (113). The most typical presentation of the T wave may be biphasic (114) or notched (75,114,115), and is most prominent in the precordial leads (114,115). In addition, T wave alternans is an infrequently recorded highly arrhythmogenic ECG finding with transient beat-to-beat changes in amplitude, shape, and polarity of the T wave during sinus rhythm without concomitant QRS changes (116-118).

Bradycardia and Sinus Pauses

Signs of sinus node dysfunction, e.g. sinus bradycardia or sinus pauses (70,119,120), and lower than expected heart rate during exercise have been reported (33,121-123). Slow heart rates are particularly striking in younger children (122). During submaximal exercise testing, many long-QT syndrome patients reach a heart rate level lower than that achieved by healthy controls matched by sex and age (124,125). Sinus pauses may play a role in the initiation of pause-dependent torsades de pointes arrhythmias (73,74,126). Long-QT syndrome might also be complicated by atrioventricular conduction disturbances, which is generally associated with poor prognosis (50,81,123).

Electrophysiological Testing

One of the first comprehensive electrophysiological (EP) studies in long-QT syndrome patients was performed by Wellens et al. (127). The absence of inducibility by programmed stimulation indicates that the arrhythmias in long-QT syndrome are probably not the result of reentrant circuits, but reentry probably plays a role in the perpetuation of torsades de

FIGURE 1.2

Genotype-specific ECG patterns in the congenital long-QT syndrome.

(A). The two most common

LQT-1 ECG patterns:

(a) broad-based T wave pattern,

(b) normal-appearing T wave

pattern. (B). The two most

frequently encountered LQT-2

ECG manifestation: (a) obvious

bifid T waves, (b) subtle bifid

T wave with a second component

on top of the T wave in limb and

left precordial leads (or

alternatively the second

component on the downslope of

T wave; not shown). (C).

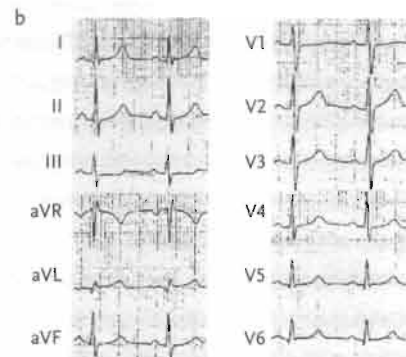
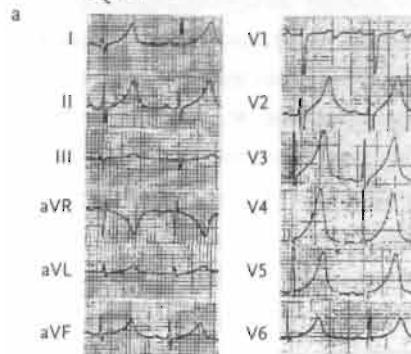
Most typical LQT-3 ECG pattern:

(a) late-onset peaked/biphasic

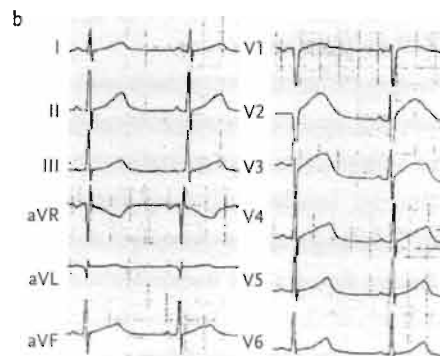
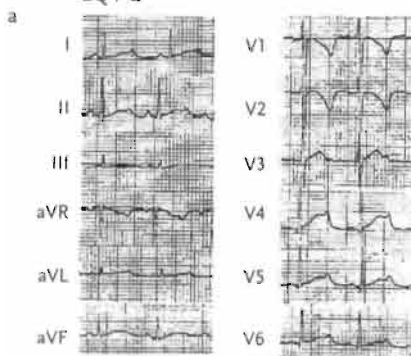
T wave. Modified from:

Zhang et al. 2000 [140].

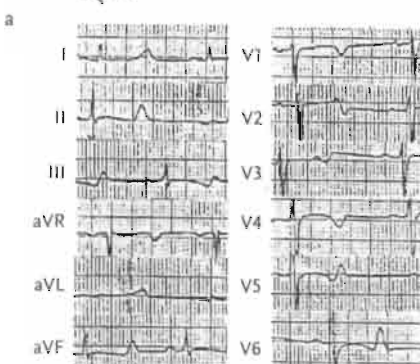
A LQT-1



B LQT-2



C LQT-3



pointes arrhythmias in long-QT syndrome. It is therefore generally believed that EP studies using one or more premature stimuli during ventricular pacing are of limited value in the diagnosis and treatment of patients with the long-QT syndrome (128,129). On the other hand, torsades de pointes might be inducible using short-long-short sequences (74,130). In addition, changes in heart rate provoked by for example the Valsalva maneuver or EP protocols may lead to clear changes in the T wave or ventricular tachycardia (75).

Response to Exercise

The standard resting ECG as a diagnostic criterion may misclassify members of long-QT syndrome families (48,131,132). Therefore, an exercise test has been suggested to enhance diagnostic accuracy, as shortening of QT-interval was shown to be inadequate in LQTS patients (4,65,133-136). In addition, a submaximal heart rate response during exercise has been reported (50,124,134). In a recent study by Swan et al. (131), a reduced maximum heart rate during exercise was found for LQT-1 patients, whereas this was normal for LQT-2 patients. During recovery from exercise, LQT-1 patients showed an exaggeration of the QT-interval prolongation compared to LQT-2 patients (131). Finally, Schwartz et al. reported that LQT-3 patients display a higher degree of QT-interval shortening in response to increase in heart rate than LQT-2 patients (89) (TABLE 1.2). Holter monitoring may also be useful (137), but well-defined criteria for QTc separation of long-QT syndrome from normal patients are currently not available. Studies have demonstrated that QT-intervals up to 500 ms occur in a significant percentage of healthy individuals (138). Therefore, a QTc > 500 ms, particularly in association with T wave abnormalities, would appear to be necessary to support the diagnosis of long-QT syndrome (54).

Genotype-Specific Electrocardiographic Phenotypes in the Congenital Long-QT Syndrome

The different time- and voltage-dependence of the ionic currents involved in long-QT syndrome are probably responsible for distinct ECG phenotypes that have been reported for the different genotypes. Initial studies by Moss et al. (34,139) reported an association of certain T wave patterns with LQT-1, LQT-2, and LQT-3. Recently, Zhang et al. (140) recognized 10 typical ST-T wave patterns that are genotype-specific (4 LQT-1, 4 LQT-2, and 2 LQT-3) (see FIGURE 1.2 for the most important ECG patterns). These ECG characteristics, however, cannot be used to diagnose the type of long-QT syndrome, but are rather useful to select which gene should be investigated first when performing genetic analysis.

Treatment of Asymptomatic Patients with ECG Characteristics of Congenital Long-QT Syndrome

Treatment of asymptomatic patients is still controversial, because the majority of long-QT syndrome patients will never experience symptoms (34,35) and sudden death during the first syncopal episode is unlikely to occur (34). While waiting for more definitive data, Schwartz recommended to begin treatment for asymptomatic patients only in the following six conditions: in those with congenital deafness; in neonates and for the first year of life because of the enhanced risk during the first months in life; in siblings of children who have already died suddenly; in patients with documented evidence of T wave alternans; when the QTc exceeds 600 ms; and whenever there is manifest anxiety or explicit request for treatment (88).

3. Mutation Carriers Without Symptoms or Electrocardiographic Characteristics of Long-QT Syndrome

It is estimated that approximately 10% of all mutation carriers have a normal QTc interval < 440 ms (140). However, only 2% of all long-QT syndrome mutation carriers have a normal ST-T wave pattern with a normal QT-interval. Priori et al. (141) showed that in some families, penetrance of clinical symptoms and QT-interval prolongation may be as low as 25%. This implies that family members considered normal on clinical and electrocardiographic grounds could be silent gene carriers displaying a very mild phenotype (19). They would be unexpectedly at risk of generating affected offspring and perhaps also of developing torsades de pointes arrhythmias if exposed to either cardiac or noncardiac drugs that block potassium channels (9,10). It is therefore recommended to perform molecular screening in all family members of positively genotyped patients (21). Few long-QT syndrome patients without ECG abnormalities present with sudden death as their first symptom (103), although preliminary data suggest that sudden death can occur in silent gene carriers (142). Awaiting more definitive data, conservative management of silent gene carriers seems reasonable, as the value of β -blocker therapy in this group of patients is still unknown.

4. Patients Carrying Mutations or Polymorphisms Associated With Drug-provoked Long-QT Syndrome

Some patients carry a predisposition for drug-induced torsades de pointes arrhythmias on the basis of congenital long-QT syndrome-related ion channel mutations (7,95,143). These patients are usually clinically asymptomatic until administration of a drug. A genetic

Gene	Channel	Drug	Usage	Reference
KCNQ1	I _{Ks}	Mefloquine	Antimalarial	(145)
KCNQ1	I _{Ks}	Disopyramide	Antiarrhythmic	(145)
KCNQ1	I _{Ks}	Terfenadine	Antihistamine	(145)
KCNQ1	I _{Ks}	Cisapride	Cholinergic antagonist	(10)
SCN5A	I _{Na}	Halofantrine	Antimalarial	(146)
MiRP1	I _{Kr}	Clarithromycin	Antibiotic	(16)
MiRP1	I _{Kr}	Quinidine	Antiarrhythmic	(9)
MiRP1	I _{Kr}	Sulfamethoxazole	Antibiotic	(9)
MiRP1	I _{Kr}	Procainamide	Antiarrhythmic	(9)
MiRP1	I _{Kr}	Oxatomide	Antihistamine	(9)

Modified from: Piippo et al. 2001 (146).

TABLE 1.3

Drugs that have been reported to provoke ventricular tachycardia in the presence of a specific mutation in one of the long-QT syndrome genes.

predisposition to drug-provoked long-QT syndrome torsades de pointes can be caused by mutations in the KCNE2 subunit of the I_{Kr} potassium channel (16,144) or a mutation in the KCNQ1 subunit of the I_{Ks} channel (10,145) (TABLE 1.3). In addition, a polymorphism in the KCNE1 gene (147), as well as two relatively common polymorphisms in KCNE2 (allelic frequency in both cases around 1.6%) have been associated with quinidine- and erythromycin-induced long-QT syndrome (9,16). Drug-provoked long-QT syndrome has also been linked to mutation in SCN5A (146).

However, it should be noted that in most patients with acquired long-QT syndrome (>85%), no ion channel mutations have been identified thus far. In this case, acquired long-QT syndrome is thought to result from electrolyte disturbances, hypertrophy, or treatment with commonly used medications, including some antiarrhythmic, antihistamine, antibiotic, psychoactive, and gastrointestinal prokinetic agents (148). In patients without ion channel mutations, it is believed that pro-arrhythmia is induced by block of the potassium current I_{Kr} (149,172). Recent studies have shed some light on the fact why so many structurally diverse compounds block KCNH2 channels but not other potassium channels. Because the KCNH2 channel has a unique group of amino acids in the S6 domain that are not present in other voltage-gated K⁺ channels (K_v1-K_v4), many drugs preferentially block KCNH2 channels (9), placing patients at risk for cardiac arrhythmias. It should be noted that acquired long-QT syndrome occurs more often in females (150).

Genetic diagnostic approaches in patients with acquired long-QT syndrome should be restricted to centers with sufficient experience in the genetic identification of these patients. The relevance of the polymorphisms is not clear yet, and there is no well-defined set of genes that have to be analyzed. A pragmatic approach is to provide a list of compounds that should not be used in the future and should be known to both mutation carriers and patients with long-QT syndrome.

Summary

The congenital long-QT syndrome is a potentially life-threatening condition characterized clinically by prolonged QT-intervals, syncope, and sudden cardiac death. The abnormally prolonged repolarization is the result of mutations in genes encoding cardiac ion channels. The diagnosis of long-QT syndrome is based on clinical, electrocardiographic, and genetic criteria. Beta-blocking therapy is important in the treatment of long-QT syndrome, although pacemakers and ICD's are useful in certain categories of patients. In the near future, mutation-specific treatment will probably become a novel approach to this potentially lethal syndrome.

Acknowledgments

The authors wish to thank Drs. R.S. Kass and A.A. Wilde for sharing with us their expertise.

References

- Wang Q, Shen J, Splawski I, Atkinson D, Li Z, Robinson JL, Moss AJ, Towbin JA, Keating MT. *SCN5A* mutations associated with an inherited cardiac arrhythmia, long-QT syndrome. *Cell* 1995;80:805-11.
- Schwartz PJ, Locati E. The idiopathic long-QT syndrome: pathogenetic mechanisms and therapy. *Eur Heart J* 1985;6 Suppl D:103-14.
- Vincent GM. The molecular genetics of the long-QT syndrome: genes causing fainting and sudden death. *Annu Rev Med* 1998;49:263-74.
- Romano C, Gemme G, Pongiglione R. Aritmie cardiache rare dell'eta pediatrica. *Clin Pediatr* 1963;45:656-83.
- Ward OC. A new familial cardiac syndrome in children. *J Irish Med Assoc* 1964;54:103-06.
- Jervell A, Lange-Nielsen F. Congenital deaf-mutism, functional heart disease with prolongation of the QT-interval, and sudden death. *Am Heart J* 1957;54:59-68.
- Roden DM. Mechanisms and management of proarrhythmia. *Am J Cardiol* 1998;82:491-571.
- Kass RS. Genetically induced reduction in small currents has major impact. *Circulation* 1997;96:1720-21.
- Sesti F, Abbott GW, Wei J, Murray KT, Saksena S, Schwartz PJ, Priori SG, Roden DM, George AL Jr, Goldstein SA. A common polymorphism associated with antibiotic-induced cardiac arrhythmia. *Proc Natl Acad Sci U S A* 2000;97:10613-18.
- Napolitano C, Schwartz PJ, Brown AM, Ronchetti E, Bianchi L, Pinnavaia A, Acquaro G, Priori SG. Evidence for a cardiac ion channel mutation underlying drug-induced QT prolongation and life-threatening arrhythmias. *J Cardiovasc Electrophysiol* 2000;11:691-96.
- Keating M, Atkinson D, Dunn C, Timothy K, Vincent GM, Leppert M. Linkage of a cardiac arrhythmia, the long-QT syndrome, and the Harvey ras-1 gene. *Science* 1991;252:704-06.
- Keating M, Dunn C, Atkinson D, Timothy K, Vincent GM, Leppert M. Consistent linkage of the long-QT syndrome to the Harvey ras-1 locus on chromosome 11. *Am J Hum Genet* 1991;49:1335-39.
- Jiang C, Atkinson D, Towbin JA, Splawski I, Lehmann MH, Li H, Timothy K, Taggart RT, Schwartz PJ, Vincent GM. Two long-QT syndrome loci map to chromosomes 3 and 7 with evidence for further heterogeneity. *Nat Genet* 1994;8:141-47.
- Schott JJ, Charpentier F, Peltier S, Foley P, Drouin E, Bouhour JB, Donnelly P, Vergnaud G, Bachner L, Moisan JP. Mapping of a gene for long-QT syndrome to chromosome 4q25-27. *Am J Hum Genet* 1995;57:1114-22.
- Splawski I, Tristani-Firouzi M, Lehmann MH, Sanguinetti MC, Keating MT. Mutations in the *hminK* gene cause long-QT syndrome and suppress I_{Ks} function. *Nat Genet* 1997;17:338-40.
- Abbott GW, Sesti F, Splawski I, Buck ME, Lehmann MH, Timothy KW, Keating MT, Goldstein SA. *MIRP1* forms I_{Kr} potassium channels with *HERG* and is associated with cardiac arrhythmia. *Cell* 1999;97:175-87.
- Splawski I, Shen J, Timothy KW, Lehmann MH, Priori S, Robinson JL, Moss AJ, Schwartz PJ, Towbin JA, Vincent GM, Keating MT. Spectrum of mutations in long-QT syndrome genes. *KvLQT1*, *HERG*, *SCN5A*, *KCNE1*, and *KCNE2*. *Circulation* 2000;102:1178-85.
- Schulze-Bahr E, Haverkamp W, Wedekind H, Rubie C, Hordt M, Borggrefe M, Assmann G, Breithardt G, Funke H. Autosomal recessive long-QT syndrome (Jervell Lange-Nielsen syndrome) is genetically heterogeneous. *Hum Genet* 1997;100:573-76.

19. Priori SG, Schwartz PJ, Napolitano C, Bianchi L, Dennis A, De Fusco M, Brown AM, Casari G. A recessive variant of the Romano-Ward long-QT syndrome? *Circulation* 1998;97:2420-25.
20. Geelen JL, Doevendans PA, Jongbloed RJ, Wellens HJ, Geraedts JP. Molecular genetics of inherited long-QT syndromes. *Eur Heart J* 1998;19:1427-33.
21. Priori SG, Napolitano C, Schwartz PJ. Low penetrance in the long-QT syndrome: clinical impact. *Circulation* 1999;99:529-33.
22. Sanguinetti MC, Curran ME, Spector PS, Keating MT. Spectrum of *HERG* K⁺-channel dysfunction in an inherited cardiac arrhythmia. *Proc Natl Acad Sci U S A* 1996;93:2208-12.
23. Barhanin J, Lesage F, Guillemare E, Fink M, Lazdunski M, Romey G. *KvLQT1* and *IsK* (*hminK*) proteins associate to form the I_{Ks} cardiac potassium current. *Nature* 1996;384:78-80.
24. Sanguinetti MC, Curran ME, Zou A, Shen J, Spector PS, Atkinson DL, Keating MT. Coassembly of *KvLQT1* and *hminK* (*IsK*) proteins to form cardiac I_{Ks} potassium channel. *Nature* 1996;384:80-83.
25. Chouabe C, Neyroud N, Guicheney P, Lazdunski M, Romey G, Barhanin J. Properties of *KvLQT1* K⁺ channel mutations in Romano-Ward and Jervell and Lange-Nielsen inherited cardiac arrhythmias. *EMBO J* 1997;16:5472-79.
26. Bennett PB, Yazawa K, Makita N, George AL Jr. Molecular mechanism for an inherited cardiac arrhythmia. *Nature* 1995;376:683-85.
27. Dumaine R, Wang Q, Keating MT, Hartmann HA, Schwartz PJ, Brown AM, Kirsch GE. Multiple mechanisms of Na⁺ channel-linked long-QT syndrome. *Circ Res* 1996;78:916-24.
28. Clancy CE, Rudy Y. Linking a genetic defect to its cellular phenotype in a cardiac arrhythmia. *Nature* 1999;400:566-69.
29. An RH, Wang XL, Kerem B, Benhorin J, Medina A, Goldmit M, Kass RS. Novel LQT-3 mutation affects Na⁺ channel activity through interactions between α - and β 1-subunits. *Circ Res* 1998;83:141-46.
30. Schwartz PJ, Moss AJ. Prolonged Q-T interval: what does it mean? *J Cardiovasc Med* 1982;7:1317-30.
31. Schwartz PJ. The idiopathic long-QT syndrome: the need for a prospective registry. *Eur Heart J* 1983;4:529-31.
32. Moss AJ, Schwartz PJ, Crampton RS, Locati E, Carleen E. The long-QT syndrome: a prospective international study. *Circulation* 1985;71:17-21.
33. Moss AJ, Schwartz PJ, Crampton RS, Zivoni D, Locati EH, MacCluer J, Hall WJ, Weitkamp L, Vincent GM, Garson A Jr. The long-QT syndrome. Prospective longitudinal study of 328 families. *Circulation* 1991;84:1136-44.
34. Zareba W, Moss AJ, Schwartz PJ, Vincent GM, Robinson JL, Priori SG, Benhorin J, Locati EH, Towbin JA, Keating MT, Lehmann MH, Hall WJ. Influence of genotype on the clinical course of the long-QT syndrome. International Long-QT Syndrome Registry Research Group. *N Engl J Med* 1998;339:960-65.
35. Schwartz PJ, Priori SG, Spazzolini C, Moss AJ, Vincent GM, Napolitano C, Denjoy I, Guicheney P, Breithardt G, Keating MT, Towbin JA, Beggs AH, Brink P, Wilde AA, Toivonen L, Zareba W, Robinson JL, Timothy KW, Corfield V, Wattanasirichaigoon D, Corbett C, Haverkamp W, Schulze-Bahr E, Lehmann MH, Schwartz K, Coumel P, Bloise R. Genotype-phenotype correlation in the long-QT syndrome: gene-specific triggers for life-threatening arrhythmias. *Circulation* 2001;103:89-95.
36. Schouten EG, Dekker JM, Meppelink P, Kok FJ, Vandenbroucke JP, Pool J. QT-interval prolongation predicts cardiovascular mortality in an apparently healthy population. *Circulation* 1991;84:1516-23.
37. de Bruyne MC, Hoes AW, Kors JA, Hofman A, van Bommel JH, Grobbee DE. Prolonged QT-interval predicts cardiac and all-cause mortality in the elderly. The Rotterdam Study. *Eur Heart J* 1999;20:278-84.
38. Atiga WL, Calkins H, Lawrence JH, Tomaselli GF, Smith JM, Berger RD. Beat-to-beat repolarization lability identifies patients at risk for sudden cardiac death. *J Cardiovasc Electrophysiol* 1998;9:899-908.

39. Bazett HC. An analysis of the time-relations of electrocardiograms. *Heart* 1920;7:353-70.
40. Rautaharju PM, Zhou SH, Wong S, Calhoun HP, Berenson GS, Prineas R, Davignon A. Sex differences in the evolution of the electrocardiographic QT-interval with age. *Can J Cardiol* 1992;8:690-95.
41. Stramba-Badiale M, Spagnolo D, Bosi G, Schwartz PJ. Are gender differences in QTc present at birth? MISNES Investigators. Multicenter Italian Study on Neonatal Electrocardiography and Sudden Infant Death Syndrome. *Am J Cardiol* 1995;75:1277-78.
42. Lehmann MH, Timothy KW, Frankovich D, Fromm BS, Keating M, Locati EH, Taggart RT, Towbin JA, Moss AJ, Schwartz PJ, Vincent GM. Age-gender influence on the rate-corrected QT-interval and the QT-heart rate relation in families with genotypically characterized long-QT syndrome. *J Am Coll Cardiol* 1997;29:93-99.
43. Locati EH, Zareba W, Moss AJ, Schwartz PJ, Vincent GM, Lehmann MH, Towbin JA, Priori SG, Napolitano C, Robinson JL, Andrews M, Timothy K, Hall WJ. Age- and sex-related differences in clinical manifestations in patients with congenital long-QT syndrome: findings from the International LQTS Registry. *Circulation* 1998;97:2237-44.
44. Merri M, Benhorin J, Alberti M, Locati E, Moss AJ. Electrocardiographic quantitation of ventricular repolarization. *Circulation* 1989;80:1301-08.
45. Davignon A, Rautaharju B, Boisselle E. Normal ECG standards for infants and children. *Pediatr Cardiol* 1980;1:123-31.
46. Schwartz PJ, Moss AJ, Vincent GM, Crampton RS. Diagnostic criteria for the long-QT syndrome. An update. *Circulation* 1993;88:782-84.
47. Hashiba K. Hereditary QT prolongation syndrome in Japan: genetic analysis and pathological findings of the conducting system. *Jpn Circ J* 1978;42:1133-50.
48. Vincent GM, Timothy KW, Leppert M, Keating M. The spectrum of symptoms and QT-intervals in carriers of the gene for the long-QT syndrome. *N Engl J Med* 1992;327:846-52.
49. Rashba EJ, Zareba W, Moss AJ, Hall WJ, Robinson J, Locati EH, Schwartz PJ, Andrews M. Influence of pregnancy on the risk for cardiac events in patients with hereditary long-QT syndrome. LQTS Investigators. *Circulation* 1998;97:451-56.
50. Schwartz PJ, Periti M, Malliani A. The long-QT syndrome. *Am Heart J* 1975;89:378-90.
51. Pham TV, Sosunov EA, Gainullin RZ, Danilo P Jr, Rosen MR. Impact of sex and gonadal steroids on prolongation of ventricular repolarization and arrhythmias induced by I_K -blocking drugs. *Circulation* 2001;103:2207-12.
52. Tanabe S, Hata T, Hiraoka M. Effects of estrogen on action potential and membrane currents in guinea pig ventricular myocytes. *Am J Physiol* 1999;277:H826-33.
53. Doevendans PA, Wilde AA (eds.). Cardiovascular Genetics. Dordrecht, Netherlands: Kluwer Academic Publisher 2001.
54. Vincent GM, Timothy K, Fox J, Zhang L. The inherited long-QT syndrome: from ion channel to bedside. *Cardiol Rev* 1999;7:44-55.
55. van den Berg MP, Wilde AA, Viersma TJW, Brouwer J, Haaksma J, van der Hout AH, Stolte-Dijkstra I, Bezzina TCR, Van Langen IM, Beaufort-Krol GC, Cornel JH 2nd, Crijns HJ. Possible bradycardic mode of death and successful pacemaker treatment in a large family with features of long-QT syndrome type 3 and Brugada syndrome. *J Cardiovasc Electrophysiol* 2001;12:630-36.
56. Wilde AA, Roden DM. Predicting the long-QT genotype from clinical data: from sense to science. *Circulation* 2000;102:2796-98.
57. Barlow JB, Bosman CK, Craig Cochrane JW. Congenital cardiac arrhythmias. *Lancet* 1964;2:531 (letter).

58. Dessertenne F. La tachycardie ventriculaire à deux foyers opposés variables. *Arch Mal Coeur Vaiss* 1966;59:263-72.
59. Wilde AA, Jongbloed RJ, Doevendans PA, Duren DR, Hauer RN, van Langen IM, van Tintelen JP, Smeets HJ, Meyer H, Geelen JL. Auditory stimuli as a trigger for arrhythmic events differentiate *HERG*-related (LQTS2) patients from *KvLQT1*-related patients (LQTS1). *J Am Coll Cardiol* 1999;33:327-32.
60. Moss AJ, Robinson JL, Gessman L, Gillespie R, Zareba W, Schwartz PJ, Vincent GM, Benhorin J, Heilbron EL, Towbin JA, Priori SG, Napolitano C, Zhang L, Medina A, Andrews ML, Timothy K. Comparison of clinical and genetic variables of cardiac events associated with loud noise versus swimming among subjects with the long-QT syndrome. *Am J Cardiol* 1999;84:876-79.
61. Ali RH, Zareba W, Moss AJ, Schwartz PJ, Benhorin J, Vincent GM, Locati EH, Priori S, Napolitano C, Towbin JA, Hall WJ, Robinson JL, Andrews ML, Zhang L, Timothy K, Medina A. Clinical and genetic variables associated with acute arousal and nonarousal-related cardiac events among subjects with long-QT syndrome. *Am J Cardiol* 2000;15:457-61.
62. de Jager T, Corbett CH, Badenhorst JC, Brink PA, Corfield VA. Evidence of a long-QT founder gene with varying phenotypic expression in South African families. *J Med Genet* 1996;33:567-73.
63. Schwartz PJ, Locati E, Napolitano C, Priori SG. The long-QT syndrome. In: Zipes DP, Jalife J (eds.) *Cardiac electrophysiology. From cell to bedside*. 2nd ed. Philadelphia: WB Saunders 1995: 778-811.
64. Shimizu W, Antzelevitch C. Cellular basis for the ECG features of the LQT-1 form of the long-QT syndrome: effects of beta-adrenergic agonists and antagonists and sodium channel blockers on transmural dispersion of repolarization and torsades de pointes. *Circulation* 1998;98:2314-22.
65. Maron BJ, Moller JH, Seidman CE, Vincent GM, Dietz HC, Moss AJ, Towbin JA, Sondheimer HM, Pyeritz RE, McGee G, Epstein AE. Impact of laboratory molecular diagnosis on contemporary diagnostic criteria for genetically transmitted cardiovascular diseases: hypertrophic cardiomyopathy, long-QT syndrome, and Marfan syndrome. A statement for healthcare professionals from the Councils on Clinical Cardiology, Cardiovascular Disease in the Young, and Basic Science, American Heart Association. *Circulation* 1998;98:1460-71.
66. Wellens HJ, Vermeulen A, Durrer D. Ventricular fibrillation occurring on arousal from sleep by auditory stimuli. *Circulation* 1972;46:661-65.
67. Nakajima T, Misu K, Iwasawa K, Tamiya E, Segawa K, Matsuo H, Hada K. Auditory stimuli as a major cause of syncope in a patient with idiopathic long-QT syndrome. *Jpn Circ J* 1995;59:241-46.
68. Moss AJ, Zareba W, Hall WJ, Schwartz PJ, Crampton RS, Benhorin J, Vincent GM, Locati EH, Priori SG, Napolitano C, Medina A, Zhang L, Robinson JL, Timothy K, Towbin JA, Andrews ML. Effectiveness and limitations of beta-blocker therapy in congenital long-QT syndrome. *Circulation* 2000;101:616-23.
69. Garza LA, Vick RL, Nora JJ, McNamara DG. Heritable Q-T prolongation without deafness. *Circulation* 1970;41:39-48.
70. James TN. Congenital deafness and cardiac arrhythmias. *Am J Cardiol* 1967;62:627-43.
71. Johansson BW, Jorming B. Hereditary prolongation of QT-interval. *Br Heart J* 1972;34:744-51.
72. Grubb BP. The use of oral labetalol in the treatment of arrhythmias associated with the long-QT syndrome. *Chest* 1991;100:1724-25.
73. Brachmann J, Scherlag BJ, Rosenshtraukh LV, Lazzara R. Bradycardia-dependent triggered activity: relevance to drug-induced multiform ventricular tachycardia. *Circulation* 1983;68:846-56.
74. Cranefield PF, Aronson RS. Torsade de pointes and other pause-induced ventricular tachycardias: the short-long-short sequence and early afterdepolarizations. *Pacing Clin Electrophysiol* 1988;11:670-78.

75. Jackman WM, Friday KJ, Anderson JL, Aliot EM, Clark M, Lazzara R. The long-QT syndromes: a critical review, new clinical observations and a unifying hypothesis. *Prog Cardiovasc Dis* 1988;31:115-72.
76. Ratskin RA, Hunt D, Russell RO, Rackley CE. Q-T interval prolongation, paroxysmal ventricular arrhythmias, and convulsive syncope. *Ann Intern Med* 1971;75:919-24.
77. Roy PR, Emanuel R, Ismail SA, El Tayib MH. Hereditary prolongation of the Q-T interval. Genetic observations and management in three families with twelve affected members. *Am J Cardiol* 1976;37:237-43.
78. Di Segni E, David D, Katzenstein M, Klein HO, Kaplinsky E, Levy MJ. Permanent overdrive pacing for the suppression of recurrent ventricular tachycardia in a newborn with long-QT syndrome. *J Electrocardiol* 1980;13:189-92.
79. Medina-Ravell V, Castellanos A, Portillo-Acosta B, Maduro-Maytin C, Rodriguez-Salas L, Hernandez-Arenas M, La Salle-Toro R, Mendoza-Mujica I, Ortega-Maldonado M, Berkovits BV. Management of tachyarrhythmias with dual-chamber pacemakers. *PACE* 1983;6:333-45.
80. Wilmer CI, Stein B, Morris DC. Atrioventricular pacemaker placement in Romano-Ward syndrome and recurrent torsades de pointes. *Am J Cardiol* 1987;59:171-72.
81. Scott WA, Dick M. Two:one atrioventricular block in infants with congenital long-QT syndrome. *Am J Cardiol* 1987;60:1409-10.
82. Viskin S. Cardiac pacing in the long-QT syndrome: review of available data and practical recommendations. *J Cardiovasc Electrophysiol* 2000;11:593-600.
83. Benhorin J, Taub R, Goldmit M, Kerem B, Kass RS, Windman I, Medina A. Effects of flecainide in patients with new *SCN5A* mutation: mutation-specific therapy for long-QT syndrome? *Circulation* 2000;101:1698-706.
84. Eldar M, Griffin JC, Abbott JA, Benditt D, Bhandari A, Herre JM, Benson DW, Scheinman MM. Permanent cardiac pacing in patients with the long-QT syndrome. *J Am Coll Cardiol* 1987;10:600-07.
85. Silka MJ, Kron J, Dunnigan A, Dick M. Sudden cardiac death and the use of implantable cardioverter-defibrillators in pediatric patients. The Pediatric Electrophysiology Society. *Circulation* 1993;87:800-07.
86. Groh WJ, Silka MJ, Oliver RP, Halperin BD, McAnulty JH, Kron J. Use of implantable cardioverter-defibrillators in the congenital long-QT syndrome. *Am J Cardiol* 1996;78:703-06.
87. Dorostkar PC, Eldar M, Belhassen B, Scheinman MM. Long-term follow-up of patients with long-QT syndrome treated with beta-blockers and continuous pacing. *Circulation* 1999;100:2431-36.
88. Schwartz PJ. The long-QT syndrome. Armonk, NY: Futura Publishing Company, Inc. 1997.
89. Schwartz PJ, Priori SG, Locati EH, Napolitano C, Cantu F, Towbin JA, Keating MT, Hammoude H, Brown AM, Chen LS. Long-QT syndrome patients with mutations of the *SCN5A* and *HERG* genes have differential responses to Na^+ channel blockade and to increases in heart rate. Implications for gene-specific therapy. *Circulation* 1995;92:3381-86.
90. Ackerman MJ, Tester DJ, Porter CJ. Swimming, a gene-specific arrhythmogenic trigger for inherited long-QT syndrome. *Mayo Clin Proc* 1999;74:1088-94.
91. Sanguinetti MC, Jurkiewicz NK. Role of external Ca^{2+} and K^+ in gating of cardiac delayed rectifier K^+ currents. *Pflugers Arch* 1992;420:180-86.
92. Sanguinetti MC, Jiang C, Curran ME, Keating MT. A mechanistic link between an inherited and an acquired cardiac arrhythmia: *HERG* encodes the I_{Kr} potassium channel. *Cell* 1995;81:299-307.
93. Choy AM, Lang CC, Chomsky DM, Rayos GH, Wilson JR, Roden DM. Normalization of acquired QT prolongation in humans by intravenous potassium. *Circulation* 1997;96:2149-54.

94. Compton SJ, Lux RL, Ramsey MR, Strelch KR, Sanguinetti MC, Green LS, Keating MT, Mason JW. Genetically defined therapy of inherited long-QT syndrome. Correction of abnormal repolarization by potassium. *Circulation* 1996;94:1018-22.
95. Kubota T, Shimizu W, Kamakura S, Horie M. Hypokalemia-induced long-QT syndrome with an underlying novel missense mutation in S4-S5 linker of *KCNQ1*. *J Cardiovasc Electrophysiol* 2000;11:1048-54.
96. Tan HL, Alings M, Van Olden RW, Wilde AA. Long-term (subacute) potassium treatment in congenital *HERG*-related long-QT syndrome (LQTS2). *J Cardiovasc Electrophysiol* 1999;10:229-33.
97. Shimizu W, Kurita T, Matsuo K, Suyama K, Aihara N, Kamakura S, Towbin JA, Shimomura K. Improvement of repolarization abnormalities by a K^+ channel opener in the LQT-1 form of congenital long-QT syndrome. *Circulation* 1998;97:1581-88.
98. Rosero SZ, Zareba W, Robinson J, Moss A. Gene-specific therapy for long-QT syndrome: QT shortening with lidocaine and tocainide in patients with mutations of the sodium channel gene. *Ann Noninv Electrophys* 1997;3:274-78.
99. Sicouri S, Antzelevitch D, Heilmann C, Antzelevitch C. Effects of sodium channel block with mexiletine to reverse action potential prolongation in *in vitro* models of the long-QT syndrome. *J Cardiovasc Electrophysiol* 1997;8:1280-90.
100. Priori SG, Napolitano C, Schwartz PJ, Bloise R, Crotti L, Ronchetti E. The elusive link between LQT-3 and Brugada syndrome: the role of flecainide challenge. *Circulation* 2000;102:945-47.
101. Brugada P, Brugada J. Right bundle branch block, persistent ST segment elevation and sudden cardiac death: a distinct clinical and electrocardiographic syndrome. A multicenter report. *J Am Coll Cardiol* 1992;20:1391-96.
102. Cowan JC, Yusoff K, Moore M, Amos PA, Cold AE, Bourke JP, Tansuphaswadikul S, Campbell RW. Importance of lead selection in QT-interval measurement. *Am J Cardiol* 1988;61:83-87.
103. Garson AJ. How to measure the QT-interval - what is normal? *Am J Cardiol* 1993;72:14B-16B.
104. Morganroth J, Brown AM, Critz S, Crumb WJ, Kunze DL, Lacerda AE, Lopez H. Variability of the QTc interval: impact on defining drug effect and low-frequency cardiac event. *Am J Cardiol* 1993;72:26B-31B.
105. Day CP, McComb JM, Campbell RW. QT dispersion: an indication of arrhythmia risk in patients with long-QT-intervals. *Br Heart J* 1990;63:342-44.
106. Linker NJ, Colonna P, Kekwick CA, Till J, Camm AJ, Ward DE. Assessment of QT dispersion in symptomatic patients with congenital long-QT syndromes. *Am J Cardiol* 1992;69:634-38.
107. Priori SG, Napolitano C, Diehl L, Schwartz PJ. Dispersion of the QT-interval. A marker of therapeutic efficacy in the idiopathic long-QT syndrome. *Circulation* 1994;89:1681-89.
108. Wilson FN, MacLeod AG, Barker PS, Johnston FD. The determination and the significance of the areas of the ventricular deflections of the electrocardiogram. *Am Heart J* 1934;10:46-61.
108. Malik M, Acar B, Gang Y, Yap YG, Hnatkova K, Camm AJ. QT dispersion does not represent electrocardiographic interlead heterogeneity of ventricular repolarization. *J Cardiovasc Electrophysiol* 2000;11:835-43.
110. Sylven JC, Horacek BM, Spencer CA, Klassen GA, Montague TJ. QT-interval variability on the body surface. *J Electrocardiol* 1984;17:179-88.
111. Vassallo JA, Cassidy DM, Kindwall KE, Marchlinski FE, Josephson ME. Nonuniform recovery of excitability in the left ventricle. *Circulation* 1988;78:1365-72.
112. Hii JT, Wyse DG, Gillis AM, Duff HJ, Solylo MA, Mitchell LB. Precordial QT-interval dispersion as a marker of torsades de pointes. Disparate effects of class IA antiarrhythmic drugs and amiodarone. *Circulation* 1992;86:1376-82.

113. Benhorin J, Merri M, Alberti M, Locati E, Moss AJ, Hall WJ, Cui L. Long-QT syndrome. New electrocardiographic characteristics. *Circulation* 1990;82:521-27.
114. Malfatto G, Beria G, Sala S, Bonazzi O, Schwartz PJ. Quantitative analysis of T wave abnormalities and their prognostic implications in the idiopathic long-QT syndrome. *J Am Coll Cardiol* 1994;23:296-301.
115. Lehmann MH, Suzuki F, Fromm BS, Frankovich D, Elko P, Steinman RT, Fresard J, Baga JJ, Taggart RT. T wave "humps" as a potential electrocardiographic marker of the long-QT syndrome. *J Am Coll Cardiol* 1994;24:746-54.
116. Nearing BD, Huang AH, Verrier RL. Dynamic tracking of cardiac vulnerability by complex demodulation of the T wave. *Science* 1991;252:437-40.
117. Schwartz PJ, Malliani A. Electrical alternation of the T-wave: clinical and experimental evidence of its relationship with the sympathetic nervous system and with the long-QT syndrome. *Am Heart J* 1975;89:45-50.
118. Hiejima K, Sano T. Electrical alternans of TU wave in Romano-Ward syndrome. *Br Heart J* 1976;38:767-70.
119. Schwartz PJ. The long-QT syndrome. In: Kulbertus HE, Wellens HJ (eds.) *Sudden death. The Hague: M. Nijhoff* 1980: 358-78.
120. Schwartz PJ. Idiopathic long-QT syndrome: progress and questions. *Am Heart J* 1985;109:399-411.
121. Hiejima K, Suzuki F, Satake S, Ishihara K. Electrophysiologic studies of Jervell Lange-Nielsen syndrome. *Chest* 1981;79:446-48.
122. Vincent GM. The heart rate of Romano-Ward syndrome patients. *Am Heart J* 1986;112:61-64.
123. Gorgels AP, Al Fadel F, Zaman L, Kantoch MJ, Al Halees Z. The long-QT syndrome with impaired atrioventricular conduction: a malignant variant in infants. *J Cardiovasc Electrophysiol* 1998;9:1225-32.
124. Kugler JD. Sinus nodal dysfunction in young patients with long-QT syndrome. *Am Heart J* 1991;121:1132-36.
125. Curtiss EI, Heibel RH, Shaver JA. Autonomic maneuvers in hereditary Q-T interval prolongation (Romano-Ward syndrome). *Am Heart J* 1978;95:420-28.
126. Viswanathan PC, Rudy Y. Pause induced early afterdepolarizations in the long-QT syndrome: a simulation study. *Cardiovasc Res* 1999;42:530-42.
127. Wellens HJ, Lie KI. Ventricular tachycardia: the value of programmed electrical stimulation. In: Krikler DM, Goodwin JF (eds.) *Cardiac arrhythmias. W.B. Saunders* 1975:182-94.
128. Bhandari AK, Shapiro WA, Morady F, Shen EN, Mason J, Scheinman MM. Electrophysiologic testing in patients with the long-QT syndrome. *Circulation* 1985;71:63-71.
129. Coumel P, Leclercq JF, Lucet V. Possible mechanisms of the arrhythmias in the long-QT syndrome. *Eur Heart J* 1985;6 Suppl D:115-29.
130. Viskin S, Alla SR, Barron HV, Heller K, Saxon L, Kitzis I, Hare GF, Wong MJ, Lesh MD, Scheinman MM. Mode of onset of torsades de pointes in congenital long-QT syndrome. *J Am Coll Cardiol* 1996;28:1262-68.
131. Swan H, Viitasalo M, Piippo K, Laitinen P, Kontula K, Toivonen L. Sinus node function and ventricular repolarization during exercise stress test in long-QT syndrome patients with *KvLQT1* and *HERG* potassium channel defects. *J Am Coll Cardiol* 1999;34:823-29.
132. Schwartz SP, De Salo Pool N. Transient ventricular fibrillation. III. The effects of bodily rest, atropine sulphate, and exercise on patients with transient ventricular fibrillation during established auriculoventricular dissociation. A study of the influence of the extrinsic nerves on the idioventricular pacemaker of the heart. *Am Heart J* 1958;39:361-86.

133. Phillips J, Ichinose H. Clinical and pathologic studies in the hereditary syndrome of a long-QT-interval, syncopal spells and sudden death. *Chest* 1970;58:236-43.
134. Vincent GM, Jaiswal D, Timothy KW. Effects of exercise on heart rate, QT, QTc and QT/QTs in the Romano-Ward inherited long-QT syndrome. *Am J Cardiol* 1991;68:498-503.
135. Shimizu W, Ohe T, Kurita T, Shimomura K. Differential response of QTU interval to exercise, isoproterenol, and atrial pacing in patients with congenital long-QT syndrome. *Pacing Clin Electrophysiol* 1991;14:1966-70.
136. Merri M, Moss AJ, Benhorin J, Locati EH, Alberti M, Badilini F. Relation between ventricular repolarization duration and cardiac cycle length during 24-hour Holter recordings. Findings in normal patients and patients with long-QT syndrome. *Circulation* 1992;85:1816-21.
137. Eggeling T, Osterhues HH, Hoehner M, Gabrielsen FG, Weismueller P, Hombach V. Value of Holter monitoring in patients with the long-QT syndrome. *Cardiology* 1992;81:107-14.
138. Molnar J, Zhang F, Weiss J, Ehler FA, Rosenthal JE. Diurnal pattern of QTc interval: how long is prolonged? Possible relation to circadian triggers of cardiovascular events. *J Am Coll Cardiol* 1996;27:76-83.
139. Moss AJ, Zareba W, Benhorin J, Locati EH, Hall WJ, Robinson JL, Schwartz PJ, Towbin JA, Vincent GM, Lehmann MH. ECG T-wave patterns in genetically distinct forms of the hereditary long-QT syndrome. *Circulation* 1995;92:2929-34.
140. Zhang L, Timothy KW, Vincent GM, Lehmann MH, Fox J, Giulio LC, Shen J, Splawski I, Priori SG, Compton SJ, Yanowitz F, Benhorin J, Moss AJ, Schwartz PJ, Robinson JL, Wang Q, Zareba W, Keating MT, Towbin JA, Napolitano C, Medina A. Spectrum of ST-T-wave patterns and repolarization parameters in congenital long-QT syndrome: ECG findings identify genotypes. *Circulation* 2000;102:2849-55.
141. Priori SG, Barhanin J, Hauer RN, Haverkamp W, Jongsma HJ, Kleber AG, McKenna WJ, Roden DM, Rudy Y, Schwartz K, Schwartz PJ, Towbin JA, Wilde AM. Genetic and molecular basis of cardiac arrhythmias: impact on clinical management parts I and II. *Circulation* 1999;99:518-28.
142. Vincent GM, Timothy K, Fox J, Zhang L. Long-QT syndrome patients with normal to borderline prolonged QTc intervals are at risk for syncope, cardiac arrest and sudden death. *Circulation* 1999;100(18S):1245 (abstract).
143. Ackerman MJ. The long-QT syndrome: ion channel diseases of the heart. *Mayo Clin Proc* 1998;73:250-69.
144. Wei J, Abbott GW, Sesti F, Goldstein SA, Schwartz PJ, Saksena S, Murray KT, George AL. Prevalence of KCNE2 (MiRP1) mutations in acquired long-QT syndrome. *Circulation* 1999;100(18S):1495 (abstract).
145. Donger C, Denjoy I, Berthet M, Neyroud N, Cruaud C, Bennaceur M, Chivoret G, Schwartz K, Coumel P, Guicheney P. KvLQT1 C-terminal missense mutation causes a forme fruste long-QT syndrome. *Circulation* 1997;96:2778-81.
146. Piippo K, Holmstrom S, Swan H, Viitasalo M, Raatikka M, Toivonen L, Kontula K. Effect of the antimalarial drug halofantrine in the long-QT syndrome due to a mutation of the cardiac sodium channel gene SCN5A. *Am J Cardiol* 2001;87:909-11.
147. Wei J, Yang ICH, Tapper AR, Murray KT, Viswanathan PC, Rudy Y, Bennett PB, Norris K, Balser JR, Roden DM, George AL. KCNE1 polymorphism confers risk of drug-induced long-QT syndrome by altering kinetic properties of I_{Ks} potassium channels. *Circulation* 1999;100(18S):1495 (abstract).
148. Roden DM. Acquired long-QT syndromes and the risk of proarrhythmia. *J Cardiovasc Electrophysiol* 2000;11:938-40.

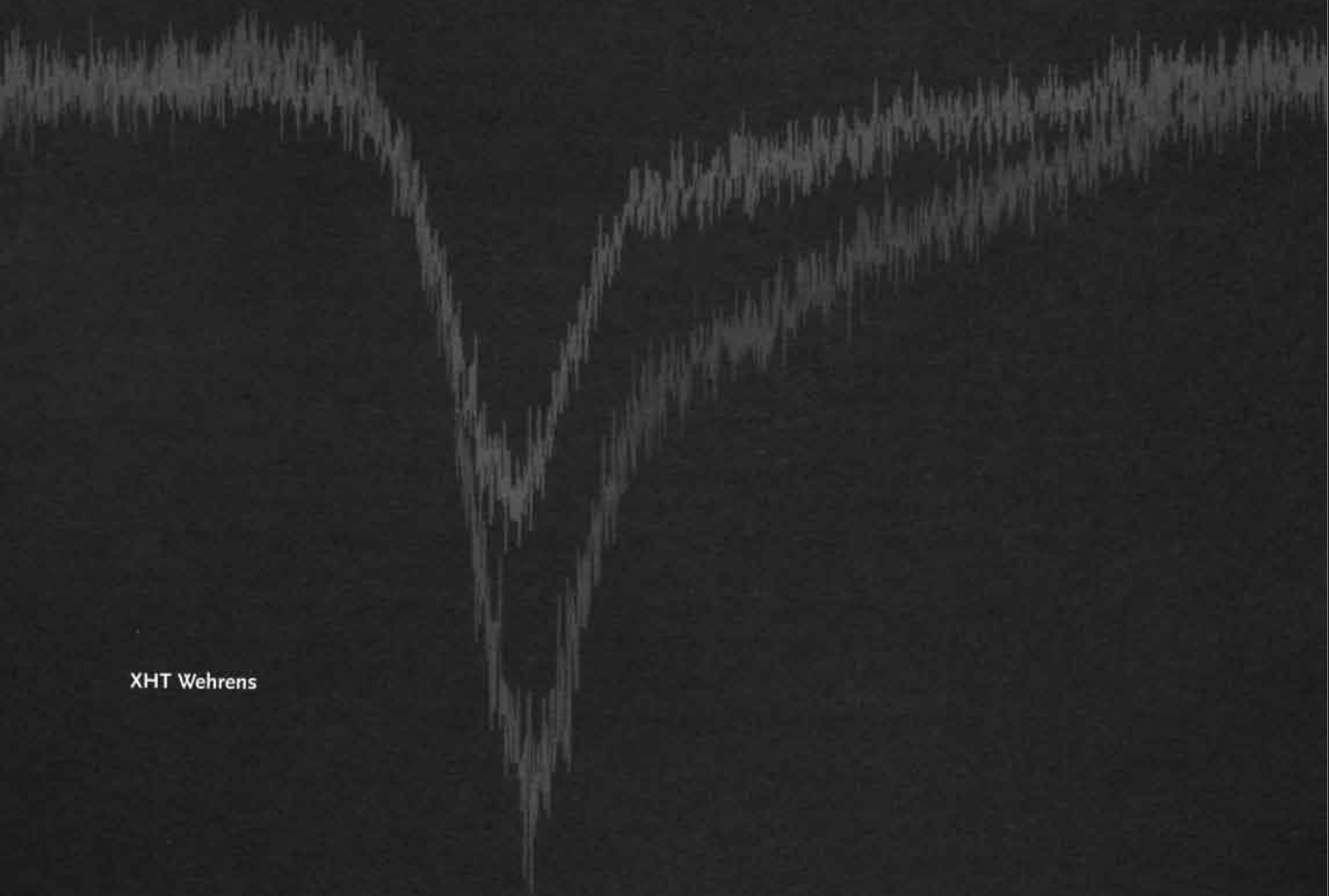
149. Roden DM, Lazzara R, Rosen M, Schwartz PJ, Towbin J, Vincent GM. Multiple mechanisms in the long-QT syndrome. Current knowledge, gaps, and future directions. The SADS Foundation Task Force on LQTS. *Circulation* 1996;94:1996-2012.
150. Lehmann MH, Hardy S, Archibald D, Quart B, MacNeil DJ. Sex difference in risk of torsades de pointes with d,l-sotalol. *Circulation* 1996;94:2535-41.
151. Meissner FL. Taubstummenheit und taubstummenbildung. *Leipzig/ Heidelberg: C.F. Winter'sche Verlagshandlung*, 1856.
152. Morquio L. Sur une maladie infantile et familiale caractérisée par des modifications permanentes du poulx, des attaques épileptiformes et al morte subite. *Arch Med Enf* 1901;4:467-75.
153. Latham AD, Munro TA. Familial myoclonus epilepsy associated with deaf-mutism in a family showing other psychobiological abnormalities. *Ann Eugen Lond* 1937;8:166-75.
154. Herrlin KM, Moller T. A case of cardiac syncope. *Acta Paediatrica* 1953;42:391.
155. Romano C. Congenital cardiac arrhythmias. *Lancet* 1965; i:658-59.
156. Levine SA, Woodworth CR. Congenital deafmutism, prolonged Q-T interval, syncopal attacks and sudden death. *New Engl J Med* 1958;259:412-17.
157. Fraser GR, Forgett P, James TN. Congenital deafness associated with electrocardiographic abnormalities. *Quart J Med* 1964;33:361-85.
158. James TN. Congenital deafness and cardiac arrhythmias. *Am J Cardiol* 1967;627:627-43.
159. Splawski I, Timothy KW, Vincent GM, Atkinson DL, Keating MT. Molecular basis of the long-QT syndrome associated with deafness. *N Engl J Med* 1997;336:1562-67.
160. Fraser GR, Froggatt P, Murphy T. Genetical aspects of the cardio-auditory syndrome of Jervell and Lange-Nielsen (congenital deafness and electrocardiographic abnormalities). *Ann Hum Genet Lond* 1964;28:133-57.
161. Mathews EC, Blount AW, Townsend JL. Q-T prolongation and ventricular arrhythmias, with and without deafness, in the same family. *Am J Cardiol* 1972;29:702-11.
162. Crampton R. Preeminence of the left stellate ganglion in the long-QT syndrome. *Circulation* 1979;59:769-78.
163. Ben-David J, Zipes DP. Differential response to right and left ansae subclaviae stimulation of early afterdepolarizations and ventricular tachycardia induced by cesium in dogs. *Circulation* 1988;78:1241-50.
164. Moss AJ, McDonald J. Unilateral cervicothoracic sympathetic ganglionectomy for the treatment of long-QT-interval syndrome. *N Engl J Med* 1971;285:903-04.
165. Yanowitz F, Preston JB, Abildskov JA. Functional distribution of right and left stellate innervation to the ventricles: production of neurogenic electrocardiographic changes by unilateral alteration of sympathetic tone. *Circ Res* 1966;18:416-28.
166. Muller KD, Jakob H, Neuzner J, Grebe SF, Schlepper M, Pitschner HF. ¹²³I-metaiodobenzylguanidine scintigraphy in the detection of irregular regional sympathetic innervation in long-QT syndrome. *Eur Heart J* 1993;14:316-25.
167. Gohl K, Feistel H, Weikl A, Bachmann K, Wolf F. Congenital myocardial sympathetic dysinnervation (CMSD) - a structural defect of idiopathic long-QT syndrome. *Pacing Clin Electrophysiol* 1991;14:1544-53.
168. Calkins H, Lehmann MH, Allman K, Wieland D, Schwaiger M. Scintigraphic pattern of regional cardiac sympathetic innervation in patients with familial long-QT syndrome using positron emission tomography. *Circulation* 1993;87:1616-21.

169. Nador F, Beria G, De Ferrari GM, Stramba-Badiale M, Locati EH, Lotto A, Schwartz PJ. Unsuspected echocardiographic abnormality in the long-QT syndrome. Diagnostic, prognostic, and pathogenetic implications. *Circulation* 1991;84:1530-42.
170. Schwartz PJ, Verrier RL, Lown B. Effect of stellectomy and vagotomy on ventricular refractoriness in dogs. *Circ Res* 1977;40:536-40.
171. Schwartz PJ, Zaza A, Locati E, Moss AJ. Stress and sudden death. The case of the long-QT syndrome. *Circulation* 1991;83:1171-80.
172. Mitcheson JS, Chen J, Lin M, Culbertson C, Sanguinetti MC. A structural basis for drug-induced long-QT syndrome. *Proc Natl Acad Sci U S A* 2000;97:12329-33

Chapter 2

The Cardiac Sodium Channel

XHT Wehrens



Introduction

Voltage-gated sodium (Na^+) channels are transmembrane proteins responsible for the rapid upstroke of the cardiac action potential and for rapid impulse conduction through cardiac tissue (for review, see (1,2)). Mutations in the gene encoding the cardiac Na^+ channel (*SCN5A*) have been linked to three forms of primary electrical disease: the long-QT syndrome (LQTS) (3), the Brugada syndrome (BrS) (4), and cardiac conduction defects (CCD) (5,6). This chapter will review the physiology, molecular biology, biophysics, pharmacology, modulation and regulation of the cardiac Na^+ channel, and the relevance to the congenital long-QT syndrome.

Sodium Channel Current

The upstroke of the action potential of cardiomyocytes and cells of the specialized conduction system is due to a transient increase in membrane permeability to Na^+ ions. Na^+ channels can be viewed upon as macromolecular protein tunnels that span the lipid bilayer of the cell membrane, which allow ions to flow in or out the cell in a very efficient fashion (up to 10^6 per second) (7,8). This flow of ions creates electrical currents large enough to produce rapid changes in transmembrane voltage, which is the electrical potential difference between the cell interior and exterior. The very rapid rates of rise of the action potentials in these cells predict that the currents responsible for these voltage changes are rather large (about 1 mA/cm^2) (8). Sodium currents were first studied under voltage-clamp in several multicellular cardiac preparations (9,10), but have now also been thoroughly investigated in single cell preparations (11), internally perfused canine cardiac Purkinje cells (12), and embryonic mouse cardiomyocytes (13). Measurements of single sodium channel activity have also been carried out in membranes of rat (14), rabbit (15), canine (12), guinea pig (14), and mouse cardiomyocytes (16,17). Although the role of Na^+ channel currents in initiating action potentials and impulse propagation is well known, it has not been as well understood that Na^+ channel activity can also contribute to the duration of the action potential. A very small fraction of Na^+ channels fail to enter the inactivated state of the channel and thus create a small persistent current during the action

potential plateau phase, that has been referred to as 'window current' through Na^+ channels (18).

Molecular Architecture of Voltage-gated Na^+ Channels

The tetrodotoxin (TTX)-sensitive Na^+ channel is a heterotrimeric voltage-gated ion channel that is highly selective for Na^+ over other ions (8). The voltage-gated Na^+ channel consists of three glycoprotein subunits: a principal α -subunit of 260 kDa (19), which is associated with a β_1 -subunit of 36 kDa (20,21), and linked to a β_2 -subunit of 33 kDa (20,22). The primary structure of the α -subunit consists of four homologous transmembrane domains (DI-DIV) each containing six membrane-spanning segments (S1-S6) with a central pore region (23-25). The region between segment 5 and 6 of each of the four domains is called the P-region because it contributes to the pore of the channel (FIGURE 2.1).

In 1992, Gellens et al. (26) cloned and characterized the cardiac sodium channel α -subunit gene (*SCN5A*). The *SCN5A* gene consists of 28 exons and spans approximately 80 kb on chromosome 3p21 (27,28). The *SCN5A* gene encodes Nav 1.5 Na^+ channels, that belong to the same family as the neuronal and skeletal muscle isoforms (29,30). Nav 1.5 channels have been detected in adult heart (*hH1*) (19), and in embryonic and denervated muscle (*hSkM2*) (31). Recent observations indicate that *SCN5A* is also expressed in the brain (32,33). The expression is localized to the limbic system and certain autonomic structures (32,33), which might implicate the cardiac Na^+ channel in sudden unexplained death in epilepsy (34).

At least two α -subunit mRNA transcripts, Nav 1.1 and Nav 1.5, have been identified in rat (19) and rabbit heart (35). Nav 1.5 cardiac Na^+ channels are localized at the cell surface and T-tubular membranes of cardiomyocytes, but also at terminal intercalated disk membranes (36). In addition, Nav 1.1 antibody labeling was observed along Z lines in longitudinal sections (37). Whether the subcellular localization of Na^+ channels may play a role in anisotropic or saltatory conduction, or as a localized voltage-dependent current amplifier, remains to be established (36).

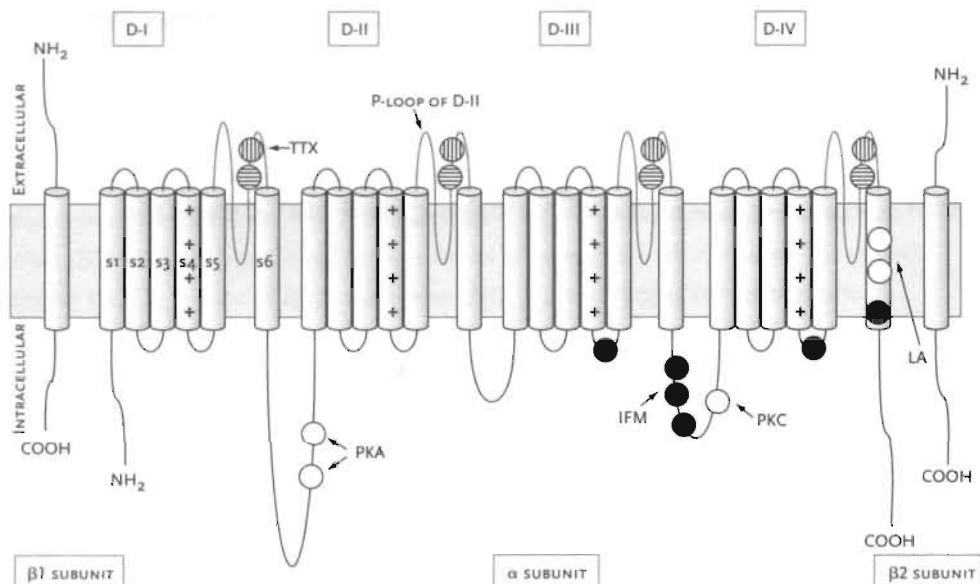


FIGURE 2.1

Structure of the cardiac Na⁺ channel α and β subunits. The α subunit consists of four homologous domains, D-I to D-IV. Each domain consists of six transmembrane segments, named S1-S6 (indicated in D-I). The voltage-sensors (S4 segments) important for voltage-dependent activation are indicated with '+++'. P-loops (S5-S6) are colored grey (the P-loop of D-II is indicated with an arrow). The circles in the P-loops correspond with residues forming the two rings contributing to the outer pore and selectivity filter, which are also important for tetrodotoxin (TTX) binding to the Na⁺ channel. Residues important for inactivation, such as the IFM-motif in the III-IV linker, and the docking sites for the fast-inactivation particle, are represented with black circles. The local anesthetic (LA) binding site in DIV-S4 is indicated with two white circles. The PKA (Ser 525, Ser 528) and PKC (Ser 1503)-binding sites are also shown. The cardiac Na⁺ channel β1 and β2 subunits consist of a single membrane-spanning segment, with a short intracellular C-terminus and a larger extracellular N-terminus.

Physical Model

Few studies are available on the actual three-dimensional structure of Na⁺ channels. Sato et al. (25) were the first to perform electron microscopy studies on the Na⁺ channel isolated from *Electrophorus electricus* electroplax (electrical eel). A higher resolution was obtained using helium-cooled cryo-electron microscopy and single-particle image analysis of solubilized Na⁺ channels (38). The channel has a bell-shaped outer surface of 13.5 nm in height and 10.0 nm in side length at the square-shaped bottom, and a spherical top with a diameter of 6.5 nm (FIGURE 2.2). Several inner cavities are connected to four small holes and eight orifices close to the extracellular and cytoplasmic membrane surfaces.

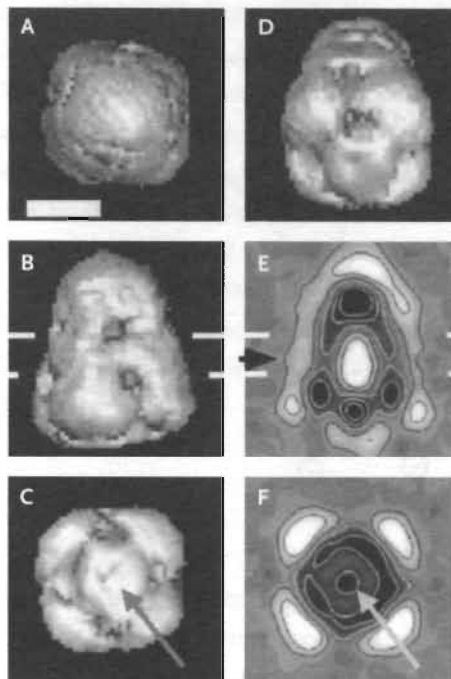


FIGURE 2.2

Surface representation of the Na⁺ channel protein (A-D). (A) Top view, (B) Side view, (C) Bottom view, (D) View at an oblique angle. Axial section (E) and perpendicular section (F) marked by the black arrow in E. The white arrows in C and F indicate the central pore of the Na⁺ channel. White bars (in B and E) delineate the lipid bilayer. Scale bar, 5.0 nm. Adapted from (38).

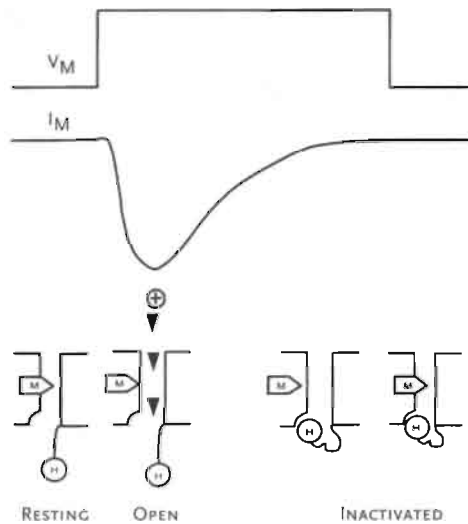
Na⁺ Channel Permeation

The first functional view of the Na⁺ channel was formulated by Hodgkin and Huxley (7) on the basis of voltage-clamp experiments, and provided a rationale for excitability based on the elementary properties of cation *permeation* (flux through the pore) and *gating* (dynamic conformational changes in response to membrane potential fluctuations). Although their physical model to explain transient membrane current was revolutionary at the time it was published (FIGURE 2.3), current theory involves a much more complicated scheme of conformational states underlying sodium channel function (39).

The Na⁺ channel pore is the region of the molecule that is specialized to recognize Na⁺ ions and to catalyze their transfer across the membrane. The central ion-conduction pore of the Na⁺ channel is lined by the S5-S6 linkers (P-loops) from each of the four domains of the channel. These loops, which are highly conserved among various

FIGURE 2.3

The Hodgkin-Huxley model of Na^+ channel gating. The upper trace shows a voltage step and the middle trace, the resulting membrane current. The lower panel shows a physical model to account for the transient current. In the resting state, the activation gate (m) is in the closed position and the inactivation gate (h) is in the open position. After depolarization, the m gate assumes the open position, sodium ions move into the cell. The h gate then moves into the closed position blocking ion movement. When the membrane is returned to the resting level, the m gate moves into the closed position (deactivation). After a variable interval, the h gate moves into the open position (recovery from inactivation) (courtesy of Dr A. Grànt (45)).



species, determine selectivity and conductance properties of the channel (40). Each of these four P-loop domains has a unique primary structure and a different positioning relative to the permeation pathway (41-43). Cysteine scanning accessibility mutagenesis experiments suggest that the domain II pore loop is most superficial, domains I and III intermediate, and domain IV distinctly deeper, judged by the voltage-dependence of Cd^{2+} block of the mutated Na^+ channels (41). Motions in the Na^+ channel pore were demonstrated by introducing pairs of cysteine residues throughout the pore-lining segment (44). Domains I and II were found to be closely apposed, because of their ability to form disulfide bonds, which implies protein dynamics that allow at least occasional proximity.

Outer Pore and Selectivity Filter

The segments that line the pore and define the ion selectivity and conductance of the Na^+ channel have been identified. The extracellular mouth of the pore plays an important role in TTX and saxitoxin (STX) binding to the Na^+ channel (8). These toxins are small rigid molecules of known crystal structure and have been proven crucial in defining the ion conduction pathway of sodium channels (45). Noda et al. (46) and Terlau et al. (47) identified residues in the ascending limb of the P-loop (the most important one being Glu 387 in brain type II sodium channel) using site-directed mutagenesis that impair affinity for TTX. These residues are likely to surround the extracellular opening of the pore and contribute to a receptor site for TTX.

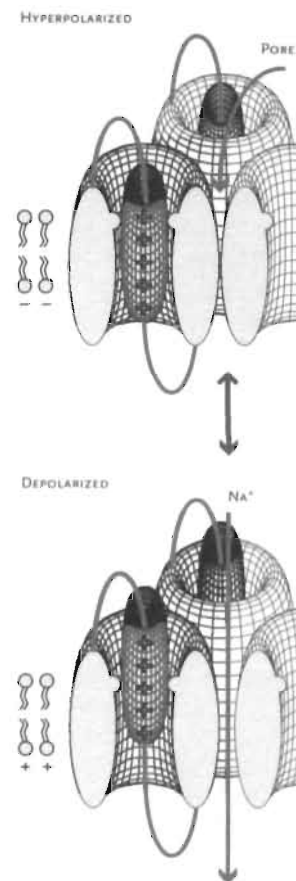
In addition, a second ring of four amino acids located three residues on the amino terminal site of these is also required for TTX binding (48). The cardiac isoform of the Na^+ channel is relatively resistant to TTX (IC_{50} in μM range) when compared to the brain and skeletal muscle isoforms (IC_{50} in nM range). A cysteine at position 373 in the cardiac isoform (in the P-loop of domain I) is responsible for this phenomenon (49) (FIGURE 2.1). The same amino-acid difference is also responsible for the susceptibility of the heart isoform to Cd^{2+} block, compared to the relatively insensitive neuronal and skeletal muscle isoforms (50). In addition, mutation of only one amino-acid in the P-loop of domain III (K1419 in *SCN5A*) is sufficient to confer Ca^{2+} -channel-like properties to the Na^+ channel (40). Mutations of the tetrad WDGL (amino-acids 1713-1716 in *SCN5A*) in the D-IV P-loop affect selectivity among monovalent cations (41).

Na⁺ Channel Gating

Voltage-dependent Activation

Activation of the voltage-gated Na^+ channel is thought to result from a voltage-driven conformational change that opens a transmembrane pore through the protein. The voltage-dependence of activation of the Na^+ channel derives from the OUTWARD MOVEMENT OF GATING CHARGES in response to changes in the electrical field (7,51). Recent studies indicate that approximately 12 electronic charges in the Na^+ channel protein move across the membrane electric field during activation (52). Because sequence analysis of the Na^+ channel α -subunit revealed that the fourth transmembrane segment (S4) in each of the four domains contained repeated motifs of a positively charged residue followed by two hydrophobic residues, it was postulated that the S4 segment might serve as the key voltage-sensor that underlies channel activation (53,54), which was subsequently confirmed by mutagenesis studies (55-57). Changes in transmembrane potential exert a force on these gating charges, and initiate conformational changes in each domain of the channel protein that lead to activation.

In the process of activation, several charged residues in each S4 segment actually transverse the membrane through a narrow tunnel formed by other, not yet identified regions of the channel (58,59). The sliding helix (60) or helical screw (61) models of gating propose that these positively charged amino residues are stabilized in the transmembrane



Membrane depolarization causes outward movement of the positively-charged S4 segments, which leads to channel activation.

environment by forming ion pairs with negatively charged residues in adjacent transmembrane segments. Depolarization of the membrane was proposed to release the S4 segments to move outward along a spiral path, initiating a conformational change that opens the pore. Although this model was quite speculative when it was proposed, its major features have now received direct experimental support from work on both sodium and potassium channels (58,59,62).

Fast Inactivation

Voltage-dependent inactivation of Na⁺ channels is a consequence of the voltage-dependent activation (51,63). Inactivation is characterized by at least two distinguishable kinetic components, an initial rapid component (fast inactivation) and a slower component (slow inactivation). Using site-directed mutagenesis (55,64) and peptide-specific antibodies (65), the cytoplasmic linker between domains III and IV of the Na⁺ channel α -subunit has been identified as a key structural component that contributes to fast inactivation. This cytoplasmic linker serves as the inactivation gate that occludes the Na⁺ channel pore from the cytoplasmic side of the membrane during maintained depolarization (so-called 'ball-and-chain' model) (51). The residues that form a hydrophobic triplet (IFM) in the III-IV linker are involved in inactivation gating (64). The IFM motif has been suggested to function as a 'latch' that holds the inactivation gate shut. A cysteine scanning study of the residues I1485, F1486, and M1487 in the human cardiac Na⁺ channel revealed that these amino-acids contribute to stabilizing the fast-inactivation particle in analogy to the brain Na⁺ channel (66-68). However, peptide-binding studies suggest that inactivation may not involve simple occlusive block of the inner mouth of the pore (69). Glycine and proline residues that flank the IFM motif may serve as molecular hinges to allow closure of the inactivation gate like a hinged lid ('hinged-lid model') (64,70).

Mutagenesis studies have identified a number of additional residues that reside in cytoplasmic loci consistent with 'docking sites' for the inactivation gate. Residues on S6 segment of domain IV form part of the intracellular mouth of the pore, and are thought to form part of the hydrophobic receptor site for the inactivation gate (71) or may stabilize the inactivated state through an indirect mechanism (72). Residues in cytoplasmic loops proximal to the III-IV linker including the domain III (73) and domain IV S4-5 loops also may form part of the 'docking site' (69,74-76) (FIGURE 2.1).

Slow Inactivation

In most published SCHEMES OF THE CARDIAC Na⁺ CHANNEL, slow inactivation follows fast

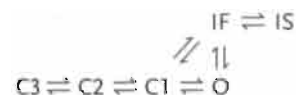
inactivation (39). Structural determinants of slow inactivation are less well known. The slow inactivation mechanism is unaffected when fast inactivation is prevented by protease treatment (78) or when movement of the inactivation gate is blocked by specific antibodies (65), and therefore likely to be an independent gating process. It has been shown that transposition of all four cardiac isoform P-loops into the human skeletal muscle isoform (*hSkM1*) backbone conferred heart isoform-like slow inactivation properties on the chimeric construct, suggesting a role for the P-loops in slow inactivation (79,80). Changes in flexibility of the P-loops may affect slow inactivation (81). Recently, a single residue in the D-II P-loop of the cardiac Na⁺ channel (I891) has been shown to regulate the steady-state ability of slow inactivation (82). It is suggested that slow inactivation in Na⁺ channels involves conformational changes in the outer pore in a fashion analogous to C-type inactivation in K⁺ channels (83-85). On the other hand, it has been suggested that other voltage-dependent structures play a role in slow inactivation. A region near the midpoint of the S₄ segment of D-IV has been shown to play an important role in slow inactivation (86,87), and suggests a role of S₄ segments in slow inactivation.

Coupling of Activation to Inactivation

In neuronal tissue, sodium channel inactivation derives most of its voltage-dependence from coupling to the activation process driven by transmembrane movements of the S₄ voltage sensors (51,197). In heart tissue, however, the thesis has always been defended that the coupling between activation and inactivation is relatively weak. While channels can inactivate from a closed state, inactivation is facilitated by previous opening of the channel (39). There is accumulating evidence that outward movement of the S₄ segment in domains III and IV is the signal to initiate fast inactivation of the sodium channel by closure of the intracellular inactivation gate (68,88-90). An alternative mechanism based on physical interaction between regions on the S₄-S₅ linker of DIV and the DIII-DIV inactivation particle has also been proposed (75,76). Such an association could be sensitive to changes in the conformation of S₄-S₅ of DIV, which are the result of movement of the voltage sensor of that domain during activation. This could lead to a change in the position of the inactivation gate relative to its docking sites.

Inner Pore and Local Anesthetic Binding Site

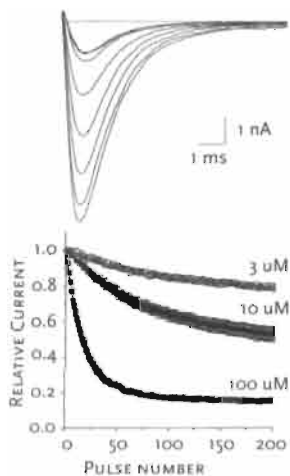
Class I antiarrhythmic drugs such as lidocaine, quinidine, and flecainide (91,92) act by inhibiting ionic currents through Na⁺ channels. Tertiary amine local anesthetics, such as procaine and etidocaine, which are chemically related to lidocaine, act in a similar manner.



Markov model of the sodium channel (39). C=closed state; O=open state; IF=fast-inactivated state; IS=slow-inactivated state. Inactivation can also occur from the closed state in the absence of channel opening (so-called closed-state inactivation C1→IF).

The efficacy of these drugs stems from their ability to selectively inhibit Na^+ channels during abnormal membrane depolarizations and rapid bursts of action potentials that characterize cardiac and neuronal pathologies (93).

It is thought that the selectivity of local anesthetics (LA) and antiarrhythmic drugs for depolarized Na^+ channels results from the preferential binding of these drugs to open and/or inactivate channel states that predominate at depolarized membrane potentials, rather than the resting channel states that predominate at more hyperpolarized membrane potentials. The state-dependent drug action can be explained by an allosteric model in which a modulated drug receptor is in a low affinity conformation when the channel is resting, and converts to a high affinity conformation when the channel is open and/or inactivated (93,94). This concept is often being referred to as the 'modulated receptor model' (93,94), and attributes the complex time- and voltage-dependent effects of LA and antiarrhythmics to distinct binding affinities for the three putative gated conformational states of the Na^+ channel (closed - opened - inactivated) (7). Mild suppression of Na^+ current during, isolated, brief depolarizations is attributed to low affinity binding for the closed channel conformation (tonic block), while far greater current suppression during repetitive depolarization, also known as USE-DEPENDENCE (95), is attributed to binding to states occupied during depolarization (either open or inactivated). Importantly, this model implies not only distinct high and low affinity drug-receptor sites, but also a complex interrelationship between channel gating and drug action. Lipid-soluble drug forms are thought to reach the receptor via a hydrophobic region of the membrane, while charged and less lipid-soluble forms pass via a hydrophilic region (inner channel mouth). The hydrophilic pathway is open only when the sodium channel opens.



Development of use-dependent lidocaine-block upon repetitive depolarizations; note the gradual decrease in Na^+ channel amplitude (top). Time course of UDB in the presence of 3, 10, and 100 μM lidocaine (bottom).

Hille (94) has proposed that the binding site for both neutral and charged drugs that are used as local anesthetics and antiarrhythmic agents lies between the channel gates and the selectivity filter. Starmer et al. (96) have attempted to simplify and formalize some of these concepts mathematically. Thus, in their 'guarded receptor model', the binding site is guarded by the channel gates; a drug can bind to its receptor (and inhibit current) only after the gate is open and the receptor is unguarded.

Local anesthetics and related anti-arrhythmic drugs are thought to bind to a receptor site on the Na^+ channel that is accessible only from the intracellular side of the membrane, and is more accessible when the Na^+ channel is open (8,97). Mutagenesis experiments of Na^+ channels revealed that the local anesthetic receptor is confined to the DIVS6 segment (98,99). High-affinity binding of local anesthetics to the inactivated state of the Na^+ channel requires two critical amino acid residues, Phe-1764 and Tyr-1771,

located in the DIVS6 transmembrane segment in the brain IIA channel (corresponding to F1760 and Y1767 in *SCN5A*) (99). The current concept is that the tertiary amino group of local anesthetics interact with Phe-1764, which is located deeply in the pore, and that the aromatic moiety of the local anesthetics interact with Tyr-1771, which is located nearer to the intracellular side of the pore (99) (see FIGURE 2.4). It is noteworthy that at least one of the residues implicated in LA block (F1764) importantly affects inactivation gating (71,72). While it is likely that DIVS6 forms part of the local anesthetic receptor, the fact that mutations in this location also influence inactivation gating makes it difficult to exclude the possibility that some of the mutational effects on drug action are indirect. In support of this observation, recent studies have shown that mutations in the outer pore, C-terminal to the selectivity filter and putative LA binding site, alter inactivation and LA block (100,101).

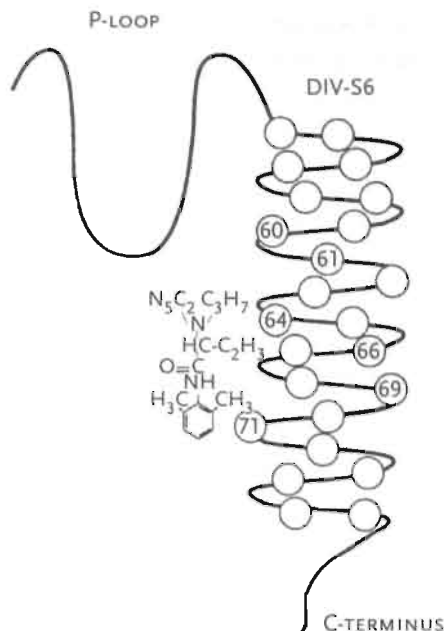


FIGURE 2.4
Proposed orientation of amino acids in the sixth transmembrane segment of DIV of the Na⁺ channel with respect to bound local anesthetic molecule in the conduction pore. The DIV pore loop, which probably also contributes to the receptor site, is shown as well. Amino acid positions 1760, 1764, and 1771 are shown facing the pore lumen. From: (102).

Modulation by Auxiliary β -subunits

Auxiliary β -subunits do not form the ion-conducting pore but rather modulate channel Na⁺ gating and cell surface expression levels, and interact with extracellular matrix and cell adhesion molecules (103). Although no mutations in β -subunits have been linked to one of the inherited arrhythmogenic syndromes, a mutation in the β_1 gene (*SCN1B*) (104,105) has been implicated to play a role in febrile seizures and generalized epilepsy (34).

Brain sodium channels are composed of a single pore-forming α -subunit, non-covalently bound to a β_1 -subunit, and linked to the β_2 -subunit by a disulfide bond, in a 1:1:1 stoichiometry (20,22,62,106). Expression of the Na⁺ channel α -subunit alone resulted

in functional sodium channels (65). Co-expression studies of brain Na⁺ channel α -subunits with the β 1-subunit have demonstrated larger peak I_{Na} amplitude, acceleration of activation and inactivation, and a more negative voltage-dependence of steady-state inactivation than the α -subunit expressed alone (21,104,107-110).

The subunit structure of cardiac sodium channels has been controversial for a long time. Recently, however, Malhotra et al. (37) determined that cardiac Na⁺ channels in rat and mouse cardiac myocytes are composed of α -, β 1- and β 2-subunits. In addition, a β 3-subunit has been identified in human and rat heart (111), and a splice-variant of the β 1-subunit (β 1A) has been identified in rat heart (112). Their functional roles in modulating cardiac sodium channels, however, remain to be determined.

Nav 1.5 Na⁺ channel and β 1 co-expression has been studied in heterologous expression systems with variable and conflicting results (104,108,110,113-115). When expressed in *Xenopus* oocytes, Nav 1.5 channels alone show gating and blocking properties comparable to native Na⁺ channels (49). While studies consistently show that β 1-subunit coexpression in *Xenopus* oocytes enhances the current magnitude, studies differ in regard to whether gating effects are present (110) or absent (116). Some groups have reported that β 1 has no observable effects on Nav 1.5 functional expression (104,108), while other reported modulation of channel sensitivity to lidocaine block and subtle changes in channel kinetics and gating properties in response to β 1 expression (37,114,115). The recent study by Malhotra et al. (37) showed that in HEK cells, co-expression with β 1 shifts the voltage-dependence of inactivation, whereas β 2 does not. The voltage-dependence of activation is not modified by β -subunit coexpression (37). A possible explanation for the inconsistent results reported in previous studies is that some HEK cell lines express endogenously the β 1 α -subunit, which could confound the electrophysiological measurements (117). Finally, rat Nav 1.1 α -subunits are also modulated by β 1- and β 2-subunits when expressed in oocytes (118).

Structural correlates for the noncovalent α - β 1 subunit interaction are thought to reside on the extracellular and intramembraneous domains of the β 1-subunit (119-121) and domain I and IV P-loops within the α -subunit (80,120,122). McCormick (121) showed that the immunoglobulin (Ig)-fold of the β 1 extracellular domain serves as a scaffold that presents charged residues or interaction with the α -subunit. In addition, the cytoplasmic C-terminal domain of the α -subunit has been implicated to play a yet unknown role in the interaction with the β 1-subunit (115,120).

Cardiac β -subunits, which are type I topology membrane proteins (123), are characterized by one large extracellular domain at the aminoterminal, a single

transmembrane region, and a shorter intracellular C-terminal domain (124). A surprising finding from determination of the primary structures of the β_1 and β_2 -subunits (21,22) was their close relationship to the large family of cell adhesion molecules of the immunoglobulin superfamily (125). No other auxiliary subunits of ion channels have related structures (62). Both β -subunits interact with extracellular matrix molecules and participate in homophilic cell adhesion, resulting in cellular aggregation and recruitment of ankyrin to the plasma membrane at point of cell-cell contact (103). The presence of β -subunits in cardiac myocytes may facilitate sodium channel localization and clustering to discrete functional domains via cell-adhesive interactions. Interestingly, the putative cytoplasmic region of both β_1 and β_3 contains a sequence YLAI 16 amino acids from the end of the predicted transmembrane sequence. The position and sequence of this motif fits the consensus for an internalization signal recognized by clathrin-coated pits, suggesting a possible role for β -subunits in the movement of sodium channels between cellular compartments (111).

Ankyrins are a family of spectrin-binding proteins associated with the cytoplasmic surface of the plasma membrane in many cell types. Ankyrins associate via their membrane binding domains with several ion channels (126). Sodium channels in ankyrin β -knockout mice display a reduced current density and abnormal Na^+ channel kinetics that lead to action potential prolongation and abnormal QT-rate adaptation (17), suggesting that a proper functional localization of Na^+ channels is essential. In line with these results, Undrovinas et al. (127) have demonstrated that breakup of the actin-based cardiomyocyte cytoskeleton with cytochalasin D produced late Na^+ current at hyperpolarizing test potentials, and suggested a role for the cytoskeleton in regulating Na^+ channel gating.

Transcriptional and Posttranslational Modification of Na^+ Channel Expression

Transcriptional Control of Na^+ Channel Gene Expression

Control of excitability can occur at the genomic level by transcriptional regulation of ion channel genes. The expression of Na^+ channels is developmentally regulated (13) and tissue restricted. Patterns of certain electrical activity can also influence transcriptional activity, e.g. seizures alter Na^+ gene expression in the brain (128). Denervation induces the

expression of the cardiac isoform of the Na⁺ channel in skeletal muscle, while transiently suppressing the expression of the mature skeletal muscle isoform (31). Chronic exposure to antiarrhythmic drugs which block Na⁺ channels can increase the steady-state levels of Na⁺ mRNA, which would counteract the effects of channel blockade (129). In addition, chronic treatment with n-3 polyunsaturated fatty acids, which are known to prevent fatal ventricular arrhythmias (130), reduced mexiletine-induced increase in cardiac Na⁺ channel expression in cultured neonatal cardiac myocytes (131). Finally, an increased expression of neuronal subtype Na⁺ channels was identified in post myocardial infarction remodeled myocardium, with a reversion toward the fetal phenotype (132).

Post-translational Modification of Na⁺ Channel Expression

All Na⁺ channel subunits are modified by glycosylation. The β_1 , β_2 , and brain and muscle α -subunits are heavily glycosylated (25-40%) (133,134), whereas the cardiac α -subunit is composed by 5% carbohydrates (135). Sialic acid is a prominent component of the N-linked carbohydrate of the Na⁺ channel. Neurominidase treatment to remove sialic acid from expressed skeletal muscle channels produces a depolarizing shift of steady-state inactivation (136). Local surface charge is also importantly influenced by charged amino acid residues that stud the outer mouth of the pore, although the predominant effects in this case are on permeation rather than gating (41,47). Recently, it has been shown that incomplete glycosylation during post-translational processing may contribute to Na⁺ channel-dependent arrhythmogenesis in mice with heart failure (137).

Regulation of the Na⁺ Channel

There is evidence that the cardiac Na⁺ channel may be the target of modulation by cAMP-dependent protein kinase A (PKA) and protein kinase C (PKC), although the experimental evidence for modulation of this channel is not as well established as it is for other ion channels. Cyclic nucleotide-dependent phosphorylation sites have been mostly studied in the α -subunit of the voltage-gated brain sodium channel type IIA (138-140). Within the intracellular linker region between D1S6 and D2S1 (ID 1-2) of the α -subunit of the rat brain IIA sodium channel five sites matching PKA consensus sequences are found (141), four of which have been shown biochemically to be involved in PKA phosphorylation of the

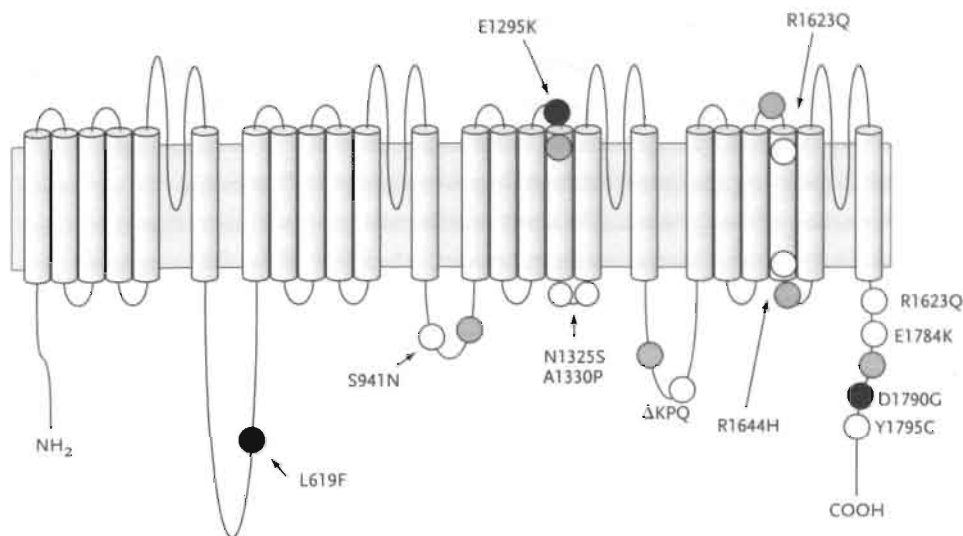


FIGURE 2-5
Structure of the cardiac Na⁺ channel α-subunit. Indicated with the circles are long-QT syndrome mutations with the respective amino-acid substitutions or deletions. The white circles represent mutations that have been characterized electrophysiologically, grey circles have not been characterized yet, and black circles represent mutations characterized in this thesis.

channel (119,140). Phosphorylation at the second PKA site (Ser 537) is necessary and sufficient to diminish amplitude in brain Na⁺ channels (141).

The cardiac sodium channel has eight candidate consensus PKA phosphorylation sites of the form KRXXS*, RXXS*, or RXS* in the I-II linker, all of which are distinct from the neuronal channel. *In vitro* studies of expressed rat cardiac Na⁺ channels demonstrated cAMP-dependent phosphorylation of only two of these serines (Ser 526 and Ser 529, corresponding with Ser 525 and Ser 528 in the human isoform) (142). Phosphorylation by PKA at these sites augments the Na⁺ current (142-144), by increasing the number of Na⁺ channels in the plasma membrane (145,146). Modulation of cardiac Na⁺ channel gating has also been demonstrated, including changes in the voltage-dependence of channel activation and inactivation (146-149).

The effects of upstream receptor-activated stimulation are less clear, with both increases and decreases in current being reported after treatment with cAMP-elevating agents or membrane-permeant cAMP analogs (148). In addition to the indirect pathway mediated by G-proteins acting through second messenger cascades, a direct membrane-delimited G-protein regulatory pathway involving direct interaction of the stimulatory G-protein α-subunit with the cardiac Na⁺ channel has been proposed (144,145,147,148,150). Protein kinase C (PKC) also modulates cardiac Na⁺ channels, both reducing the maximal conductance of the channel and altering gating. Both effects are largely attributable to

phosphorylation of a serine residue in the III-IV linker that is conserved in the neuronal and cardiac isoform (151). Interestingly, while PKC phosphorylation of this residue reduces Na^+ current in both isoforms, the gating defects diverge. Phosphorylation of Serine 1503 in the cardiac isoform induces a negative shift in the voltage-dependence of steady-state inactivation (implying stabilized inactivation), while in brain Na^+ channels, phosphorylation of the same residues slows and destabilizes inactivation (64,151). Because the III/IV linker sequences are conserved, interaction of the phosphorylated serine with other domains may differ for the two isoforms.

Slip-mode Conductance of the Cardiac Na^+ Channel

Nav 1.5 Na^+ channels can become permeable to Ca^{2+} after activation of protein kinase A (152). This slip-mode conductance of the Na^+ channel only occurs in transfected cells in the presence of both β_1 and β_2 -subunits (153). The Ca^{2+} flux through this pathway can increase subcellular Ca^{2+} and thereby activate sarcoplasmic reticulum (SR) Ca^{2+} release, Ca^{2+} sparks, and the Ca^{2+} transient. This is an intriguing finding, as consensus PKA sites are remote from the pore and selectivity filter. Yet sympathetic stimulation results in a dramatic change in the calcium selectivity of the sodium channel. The mechanism involved in this potentially physiologically important phenomenon remains to be further established.

Long-QT Syndrome Na^+ Channel Mutations

Mutations in the cardiac Na^+ channel α -subunit gene *SCN5A* were linked to LQTS by a candidate gene approach and positional cloning (3). First, the LQT-3 locus was mapped to chromosome 3p21-24 (154). Subsequently, the *SCN5A* gene was mapped to chromosome 3p21 (28), and mutations in *SCN5A* were linked to type 3 LQTS (3).

Seventeen distinct mutations associated with LQT-3 (see FIGURE 2.5) have been reported to date. The first mutation discovered was a 3-amino acids deletion (residues 1505-1507) in the cytoplasmic linker region between DIII and DIV of the Na^+ channel α -subunit (ΔKPQ mutation). Other mutations involve amino acid substitutions ($n=15$) and a deletion ($n=1$) (TABLE 2.1). In this thesis, the biophysical properties of D1790G, and the novel E1295K and L619F mutant LQT-3 Na^+ channels will be described (FIGURE 2.5; and CHAPTERS 3, 5, and 6).

ΔKPQ Mutation (Deletion K1505, P1506, Q1507): Defect in the Inactivation Lid

The first functional phenotype reported, and hence the 'prototypical LQT-3 phenotype' is caused by the ΔKPQ mutation (28,64). Using two-electrode voltage-clamp recordings from *Xenopus laevis* oocytes, a TTX-sensitive persistent Na⁺ current of less than 5% of the peak inward current was identified during prolonged repolarizations (28). In addition, time constants for current decay were decreased in the ΔKPQ mutant, and there was a -6 mV shift of the potential at which half of the current is inactivated (28). At the single channel level, brief dispersed reopenings and infrequent long-lasting bursts of openings were responsible for the macroscopic non-inactivating Na⁺ current (28,165,166). ΔKPQ mutant Na⁺ channels were also studied in human embryonic kidney (HEK) cells using whole-cell patch-clamp analysis (158,166,167). The presence of a non-inactivating Na⁺ current during prolonged depolarizations was confirmed. In HEK cells, current inactivation was speeded, recovery from inactivation faster, and the voltage-dependence of inactivation shifted towards more negative potentials (158,166).

Nucleotide change	Aminoacid substitution	Channel domain	Exon	No of RW families	Reference
AA2971TC	S941N	DII/DIII	16	1	(155)
G3340A	D1114N	DII/DIII	18	1	(156)
C3911T	T1304M	DIII/S4	22	1	(157)
A3974G	N1325S	DIII/S4-5	23	1	(158)
G4138A	A1330P	DIII/S4-5	23	1	(159)
C4501G	L1501V	DIII/DIV	26	1	(156)
del4511-4519	del1505-1507	DIII/DIV	26	4	(3)
del4850-4852	delF1617	DIV/S3-4	28	1	(156)
G4868A	R1623Q	DIV/S4	28	2	(156,160)
G4868T	R1623L	DIV/S4	28	1	(156)
G4931A	R1644H	DIV/S4	28	2	(156,158)
G4934T	T1645M	DIV/S4	28	1	(157)
G5329A	V1777M	C-terminus	28	1	(161)
G5349A	E1784K	C-terminus	28	2	(156,162)
G5360A	S1787N	C-terminus	28	1	(156)
A5359G	D1790G	C-terminus	28	1	(163)
A5384G	Y1795C	C-terminus	28	1	(164)

TABLE 2.1
Summary of all published
SCN5A mutations.

N1325S and R1644H Mutation: Defect in Inactivation Lid Docking Site

The N1325S mutation occurs in the S4-S5 region of domain III, R1644H near the cytoplasmic end of the S4 segment of domain IV. Both regions are highly conserved between the cardiac, skeletal muscle, and brain IIa isoforms suggesting their importance (26,53,168). Both the N1325S and R1644H mutations lead to persistent, non-inactivating Na^+ current (158,165). The N1325S mutation also causes a negative shift in the voltage-dependence of inactivation and slower recovery from inactivation (158,165). Interestingly, mutation T1645M (directly adjacent to residue R1644) in the first cytoplasmic residue of the S4-S5 linker in domain IV has also been associated with LQT-3 (157).

S941N Mutation: Sudden Infant Death Syndrome

The sporadic *SCN5A* mutation S941N was identified in a 44-day old infant with congenital LQTS, resuscitated from ventricular fibrillation. The aspartate at amino-acid position 941 (Asp941) is located in the highly conserved intracellular loop between the second and third transmembrane domains of *SCN5A* (27). When expressed in *Xenopus* oocytes, this mutation was characterized by a late sodium current of 1.8-2.5% (155). The mechanism by which a substitution in this part of the channel protein leads to a persistent inward current is not yet understood.

R1623Q Mutation: Uncoupling of Activation-inactivation

The *de novo* missense mutation R1623Q was identified in a Japanese girl severely affected by a sporadic form of the long-QT syndrome (169). The positively charged R1623 is the outermost residue of the S4 segment of domain IV. When expressed heterologously in *Xenopus* oocytes, a small non-inactivating current was found at the end of the 100 ms depolarizations (< 3% of peak current) (170), comparable to previously described LQT-3 mutations. Striking difference between R1623Q and WT current was a slowed rate of macroscopic current decay, a unique feature not observed in other mutations reported in familial LQTS mutations (28,158,165).

During single channel recordings, the R1623Q exhibited multiple, prolonged openings early in the depolarization period, which give rise to the slow decay. The ability of open channels to inactivate is impaired (160,170). The underlying mechanism may involve uncoupling activation from inactivation (59,171). In addition, Kambouris et al. (172) reported that the voltage-dependence of availability of I_{Na} was shifted to more negative potentials when expressed in *Xenopus* oocytes, indicating that inactivation from closed states is increased. A slowing of open-state inactivation with co-existent enhancement of

closed-state inactivation for this *SCN5A* mutation is consistent with gating phenotypes reported for mutations in the domain IV-S4 segment of the human skeletal muscle Na⁺ channel (*hSkM1*) linked to paramyotonia congenita (171,173). The precise mechanism of impaired inactivation of the R1623Q mutation may be a functional defect in activation-inactivation coupling of the Na⁺ channel that has been previously reported in the paramyotonia congenita mutations R1448H/C (65).

Genetic analysis of LQTS families enrolled in the International Long-QT Registry has indicated that the C-terminus of the *SCN5A* gene is a hot-spot for LQT-3 mutations (156). Approximately 30% of all LQT-3 mutations have been identified in this part of the Na⁺ channel.

E1784K Mutation: C-terminal Mutation

The E1784K mutation occurs in a highly conserved acidic domain immediately following the D4/S6 segment, within the carboxy terminus of the cardiac Na⁺ channel (162). Electrophysiological analysis of E1784K channels in *Xenopus* oocytes (162) and HEK cells (174) revealed a 2-4% maintained Na⁺ current, a -12 mV negative shift in the V_{1/2} of steady-state inactivation, and a faster recovery from inactivation. These results suggest a destabilization of the inactivated state of the Na⁺ channel. Additional mutagenesis experiments in the early C-terminus domain suggest that the biophysical mechanism may be allosteric rather than caused by direct interference with channel-gating properties (162). The early part of the C-terminus (adjacent to DIV-S6) of the human cardiac Na⁺ channel has clusters of negatively charged amino acid residues (162). Little research has been performed as to the function of this highly conserved segment of the Na⁺ channel. The accentuation of the functional defect by the β_1 -subunit was observed in the E1784K and the nearby D1790G mutations. It is, however, difficult to reconcile these findings with the work of other groups demonstrating that the cytoplasmic domain of the β_1 -subunit might not be required for its functional effects on mammalian sodium channels (119-121).

D1790G Mutations: Impaired α - β_1 Subunit Interaction

The D1790G (negatively charged aspartic acid to a neutral glycine) mutation is also located in the C-terminal part of the channel (163). In contrast to most other LQT-3 mutations, it does not lead to a sustained Na⁺ current when studied in a heterologous expression system (115). Although a disturbed interaction between the α and β_1 -subunit of the cardiac Na⁺ channel were suggested to cause the D1790G phenotype, the exact mechanism by which this mutation may lead to an arrhythmogenic phenotype remained to be established.

ANDREI ANDREYEVICH MARKOV
 was a graduate of Saint
 Petersburg University (1878),
 where he began as a professor in
 1886. Markov's early work was
 mainly in number theory and
 analysis, continued fractions,
 limits of integrals, approximation
 theory and the convergence of
 series. Markov is particularly
 remembered for his study of
 Markov chains, sequences
 of random variables in which the
 future variable is determined by
 the present variable but is
 independent of the way in which
 the present state arose from its
 predecessors. This work launched
 the theory of stochastic processes.

In CHAPTER 3 of this thesis, novel insights in the electrophysiological consequences of this mutation will be described.

Interestingly, the mutation E1784K (negatively charged glutamic acid to positively charged lysine), located only 6 aminoacids away from D1790G, does lead to sustained inward current. In contrast, the mutation E1784D (a mutation conserving the negative charge) was indistinguishable from wild-type current with respect to sustained current (174). This implies that subtle changes in amino-acid charges in the early carboxyterminal domain may have profound effects on gating of the cardiac Na⁺ channel.

Arrhythmogenic Mechanism of the Non-inactivating Na⁺ Current

The fact that several LQTS Na⁺ channel mutations spanning nearly the entire α -subunit, modify fast inactivation suggests that Na⁺ channel inactivation depends upon complex ensembled interactions among many structural domains. Incomplete inactivation leading to persistent inward current has been shown to be a common consequence of most of the identified SCN5A mutations (28,158,160,162,165-167,170). This resultant non-inactivating component of Na⁺ channel current exceeds the physiological levels of Na⁺ current during the action potential plateau phase (18,175).

Using a single-channel based MARKOVIAN computational model, Clancy and Rudy (39) were able to demonstrate elegantly that sustained Na⁺ current during the plateau phase of the action potential may lead to arrhythmogenic consequences at the cellular level. Although the amplitude of the persistent current is very small, only 1% of the peak I_{Na}, it is sufficient to shift the delicate balance of currents that exists during the action potential plateau (176-179). The additional current carried by sodium acts in opposition to repolarizing outward currents and prolongs the APD (39).

Molecular Pharmacology of LQT-3 Na⁺ Channel Mutations

The precise identification of genetic defects that cause different forms of LQTS opened up the possibility of discovering new therapeutic approaches to the management of this disorder based on the molecular pharmacology of the mutant ion channels encoded by the specific gene defects (180). Because it is possible to investigate the functional properties of the mutant genes using heterologous expression systems, *in vitro* tests can be carried out

to identify unique drug-channel interactions that may occur as a consequence of the interrupted gene defect and that may be exploited to devise novel pharmacological approaches to disease management (CHAPTER 4).

Class IB antiarrhythmics, such as lidocaine and mexiletine, are drugs that block Na^+ channels in a voltage-dependent manner. As discussed previously, channel block depends on the state of the channel in a complex manner, being influenced by the relative number of resting, open, and/or inactivated channels (93,94,181). Because certain Na^+ channel mutations that underlie LQT-3 have been shown to modify inactivation (28), it is very likely that these mutant Na^+ channels will be modified in a unique manner by local anesthetic drugs.

There have been several reports indicating that such a specific interaction is indeed clinically relevant. Experiments carried out in transfected HEK cells (180) and *Xenopus* oocytes (182) revealed that maintained Na^+ current through non-inactivating mutant channels was more sensitive to local anesthetic block than peak inward current. This suggests that Na^+ channel current that underlies impulse conduction (peak current) will be less sensitive to class IB drugs than currents that underlie QT prolongation in carriers of LQT-3 gene mutations. This observation has been reinforced in preliminary clinical pharmacological studies (183,184). Schwartz et al. showed that the class IB agent mexiletine effectively shortens the QT-interval of patients identified as carriers of the *SCN5A* gene mutations ΔKPQ and R1644H (183). In addition, Rosero et al. (184) reported QT-interval shortening in two ΔKPQ carriers by short-term intravenous lidocaine and long-term oral tocainide therapy.

When more LQT-3 Na^+ channels were characterized electrophysiologically, it became clear that class IB Na^+ channel blockers might not constitute a universal approach to LQT-3. As predicted on the basis of the absence of maintained current in D1790G mutant Na^+ channels (115), lidocaine did not correct QT-interval prolongation in two patients with the D1790G mutation (185). However, the class IC antiarrhythmic agent flecainide did shorten QT-intervals and other repolarization parameters in D1790G mutation carriers significantly (185). The molecular basis of this observation is the subject of CHAPTER 4 in this thesis.

Other Arrhythmogenic Syndromes Caused by Na⁺ Channel Mutations

Na⁺ channel mutations can also cause the Brugada syndrome, a hereditary cardiac disease characterized by right bundle-branch block (RBBB), an elevation of the ST segment in leads V₁ through V₃ on the electrocardiogram, and ventricular fibrillation that can lead to sudden cardiac death (186). In patients with Brugada syndrome, missense mutations T1620M (4), R1512W (174), A1924T (187), splice-donor, and frameshift mutations have been identified in *SCN5A* (4). For further information on the electrophysiological phenotypes of these Na⁺ channel mutations, the reader is referred to the reviews by Bezzina et al. (2) and Vatta et al. (188).

Although LQTS and Brugada syndrome are known as distinct disorders, a recent study reported a mutation in the *SCN5A* gene that causes both syndromes (189). An in-frame insertion of three nucleotides in the carboxyterminal region resulting in an additional aspartate at position 1795 was found to be responsible for this 'overlap syndrome'. Subsequent reports described the biophysical phenotype of this Na⁺ channel mutation (190,191).

Progressive slowing of cardiac conduction is a common electrophysiological manifestation of the progressive fibrosis in the conduction system of elderly patients (192). Progressive cardiac conduction disease (PCCD) or Lev-Lenegre syndrome, was first recognized as such by Drs. Lev (193) and Lenegre (194), and is characterized by progressive impairment of cardiac conduction through the His-Purkinje system leading to right or left bundle branch block. This may deteriorate into complete atrioventricular block, causing syncope and sudden death. Surprisingly, Schott et al. (5) demonstrated that a single nucleotide deletion at position 5280 in *SCN5A* causes early-onset PCCD in a Dutch family. Deletion of G5280 is predicted to lead to a frame-shift resulting in a stop-codon. The resulting truncated channels might contribute to an overall reduced Na⁺ current density, which might explain slow conduction in these patients.

Tan et al. (6) reported a *SCN5A* mutation that causes a sustained sinoatrial and atrioventricular conduction defect with pathological slowing of the cardiac rhythm in the absence of other cardiac abnormalities. The missense mutation G514C was identified in the channel protein. The gating defects of this mutation are likely to cause slow myocardial conduction, but do not provoke rapid cardiac arrhythmias associated with LQTS and Brugada syndrome (6). A previous study reported linkage of an isolated cardiac conduction

disease to chromosome 19q13.3. It is interesting to note that the gene encoding the β_1 -subunit of the cardiac Na^+ channel maps to a locus on chromosome 19q13.1-2 (105).

Aim of This Thesis

The identification and study of *SCN5A* mutations related to the congenital long-QT syndrome may serve several purposes (TABLE 2.2). Common techniques to characterize functional defects related to mutations in the cardiac sodium channel included heterologous expression studies in *Xenopus laevis* oocytes (28) and human embryonic kidney (HEK) cells (115). More recently, transgenic mice have been used to study the functional consequences of sodium channel mutations on the cellular and whole organism level (195).

Although considerable progress has been made in terms of the biophysical characterization of long-QT syndrome-related Na^+ channel mutations, few of the mechanisms so far are really fully understood. For example, the D1790G mutation was the first Na^+ channel mutation identified, that did not lead to non-inactivating current upon prolonged depolarization (115). Although it was initially suggested that defective α - β_1 subunit interactions underlie the channel defect (115), it was not obvious from these data how this might prolong cellular action potentials. In CHAPTER 3, we extended these findings by incorporated whole-cell patch-clamp data of the D1790G mutation into the Luo-Rudy computer model of the ventricular action potential.

Motivations to Identify and Characterize *SCN5A* Mutations

1. Identification of patients with symptoms of the long-QT syndrome mutation
2. Screening of (asymptomatic) family members of long-QT syndrome patients
3. Study of structure-function relationship of the sodium channel
4. Study of molecular pharmacology

Methods to Characterize *SCN5A* Mutations

1. Heterologous expression studies in *Xenopus laevis* oocytes
2. Heterologous expression studies in HEK cells
3. Transgenic mice

TABLE 2.2

*The rationale and methods of studying *SCN5A* mutations.*

A recent clinical study by Benhorin et al. (185) showed that in carriers of the D1790G mutation, class IB sodium channel blockers were ineffective, whereas class IC blocker flecainide significantly shortened all heart rate-corrected repolarization parameters. In CHAPTER 4, we investigated the molecular pharmacological basis of this intriguing clinical observation. Other clinical studies support the idea that considerable heterogeneity exists in carriers of long-QT syndrome related ion channel mutations (183,196). In an attempt to assess whether this was also true for carriers of different Na⁺ channel mutations, we studied two novel SCN5A mutations, E1295K (CHAPTER 5) and L619F (CHAPTER 6).

Finally, after describing several novel mechanisms by which Na⁺ channel mutations may prolong ventricular action potentials, and thus the QT-interval on the electrocardiogram, we summarize current concepts regarding the LQT-3 phenotypes. We discuss these data in perspective of the structure-function relationship of the cardiac Na⁺ channel, and review the implications of our findings for the mutation-specific treatment of the long-QT syndrome type 3.

References

1. Balser JR. Structure and function of the cardiac sodium channels. *Cardiovasc Res* 1999;42:327-38.
2. Bezzina CR, Rook MB, Wilde AA. Cardiac sodium channel and inherited arrhythmia syndromes. *Cardiovasc Res* 2001;49:257-71.
3. Wang Q, Shen J, Splawski I, Atkinson D, Li Z, Robinson JL, Moss AJ, Towbin JA, Keating MT. *SCN5A* mutations associated with an inherited cardiac arrhythmia, long-QT syndrome. *Cell* 1995;80:805-17.
4. Chen Q, Kirsch GE, Zhang D, Brugada R, Brugada J, Brugada P, Potenza D, Moya A, Borggrefe M, Breithardt G, Ortiz-Lopez R, Wang Z, Antzelevitch C, O'Brien RE, Schulze-Bahr E, Keating MT, Towbin JA, Wang Q. Genetic basis and molecular mechanism for idiopathic ventricular fibrillation. *Nature* 1998;392:293-96.
5. Schott JJ, Alshinawi C, Kyndt F, Probst V, Hoorntje TM, Hulsbeek M, Wilde AA, Escande D, Mannens MM, Le Marec H. Cardiac conduction defects associate with mutations in *SCN5A*. *Nat Genet* 1999;23:20-21.
6. Tan HL, Bink-Boelkens MT, Bezzina CR, Viswanathan PC, Beaufort-Krol GC, van Tintelen PJ, Van den Berg MP, Wilde AA, Balser JR. A sodium-channel mutation causes isolated cardiac conduction disease. *Nature* 2001;409:1043-47.
7. Hodgkin AL, Huxley AF. A quantitative description of membrane current and its application to conduction and excitation in nerve. *J Physiol* 1952;117:500-44.
8. Hille B. Ionic channels of excitable membranes. (2nd ed). Sunderland, MA: Sinauer Associates, 1992.
9. Colatsky TJ. Voltage clamp measurements of sodium channel properties in rabbit cardiac Purkinje fibres. *J Physiol* 1980;305:215-34.
10. Ebihara L, Johnson EA. Fast sodium current in cardiac muscle. A quantitative description. *Biophys J* 1980;32:779-90.
11. Brown AM, Lee KS, Powell T. Sodium current in single rat heart muscle cells. *J Physiol* 1981;318:479-500.
12. Makielski JC, Sheets MF, Hanck DA, January CT, Fozzard HA. Sodium current in voltage clamped internally perfused canine cardiac Purkinje cells. *Biophys J* 1987;52:1-11.
13. Davies MP, An RH, Doevendans P, Kubalak S, Chien KR, Kass RS. Developmental changes in ionic channel activity in the embryonic murine heart. *Circ Res* 1996;78:15-25.
14. Kunze DL, Lacerda AE, Wilson DL, Brown AM. Cardiac Na⁺ currents and the inactivating, reopening, and waiting properties of single cardiac Na channels. *J Gen Physiol* 1985;86:691-719.
15. Grant AO, Starmer CF, Strauss HC. Unitary sodium channels in isolated cardiac myocytes of rabbit. *Circ Res* 1983;53:823-29.
16. Benndorf K. Properties of single cardiac Na⁺ channels at 35 degrees C. *J Gen Physiol* 1994;104:801-20.
17. Chauhan VS, Tuvia S, Buhusi M, Bennett V, Grant AO. Abnormal cardiac Na⁺ channel properties and QT heart rate adaptation in neonatal ankyrin(B) knockout mice. *Circ Res* 2000;86:441-47.
18. Attwell D, Cohen I, Eisner D, Ohba M, Ojeda C. The steady state TTX-sensitive ("window") sodium current in cardiac Purkinje fibres. *Pflugers Arch* 1979;379:137-42.
19. Rogart RB, Cribbs LL, Muglia LK, Kephart DD, Kaiser MW. Molecular cloning of a putative tetrodotoxin-resistant rat heart Na⁺ channel isoform. *Proc Natl Acad Sci U S A* 1989;86:8170-74.
20. Hartshorne RP, Messner DJ, Coppersmith JC, Catterall WA. The saxitoxin receptor of the sodium channel from rat brain. Evidence for two nonidentical beta subunits. *J Biol Chem* 1982;257:13888-91.

21. Isom LL, De Jongh KS, Patton DE, Reber BF, Offord J, Charbonneau H, Walsh K, Goldin AL, Catterall WA. Primary structure and functional expression of the β 1-subunit of the rat brain sodium channel. *Science* 1992;256:839-42.
22. Isom LL, Ragsdale DS, De Jongh KS, Westenbroek RE, Reber BF, Scheuer T, Catterall WA. Structure and function of the β 2-subunit of brain sodium channels, a transmembrane glycoprotein with a CAM motif. *Cell* 1995;83:433-42.
23. Catterall WA. Structure and function of voltage-gated ion channels. *Annu Rev Biochem* 1995;64:493-531.
24. Fozzard HA, Hanck DA. Structure and function of voltage-dependent sodium channels: comparison of brain II and cardiac isoforms. *Physiol Rev* 1996;76:887-926.
25. Sato C, Sato M, Iwasaki A, Doi T, Engel A. The sodium channel has four domains surrounding a central pore. *J Struct Biol* 1998;121:314-25.
26. Gellens ME, George AL Jr, Chen LQ, Chahine M, Horn R, Barchi RL, Kallen RG. Primary structure and functional expression of the human cardiac tetrodotoxin-insensitive voltage-dependent sodium channel. *Proc Natl Acad Sci U S A* 1992;89:554-58.
27. Wang Q, Li Z, Shen J, Keating MT. Genomic organization of the human *SCN5A* gene encoding the cardiac sodium channel. *Genomics* 1996;34:9-16.
28. Bennett PB, Yazawa K, Makita N, George AL Jr. Molecular mechanism for an inherited cardiac arrhythmia. *Nature* 1995;376:683-85.
29. Goldin AL. Diversity of mammalian voltage-gated sodium channels. *Ann N Y Acad Sci* 1999;868:38-50.
30. Goldin AL, Barchi RL, Caldwell JH, Hofmann F, Howe JR, Hunter JC, Kallen RG, Mandel G, Meisler MH, Netter YB, Noda M, Tamkun MM, Waxman SG, Wood JN, Catterall WA. Nomenclature of voltage-gated sodium channels. *Neuron* 2001;28:365-68.
31. Kallen RG, Sheng ZH, Yang J, Chen LQ, Rogart RB, Barchi RL. Primary structure and expression of a sodium channel characteristic of denervated and immature rat skeletal muscle. *Neuron* 1990;4:233-42.
32. Hartmann HA, Colom LV, Sutherland ML, Noebels JL. Selective localization of cardiac *SCN5A* sodium channels in limbic regions of rat brain. *Nat Neurosci* 1999;2:593-95.
33. Donahue LM, Coates PW, Lee VH, Ippensen DC, Arze SE, Poduslo SE. The cardiac sodium channel mRNA is expressed in the developing and adult rat and human brain. *Brain Res* 2000;887:335-43.
34. Wallace RH, Wang DW, Singh R, Scheffer IE, George AL Jr, Phillips HA, Saar K, Reis A, Johnson EW, Sutherland GR, Berkovic SF, Mulley JC. Febrile seizures and generalized epilepsy associated with a mutation in the Na^+ channel β 1-subunit gene *SCN1B*. *Nat Genet* 1998;19:366-70.
35. Baruscotti M, Westenbroek R, Catterall WA, DiFrancesco D, Robinson RB. The newborn rabbit sinoatrial node expresses a neuronal type I-like Na^+ channel. *J Physiol* 1997;498:641-48.
36. Cohen SA. Immunocytochemical localization of *rH1* sodium channel in adult rat heart atria and ventricle. Presence in terminal intercalated disks. *Circulation* 1996;94:3083-86.
37. Malhotra JD, Chen C, Rivolta I, Abriel H, Malhotra R, Mattei LN, Brosius FC, Kass RS, Isom LL. Characterization of sodium channel α and β -subunits in rat and mouse cardiac myocytes. *Circulation* 2001;103:1303-10.
38. Sato C, Ueno Y, Asai K, Takahashi K, Sato M, Engel A, Fujiyoshi Y. The voltage-sensitive sodium channel is a bell-shaped molecule with several cavities. *Nature* 2001;409:1047-51.
39. Clancy CE, Rudy Y. Linking a genetic defect to its cellular phenotype in a cardiac arrhythmia. *Nature* 1999;400:566-69.
40. Heinemann SH, Terlau H, Stuhmer W, Imoto K, Numa S. Calcium channel characteristics conferred on the sodium channel by single mutations. *Nature* 1992;356:441-43.
41. Chiamvimonvat N, Perez-Garcia MT, Ranjan R, Marban E, Tomaselli GF. Depth asymmetries of the

- pore-lining segments of the Na⁺ channel revealed by cysteine mutagenesis. *Neuron* 1996;16:1037-47.
42. Perez-Garcia MT, Chiamvimonvat N, Ranjan R, Balser JR, Tomaselli GF, Marban E. Mechanisms of sodium/calcium selectivity in sodium channels probed by cysteine mutagenesis and sulfhydryl modification. *Biophys J* 1997;72:989-96.
 43. Yamagishi T, Janacki M, Marban E, Tomaselli GF. Topology of the P segments in the sodium channel pore revealed by cysteine mutagenesis. *Biophys J* 1997;73:195-204.
 44. Benitah JP, Ranjan R, Yamagishi T, Janacki M, Tomaselli GF, Marban E. Molecular motions within the pore of voltage-dependent sodium channels. *Biophys J* 1997;73:603-13.
 45. Grant AO. Molecular biology of sodium channels and their role in cardiac arrhythmias. *Am J Med* 2001;110:296-305.
 46. Noda M, Suzuki H, Numa S, Stuhmer W. A single point mutation confers tetrodotoxin and saxitoxin insensitivity on the sodium channel II. *FEBS Lett* 1989;259:213-16.
 47. Terlau H, Heinemann SH, Stuhmer W, Pusch M, Conti F, Imoto K, Numa S. Mapping the site of block by tetrodotoxin and saxitoxin of sodium channel II. *FEBS Lett* 1991;293:93-96.
 48. Catterall WA. Structure and function of voltage-gated ion channels. *Trends Neurosci* 1993;16:500-06.
 49. Satin J, Kyle JW, Chen M, Rogart RB, Fozzard HA. The cloned cardiac Na⁺ channel α -subunit expressed in *Xenopus* oocytes show gating and blocking properties of native channels. *J Membr Biol* 1992;130:11-22.
 50. Backx PH, Yue DT, Lawrence JH, Marban E, Tomaselli GF. Molecular localization of an ion-binding site within the pore of mammalian sodium channels. *Science* 1992;257:248-51.
 51. Armstrong CM. Sodium channels and gating currents. *Physiol Rev* 1981;61:644-83.
 52. Hirschberg B, Rovner A, Lieberman M, Patlak J. Transfer of twelve charges is needed to open skeletal muscle Na⁺ channels. *J Gen Physiol* 1995;106:1053-68.
 53. Noda M, Ikeda T, Suzuki H, Takeshima H, Takahashi T, Kuno M, Numa S. Expression of functional sodium channels from cloned cDNA. *Nature* 1986;322:826-28.
 54. Catterall WA. Structure and function of voltage-sensitive ion channels. *Science* 1988;242:50-61.
 55. Stuhmer W, Conti F, Suzuki H, Wang XD, Noda M, Yahagi N, Kubo H, Numa S. Structural parts involved in activation and inactivation of the sodium channel. *Nature* 1989;339:597-603.
 56. Kontis KJ, Rounaghi A, Goldin AL. Sodium channel activation gating is affected by substitutions of voltage sensor positive charges in all four domains. *J Gen Physiol* 1997;110:391-401.
 57. Mitrovic N, George AL, Horn R. Independent versus coupled inactivation in sodium channels. Role of the domain 2 S4 segment. *J Gen Physiol* 1998;111:451-62.
 58. Yang N, Horn R. Evidence for voltage-dependent S4 movement in sodium channels. *Neuron* 1995;15:213-18.
 59. Yang N, George AL, Horn R. Molecular basis of charge movement in voltage-gated sodium channels. *Neuron* 1996;16:113-22.
 60. Catterall WA, Schmidt JW, Messner DJ, Feller DJ. Structure and biosynthesis of neuronal sodium channels. *Ann N Y Acad Sci* 1986;479:186-203.
 61. Guy HR, Seetharamulu P. Molecular model of the action potential sodium channel. *Proc Natl Acad Sci U S A* 1986;83:508-12.
 62. Dock W. Transitory ventricular fibrillation as a cause of syncope and its prevention by quinidine sulphate. *Am Heart J* 1929;4:709-14.
 63. Aldrich RW, Corey DP, Stevens CF. A reinterpretation of mammalian sodium channel gating based on single channel recording. *Nature* 1983;306:436-41.
 64. West JW, Patton DE, Scheuer T, Wang Y, Goldin AL, Catterall WA. A cluster of hydrophobic amino acid residues required for fast Na⁺ channel inactivation. *Proc Natl Acad Sci U S A* 1992;89:10910-14.

65. Vassilev P, Scheuer T, Catterall WA. Inhibition of inactivation of single sodium channels by a site-directed antibody. *Proc Natl Acad Sci U S A* 1989;86:8147-51.
66. Hartmann HA, Tiedeman AA, Chen SF, Brown AM, Kirsch GE. Effects of III-IV linker mutations on human heart Na⁺ channel inactivation gating. *Circ Res* 1994;75(1):114-22.
67. Deschenes I, Trottier E, Chahine M. Cysteine scanning analysis of the IFM cluster in the inactivation gate of a human heart sodium channel. *Cardiovasc Res* 1999;42:521-29.
68. Sheets MF, Kyle JW, Hanck DA. The role of the putative inactivation lid in sodium channel gating current immobilization. *J Gen Physiol* 2000;115:609-20.
69. Tang L, Kallen RG, Horn R. Role of an S4-S5 linker in sodium channel inactivation probed by mutagenesis and a peptide blocker. *J Gen Physiol* 1996;108:89-104.
70. Kellenberger S, Scheuer T, Catterall WA. Movement of the Na⁺ channel inactivation gate during inactivation. *J Biol Chem* 1996;271:30971-79.
71. McPhee JC, Ragsdale DS, Scheuer T, Catterall WA. A mutation in segment IVS6 disrupts fast inactivation of sodium channels. *Proc Natl Acad Sci U S A* 1994;91:12346-50.
72. McPhee JC, Ragsdale DS, Scheuer T, Catterall WA. A critical role for transmembrane segment IVS6 of the sodium channel α -subunit in fast inactivation. *J Biol Chem* 1995;270:12025-34.
73. Smith MR, Goldin AL. Interaction between the sodium channel inactivation linker and domain III S4-S5. *Biophys J* 1997;73:1885-95.
74. McPhee JC, Ragsdale DS, Scheuer T, Catterall WA. A critical role for the S4-S5 intracellular loop in domain IV of the sodium channel α -subunit in fast inactivation. *J Biol Chem* 1998;273:1121-29.
75. Lerche H, Peter W, Fleischhauer R, Pika-Hartlaub U, Malina T, Mitrovic N, Lehmann-Horn F. Role in fast inactivation of the IV/S4-S5 loop of the human muscle Na⁺ channel probed by cysteine mutagenesis. *J Physiol* 1997;505:345-52.
76. Tang L, Chehab N, Wieland SJ, Kallen RG. Glutamine substitution at alanine 1649 in the S4-S5 cytoplasmic loop of domain 4 removes the voltage sensitivity of fast inactivation in the human heart sodium channel. *J Gen Physiol* 1998;111:639-52.
77. Schwartz SP, Jezer A. The action of quinine and quinidine of patients with transient ventricular fibrillation. *Am Heart J* 1934;9:792-801.
78. Rudy B. Slow inactivation of the sodium conductance in squid giant axons. Pronase resistance. *J Physiol* 1978;283:1-21.
79. Balser JR, Nuss HB, Chiamvimonvat N, Perez-Garcia MT, Marban E, Tomaselli GF. External pore residue mediates slow inactivation in mu 1 rat skeletal muscle sodium channels. *J Physiol* 1996;494:431-42.
80. Vilin YY, Makita N, George AL, Ruben PC. Structural determinants of slow inactivation in human cardiac and skeletal muscle sodium channels. *Biophys J* 1999;77:1384-93.
81. Benitah JP, Chen Z, Balser JR, Tomaselli GF, Marban E. Molecular dynamics of the sodium channel pore vary with gating: interactions between P-segment motions and inactivation. *J Neurosci* 1999;19:1577-85.
82. Vilin YY, Fujimoto E, Ruben PC. A single residue differentiates between human cardiac and skeletal muscle Na⁺ channel slow inactivation. *Biophys J* 2001;80:2221-30.
83. Hoshi T, Zagotta WN, Aldrich RW. Two types of inactivation in Shaker K⁺ channels: effects of alterations in the carboxy-terminal region. *Neuron* 1991;7:547-56.
84. Townsend C, Horn R. Effect of alkali metal cations on slow inactivation of cardiac Na⁺ channels. *J Gen Physiol* 1997;110:23-33.
85. Todt H, Dudley SC, Kyle JW, French RJ, Fozzard HA. Ultra-slow inactivation in mu 1 Na⁺ channels is produced by a structural rearrangement of the outer vestibule. *Biophys J* 1999;76:1335-45.

86. Vedantham V, Cannon SC. Rapid and slow voltage-dependent conformational changes in segment IVS6 of voltage-gated Na⁺ channels. *Biophys J* 2000;78:2943-58.
87. Mitrovic N, George AL, Horn R. Role of domain 4 in sodium channel slow inactivation. *J Gen Physiol* 2000;115:707-18.
88. Chen LQ, Santarelli V, Horn R, Kallen RG. A unique role for the S4 segment of domain 4 in the inactivation of sodium channels. *J Gen Physiol* 1996;108:549-56.
89. Sheets MF, Kyle JW, Kallen RG, Hanck DA. The Na⁺ channel voltage sensor associated with inactivation is localized to the external charged residues of domain IV, S4. *Biophys J* 1999;77:747-57.
90. Cha A, Ruben PC, George AL, Fujimoto E, Bezanilla F. Voltage sensors in domains III and IV, but not I and II, are immobilized by Na⁺ channel fast inactivation. *Neuron* 1999;22:73-87.
91. Vaughan Williams EM. A classification of antiarrhythmic actions reassessed after a decade of new drugs. *J Clin Pharmacol* 1984;24:129-47.
92. Harrison DC. Antiarrhythmic drug classification: new science and practical applications. *Am J Cardiol* 1985;56:185-87.
93. Hondeghem LM, Katzung BG. Time- and voltage-dependent interactions of antiarrhythmic drugs with cardiac sodium channels. *Biochim Biophys Acta* 1977;472:373-98.
94. Hille B. Local anesthetics: hydrophilic and hydrophobic pathways for the drug-receptor reaction. *J Gen Physiol* 1977;69:497-515.
95. Courtney KR. Mechanism of frequency-dependent inhibition of sodium currents in frog myelinated nerve by the lidocaine derivative GEA. *J Pharmacol Exp Ther* 1975;195:225-36.
96. Starmer CF, Grant AO, Strauss HC. Mechanisms of use-dependent block of sodium channels in excitable membranes by local anesthetics. *Biophys J* 1984;46:15-27.
97. McCormack K, Tanouye MA, Iverson LE, Lin JW, Ramaswami M, McCormack T, Campanelli JT, Mathew MK, Rudy B. A role for hydrophobic residues in the voltage-dependent gating of Shaker K⁺ channels. *Proc Natl Acad Sci U S A* 1997;88:2931-35.
98. Ragsdale DS, McPhee JC, Scheuer T, Catterall WA. Molecular determinants of state-dependent block of Na⁺ channels by local anesthetics. *Science* 1994;265:1724-28.
99. Ragsdale DS, McPhee JC, Scheuer T, Catterall WA. Common molecular determinants of local anesthetic, antiarrhythmic, and anticonvulsant block of voltage-gated Na⁺ channels. *Proc Natl Acad Sci U S A* 1996;93:9270-75.
100. Kambouris NG, Hastings LA, Stepanovic S, Marban E, Tomaselli GF, Balser JR. Mechanistic link between lidocaine block and inactivation probed by outer pore mutations in the rat $\mu 1$ skeletal muscle sodium channel. *J Physiol* 1998;512:693-705.
101. Li RA, Tsushima RG, Himmeldirk K, Dime DS, Backx PH. Local anesthetic anchoring to cardiac sodium channels. Implications into tissue-selective drug targeting. *Circ Res* 1999;85:88-98.
102. Grant AO, Whalley DW, Wendt DJ. Pharmacology of the cardiac sodium channels. In: Zipes DP, Jalife J (eds). *Cardiac electrophysiology. From cell to bedside*. Philadelphia: WB Saunders, 2000:133-41.
103. Isom LL. Sodium channel β -subunits: anything but auxiliary. *Neuroscientist* 2001;7:42-54.
104. Makita N, Bennett PB, George AL. Voltage-gated Na⁺ channel $\beta 1$ -subunit mRNA expressed in adult human skeletal muscle, heart, and brain is encoded by a single gene. *J Biol Chem* 1994;269:7571-78.
105. Makita N, Sloan-Brown K, Weghuis DO, Ropers HH, George AL. Genomic organization and chromosomal assignment of the human voltage-gated Na⁺ channel $\beta 1$ -subunit gene (SCN1B). *Genomics* 1994;23:628-34.
106. Hartshorne RP, Catterall WA. The sodium channel from rat brain. Purification and subunit composition. *J Biol Chem* 1984;259:1667-75.

107. McClatchey AI, Cannon SC, Slaugenhaupt SA, Gusella JF. The cloning and expression of a sodium channel β 1-subunit cDNA from human brain. *Hum Mol Genet* 1993;2:745-49.
108. Yang JS, Bennett PB, Makita N, George AL, Barchi RL. Expression of the sodium channel β 1-subunit in rat skeletal muscle is selectively associated with the tetrodotoxin-sensitive α -subunit isoform. *Neuron* 1993;11:915-22.
109. Patton DE, Isom LL, Catterall WA, Goldin AL. The adult rat brain β 1-subunit modifies activation and inactivation gating of multiple sodium channel α subunits. *J Biol Chem* 1994;269:17649-55.
110. Nuss HB, Chiamvimonvat N, Perez-Garcia MT, Tomaselli GF, Marban E. Functional association of the β 1-subunit with human cardiac (*hH1*) and rat skeletal muscle (*mu 1*) sodium channel α -subunits expressed in *Xenopus* oocytes. *J Gen Physiol* 1995;106:1171-91.
111. Morgan K, Stevens EB, Shah B, Cox PJ, Dixon AK, Lee K, Pinnock RD, Hughes J, Richardson PJ, Mizuguchi K, Jackson AP. Beta 3: an additional auxiliary subunit of the voltage-sensitive sodium channel that modulates channel gating with distinct kinetics. *Proc Natl Acad Sci U S A* 2000;97:2308-13.
112. Kazen-Gillespie KA, Ragsdale DS, D'Andrea MR, Mattei LN, Rogers KE, Isom LL. Cloning, localization, and functional expression of sodium channel β 1A-subunits. *J Biol Chem* 2000;275:1079-88.
113. Qu Y, Isom LL, Westenbroek RE, Rogers JC, Tanada TN, McCormick KA, Scheuer T, Catterall WA. Modulation of cardiac Na^+ channel expression in *Xenopus* oocytes by β 1-subunits. *J Biol Chem* 1995;270:25696-701.
114. Makielski JC, Limberis JT, Chang SY, Fan Z, Kyle JW. Coexpression of β 1 with cardiac sodium channel α -subunits in oocytes decreases lidocaine block. *Mol Pharmacol* 1996;49:30-39.
115. An RH, Wang XL, Kerem B, Benhorin J, Medina A, Goldmit M, Kass RS. Novel LQT-3 mutation affects Na^+ channel activity through interactions between α - and β 1-subunits. *Circ Res* 1998;83:141-46.
116. Qu Y, Rogers J, Tanada T, Scheuer T, Catterall WA. Molecular determinants of drug access to the receptor site for antiarrhythmic drugs in the cardiac Na^+ channel. *Proc Natl Acad Sci U S A* 1995;92:11839-43.
117. Moran O, Nizzari M, Conti F. Endogenous expression of the β 1A sodium channel subunit in HEK-293 cells. *FEBS Lett* 2000;473:132-34.
118. Smith RD, Goldin AL. Functional analysis of the rat I sodium channel in *Xenopus* oocytes. *J Neurosci* 1998;18:811-20.
119. Chen C, Cannon SC. Modulation of Na^+ channel inactivation by the β 1-subunit: a deletion analysis. *Pflugers Arch* 1995;431:186-95.
120. Makita N, Bennett PB, George AL. Molecular determinants of β 1-subunit-induced gating modulation in voltage-dependent Na^+ channels. *J Neurosci* 1996;16:7117-27.
121. McCormick KA, Isom LL, Ragsdale D, Smith D, Scheuer T, Catterall WA. Molecular determinants of Na^+ channel function in the extracellular domain of the β 1-subunit. *J Biol Chem* 1998;273:3954-62.
122. Qu Y, Rogers JC, Chen SF, McCormick KA, Scheuer T, Catterall WA. Functional roles of the extracellular segments of the sodium channel α -subunit in voltage-dependent gating and modulation by β 1-subunits. *J Biol Chem* 1999;274:32647-54.
123. Wickner WT, Lodish HF. Multiple mechanisms of protein insertion into and across membranes. *Science* 1985;230:400-07.
124. Eubanks J, Srinivasan J, Dinulos MB, Distech CM, Catterall WA. Structure and chromosomal localization of the β 2-subunit of the human brain sodium channel. *Neuroreport* 1997;8:2775-79.
125. Isom LL, Catterall WA. Na^+ channel subunits and Ig domains. *Nature* 1996;383:307-08.
126. Malhotra JD, Kazen-Gillespie K, Hortsch M, Isom LL. Sodium channel β -subunits mediate

- homophilic cell adhesion and recruit ankyrin to points of cell-cell contact.
J Biol Chem 2000;275:11383-88.
127. Undrovinas AI, Shander GS, Makielski JC. Cytoskeleton modulates gating of voltage-dependent sodium channel in heart. *Am J Physiol* 1995;269:H203-14.
 128. Gastaldi M, Robaglia-Schlupp A, Massacrier A, Planells R, Cau P. mRNA coding for voltage-gated sodium channel β 2-subunit in rat central nervous system: cellular distribution and changes following kainate-induced seizures. *Neurosci Lett* 1998;249:53-56.
 129. Duff HJ, Offord J, West J, Catterall WA. Class I and IV antiarrhythmic drugs and cytosolic calcium regulate mRNA encoding the sodium channel α -subunit in rat cardiac muscle. *Mol Pharmacol* 1992;42:570-74.
 130. Kang JX, Leaf A. Antiarrhythmic effects of polyunsaturated fatty acids. Recent studies. *Circulation* 1996;94:1774-80.
 131. Kang JX, Li Y, Leaf A. Regulation of sodium channel gene expression by class I antiarrhythmic drugs and n-3 polyunsaturated fatty acids in cultured neonatal rat cardiac myocytes. *Proc Natl Acad Sci U S A* 1997;94:2724-28.
 132. Huang B, El Sherif T, Gidh-Jain M, Qin D, el Sherif N. Alterations of sodium channel kinetics and gene expression in the postinfarction remodeled myocardium. *J Cardiovasc Electrophysiol* 2001;12:218-25.
 133. Roberts RH, Barchi RL. The voltage-sensitive sodium channel from rabbit skeletal muscle. Chemical characterization of subunits. *J Biol Chem* 1987;262:2298-303.
 134. James WM, Agnew WS. Alpha-(2 \rightarrow 8)-polysialic acid immunoreactivity in voltage-sensitive sodium channel of eel electric organ. *Proc R Soc Lond B Biol Sci* 1989;237:233-45.
 135. Cohen SA, Levitt LK. Partial characterization of the rH1 sodium channel protein from rat heart using subtype-specific antibodies. *Circ Res* 1993;73:735-42.
 136. Bennett E, Urcan MS, Tinkle SS, Koszowski AG, Levinson SR. Contribution of sialic acid to the voltage dependence of sodium channel gating. A possible electrostatic mechanism. *J Gen Physiol* 1997;109:327-43.
 137. Ufret-Vincenty CA, Baro DJ, Lederer WJ, Rockman HA, Quinones LE, Santana LF. Role of sodium channel deglycosylation in the genesis of cardiac arrhythmias in heart failure. *J Biol Chem* 2001;276:28197-203.
 138. Gershon E, Weigl L, Lotan I, Schreibleymer W, Dascal N. Protein kinase A reduces voltage-dependent Na^+ current in *Xenopus* oocytes. *J Neurosci* 1992;12:3743-52.
 139. Li M, West JW, Lai Y, Scheuer T, Catterall WA. Functional modulation of brain sodium channels by cAMP-dependent phosphorylation. *Neuron* 1992;8:1151-59.
 140. Li M, West JW, Numann R, Murphy BJ, Scheuer T, Catterall WA. Convergent regulation of sodium channels by protein kinase C and cAMP-dependent protein kinase. *Science* 1993;261:1439-42.
 141. Smith RD, Goldin AL. Phosphorylation at a single site in the rat brain sodium channel is necessary and sufficient for current reduction by protein kinase A. *J Neurosci* 1997;17:6086-93.
 142. Murphy BJ, Rogers J, Perdichizzi AP, Colvin AA, Catterall WA. cAMP-dependent phosphorylation of two sites in the α -subunit of the cardiac sodium channel. *J Biol Chem* 1996;271:28837-43.
 143. Schreibleymer W, Frohnwieser B, Dascal N, Platzer D, Spreitzer B, Zechner R, Kallen RG, Lester HA. Beta-adrenergic modulation of currents produced by rat cardiac Na^+ channels expressed in *Xenopus laevis* oocytes. *Receptors Channels* 1994;2:339-50.
 144. Frohnwieser B, Chen LQ, Schreibleymer W, Kallen RG. Modulation of the human cardiac sodium channel α -subunit by cAMP-dependent protein kinase and the responsible sequence domain. *J Physiol* 1997;498:309-18.

145. Lu T, Lee HC, Kabat JA, Shibata EF. Modulation of rat cardiac sodium channel by the stimulatory G protein α -subunit. *J Physiol* 1999;518:371-84.
146. Zhou J, Yi J, Hu N, George AL Jr, Murray KT. Activation of protein kinase A modulates trafficking of the human cardiac sodium channel in *Xenopus* oocytes. *Circ Res* 2000;87:33-38.
147. Ono K, Fozzard HA, Hanck DA. Mechanism of cAMP-dependent modulation of cardiac sodium channel current kinetics. *Circ Res* 1993;72:807-15.
148. Schubert B, VanDongen AM, Kirsch GE, Brown AM. Beta-adrenergic inhibition of cardiac sodium channels by dual G-protein pathways. *Science* 1989;245:516-19.
149. Gintant GA, Liu DW. Beta-adrenergic modulation of fast inward sodium current in canine myocardium. Syncytial preparations versus isolated myocytes. *Circ Res* 1992;70:844-50.
150. Matsuda JJ, Lee H, Shibata EF. Enhancement of rabbit cardiac sodium channels by beta-adrenergic stimulation. *Circ Res* 1992;70:199-207.
151. Qu Y, Rogers JC, Tanada TN, Catterall WA, Scheuer T. Phosphorylation of S1505 in the cardiac Na^+ channel inactivation gate is required for modulation by protein kinase C. *J Gen Physiol* 1996;108:375-79.
152. Santana LF, Gomez AM, Lederer WJ. Ca^{2+} flux through promiscuous cardiac Na^+ channels: slip-mode conductance. *Science* 1998;279:1027-33.
153. dos Santos Cruz J, Santana LF, Frederick CA, Isom LL, Malhotra JD, Mattei LN, Kass RS, Xia J, An RH, Lederer WJ. Whether 'slip-mode conductance' occurs. *Science* 1999;284:716a-23a.
154. Jiang C, Atkinson D, Towbin JA, Splawski I, Lehmann MH, Li H, Timothy K, Taggart RT, Schwartz PJ, Vincent GM. Two long-QT syndrome loci map to chromosomes 3 and 7 with evidence for further heterogeneity. *Nat Genet* 1994;8:141-47.
155. Schwartz PJ, Priori SG, Dumaine R, Napolitano C, Antzelevitch C, Stramba-Badiale M, Richard TA, Berti MR, Bloise R. A molecular link between the sudden infant death syndrome and the long-QT syndrome. *N Engl J Med* 2000;343:262-67.
156. Splawski I, Shen J, Timothy KW, Lehmann MH, Priori S, Robinson JL, Moss AJ, Schwartz PJ, Towbin JA, Vincent GM, Keating MT. Spectrum of mutations in long-QT syndrome genes. *KvLQT1*, *HERG*, *SCN5A*, *KCNE1*, and *KCNE2*. *Circulation* 2000;102:1178-85.
157. Wattanasirichaigoon D, Vesely MR, Duggal P, Levine JC, Blume ED, Wolff GS, Edwards SB, Beggs AH. Sodium channel abnormalities are infrequent in patients with long-QT syndrome: identification of two novel *SCN5A* mutations. *Am J Med Genet* 1999;86:470-76.
158. Wang DW, Yazawa K, George AL Jr, Bennett PB. Characterization of human cardiac Na^+ channel mutations in the congenital long-QT syndrome. *Proc Natl Acad Sci U S A* 1996;93:13200-05.
159. Wedekind H, Smits JP, Schulze-Bahr E, Arnold R, Veldkamp MW, Bajanowski T, Borggreffe M, Brinkmann B, Warnecke I, Funke H, Bhuiyan ZA, Wilde AA, Breithardt G, Haverkamp W. *De novo* mutation in the *SCN5A* gene associated with early onset of sudden infant death. *Circulation* 2001;104:1158-64.
160. Makita N, Shirai N, Nagashima M, Matsuoka R, Yamada Y, Tohse N, Kitabatake A. A *de novo* missense mutation of human cardiac Na^+ channel exhibiting novel molecular mechanisms of long-QT syndrome. *FEBS Lett* 1998;423:5-9.
161. Lupoglazoff JM, Cheav T, Baroudi G, Berthet M, Denjoy I, Cauchemez B, Extramiana F, Chahine M, Guicheney P. Homozygous *SCN5A* mutation in long-QT syndrome with functional two-to-one atrioventricular block. *Circ Res* 2001;89:E16-21.
162. Wei J, Wang DW, Alings M, Fish F, Wathen M, Roden DM, George AL Jr. Congenital long-QT syndrome caused by a novel mutation in a conserved acidic domain of the cardiac Na^+ channel. *Circulation* 1999;99:3165-71.

163. Benhorin J, Goldmit M, MacCluer JW, Blangero J, Goffen R, Leibovitch A, Rahat A, Wang Q, Medina A, Towbin J, Kerem B. Identification of a new *SCN5A* mutation, D1840G, associated with the long-QT syndrome. *Hum Mutat* 1998;12:72.
164. Rivolta I, Abriel H, Tateyama M, Liu H, Memmi M, Vardas P, Napolitano C, Priori SG, Kass RS. Inherited Brugada and LQT-3 syndrome mutations of a single residue of the cardiac sodium channel confer distinct channel and clinical phenotypes. *J Biol Chem* 2001;276:30623-30.
165. Dumaine R, Wang Q, Keating MT, Hartmann HA, Schwartz PJ, Brown AM, Kirsch GE. Multiple mechanisms of Na^+ channel-linked long-QT syndrome. *Circ Res* 1996;78:916-24.
166. Chandra R, Starmer CF, Grant AO. Multiple effects of ΔKPQ deletion mutation on gating of human cardiac Na^+ channels expressed in mammalian cells. *Am J Physiol* 1998;274:H1643-54.
167. Nagatomo T, Fan Z, Ye B, Tonkovich GS, January CT, Kyle JW, Makielski JC. Temperature dependence of early and late currents in human cardiac wild-type and long QT ΔKPQ Na^+ channels. *Am J Physiol* 1998;275:H2016-24.
168. George AL, Komisarof J, Kallen RG, Barchi RL. Primary structure of the adult human skeletal muscle voltage-dependent sodium channel. *Ann Neurol* 1992;31:131-37.
169. Yamagishi H, Furutani M, Kamisago M, Morikawa Y, Kojima Y, Hino Y, Furutani Y, Kimura M, Imamura S, Takao A, Momma K, Matsuoka R. A *de novo* missense mutation (R1623Q) of the *SCN5A* gene in a Japanese girl with sporadic long-QT syndrome. *Hum Mutat* 1998;11:481.
170. Kambouris NG, Nuss HB, Johns DC, Tomaselli GF, Marban E, Balser JR. Phenotypic characterization of a novel long-QT syndrome mutation (R1623Q) in the cardiac sodium channel. *Circulation* 1998;97:640-44.
171. Chahine M, George AL, Zhou M, Ji S, Sun W, Barchi RL, Horn R. Sodium channel mutations in paramyotonia congenita uncouple inactivation from activation. *Neuron* 1994;12:281-94.
172. Kambouris NG, Nuss HB, Johns DC, Marban E, Tomaselli GF, Balser JR. A revised view of cardiac sodium channel "blockade" in the long-QT syndrome. *J Clin Invest* 2000;105:1133-40.
173. Ji S, George AL, Horn R, Barchi RL. Paramyotonia congenita mutations reveal different roles for segments S3 and S4 of domain D4 in *hSkM1* sodium channel gating. *J Gen Physiol* 1996;107:183-94.
174. Deschenes I, Baroudi G, Berthet M, Barde I, Chalvidan T, Denjoy I, Guicheney P, Chahine M. Electrophysiological characterization of *SCN5A* mutations causing long-QT (E1784K) and Brugada (R1512W and R1432G) syndromes. *Cardiovasc Res* 2000;46:55-65.
175. Kiyosue T, Arita M. Late sodium current and its contribution to action potential configuration in guinea pig ventricular myocytes. *Circ Res* 1989;64:389-97.
176. Luo CH, Rudy Y. A dynamic model of the cardiac ventricular action potential. I. Simulations of ionic currents and concentration changes. *Circ Res* 1994;74:1071-96.
177. Luo CH, Rudy Y. A dynamic model of the cardiac ventricular action potential. II. Afterdepolarizations, triggered activity, and potentiation. *Circ Res* 1994;74:1097-13.
178. Zeng J, Rudy Y. Early afterdepolarizations in cardiac myocytes: mechanism and rate dependence. *Biophys J* 1995;68:949-64.
179. Zeng J, Laurita KR, Rosenbaum DS, Rudy Y. Two components of the delayed rectifier K^+ current in ventricular myocytes of the guinea pig type. Theoretical formulation and their role in repolarization. *Circ Res* 1995;77:140-52.
180. An RH, Bangalore R, Rosero SZ, Kass RS. Lidocaine block of LQT-3 mutant human Na^+ channels. *Circ Res* 1996;79:103-08.
181. Starmer CF. Theoretical characterization of ion channel blockade. Competitive binding to periodically accessible receptors. *Biophys J* 1987;52:405-12.

182. Wang DW, Yazawa K, Makita N, George AL Jr, Bennett PB. Pharmacological targeting of long-QT mutant sodium channels. *J Clin Invest* 1997;99:1714-20.
183. Schwartz PJ, Priori SG, Locati EH, Napolitano C, Cantu F, Towbin JA, Keating MT, Hammoude H, Brown AM, Chen LS. Long-QT syndrome patients with mutations of the *SCN5A* and *HERG* genes have differential responses to Na⁺ channel blockade and to increases in heart rate. Implications for gene-specific therapy. *Circulation* 1995;92:3381-86.
184. Rosero SZ, Zareba W, Robinson J, Moss A. Gene-specific therapy for long-QT syndrome: QT shortening with lidocaine and tocainide in patients with mutations of the sodium channel gene. *Ann Noninvasive Electrocardiol* 1997;3:274-78.
185. Benhorin J, Taub R, Goldmit M, Kerem B, Kass RS, Windman I, Medina A. Effects of flecainide in patients with new *SCN5A* mutation: mutation-specific therapy for long-QT syndrome? *Circulation* 2000;101:1698-706.
186. Brugada P, Brugada J. Right bundle branch block, persistent ST segment elevation and sudden cardiac death: a distinct clinical and electrocardiographic syndrome. A multicenter report. *J Am Coll Cardiol* 1992;20:1391-96.
187. Rook MB, Alshinawi CB, Groenewegen WA, Van Gelder IC, Van Ginneken AC, Jongsma HJ, Mannens MM, Wilde AA. Human *SCN5A* gene mutations alter cardiac sodium channel kinetics and are associated with the Brugada syndrome. *Cardiovasc Res* 1999;44:507-17.
188. Vatta M, Li H, Towbin JA. Molecular biology of arrhythmic syndromes. *Curr Opin Cardiol* 2000;15:12-22.
189. Bezzina C, Veldkamp MW, Van den Berg MP, Postma AV, Rook MB, Viersma JW, van Langen IM, Tan-Sindhunata G, Bink-Boelkens MT, Van der Hout AH, Mannens MM, Wilde AA. A single Na⁺ channel mutation causing both long-QT and Brugada syndromes. *Circ Res* 1999;85:1206-13.
190. Veldkamp MW, Viswanathan PC, Bezzina C, Baartscheer A, Wilde AA, Balser JR. Two distinct congenital arrhythmias evoked by a multidysfunctional Na⁺ channel. *Circ Res* 2000;86:E91-97.
191. Baroudi G, Chahine M. Biophysical phenotypes of *SCN5A* mutations causing long-QT and Brugada syndromes. *FEBS Lett* 2000;487:224-28.
192. Taneja T, Mahnert BW, Passman R, Goldberger J, Kadish A. Effects of sex and age on electrocardiographic and cardiac electrophysiological properties in adults. *Pacing Clin Electrophysiol* 2001;24:16-21.
193. Lev M, Kinare SG, Pick A. The pathogenesis of atrioventricular block in coronary disease. *Circulation* 1970;42:409-25.
194. Lenegre J, Moreau P. Le bloc auriculo-ventriculaire chronique. Etude anatomique, clinique et histologique. *Arch Mal Coeur Vaiss* 1963;56:867-88.
195. Nuyens D, Stengl M, Dugarmaa S, Rossenbacker T, Compennolle V, Rudy Y, Smits JF, Flameng W, Clancy CE, Moons L, Vos MA, Dewerchin M, Benndorf K, Collen D, Carmeliet E, Carmeliet P. Abrupt rate accelerations or premature beats cause life-threatening arrhythmias in mice with long-QT3 syndrome. *Nat Med* 2001;7:1021-27.
196. Schwartz PJ, Priori SG, Spazzolini C, Moss AJ, Vincent GM, Napolitano C, Denjoy I, Guicheney P, Breithardt G, Keating MT, Towbin JA, Beggs AH, Brink P, Wilde AA, Toivonen L, Zareba W, Robinson JL, Timothy KW, Corfield V, Wattanasirichaigoon D, Corbett C, Haverkamp W, Schulze-Bahr E, Lehmann MH, Schwartz K, Coumel P, Bloise R. Genotype-phenotype correlation in the long-QT syndrome: gene-specific triggers for life-threatening arrhythmias. *Circulation* 2001;103:89-95.
197. Aldrich RW, Stevens CF. Voltage-dependent gating of single sodium channels from mammalian neuroblastoma cells. *J Neurosci* 1987;7:418-31.

Chapter 3

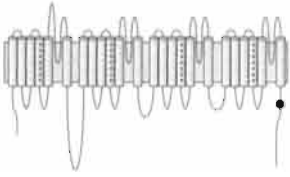
Arrhythmogenic Mechanism of the D1790G Mutation of the Human Heart Na⁺ Channel α -Subunit

Based on:

WEHRENS XHT, Abriel H, Cabo C, Benhorin J, Kass RS.

Arrhythmogenic Mechanism of an LQT-3 Mutation of the Human Heart Na⁺ Channel α -Subunit - A Computational Analysis. Circulation 2000;102:584-90.

Abstract



BACKGROUND. D1790G, a mutation of *SCN5A*, the gene that encodes the human Na^+ channel α -subunit, is linked to one form of the congenital long-QT syndrome (LQT-3). In contrast to other LQT-3-linked *SCN5A* mutations, D1790G does not promote sustained Na^+ channel activity but instead alters the kinetics and voltage-dependence of the inactivated state.

METHODS AND RESULTS. We modeled the cardiac ventricular action potential (AP) using parameters and techniques described by Luo and Rudy as our control. On this background, we modified only the properties of the voltage-gated Na^+ channel according to our patch-clamp analysis of D1790G channels. Our results indicate that D1790G-induced changes in Na^+ channel activity prolong APs in a steeply heart rate-dependent manner not directly due to changes in Na^+ entry through mutant channels but instead to alterations in the balance of net plateau currents by modulation of calcium-sensitive exchange and ion channel currents.

CONCLUSIONS. We conclude that the D1790G mutation of the Na^+ channel α -subunit can prolong the cardiac ventricular AP despite the absence of mutation-induced sustained Na^+ channel current. This prolongation is calcium-dependent, is enhanced at slow heart rates, and at sufficiently slow heart rate triggers arrhythmogenic early afterdepolarizations.

Introduction

The congenital long-QT syndrome (LQTS) is an inherited cardiac disorder that is defined in part by prolonged ventricular repolarization, an association with recurrent syncope, a propensity to polymorphous ventricular tachycardia (torsades de pointes), and sudden death (1,2). Multiple genes that encode ion channel subunits have now been shown to be linked to LQTS (3) and in most cases, the functional properties of the mutant gene products are consistent with the disease phenotype, i.e., increase of inward or decrease of outward plateau current (4,5).

LQT-3 is linked to the gene encoding the α -subunit of the cardiac voltage-gated sodium channel (*SCN5A* on chromosome 3) (6). Functional analysis of initially reported *SCN5A* mutations revealed mutant Na^+ channels that fail to inactivate completely on prolonged depolarization (7,8) and produce a small but functionally important enhancement of inward plateau current sufficient to delay repolarization and increase vulnerability of the heart to arrhythmias (9). All subsequently reported LQT-3 mutations with the exception of D1790G (DG) promote sustained Na^+ current and are expected to prolong repolarization through this common mechanism (9-14).

The purpose of the present study was to use a computational approach to determine whether or not the biophysical properties of DG mutant Na^+ channels might affect the cellular action potential (AP) through mechanisms other than a direct contribution to maintained Na^+ channel plateau current. We modeled the cardiac ventricular AP using parameters and techniques described by Luo and Rudy (15) as our control and modified only the properties of the voltage-gated Na^+ channel according to our patch-clamp analysis of DG channels. Our results indicate that the DG mutation can prolong AP duration (APD) despite the absence of mutation-induced inward Na^+ channel current during the plateau phase. Instead, the mutation indirectly affects other electrogenic pathways, which have a common interdependence on altered cellular calcium homeostasis. The computations predict DG mutation-induced AP prolongation, which is heart rate-dependent and driven by subsequent changes in the intracellular calcium transient. These results are important not only for the novel fundamental insight into the mechanistic basis of inherited arrhythmias but also because they suggest novel targets (i.e., calcium-handling proteins) as therapeutic agents.

The Luo-Rudy Model of the Ventricular Action Potential

The simulations in this chapter were conducted using the Luo-Rudy (LRd) model, a theoretical dynamic model of a mammalian ventricular action potential (FIGURE 3.51). The model is based mostly on guinea pig experimental data; it includes membrane ionic channel currents that are formulated mathematically using the Hodgkin-Huxley approach, as well as ionic pumps and exchangers. The model also accounts for processes that regulate intracellular concentration changes of Na^+ , K^+ and Ca^{2+} (9,29,30). Intracellular processes represented in the model include Ca^{2+} uptake and Ca^{2+} release by the sarcoplasmic reticulum (SR) as well as Ca^{2+} buffering by calmodulin and troponin (in the myoplasm) and calsequestrin (in the SR). As it was shown that reduced density of I_{K_S} can result in electrical and pharmacological properties that are very similar to those of M cells (31), consistent with experimental data by Liu et al. (32), M-cell properties were formulated by lowering I_{K_S} density while keeping I_{K_r} constant.

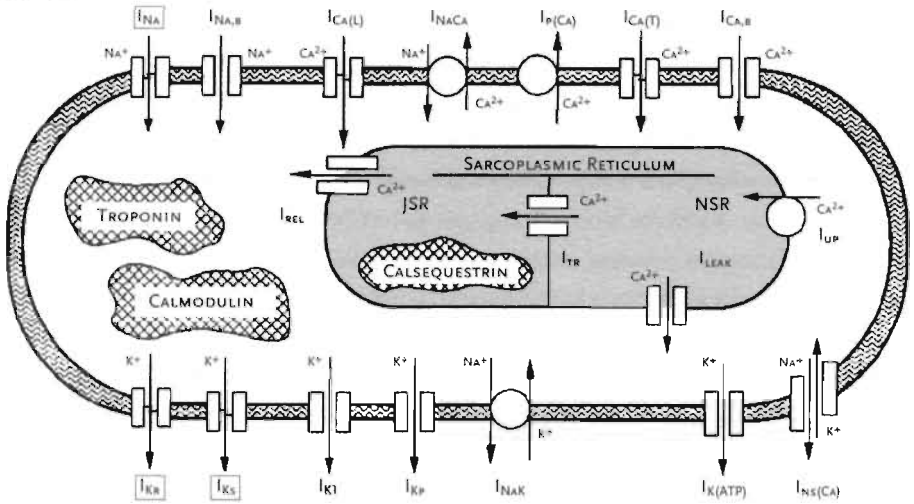


FIGURE 3.51 Schematic diagram of the Luo-Rudy mammalian ventricular cell model. I_{Na} , fast Na^+ current; $I_{Ca(L)}$, Ca^{2+} current through the L-type Ca^{2+} channel; $I_{Ca(T)}$, Ca^{2+} current through the T-type Ca^{2+} channel; I_{K_r} , fast component of the delayed rectifier K^+ current; I_{K_s} , slow component of the delayed rectifier K^+ current; I_{K_1} , inward rectifier K^+ current; I_{K_p} , plateau K^+ current; $I_{K(ATP)}$, ATP sensitive K^+ current; I_{NaK} , Na^+ - K^+ pump; I_{NaCa} , Na^+ - Ca^{2+} exchange current; $I_{p(Ca)}$, Ca^{2+} pump in the sarcolemma; $I_{Na,b}$, Na^+ background current; $I_{Ca,b}$, Ca^{2+} background current; $I_{ns(Ca)}$, nonspecific Ca^{2+} activated current (activated only under conditions of Ca^{2+} overload); I_{up} , Ca^{2+} uptake from the myoplasm to network sarcoplasmic reticulum (NSR); I_{rel} , Ca^{2+} release from the junctional sarcoplasmic reticulum (JSR); I_{leak} , Ca^{2+} leakage from NSR to myoplasm; I_{tr} , Ca^{2+} translocation from NSR to JSR; Calmodulin and Troponin, myoplasmic Ca^{2+} buffers; Calsequestrin, SR Ca^{2+} buffer.

Methods

Computer-generated AP Reconstruction

The AP was calculated by solving the differential equation $I_{ion} = -C_m(dV_m/dt)$, where I_{ion} is the total transmembrane ionic current ($\mu A/cm^2$), C_m is the specific capacitance of the membrane ($1 \mu F/cm^2$), and V_m is the transmembrane potential (mV). All ionic currents were formulated according to THE LUO-RUDY MODEL OF THE VENTRICULAR AP (15), except that the sodium current was formulated to reproduce our patch-clamp experiments in HEK 293 cells. The differential equation was solved numerically with a discretization time step of 10 μs .

Experimental parameters used in the model were determined from experimental data for voltage-dependence of steady-state activation and inactivation and the kinetics of the onset and recovery from inactivation. Parameters for Boltzmann relationships and time constants were extracted as previously described (16). Rate constants were adjusted with temperature, assuming Q_{10} factors (the factor is usually between 2 and 3 for rate constants between different states in ionic channels).

To simulate wild-type (WT) channels, we used $m_{\infty} = 1/[1 + \exp\{-(V_m + 32.5)/9\}]$ and $h_{\infty} = 1/[1 + \exp\{(V_m + 57.87)/7\}]$. To simulate DG channels, $m_{\infty} = 1/[1 + \exp\{-(V_m + 29)/10.5\}]$ and $h_{\infty} = 1/[1 + \exp\{(V_m + 74.3)/6.5\}]$ were used. In the DG channels, the time constants of onset of inactivation (τ_h) and the slow inactivation gate (τ_j) were half of those used in the WT channels. The maximum sodium conductance was 27 mS/cm^2 . In all simulations, the maximum conductance of the slow component of the delayed rectifier potassium current, I_{Ks} , was reduced by 40% to uncover AP differences between cells with WT and DG channels. These APs thus simulate endocardial or M-cell activity (5,17-20). APs were initiated by intracellular 0.5 ms current pulses ($100 \mu A/cm^2$). Initial conditions were established by stimulating cells with WT and DG channels once per second for a 3 minute period. Cells were stimulated 20 times at a constant cycle length (500-4000 ms).

Expression of Recombinant Na^+ Channels

Na^+ channels were expressed in HEK 293 cells as previously described (11). Transfections were carried out with equal amounts of Na^+ channel α -subunit cDNA (WT or DG, respectively), with $\beta 1$ - and/or $\beta 2$ -subunit cDNA subcloned individually into the pcDNA3 (Invitrogen) vector (total cDNA $2.5 \mu g$). Control experiments (data not shown) indicated no significant differences in channel activity for these subunit combinations.

Electrophysiology

Membrane currents were measured with whole-cell patch-clamp procedures (21) with Axopatch 200B amplifiers (Axon Instruments) as previously described (11). Unless noted otherwise, recordings were made at room temperature (22°C) with previously published solutions (11). Data acquisition and analysis were carried out with pClamp 7 (Axon Instruments), Excel (Microsoft), and Origin (Microcal Software). Steady-state inactivation was determined after application of 500 ms conditioning pulses applied once every 2 seconds. Recovery from inactivation was measured in paired pulse experiments, with a test pulse applied at variable times after a 100 ms conditioning pulse to -10 mV. Holding potentials were -80 mV.

Results

Biophysical Properties of DG Mutant Channels: Computational Parameter Set

FIGURE 3.1 shows families of experimental records of WT and DG mutant channels expressed in HEK 293 cells as well as analysis of the experimentally determined voltage-dependence of the time constants of the onset of inactivation. As illustrated in FIGURE 3.1A, we compared experimental recordings of WT and DG channels at 22°C (top) and 29°C (bottom). Clearly, increasing temperature speeds the kinetics of both WT and DG mutant channels, as expected (22) but it neither changes the relationship between WT and DG mutant channel time constants nor promotes DG-induced sustained inward current. FIGURE 3.1B summarizes time constants obtained by fitting experimental records with functions containing one exponential component. Although in a limited number of experiments, we previously reported no effect of the DG mutation on the kinetics of the onset of inactivation, in a more complete analysis we have found that, in fact, this mutation speeds the onset of inactivation (FIGURE 3.1) and slightly alters the voltage-dependence of activation (FIGURE 3.3). Using these data, we extrapolated the temperature coefficient (Q_{10}) of 2.1 for inactivation kinetics for both WT and DG mutant channels to compute the effects of the mutation on APs at physiological temperatures. FIGURE 3.2 shows the simulated changes in Na^+ channel currents and the time constants of the onset of inactivation generated by the computer-based model. As is the case for the experimental data, the simulated currents reflect the speeding of the onset of inactivation as a function of membrane potential but do not exhibit enhanced sustained current.

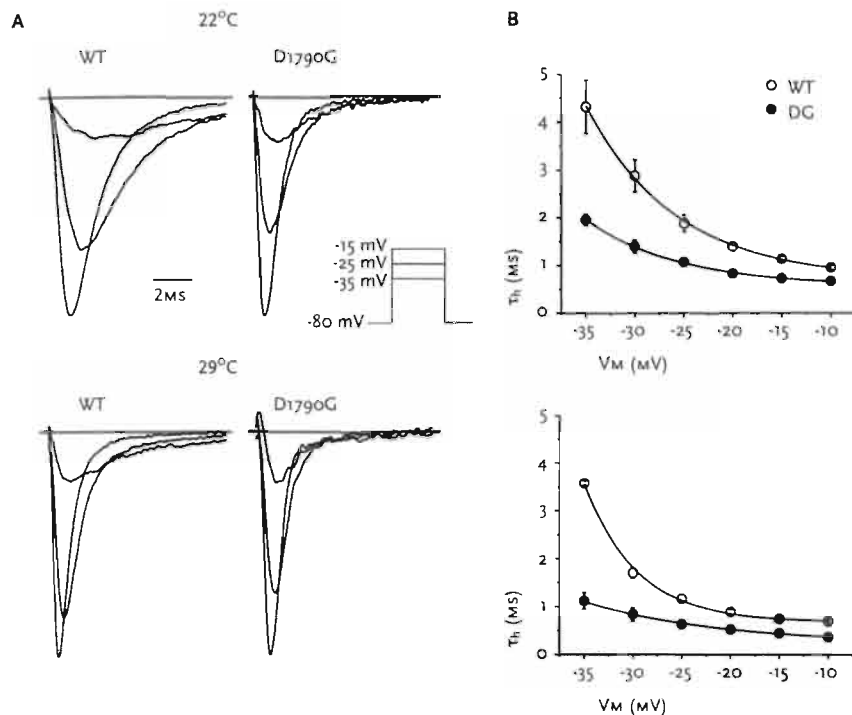


FIGURE 3.1
DG mutation speeds onset of inactivation at 22°C (top) and 29°C (bottom). **A**, Representative current traces evoked by 20 ms pulses to voltages indicated in inset for cells expressing WT or DG mutant Na⁺ channels. Maximum currents have been normalized to facilitate comparison of WT and DG current traces. **B**, Time constants (mean±SEM, $n=3$ to 7 for each data point) determined from best-fit single exponential functions to data, plotted vs test-pulse potential for WT (○) and DG (●) channels.

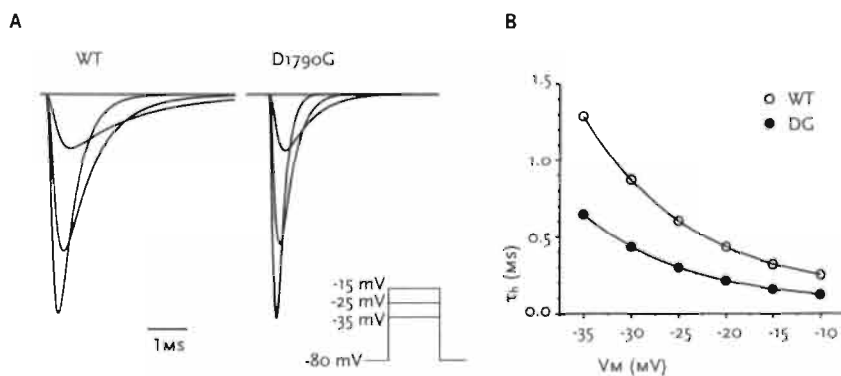


FIGURE 3.2
Effects of DG mutation on **simulated** Na⁺ channel currents. **A**, Effects of calculated time constants on computed families of WT and DG currents. **B**, Voltage-dependence of time constants of inactivation for WT and DG channels. Current traces for WT and DG Na⁺ channel currents are simulated at 37°C.

FIGURE 3.3
Experimentally determined (A) and simulated (B) effects of DG mutation on channel properties. Each panel shows steady-state inactivation and activation (top) and recovery from inactivation (bottom) for WT (○) and DG (●) channels. Theoretical curves (B) generated with parameters obtained in A in Luo and Rudy model (note that recovery from inactivation is modeled as a single exponential function) as follows: $\tau=25.2$ ms for WT; $\tau=12.6$ ms for DG.

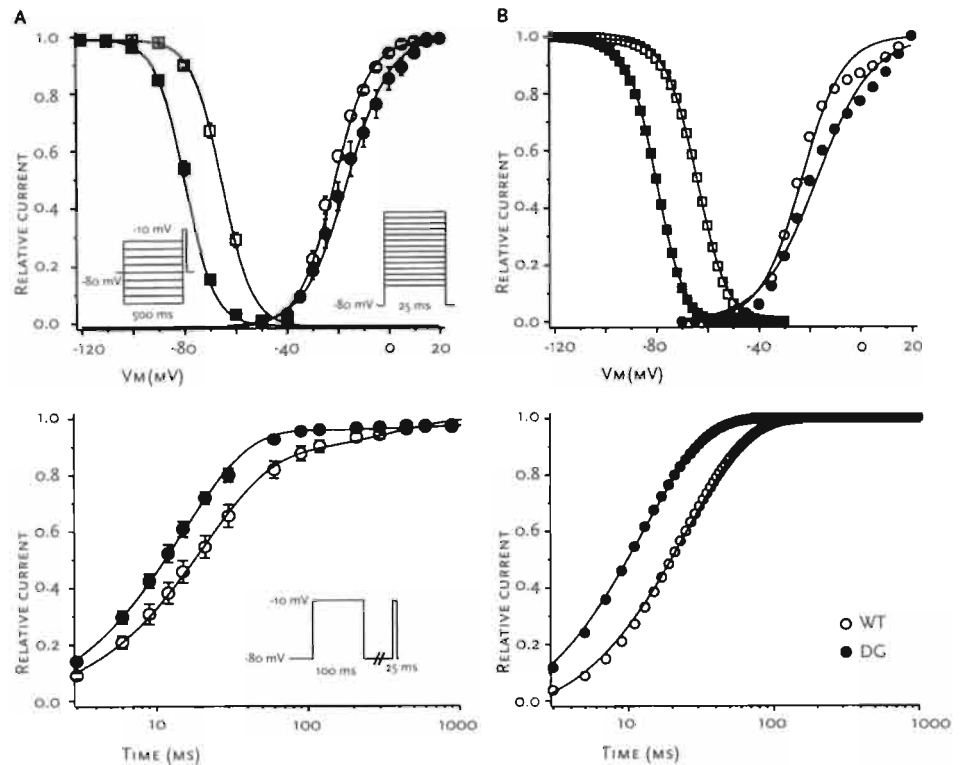


FIGURE 3.3 illustrates experimental and computational data showing the effects of the DG mutation on the voltage-dependence of steady-state inactivation and activation and on the time course of recovery from the inactivated state. For activation, peak currents (measured in 30 mmol/L $[Na^+]_o$) were normalized to driving force to determine conductance. The mutation causes a marked negative shift of the voltage-dependence of inactivation (WT, DG: $V_{1/2}$ -64, -79 mV; k 5.9, 5.5; $n=13$) with relatively minor changes in the voltage-dependence of activation, (WT, DG: $V_{1/2}$ -23, -17; K : 6.9, 9.2 ($n=6$), as we previously reported (11). The mutation also causes a small but significant speeding of the recovery process (averaged experimental time constants and relative weights are WT (○): $\tau_{fast}=20.4$ ms, $a_{fast}=0.87$, $\tau_{slow}=351$ ms, $a_{slow}=0.13$; and for DG (●): $\tau_{fast}=14.9$ ms, $a_{fast}=0.97$, $\tau_{slow}=2149$ ms, $a_{slow}=0.03$). The results obtained in experiments (A) were incorporated into the simulated channels (B).

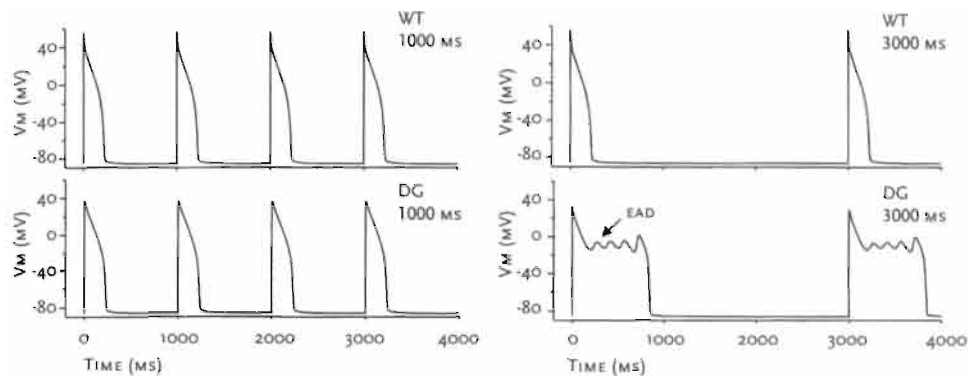


FIGURE 3.4
Effect of pacing frequency on APD and development of EADs for DG cells. First 4 (left 2 rows) and first 2 (right 2 rows) APs after trains of 20 APs at BCLs of 1000 ms (left 2 rows) and 3000 ms (right 2 rows) simulated for cells expressing WT and DG Na⁺ channels.

Simulation of Cellular Electrical Activity:

AP Prolongation That Is Heart Rate-dependent

FIGURE 3.4 shows the consequences of these mutation-induced changes in channel properties on cellular electrical activity that is predicted by the computer-generated model. At a basic cycle length (BCL) of 1000 ms, there is little effect of the DG mutation despite a significant APD prolongation. At a BCL of 3000 ms, however, it causes dramatic APD prolongation, which results in the generation of early afterdepolarizations (EADs). The results of similar calculations repeated over a series of BCLs are summarized in FIGURE 3.5, in which APD is plotted versus BCL for both WT and DG channels. The expression of mutant DG channels markedly alters this relationship. FIGURE 3.5 shows that even at moderately long BCLs (1000 to 2000 ms), the DG mutation prolongs APs compared with cells expressing WT channels. This effect becomes very pronounced (note change in vertical scale) as heart rate slows further, and at a BCL of 3000 ms, as illustrated above, the mutation-induced action prolongation is sufficient to induce EADs (arrow). Similarly, the DG mutation induces EADs after pauses in AP activity (FIGURE 3.6).

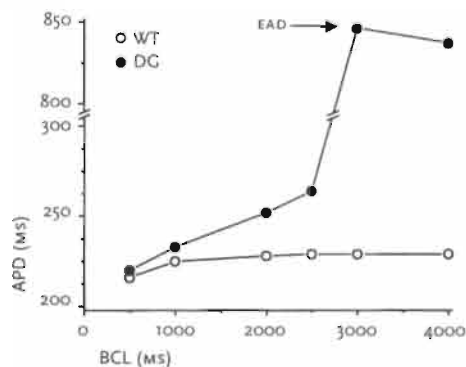


FIGURE 3.5
DG-induced AP prolongation is steeply heart rate-dependent. Plotted is relationship between APD and BCL. At BCL of 3000 ms, mutation-induced action prolongation is sufficient to induce EADs (arrow) at BCL >2500 ms.

FIGURE 3.6
Effect of DG mutation on pauses in stimulation. Last 2 APs in a train of 20 at BCL of 500 ms followed by 1500 ms pause and postpause AP. Pause in activity induces an EAD (arrow) in cells expressing DG but not WT channels.

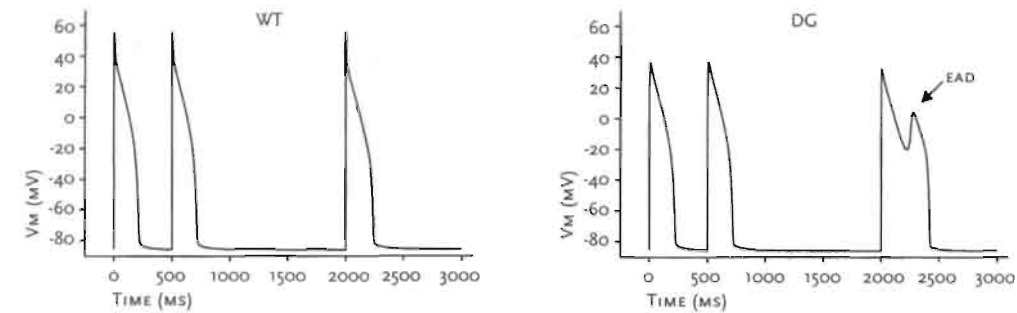
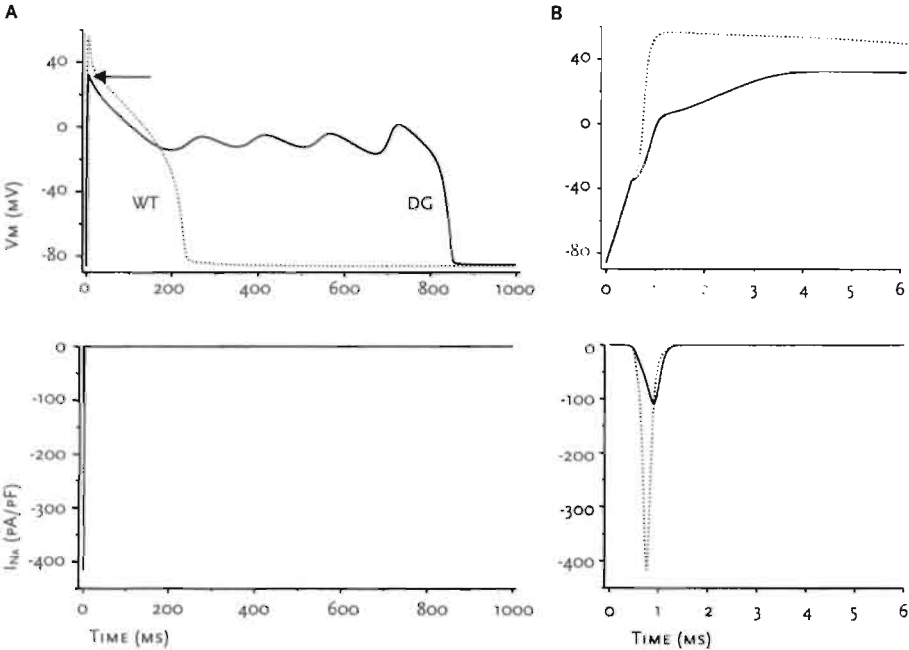


FIGURE 3.7
Effects of DG mutation on Na⁺ channel activity during AP and AP upstroke (BCL of 3000 ms). Membrane potential (top) and computed Na⁺ channel currents (bottom) for cells expressing WT (dotted lines) and DG (solid lines) channels.
A. Slow time base recording; note absence of sustained inward Na⁺ current and reduction of AP overshoot (arrow).
B. Expanded time base. DG mutation reduces contribution of Na⁺ channel activity and slows initial upstroke of AP.



Ionic Basis of DG Cellular Phenotype: A Role for $[Ca^{2+}]_i$

FIGURES 3.7 and 3.8 show the effects of the DG mutation on several key ionic pathways underlying the computed APs. These computations reflect steady-state conditions during a BCL of 3000 ms, but the patterns revealed are the same as those that occur in DG-induced pause-dependent AP prolongation (data not shown). FIGURE 3.7 focuses on computed Na^+ channel currents and illustrates current during the AP plateau (A) as well as, on an expanded time scale, during the upstroke (B). As predicted by the voltage-clamp data, the DG mutation does not promote sustained inward Na^+ current that would account for AP prolongation (A, lower row). In fact, the computations show that the overall effect of this mutation is to reduce the contribution of Na^+ channel activity to the initial upstroke and overshoot (arrow) of the AP. FIGURE 3.8 illustrates DG mutation-induced changes in other pathways that occur during the duration of the AP. The computations reveal an increase in Ca^{2+} influx through L-type Ca^{2+} channels, an increase in the magnitude of the transient change in $[Ca^{2+}]_i$, changes in Na^+/Ca^{2+} exchange current, and an initial reduction followed by prolonged activation of the slowly activating K^+ channel current, I_{Ks} .

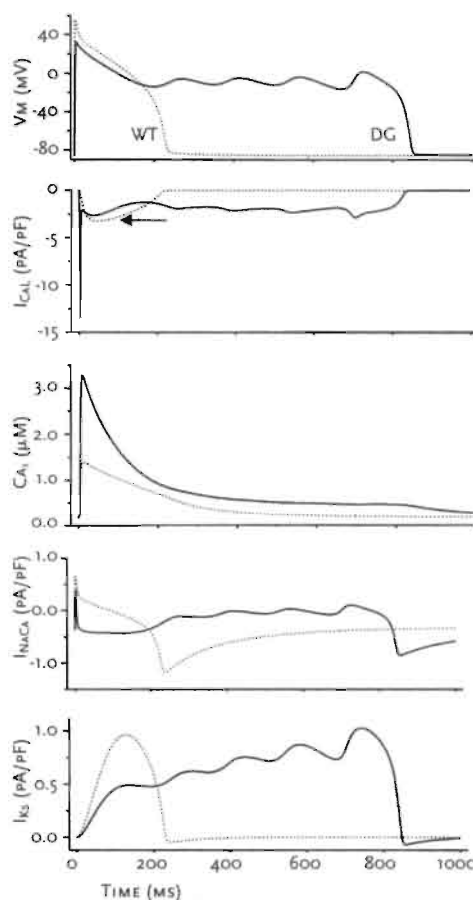
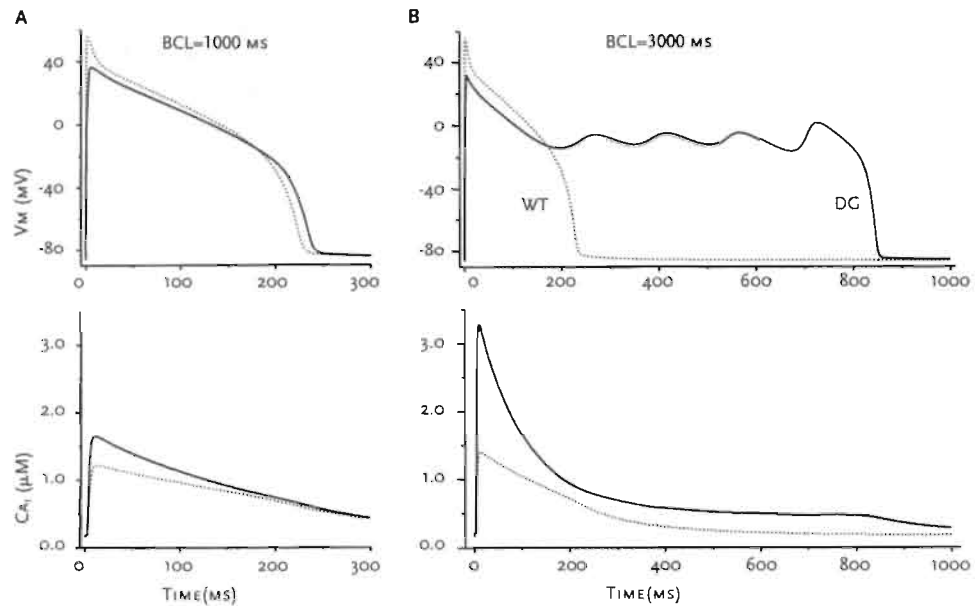


FIGURE 3.8
DG mutation affects Ca^{2+} -sensitive pathways. Simulation of effects of DG mutation on APs and key underlying pathways that occur at BCL of 3000 ms. Shown are following computations for cells expressing WT (dotted lines) and DG (solid lines) Na^+ channels (top to bottom): membrane potential; L-type Ca^{2+} channel currents; intracellular free Ca^{2+} ; Na^+/Ca^{2+} exchange current; and delayed rectifier current, I_{Ks} . Arrow in second row indicates peak Ca^{2+} influx with WT channel.

FIGURE 3.9
 DG-induced changes in Ca^{2+}
 transient are heart rate-
 dependent. Computed APs (top)
 and free calcium transients
 (bottom) shown for 1000 ms (A)
 and 3000 ms (B) BCLs.



DG-Induced Changes in $[\text{Ca}^{2+}]$; Determine Frequency-dependent APD Prolongation

Perhaps the most prominent feature of the DG cellular phenotype predicted from these computations is the marked dependence of APD on heart rate (FIGURE 3.5).

FIGURE 3.9 shows marked DG mutation-induced changes in the calcium transient that are steeply frequency-dependent. At low stimulation frequencies (long BCLs), the calcium transient in cells expressing DG Na^+ channels is increased in both amplitude and duration. At faster heart rates (BCLs on the order of 1000 ms), there is little difference between calcium transients of WT and DG-expressing cells (A). The computations thus suggest a complex calcium-dependent pathway regulating APD that becomes altered, as described above, by DG-induced changes in calcium entry. Because the effects of these changes on the calcium transient are predicted to be steeply frequency-dependent, the calculations suggest a strong interdependence on the filling and subsequent emptying of intracellular calcium stores in this process.

Discussion

Sustained Na⁺ Channel Current Is Not Necessary to Prolong the Ventricular AP

The major finding reported in this study is the fact that biophysical properties of DG mutant Na⁺ channel α -subunits prolong computer-simulated ventricular APs, even though this mutation does not promote sustained Na⁺ channel current during the AP plateau phase. This study thus extends our understanding of the molecular basis of the disease phenotype, the prolonged QT-intervals, and confirms the importance of computational studies in bridging information relating functional changes in individual ion channel subunits to predictions of cellular and even system phenotypes.

The plateau phase of the cardiac ventricular AP is maintained by a delicate balance between inward and outward movement of ions, and even very small changes in ionic currents during the plateau are expected to have marked effects on APD (4,23). The functional properties of channels encoded by DG mutant α -subunits have defied interpretation within a framework that requires direct mutation-dependent increase in Na⁺ channel current during the AP plateau, because this mutation does not promote sustained Na⁺ channel activity in the face of cellular depolarization (11). Instead, the most prominent characteristics of DG channels are a negative shift in channel availability as a function of membrane potential and a speeding of the kinetics of the onset of inactivation. However, our computations reveal the importance of these biophysical changes in channel properties to events that determine the duration of the AP and show that events that occur during the initial 5 ms of the AP can have profound effects on electrical activity that occurs during the following several hundred milliseconds.

DG-Induced Decrease in Na⁺ Channel Activity Leads to an Increase in the [Ca²⁺]_i Transient

FIGURES 3.7, 3.8, and 3.9 provide insight into the mechanism(s) by which the DG mutation delays AP repolarization. Because of the changes in Na⁺ channel kinetics, fewer channels are available for activation at the cellular resting potential, and once opened, these channels inactivate faster than WT channels. This results in a reduced Na⁺ channel current, slower upstroke, and more importantly, a less positive overshoot of the AP (FIGURE 3.7, arrow). The change in dV/dt and overshoot occurs during the very early stages of ventricular depolarization, as seen in FIGURE 3.8, and in turn causes an increase of Ca²⁺ entry via L-type Ca²⁺ channels during this crucial period of electrical activity. The primary

mechanism underlying this effect is not a change in gating parameters for Ca^{2+} channel activation and inactivation, but the effect of the DG mutation on the AP overshoot and subsequent change in the driving force for Ca^{2+} entry via L-type Ca^{2+} channels (not illustrated). With this alteration in Ca^{2+} entry, the model predicts that the subsequent Ca^{2+} transient will be altered in both time and magnitude, and as a result, all $[\text{Ca}^{2+}]_i$ -dependent processes will subsequently be altered (FIGURE 3.8). Two important ionic pathways, the $\text{Na}^+/\text{Ca}^{2+}$ exchanger (24) and the slowly activating delayed K^+ channel current, I_{Ks} (25) are affected (FIGURE 3.8). The result is a net increase of inward plateau current and corresponding increase in APD. The fundamental difference between the generation of the cellular phenotype in the case of the DG mutation compared with previously described LQT-3 mutations is that the increase of inward current does not come from a direct contribution of altered Na^+ channel activity but rather from other pathways.

The computations also reveal a critical role of I_{Ks} in the DG-induced cellular phenotype (FIGURE 3.8) as a result of the reduction in this current that occurs as a consequence of mutation-induced changes in V_m . Thus, although the disease-linked mutation is in the *SCN5A* gene, the cellular phenotype is due in part to changes in activity of channels encoded by LQT-1- and LQT-5-linked genes (26,27).

Relationship Between Cellular and Clinical Phenotypes

The work presented here is the result of incorporation of biophysical properties of human WT and DG mutant Na^+ channels expressed in a mammalian cell line into a computational model that integrates experimental data obtained from a variety of cell types and species (15). Extrapolation of these results to a precise understanding of human pathophysiology is not possible and goes beyond the scope of this study. Qualitative, but not quantitative, conclusions may be drawn from this work. Nevertheless, comparison to appropriate clinical parameters that have been measured for carriers of the DG mutation is important, and in fact, a stringent test of the validity of the methodology.

The model suggests that under steady-state pacing conditions, the Na^+ current is smaller in myocytes expressing DG mutant channels next to WT channels. This will most likely lead to a reduced rate of rise of the AP upstroke (dV/dt) as predicted for the cellular model, and this, in turn, would be expected to be reflected in a widening of the QRS complex on the ECG of mutation carriers. Indeed, DG carriers tend to have wider QRS complexes than control patients (28). The computational work clearly indicates that for this mutation, bradycardia will potentiate APD prolongation. It is interesting to note that heart rates of DG carriers have been found to be slower than those of noncarriers (10). In fact,

in several members of the DG family that have been studied, sinus slowing and even arrest may have been as significant as APD prolongation. This raises the interesting and important question as to a causal relationship between pacing and the DG mutation, a question that certainly is beyond the scope of the present study.

Role of I_{TO} in Modulating the Effect of the DG Mutation on APD

In the computations that we have carried out and reported, we have not included a contribution of the transient outward current (I_{TO}). We did, however, test for its effects in calculations, which we have not illustrated. We find, as might be expected, that if expressed at sufficiently high levels, this current will tend to offset the effects of the DG mutation and modify its influence on APD. Thus, cells expressing I_{TO} at the highest densities (epicardial cells) would be expected to have substantially shorter APDs than cells in which I_{TO} is expressed at the lowest densities (endocardial cells), because the additional contribution of DG mutant channels would then follow the same anatomic pattern (20). This pattern of channel expression would thus be expected to favor enhanced T wave dispersion (19) which, interestingly, is what is observed in carriers of the DG mutation (28). Heterogeneity in the expression of ion channel genes, no doubt, remains an important area of investigation that will be needed to provide a causal link between expression of specific gene mutations and generation of the systemic disease phenotype.

Novel Therapeutic Strategies for LQT-3

Our analysis has revealed that beat-dependent changes in intracellular calcium that occur as a consequence of the DG LQT-3 mutation should be considered major factors in generating the disease phenotype (delayed ventricular repolarization) in carriers of this gene defect. This work therefore strongly suggests that a therapeutic strategy that includes inhibition of L-type calcium channel activity may be beneficial for carriers of the DG gene defect.

In summary, our computations show that the biophysical properties of DG mutant channels are sufficient to account for a cellular phenotype consistent with LQT-3: prolongation of the ventricular AP. This occurs despite the absence of mutation-induced sustained Na^+ current. This finding not only is a necessary step in understanding the molecular basis of QT prolongation in carriers of the DG mutation but also raises the possibility that previously overlooked functional properties of other LQT-3 *SCN5A* mutations may also contribute to the disease phenotype and may require further

investigation. Furthermore, our work suggests that novel therapeutic strategies may include modulation of calcium as well as sodium channel activity.

Acknowledgments

This work was supported by US Public Health Service grant R01-HL-568105-02 (Dr Kass). Dr Abriel was supported the Swiss National Foundation for Fellowships in Medicine and Biology, Dr Wehrens by the Dutch foundation De Drie Lichten, and Dr Cabo in part by a research grant of the Whitaker Foundation.

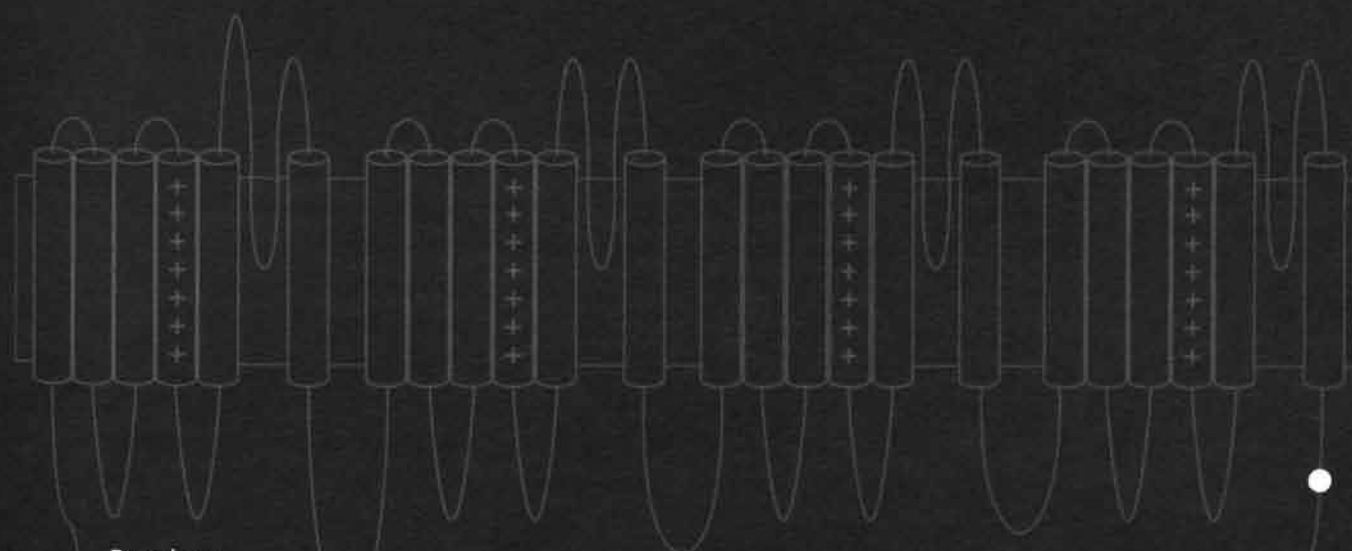
References

1. Moss AJ, Schwartz PJ, Crampton RS, Tzivoni D, Locati EH, MacCluer J, Hall WJ, Weitkamp L, Vincent GM, Garson A Jr. The long-QT syndrome: prospective longitudinal study of 328 families. *Circulation* 1991;84:1136-44.
2. Schwartz PJ, Periti M, Malliani A. The long-QT syndrome. *Am Heart J* 1975;89:378-90.
3. Yan GX, Antzelevitch C. Cellular basis for the Brugada syndrome and other mechanisms of arrhythmogenesis associated with ST-segment elevation. *Circulation* 1999;100:1660-66.
4. Kass RS. Ionic basis of electrical activity in the heart. In: Sperelakis N (ed.) *Physiology and pathophysiology of the heart*. Norwell, Mass. Kluwer Academic 1995:77-90.
5. Viswanathan PC, Rudy Y. Pause induced early afterdepolarizations in the long-QT syndrome: a simulation study. *Cardiovasc Res* 1999;42:530-42.
6. Wang Q, Shen J, Splawski I, Atkinson D, Li Z, Robinson JL, Moss AJ, Towbin JA, Keating MT. *SCN5A* mutations associated with an inherited cardiac arrhythmia, long-QT syndrome. *Cell* 1995;80:805-11.
7. Bennett PB, Yazawa K, Makita N, George AL Jr. Molecular mechanism for an inherited cardiac arrhythmia. *Nature* 1995;376:683-85.
8. Wang DW, Yazawa K, George AL Jr, Bennett PB. Characterization of human cardiac Na^+ channel mutations in the congenital long-QT syndrome. *Proc Natl Acad Sci U S A* 1996;93:13200-05.
9. Clancy CE, Rudy Y. Linking a genetic defect to its cellular phenotype in a cardiac arrhythmia. *Nature* 1999;400:566-69.
10. Benhorin J, Goldmit M, MacCluer JW, Blangero J, Goffen R, Leibovitch A, Rahat A, Wang Q, Medina A, Towbin J, Kerem B. Identification of a new *SCN5A* mutation associated with the long-QT syndrome. *Hum Mutat* 1998;12:72.
11. An RH, Wang XL, Kerem B, Benhorin J, Medina A, Goldmit M, Kass RS. Novel LQT-3 mutation affects Na^+ channel activity through interactions between α - and β_1 -subunits. *Circ Res* 1998;83:141-46.
12. Wei J, Wang DW, Alings M, Fish F, Wathen M, Roden DM, George AL Jr. Congenital long-QT syndrome caused by a novel mutation in a conserved acidic domain of the cardiac Na^+ channel. *Circulation* 1999;99:3165-71.
13. Kambouris NG, Nuss HB, Johns DC, Tomaselli GF, Marban E, Balser JR. Phenotypic characterization of a novel long-QT syndrome mutation (R1623Q) in the cardiac sodium channel. *Circulation* 1998;97:640-44.
14. Makita N, Shirai N, Nagashima M, Matsuoka R, Yamada Y, Tohse N, Kitabatake A. A *de novo* missense mutation of human cardiac Na^+ channel exhibiting novel molecular mechanisms of long-QT syndrome. *FEBS Lett* 1998;423:5-9.
15. Luo CH, Rudy Y. A dynamic model of the cardiac ventricular action potential, II: afterdepolarizations, triggered activity, and potentiation. *Circ Res* 1994;74:1097-113.
16. An RH, Bangalore R, Rosero SZ, Kass RS. Lidocaine block of LQT-3 mutant human Na^+ channels. *Circ Res* 1996;79:103-08.
17. Viswanathan PC, Shaw RM, Rudy Y. Effects of I_{Kf} and I_{Ks} heterogeneity on action potential duration and its rate dependence: a simulation study. *Circulation* 1999;99:2466-74.
18. Antzelevitch C. Ion channels and ventricular arrhythmias: cellular and ionic mechanisms underlying the Brugada syndrome. *Curr Opin Cardiol* 1999;14:274-79.

19. Antzelevitch C, Shimizu W, Yan GX, Sicouri S. Cellular basis for QT dispersion. *J Electrocardiol* 1998;30(suppl):168-75.
20. Antzelevitch C, Sicouri S, Litovsky SH, Lukas A, Krishnan SC, Di Diego JM, Gintant GA, Liu DW. Heterogeneity within the ventricular wall: electrophysiology and pharmacology of epicardial, endocardial, and M cells. *Circ Res* 1991;69:1427-49.
21. Hamill OP, Marty A, Neher E, Sakmann B, Sigworth FJ. Improved patch-clamp techniques for high-resolution current recording from cells and cell-free membrane patches. *Pflügers Arch* 1981;391:85-100.
22. Nagatomo T, Fan Z, Ye B, Tonkovich GS, January CT, Kyle JW, Makielski JC. Temperature dependence of early and late currents in human cardiac wild-type and long-QT Δ KPQ Na⁺ channels. *Am J Physiol* 1998;275:H2016-24.
23. Weidmann S. Effect of current flow on the membrane potential of cardiac muscle. *J Physiol* 1951;115:227-36.
24. Blaustein MP, Lederer WJ. Sodium/calcium exchange: its physiological implications. *Physiol Rev* 1999;79:763-854.
25. Toshe N. Calcium-sensitive delayed rectifier potassium current in guinea pig ventricular cells. *Am J Physiol* 1990;258:H1200-07.
26. Splawski I, Tristani-Firouzi M, Lehmann MH, Sanguinetti MC, Keating MT. Mutations in the *hmnK* gene cause long-QT syndrome and suppress I_{Ks} function. *Nat Genet* 1997;17:338-40.
27. Wang Q, Curran ME, Splawski I, Burn TC, Millholland JM, VanRaay TJ, Shen J, Timothy KW, Vincent GM, de Jager T, Schwartz PJ, Toubin JA, Moss AJ, Atkinson DL, Landes GM, Connors TD, Keating MT. Positional cloning of a novel potassium channel gene: *KvLQT1* mutations cause cardiac arrhythmias. *Nat Genet* 1996;12:17-23.
28. Benhorin J, Taub R, Goldmit M, Kerem B, Kass RS, Windman I, Medina A. Effects of flecainide in patients with new *SCN5A* mutation: mutation-specific therapy for long-QT syndrome? *Circulation* 2000;101:1698-706.
29. Luo CH, Rudy Y. A dynamic model of the cardiac ventricular action potential. I. Simulations of ionic currents and concentration changes. *Circ Res* 1994;74:1071-96.
30. Zeng J, Laurita KR, Rosenbaum DS, Rudy Y. Two components of the delayed rectifier K⁺ current in ventricular myocytes of the guinea pig type. Theoretical formulation and their role in repolarization. *Circ Res* 1995;77:140-52.
31. Viswanathan PC, Shaw RM, Rudy Y. Effects of I_{Kr} and I_{Ks} heterogeneity on action potential duration and its rate dependence: a simulation study. *Circulation* 1999;99:2466-74.
32. Liu DW, Antzelevitch C. Characteristics of the delayed rectifier current (I_{Kr} and I_{Ks}) in canine ventricular epicardial, midmyocardial, and endocardial myocytes. A weaker I_{Ks} contributes to the longer action potential of the M cell. *Circ Res* 1995;76:351-65.

Chapter 4

Molecular Pharmacology of the Sodium Channel Mutation D1790G
Linked to the Long-QT Syndrome



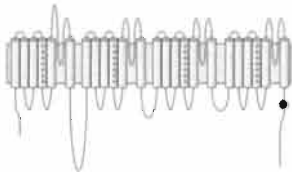
Based on:

Abriel H*, WEHRENS XHT*, Benhorin J, Kerem B, Kass RS. Molecular pharmacology of the sodium channel mutation D1790G linked to the long-QT syndrome.

Circulation 2000;102:921-25.

* contributed equally

Abstract



BACKGROUND. Multiple mutations of *SCN5A*, the gene that encodes the human Na^+ channel α -subunit, are linked to one form of the congenital long-QT syndrome (LQT-3). D1790G (DG), an LQT-3 mutation of the C-terminal region of the Na^+ channel α -subunit, alters steady-state inactivation of expressed channels but does not promote sustained Na^+ channel activity. Recently, flecainide, but not lidocaine, has been found to correct the disease phenotype, delayed ventricular repolarization, in DG carriers.

METHODS AND RESULTS. To understand the molecular basis of this difference, we studied both drugs using wild-type (WT) and mutant Na^+ channels expressed in HEK 293 cells. The DG mutation conferred a higher sensitivity to lidocaine (EC_{50} , WT=894 and DG=205 $\mu\text{mol/L}$) but not flecainide tonic block in a concentration range that is not clinically relevant. In contrast, in a concentration range that is therapeutically relevant, DG channels are blocked selectively by flecainide (EC_{50} , WT=11.0 and DG=1.7 $\mu\text{mol/L}$), but not lidocaine (EC_{50} , WT=318 and DG=176 $\mu\text{mol/L}$) during repetitive stimulation.

CONCLUSIONS. These results (1) demonstrate that the DG mutation confers a unique pharmacological response on expressed channels; (2) suggest that flecainide use-dependent block of DG channels underlies its therapeutic effects in carriers of this gene mutation; and (3) suggest a role of the Na^+ channel α -subunit C-terminus in the flecainide/channel interaction.

Introduction

The congenital long-QT syndrome is an inherited cardiac disorder defined by prolonged ventricular repolarization, recurrent syncope, a propensity to polymorphous ventricular tachycardia (torsades de pointes), and sudden death (1,2). Molecular genetic studies have identified defects in the α -subunit of the cardiac voltage-gated ion channel (*SCN5A*) that are linked to one form of the disease: LQT-3 (3). Initial functional analysis of most *SCN5A* mutations has revealed mutant Na^+ channels that fail to inactivate completely on prolonged depolarization (4-8), a property sufficient to delay repolarization of the ventricular action potential and increase vulnerability of the heart to arrhythmias (9). In contrast, the D1790G (DG) *SCN5A* mutation (10), located in the cytoplasmic region of the α -subunit C-terminus, causes a marked negative shift in the relationship between channel availability and membrane potential and alters inactivation kinetics of mutant channels (11) but does not promote sustained inward current (7).

Pharmacological analysis of LQT-3 mutant channels expressed heterologously has provided evidence that sodium channel blockers that interact with either the inactivated or open state of the channel (12,13) effectively block maintained current conducted by mutant channels (14-20), shorten action potential duration in cellular studies (21,22), and in preliminary studies correct QT prolongation in patients (22,23).

Because the biophysical properties of the DG mutation do not promote maintained current during the action potential plateau phase, it had been suggested that agents such as lidocaine would not be effective in correcting the disease phenotype linked to this mutation (7). Clinical studies (24) have confirmed this prediction but, in addition, have shown that flecainide, which preferentially blocks open but not inactivated channels (25), is effective in correcting DG-induced QT prolongation in patients carrying the DG gene defect. However, the mechanism underlying this mutation-specific therapeutic efficacy has not yet been determined.

Here, we report the pharmacological profile of DG channels expressed in a mammalian cell line and show that this point mutation confers a flecainide sensitivity that is distinct from wild type (WT) and at least one other LQT-3 mutant channel (20). Our results reveal marked drug-specific differences in channel modulation that are consistent with the clinical efficacy of both lidocaine and flecainide and suggest that over concentration ranges that are used clinically, it is the marked difference in flecainide's use-dependent block (UDB) of DG compared with WT channels that underlies its therapeutic

efficacy. The results of this study provide further support for the approach of mutation-specific pharmacology as a basis for the management of inherited cardiac arrhythmias.

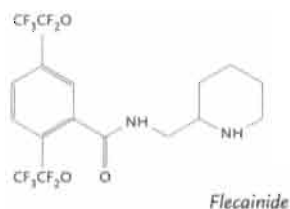
Materials and Methods

Expression of Recombinant Na⁺ Channels

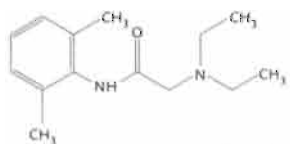
HEK 293 cells (Cold Spring Harbor Laboratories) were grown under culture conditions and transfected with equal amounts of Na⁺ channel α - (WT or DG, respectively), h β 1-, and/or h β 2-subunit cDNAs subcloned individually into the pcDNA3 (Invitrogen) vector (total cDNA, 2.5 μ g) by a lipofection procedure previously described by us (7). Control experiments (data not shown) indicated no significant differences in channel activity with or without drug for these subunit combinations. β -Subunit cDNAs were gifts of Drs L. Isom (University of Michigan, h β 2) and A. George (Vanderbilt University, h β 1), and the DG mutation was constructed as previously described (7).

Electrophysiology

Membrane currents were measured by whole-cell patch-clamp procedures (26) with Axopatch 200B amplifiers (Axon Instruments) and the following solutions (mmol/L): internal: CsCl 60, aspartic acid 50, CaCl₂ 1, MgCl₂ 1.2, HEPES 10, EGTA 11, and Na₂ATP 5; pH corrected to 7.2 with CsOH; external: NaCl 130, CsCl 5, CaCl₂ 2, MgCl₂ 1.2, HEPES 10, and glucose 5; pH corrected to 7.4 with CsOH. Drug (Sigma Chemical Co.) solutions were made from 10 mmol/L (FLECAINIDE) or 100 mmol/L (LIDOCAINE) stock solutions in H₂O. Experiments were carried out with pClamp7 software (Axon Instruments), and data were analyzed with Origin software (Microcal Software). Unless otherwise specified in the figure legends, experiments were carried out at room temperature (22°C). Measurements at higher temperature were performed with a solution heater (In-line Heater SH-27B, Warner Instrument Corp) warming the superfusate to 37°C. Recordings were made during 25 ms test pulses to -10 mV from -100 mV holding potentials. Tonic block (TB) was measured at 0.033 Hz after steady-state was achieved in the presence of drug (1 minute for lidocaine and 2 to 4 minutes for flecainide). Steady-state inactivation was measured with 5 second conditioning pulses followed by a test pulse (-10 mV), with an interpulse interval of 30 seconds. Steady-state UDB was reached in response to trains of variable numbers of



Flecainide



Lidocaine

pulses (100 to 600, -10 mV) at frequencies indicated in the figure legends. UDB was measured as block induced by pulse trains relative to TB for a given drug concentration. UDB data were normalized to currents recorded with the same protocols but in the absence of drug.

Data are represented as mean \pm SEM. Two-tailed Student's *t*-test was used to compare means; a value of $P < 0.05$ was considered statistically significant.

Results

TB of WT and Mutant Channels

Because the DG mutation alters the voltage-dependence of steady-state inactivation of expressed channels (7), we first tested for differences between the interactions of lidocaine and flecainide with the inactivated state of WT and DG channels. FIGURE 4.1 shows that lidocaine, but not flecainide, induces marked hyperpolarizing shifts in the steady-state inactivation relationship for both WT and DG channels. Furthermore, the effects of lidocaine on inactivation are approximately the same for WT and DG channels.

The lidocaine-selective shift in inactivation predicts greater TB of DG versus WT channels by lidocaine, but not flecainide, at physiologically relevant holding potentials. This prediction is confirmed in the experiments summarized in FIGURE 4.2 However, at clinically relevant concentrations (27) of lidocaine (30 $\mu\text{mol/L}$) and flecainide (3 $\mu\text{mol/L}$), neither drug discriminates between WT and DG channels on the basis of TB.

UDB: Distinctions Between WT and DG Channels

Therefore, we next compared block that accumulates with repetitive activity when DG mutant and WT channels are exposed to lidocaine and flecainide (FIGURE 4.3). Again at clinically relevant concentrations (30 $\mu\text{mol/L}$), there is no difference between lidocaine block of WT and DG channels (FIGURE 4.3A). In contrast, there is a statistically significant ($P < 0.001$) difference between flecainide UDB of DG and WT channels at the clinically relevant concentration of 3 $\mu\text{mol/L}$. This difference is evident over a broad concentration range: EC_{50} for flecainide UDB of DG channels is roughly 5 times lower than for block of WT channels (FIGURE 4.3B). In contrast, UDBs of WT or DG channels by lidocaine are

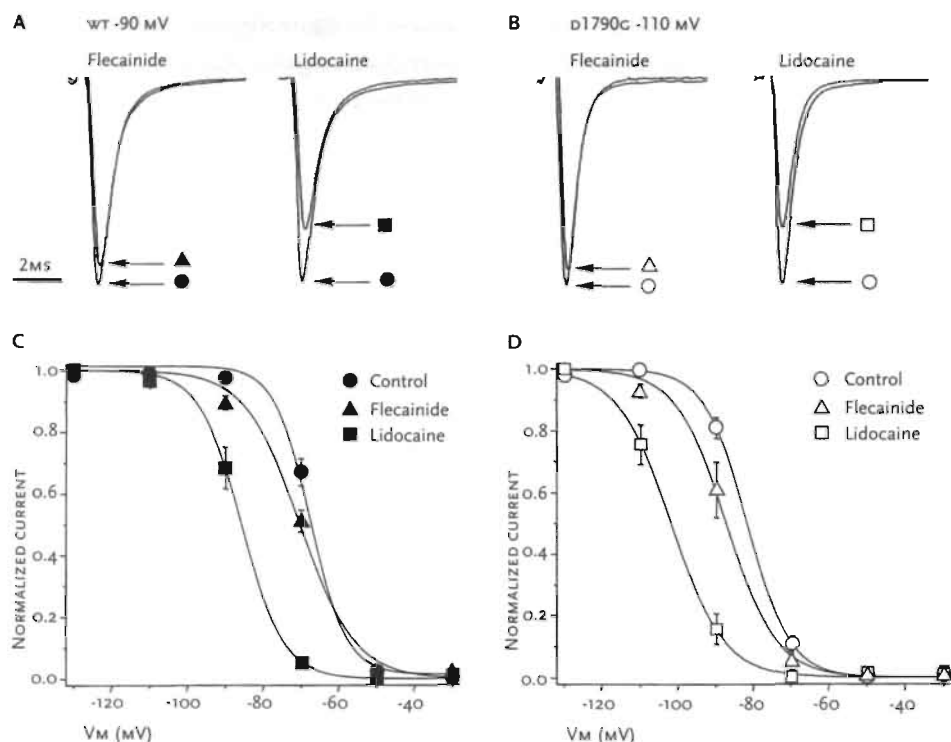


FIGURE 4.1

Effects of flecainide and lidocaine on steady-state inactivation of WT and DG channels. Steady-state availability of channels was measured (Methods) in absence and presence of each drug. **A** and **B**, Current traces, normalized to peak drug-free currents, illustrate effects of lidocaine (300 $\mu\text{mol/L}$) and flecainide (30 $\mu\text{mol/L}$). Arrows indicate drug-induced changes in peak currents for each condition. **C** and **D**, Averaged steady-state availability curves are shown in absence (circles) and presence of lidocaine (300 $\mu\text{mol/L}$, squares) and flecainide (30 $\mu\text{mol/L}$, triangles) for WT (**C**) and DG (**D**) channels. Na^+ currents elicited by -10 mV test pulses were normalized to largest currents obtained in control conditions from hyperpolarized holding potentials. Graphs show normalized current plotted against conditioning pulse voltage. Smooth lines are according to $1/[1+\exp\{(V_c-V_{1/2})/k\}]$, where V_c is conditioning potential, $V_{1/2}$ is voltage for which half the channels are not available, and k is the slope factor. $V_{1/2}$ (mV) for WT is -66.2 ± 0.9 for control, -69.8 ± 0.9 with flecainide, and -85.7 ± 1.4 with lidocaine; $V_{1/2}$ (mV) for DG is -81.8 ± 1.4 for control, -87.3 ± 2.4 with flecainide, and -102.5 ± 2.7 with lidocaine; $n=4$ cells per condition.

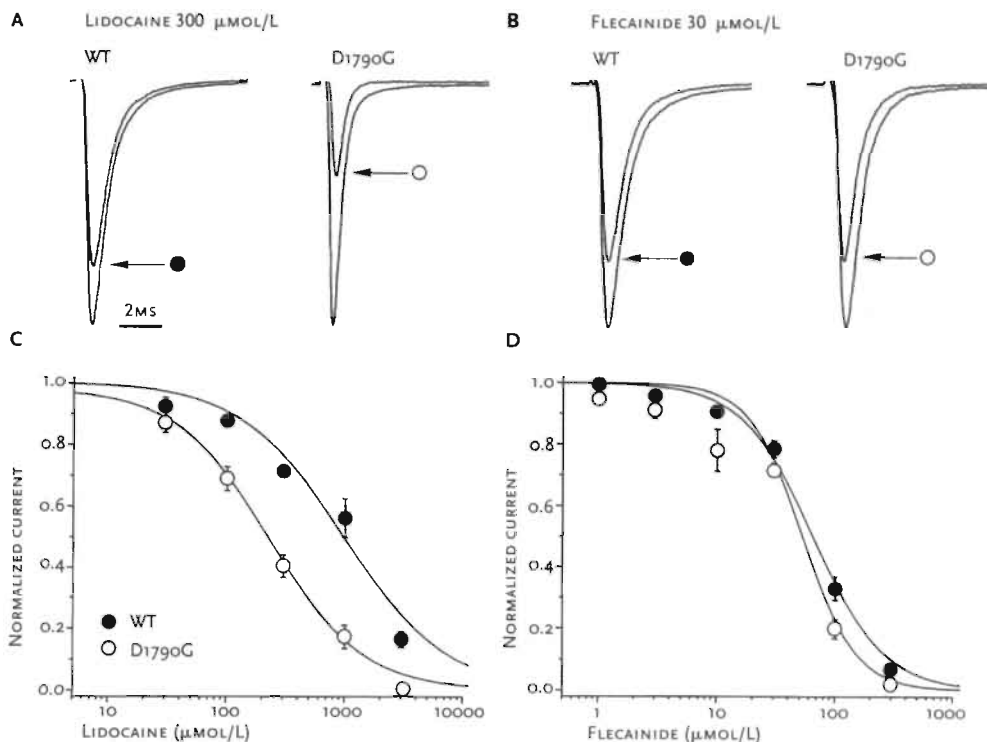


FIGURE 4.2

TB of WT and DG mutant Na^+ channels. **A** and **B**, Inhibition of Na^+ current elicited in HEK cells expressing WT or DG channels with lidocaine (**A**) or flecainide (**B**). Traces show currents in control solution and after steady-state TB was attained (arrows) 2 to 4 minutes after cell superfusate was changed to one containing lidocaine (300 $\mu\text{MOL/L}$) or flecainide (30 $\mu\text{MOL/L}$), respectively. **C** and **D**, Concentration-dependence of TB of WT (●) and DG (○) channels by lidocaine (**C**) and flecainide (**D**). Graph shows peak current after drug application, normalized to peak current in absence of drug, plotted as a function of drug concentration. Smooth lines are according to $1/(1+[drug]/EC_{50})^n$. EC_{50} for lidocaine is 894 (WT) and 205 (DG); EC_{50} for flecainide is 59.3 (WT) and 48.2 (DG); $n=3$ to 6 cells per condition.

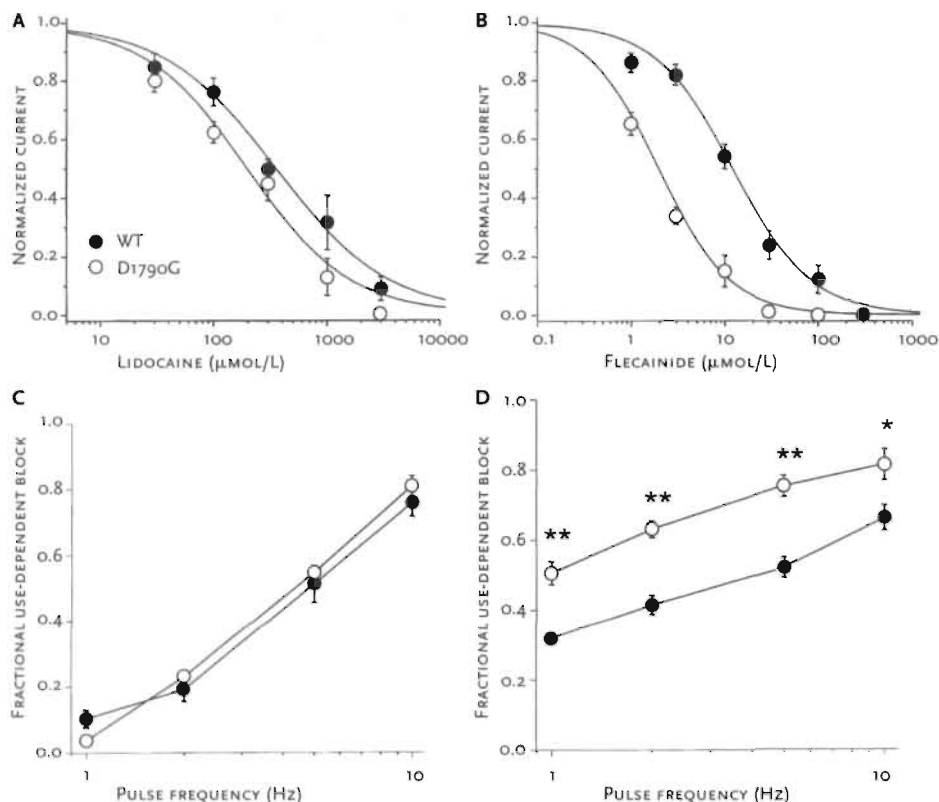


FIGURE 4.3

DG mutation increases sensitivity of channels to UDB by flecainide but not lidocaine. Concentration dependence of UDB of WT (●) and DG (○) channels by lidocaine (A) and flecainide (B). Currents were evoked by pulses applied at a frequency of 5 Hz in presence of drugs until steady-state UDB was achieved and normalized to TB levels before high-frequency train protocol was started. Smooth lines are according to $1/(1+[drug]/EC_{50})^n$. EC_{50} for lidocaine is 318 (WT) and 176 (DG); EC_{50} for flecainide is 11.0 (WT) and 1.7 (DG); $n=3$ to 6 cells per condition. C and D, Frequency-dependence of lidocaine and flecainide block of WT (●) and DG (○) channels at fixed drug concentrations. Trains of 100 to 600 pulses were applied at various frequencies in presence of lidocaine (300 μmol/L, C) or flecainide (10 μmol/L, D). Graphs show peak current during steady-state UDB normalized to peak current during first pulse of train plotted against stimulus frequency; $n=4$ cells per condition. * $P<0.05$, ** $P<0.01$.

approximately the same over all concentrations tested. In addition, the distinction in use-dependent drug action between WT and DG channels is retained when the frequency range of pulse application is extended to a broader frequency range (FIGURE 4.3C AND 4.3D).

Effect of DG Mutation on Recovery From Flecainide Block

Block that accumulates as a consequence of repetitive channel activity (UDB) is caused by a balance between the time course of the onset of block (during depolarization) and the recovery from block (during repolarization) (12,13). To understand the marked sensitivity of DG channels to UDB, we next investigated the time course of the recovery from UDB. Here, we focused only on the effects of flecainide, because there was little difference between WT and DG channels in response to UDB by lidocaine (FIGURE 4.3A AND 4.3C).

In these experiments, we applied a “conditioning” train of pulses (to -10 mV, from a -100 mV holding potential) for a fixed duration (25 ms) and frequency (25 Hz) to induce flecainide block of channels. Test pulses were then imposed after variable recovery intervals at holding potential. Currents were normalized to steady-state current levels during slow pacing (once every 30 seconds). Normalized current is plotted against recovery interval. As illustrated in FIGURE 4.4, in the absence of the drug, DG channels tend to recover faster from inactivation that occurs as a consequence of the conditioning train. In the presence of flecainide, repriming of channels is very different: now DG channels recover very slowly. Even after 10 seconds at the holding potential (-100 mV) under pulse-free conditions, only a small fraction of the flecainide-blocked current recovers. This result suggests that the flecainide-bound DG channel is very stable and that infrequent pulsing can still be very effective at accumulating block because once blocked, channels remain nonconducting for tens of seconds.

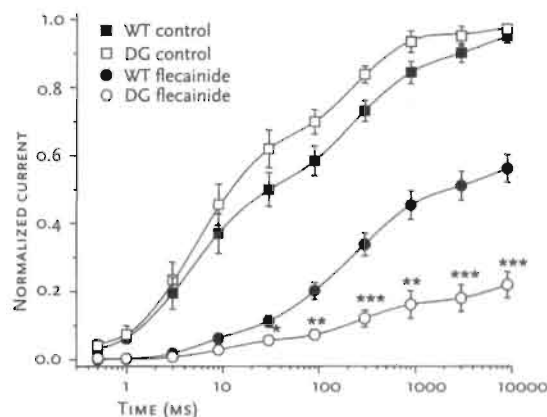


FIGURE 4.4
Effect of DG mutation on time course of recovery from inactivation and flecainide block. UDB of WT (solid symbols) and DG (open symbols) mutant channels was induced before (squares) and after (circles) application of 10 μ M/L flecainide; $n=4$ cells per condition. * $P<0.05$, ** $P<0.01$, *** $P<0.001$.

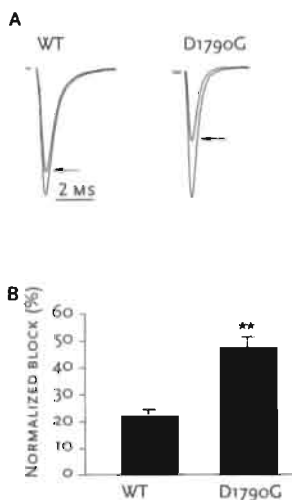


FIGURE 4.5

Preferential flecainide block of DG vs WT channels under physiological conditions.

A. Current traces before and after steady-state UDB (arrows). Shown are superimposed records of first and 100th traces in trains applied to WT (left) and DG (right) channels. **B.** Bar graphs summarize steady-state UDB plotted as fraction of current blocked in response to the pulse train; $n=6$ cells per condition.

** $P<0.01$.

Clinical Efficacy of Flecainide: Distinctions Between UDB of WT and DG Channels

The dramatic slowing of flecainide unblock caused by the DG mutation (FIGURE 4.4) has important implications for the clinical usefulness of this compound in the treatment of LQT-3 in carriers of the DG mutation. Because use-dependent flecainide block discriminates between WT and DG mutant channels (FIGURE 4.3), it is important to demonstrate UDB of DG channels under conditions that more closely resemble those encountered in the heart. Thus, we tested for differences between WT and DG channels in the response to flecainide (3 $\mu\text{mol/L}$), when longer pulses (400 ms), which mimic the duration of action potentials in LQT-3 patients, are applied at a physiological frequency (1 Hz) and temperature (37°C). These experiments (FIGURE 4.5) confirm that, even under these conditions, the extremely slow recovery from flecainide block of DG channels is sufficient to cause significantly greater block of DG versus WT channels.

Discussion

Molecular Basis for Mutation-specific Pharmacology:

Implications for a Role of C-Terminus in Inactivation and Drug Activity

The principal finding of this study is that a LQT-3-linked mutation of the heart α -subunit of the Na^+ channel dramatically and specifically changes the manner by which channels encoded by the mutant gene interact with sodium channel-blocking drugs. The mutation confers a higher sensitivity to UDB by flecainide, but not lidocaine, over a clinically relevant concentration range. Flecainide TB is not affected by the DG mutation. Our findings thus illustrate the importance of investigating mutation-induced changes not only in channel function but also in channel pharmacology.

Voltage-dependent block of Na^+ channel currents by antiarrhythmic drugs is a consequence of distinct interactions with different states of the voltage-gated Na^+ channel. Lidocaine and flecainide differ in their modes of action in that lidocaine interacts preferentially with inactivated channels, and drug block is not necessarily dependent on channel openings (25,28), whereas flecainide requires channels to open and is not dependent on channels entering the inactivated state to promote block (25,29).

We observed that the DG mutation does not influence the interaction of lidocaine with the Na^+ channel, even if TB was greater than for mutant channels (FIGURE 4.2).

Indeed, this effect is explained by the fact that lidocaine shifts the steady-state inactivation curve by the same amount for WT as for the DG mutant channel, but the DG mutation by itself already shifts this curve by -20 mV in the absence of drug. Because flecainide has a much weaker effect on the inactivation curve (FIGURE 4.1), there is little difference between flecainide-induced TB of WT and DG channels. In contrast, the DG mutation markedly increases flecainide UDB of channels, in large part because of the pronounced slowing of the repriming of DG channels in the presence of the drug (FIGURE 4.4).

This specific alteration of the sensitivity to UDB by flecainide is not a general property of all LQT-3 mutant channels. Recently, Nagatomo et al. (20) found that LQT-3 Δ KPQ mutant channels have an intrinsically higher affinity than WT channels to flecainide, but in the case of this mutation, sensitivity to both TB and UDB is increased. Thus, our data indicate that the DG point mutation causes a unique pharmacological response of the expressed channels, which is distinct not only from WT but also from Δ KPQ mutant channels.

The DG mutation is a nonconservative change from an aspartic acid to a glycine only 18 amino acids away from transmembrane segment S6 in the C-terminus of the Na⁺ channel α -subunit, a region of the channel not previously considered to play a major role in the molecular interactions of flecainide (30). Our data clearly show that this is not the case and raise the possibility that other residues of the C-terminus may also be important in determining pharmacological responses of Na⁺ channels. Importantly, one other nonconservative C-terminus LQT-3 mutation (E1784K) has been reported recently (6), and a C-terminus insertion mutation (1795insD) has been linked to both Brugada's syndrome and LQT-3 (31). Our work strongly suggests that these mutations may also modify the interactions of the encoded channels by flecainide (and probably other drugs), raising the possibility of pharmacological targeting of a broad range of mutation-induced phenotypes. As has been shown for Δ KPQ and DG channels, however, determination of the pharmacological profile must be carried out systematically on a mutation-by-mutation basis before this would be possible.

Relationship Between Molecular Pharmacology and Therapeutic Efficacy

Our data on recombinant human Na⁺ channels complement those of Benhorin et al. (24), which have shown that flecainide, but not lidocaine, significantly decreased the QTc interval in DG carriers by 10% but was without effect in control patients. This difference was even more striking when the effect of flecainide on the marked repolarization

heterogeneity seen in DG carriers was considered. Our experiments indicate that over the clinically relevant drug concentration range and under physiological conditions, flecainide discriminates between WT and DG primarily because of the pronounced effect of the DG mutation on flecainide UDB. The correlation between the clinical results and our data strongly suggests that it is this mechanism of action that underlies the therapeutic usefulness of flecainide compared with lidocaine in the treatment of carriers of the DG mutation. Interestingly, flecainide has also recently been shown to be very effective in treating carriers of the Δ KPQ LQT-3 mutation (A.J. Moss, personal communication), even though, as discussed above, the interactions of flecainide with Δ KPQ and DG mutant channels differ. In the case of both channel defects, however, recovery from the drug-blocked state is markedly slowed compared with WT channels, and it may be this common mode of action that makes this drug so useful as a therapeutic tool in the treatment of carriers of these gene defects.

In summary, we have found that the LQT-3 DG mutation changes the pharmacological response of encoded channels in a manner that differs not only from WT but also from other LQT-3 mutant channels. The pharmacological profile of DG channels shows distinct changes that occur over a therapeutically relevant concentration range. Our data provide further support for the usefulness of a mutation-specific pharmacological approach for the management of distinct inherited ion channel defects.

Acknowledgments

This work was supported by US Public Health Service grant R01-HL-568105-02 (Dr Kass). Dr Abriel was supported by the Swiss National Foundation for Fellowships in Medicine and Biology, and Dr Wehrens by the Dutch foundation De Drie Lichten.

References

1. Moss AJ, Schwartz PJ, Crampton RS, Tzivoni D, Locati EH, MacCluer J, Hall WJ, Weitkamp L, Vincent GM, Garson A Jr. The long-QT syndrome: prospective longitudinal study of 328 families. *Circulation* 1991;84:1136-44.
2. Schwartz PJ, Periti M, Malliani A. The long-QT syndrome. *Am Heart J* 1975;89:378-90.
3. Wang Q, Shen J, Splawski I, Atkinson D, Li Z, Robinson JL, Moss AJ, Towbin JA, Keating MT. *SCN5A* mutations associated with an inherited cardiac arrhythmia, long QT-syndrome. *Cell* 1995;80:805-11.
4. Bennett PB, Yazawa K, Makita N, George AL Jr. Molecular mechanism for an inherited cardiac arrhythmia. *Nature* 1995;376:683-85.
5. Wang DW, Yazawa K, George AL Jr, Bennett PB. Characterization of human cardiac Na^+ channel mutations in the congenital long QT-syndrome. *Proc Natl Acad Sci U S A* 1996;93:13200-05.
6. Wei J, Wang DW, Alings M, Fish F, Wathen M, Roden DM, George AL Jr. Congenital long-QT syndrome caused by a novel mutation in a conserved acidic domain of the cardiac Na^+ channel. *Circulation* 1999;99:3165-71.
7. An RH, Wang XL, Kerem B, Benhorin J, Medina A, Goldmit M, Kass RS. Novel LQT-3 mutation affects Na^+ channel activity through interactions between α - and β 1-subunits. *Circ Res* 1998;83:147-46.
8. Kambouris NG, Nuss HB, Johns DC, Tomaselli GF, Marban E, Balser JR. Phenotypic characterization of a novel long-QT syndrome mutation (R1623Q) in the cardiac sodium channel. *Circulation* 1998;97:640-44.
9. Clancy CE, Rudy Y. Linking a genetic defect to its cellular phenotype in a cardiac arrhythmia. *Nature* 1999;400:566-69.
10. Benhorin J, Goldmit M, MacCluer JW, Blangero J, Goffen R, Leibovitch A, Rahat A, Wang Q, Medina A, Towbin J, Kerem B. Identification of a new *SCN5A* mutation associated with the long-QT syndrome. *Hum Mutat* 1998;12:72.
11. Wehrens XHT, Abriel H, Cabo C, Benhorin J, Kass RS. Arrhythmogenic mechanism of an LQT-3 mutation of the human heart Na^+ channel α -subunit: a computational analysis. *Circulation* 2000;102:584-90.
12. Hille B. Local anesthetics: hydrophilic and hydrophobic pathways for the drug-receptor reaction. *J Gen Physiol* 1977;69:497-515.
13. Hondeghem LM, Katzung BG. Time- and voltage-dependent interactions of antiarrhythmic drugs with cardiac sodium channels. *Biochim Biophys Acta* 1977;472:373-98.
14. An RH, Bangalore R, Rosero SZ, Kass RS. Lidocaine block of LQT-3 mutant human Na^+ channels. *Circ Res* 1996;79:103-08.
15. Compton SJ, Lux RL, Ramsey MR, Strelich KR, Sanguinetti MC, Green LS, Keating MT, Mason JW. Genetically defined therapy of inherited long-QT syndrome: correction of abnormal repolarization by potassium. *Circulation* 1996;94:1018-22.
16. Dumaine R, Wang Q, Keating MT, Hartmann HA, Schwartz PJ, Brown AM, Kirsch GE. Multiple mechanisms of Na^+ channel linked long-QT syndrome. *Circ Res* 1996;78:916-24.
17. Priori SG, Napolitano C, Cantu F, Brown AM, Schwartz PJ. Differential response to Na^+ channel blockade, β -adrenergic stimulation, and rapid pacing in a cellular model mimicking the *SCN5A* and *HERG* defects present in the long-QT syndrome. *Circ Res* 1996;78:1009-15.

18. Wang DW, Yazawa K, Makita N, George AL Jr, Bennett PB. Pharmacological targeting of long-QT mutant sodium. *J Clin Invest* 1997;99:1714-20.
19. Dumaine R, Kirsch GE. Mechanism of lidocaine block of late current in long-QT mutant Na⁺ channels. *Am J Physiol* 1998;274:H477-87.
20. Nagatomo T, January CT, Makielski JC. Preferential block of late sodium current in the LQT-3 ΔKPQ mutant by the class IC antiarrhythmic flecainide. *Mol Pharmacol* 2000;57:101-07.
21. Shimizu W, Antzelevitch C. Sodium channel block with mexiletine is effective in reducing dispersion of repolarization and preventing torsades de pointes in LQT-2 and LQT-3 models of the long-QT syndrome. *Circulation* 1997;96:2038-47.
22. Schwartz PJ, Priori SG, Locati EH, Napolitano C, Cantu F, Towbin JA, Keating MT, Hammoude H, Brown AM, Chen LS. Long-QT syndrome patients with mutations of the SCN5A and HERG genes have differential responses to Na⁺ channel blockade and to increases in heart rate: implications for gene-specific therapy. *Circulation* 1995;92:3381-86.
23. Zareba W, Moss AJ, Rosero SZ, Hajj-Ali R, Konecki J, Andrews M. Gene-specific therapy for long-QT syndrome: QT shortening with lidocaine and tocainide in patients with mutation of the sodium channel gene. *Ann Noninvas Electrocardiol* 1997;2:274-78.
24. Benhorin J, Taub R, Goldmit M, Kerem B, Kass RS, Windman I, Medina A. Effects of flecainide in patients with new SCN5A mutation: mutation-specific therapy for long-QT syndrome? *Circulation* 2000;101:1698-706.
25. Ragsdale DS, McPhee JC, Scheuer T, Catterall WA. Common molecular determinants of local anesthetic, antiarrhythmic, and anticonvulsant block of voltage-gated Na⁺ channels. *Proc Natl Acad Sci U S A* 1996;93:9270-75.
26. Hamill OP, Marty A, Neher E, Sakmann B, Sigworth FJ. Improved patch-clamp techniques for high-resolution current recording from cells and cell-free membrane patches. *Pflugers Arch* 1981;391:85-100.
27. Marcus FI, Opie LH. Antiarrhythmic agents. In: Opie LH (ed.) *Drugs for the heart*. Philadelphia, PA: WB Saunders; 1997:207-47.
28. Bean BP, Cohen CJ, Tsien RW. Lidocaine block of cardiac sodium channels. *J Gen Physiol* 1983;81:613-42.
29. Anno T, Hondeghem LM. Interactions of flecainide with guinea pig cardiac sodium channels: importance of activation unblocking to the voltage dependence of recovery. *Circ Res* 1990;66:789-803.
30. Catterall WA. Molecular properties of sodium and calcium channels. *J Bioenerg Biomembr* 1996;28:219-30.
31. Bezzina C, Veldkamp MW, Van den Berg MP, Postma AV, Rook MB, Viersma JW, Van Langen IM, Tan-Sindhunata G, Bink-Boelkens MT, Van der Hout AH, Mannens MM, Wilde AA. A single Na⁺ channel mutation causing both long-QT and Brugada syndromes. *Circ Res* 1999;85:1206-13.

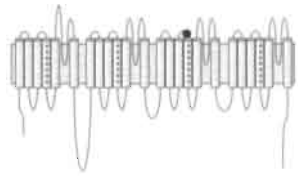
Chapter 5

Novel Arrhythmogenic Mechanism Revealed by a
Long-QT Syndrome Mutation in the Cardiac Na⁺ Channel

Based on:

Abriel H, Cabo C, WEHRENS XHT, Rivolta I, Motoike HK, Memmi M, Napolitano C, Priori SG, Kass RS. Novel Arrhythmogenic Mechanism Revealed by a Long-QT Syndrome Mutation in the Cardiac Na⁺ Channel. *Circ Res* 2001;88:740-45.

Abstract



Variant 3 of the congenital long-QT syndrome (LQT-3) is caused by mutations in the gene encoding the α -subunit of the cardiac Na^+ channel. In the present study, we report a novel LQT-3 mutation, E1295K (EK), and describe its functional consequences when expressed in HEK293 cells.

The clinical phenotype of the proband indicated QT-interval prolongation in the absence of T wave morphological abnormalities and a steep QT/R-R relationship, consistent with an LQT-3 lesion. However, biophysical analysis of mutant channels indicates that the EK mutation changes channel activity in a manner that is distinct from previously investigated LQT-3 mutations.

The EK mutation causes significant positive shifts in the half-maximal voltage ($V_{1/2}$) of steady-state inactivation and activation (+5.2 and +3.4 mV, respectively). These gating changes shift the window of voltages over which Na^+ channels do not completely inactivate without altering the magnitude of these currents. The change in voltage dependence of window currents suggests that this alteration in the voltage dependence of Na^+ channel gating may cause marked changes in action potential duration because of the unique voltage-dependent rectifying properties of cardiac K^+ channels that underlie the plateau and terminal repolarization phases of the action potential. Na^+ channel window current is likely to have a greater effect on net membrane current at more positive potentials (EK channels) where total K^+ channel conductance is low, than at more negative potentials (wild-type channels), where total K^+ channel conductance is high. These findings suggest a fundamentally distinct mechanism of arrhythmogenesis for congenital LQT-3.

Introduction

Electrical activity in the heart is the result of a complex interaction of a large number of ion channels, pumps, and exchange mechanisms that serve unique physiological roles in anatomically distinct regions (1,2). The action potential duration (APD) of ventricular cells is determined by a long-lasting (hundreds of milliseconds) depolarization or plateau phase that is controlled by a fine balance between small inward and outward ionic currents and during which there is little change in membrane potential (3). Key to an energetically favorable maintenance of depolarization are the voltage-dependent rectification properties of at least two types of potassium channel currents, I_{K1} and I_{Kr} , which restrict outward movement of potassium during the plateau but permit large outward currents during the terminal phases of repolarization as the membrane potential becomes more negative (4,5).

Physiological insight into the roles of ion channels in the control of the human cardiac action potential (AP) plateau phase has grown rapidly during the past 5 years from studies of the congenital long-QT syndrome (LQTS), an inherited cardiac arrhythmia, which is clinically characterized by prolongation of the ECG QT-interval, syncope, and sudden death (6-12). The unexpected importance of Na^+ channel activity to the control of QT-intervals has been revealed by studies of LQT-3, which is caused by mutations in the *SCN5A* gene, which codes for the α -subunit of the cardiac Na^+ channel (8,10,13).

Expression of LQT-3 mutant channels in heterologous systems has revealed mutation-induced channel activity that either directly (14-16), or indirectly (17-20) causes a small increase in net inward current over the voltage range and time course of the AP plateau. Computational analysis has shown that this increase in inward current is sufficient to explain the cellular phenotype of APD prolongation (17,21). Nevertheless, not all LQT-3 mutations alter Na^+ channel functional properties in the same manner, and distinction in mutation-induced changes in channel properties is important to document, not only because of the possibility of mutation-specific clinical phenotypes but also because such changes may have implications for therapeutic intervention.

In the present study, we report the biophysical consequences of a novel LQT-3 mutation that change a conserved negative into a positive amino acid (E1295K [EK]) in a region immediately adjacent to the extracellular portion of the S4 segment of channel domain III (DIIS4). Expression of mutant channels in a mammalian cell line indicates that the primary effect of this mutation is to cause small positive shifts in the voltage dependence of both activation and inactivation gating of the channel, which, in turn, shift

the window of voltages over which noninactivating Na^+ channel activity can be measured (22-24). These small changes in the voltage dependence of Na^+ channel gating occur over the plateau range of membrane potentials for which two cardiac K^+ channel currents, I_{K1} and I_{Kr} , show strong inward rectification (4,25-32). Window current that flows during the terminal phase of repolarization (wild-type [WT] channels), where rectification of I_{K1} and I_{Kr} is being relieved, is likely to be less effective than window current that flows over more positive voltages (EK channels) where the conductance of these two channels is minimal. The linkage of these small changes in Na^+ channel gating to delay in ventricular repolarization through LQT-3 confirms the important principle of balance of currents necessary to maintain the AP plateau phase and the role of membrane input impedance in determining the effects of small changes in ion channel currents on cellular electrical activity (3). Thus, our findings are important because they further support the concept of phenotypic heterogeneity of LQT-3 that has to be taken into account when developing new therapeutic strategies for this disorder.

Materials and Methods

Molecular Screening

Genomic DNA was extracted from peripheral blood lymphocytes by standard techniques. The coding region of the *SCN5A* gene encoding the cardiac Na^+ channel was screened using single-strand conformation polymorphism (SSCP) on polymerase chain reaction (PCR)-amplified genomic DNA samples. The abnormal conformers were directly sequenced using an ABI310 genetic analyzer or cloned (TOPO-TA cloning, Invitrogen) and sequenced using plasmid-specific oligonucleotides. SSCP shifts were also checked against a panel of genomic DNA from 300 (600 chromosomes) healthy reference individuals. The presence of a second mutation in the remaining LQTS-related genes (i.e., *KCNQ1*, *HERG*, *KCNE1*, and *KCNE2*) was excluded by molecular analysis.

Mutagenesis and Expression of Recombinant Na^+ Channels

The E1295K mutation of *SCN5A* was engineered into WT cDNA cloned in pcDNA3.1 (Invitrogen) by overlap extension using mutation-specific primers and Quik Change™ Site-Directed Mutagenesis Kit (Stratagene). The presence of the mutation was confirmed by

sequence analysis. WT and mutant Na⁺ channels were expressed in HEK293 cells. Briefly, transient transfections were carried out with equal amounts of Na⁺ channel α -subunit, with h β 1 and/or h β 2 subunits cDNA subcloned individually into the pcDNA3.1 (Invitrogen) vector (total cDNA 2.5 μ g) using a previously described procedure (17). Control experiments (data not shown) indicated no significant differences in channel activity for these subunit combinations. We found no difference in the properties of expressed channels with or without cotransfection of h β 2.

Electrophysiology

Membrane currents were measured using whole-cell patch-clamp procedures, with Axopatch 200B amplifiers (Axon Instruments, Foster City, CA). Recordings were made at room temperature (22°C) using an internal solution containing (mmol/L) CsCl 60, cesium aspartate 80, EGTA 11, MgCl₂ 1, CaCl₂ 1 (effective free calcium 100 nmol/L), HEPES 10, and Na₂-ATP 5, pH adjusted to 7.2 with CsOH. In experiments recording I/V curves, external Na⁺ was reduced to 30 mmol/L using n-methyl-glucamine as a Na⁺ substitute.

The use of these solutions in our experiments allowed us to make very stable recordings with minimal time-dependent changes in voltage-parameters of activation and inactivation.

We have carried out control experiments for both voltage-dependence of activation and inactivation. After an initial time of 1 to 2 minutes, we determined that there are no significant changes in the voltage-dependence of activation or inactivation for periods at least as long as 12 minutes (FIGURE 5.1). However, in order

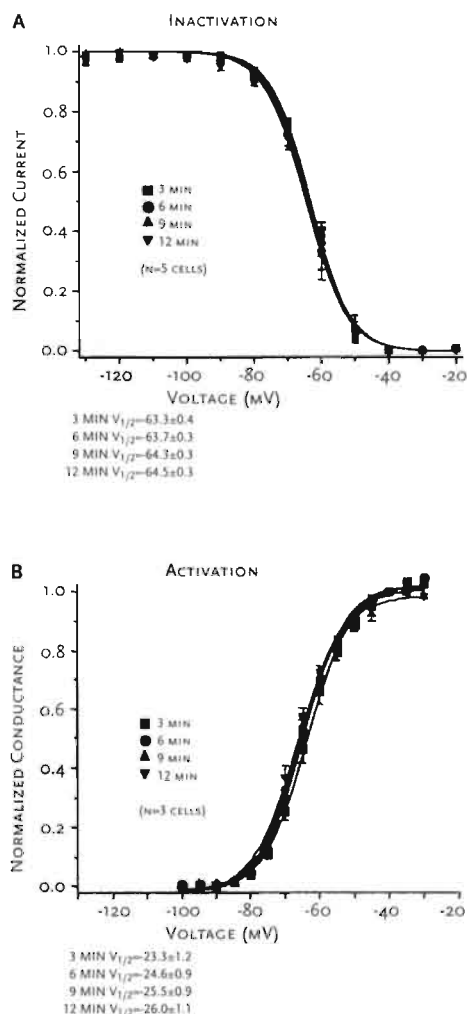


FIGURE 5.1
Stability of recordings with intracellular solution used in this study. Inactivation (A) and activation (B) curves recorded at the indicated times. We detect no significant change in the voltage-dependence of inactivation or activation over the recording periods used in this study.

to ensure reproducibility, we systematically timed each experiment and thus restrict recording times between 3 min and 8 min after rupturing the membrane to establish whole-cell conditions. pClamp 7 (Axon Instruments, Foster City, CA); EXCEL (Microsoft, Seattle, WA); and Origin (Microcal Software, Northampton, MA) were used for data acquisition and analysis. Protocols used have been described previously by us (14,17). Holding potentials were -80 mV unless otherwise indicated. Control experiments of voltage-dependence of activation and inactivation with -100 mV holding potentials did not yield significantly different values. Data are represented as mean \pm SEM. Two-tailed Student's *t*-test was used to compare means; $P < 0.05$ was considered statistically significant.

Results

Description of a New LQT-3 Mutation in a Patient with QTc Prolongation

The patient, an 18-year-old white man, was referred to us because of the documentation of QT-interval prolongation at medical checkup. No history of syncope and cardiac arrest was present. Family history was negative for syncope and sudden death. The 12-lead ECG showed normal sinus rhythm and normal atrioventricular and intraventricular conduction; a QT-interval prolongation (QTc D2: 480 ms), in the absence of T wave morphological abnormalities, was also observed. No ventricular ectopies were found at 24-hour Holter recording or elicited at the exercise stress test. Interestingly, QTc interval was shorter during relative tachycardia (both at Holter and exercise stress test, FIGURES 5.2A and 5.2B), indicating a steep QT/R-R relationship. FIGURE 5.2C, which compares the relationship between QT and R-R intervals for this proband and a noncarrier indicates almost a doubling of the QT/R-R slope for the proband. These data show an increased propensity to excessive QT prolongation at slow heart rate for the carrier of the EK mutation and suggest increased risk of arrhythmia during bradycardia. This abnormal adaptation of the QT-interval has been reported in carriers of LQT-3 mutations (33) but not in carriers of LQT-1 or LQT-2 mutations or in control subjects (33,34). Thus, the clinical phenotype suggested the possibility of an LQT-3 lesion.

Analysis of the DNA of the proband by SSCP in fact revealed an abnormal conformer in the exon 22 of the *SCN5A* gene. Subsequent DNA sequence analysis of this

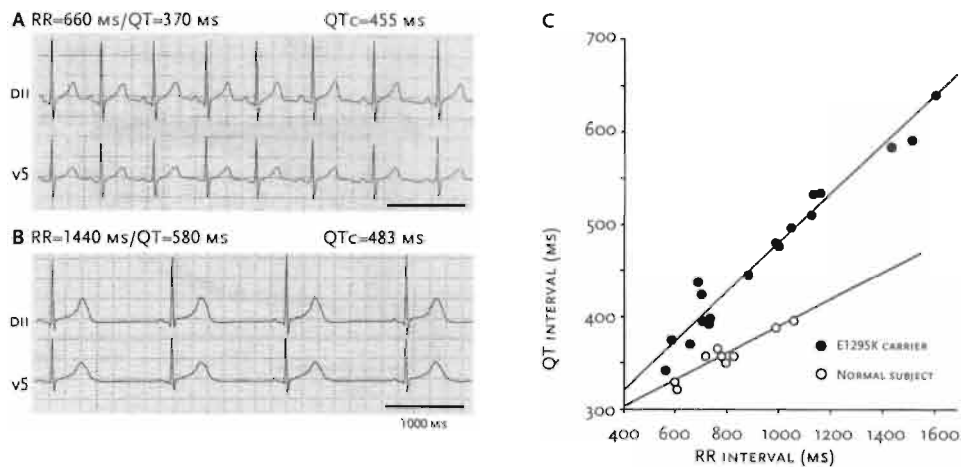


FIGURE 5.2 ECG recordings of the EK carrier during relative tachycardia (A) and bradycardia (B), showing the increase of QT corrected for heart rate with Bazett's formula (QTc) at slower heart rates. C, Analysis of the QT versus R-R interval relationship in the EK carrier measured in lead D₂ during 12-lead Holter recording for the mutation carrier and for a healthy control subject (the mother of the proband). The QT/R-R slopes were 0.254 and 0.145 for the EK patient and the control subject, respectively.

exon with specific primers for the regions of introns 21 and 22 flanking exon 22 showed a single nucleotide transition from G to A at the first base of the codon 1295 leading to the missense mutation Glu1295Lys, changing the charge at this location from negative to positive. Because this change in charge occurs close to the extracellular extremity of DIIS4, a critical contributor to channel gating, we next sought to determine whether functional changes accompany this amino acid change.

Biophysical Characterization of the EK Mutation in HEK293 Cells

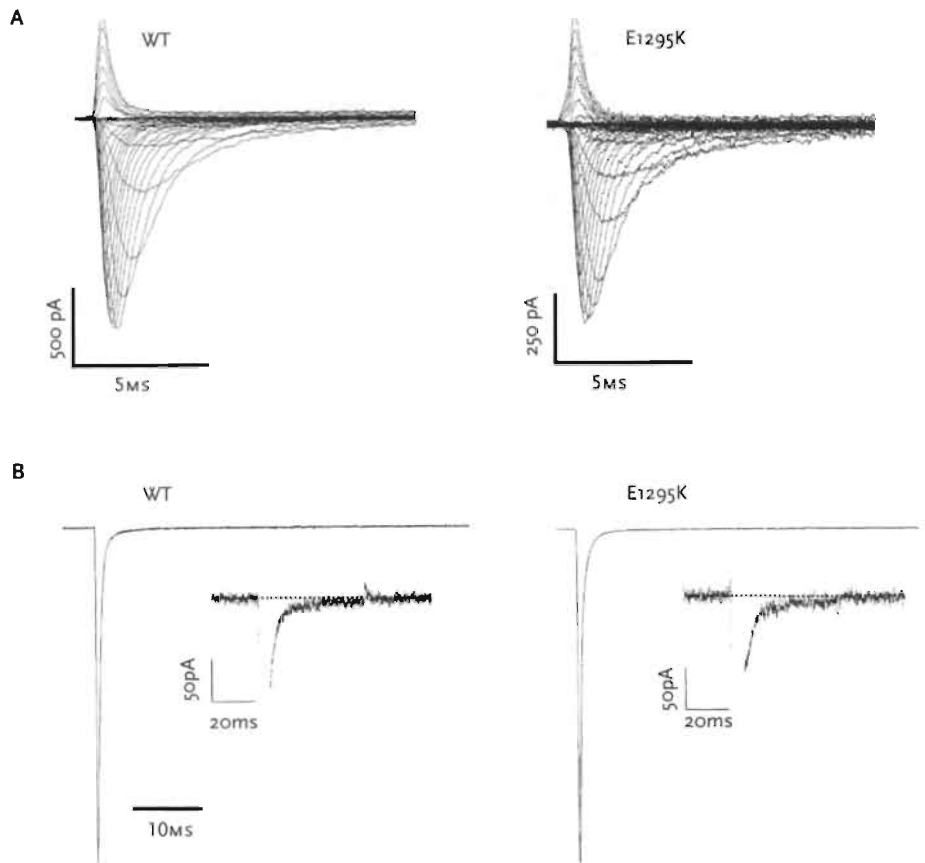
We performed a detailed characterization of mutant EK channels to look for biophysical properties that may explain the observed clinical phenotype. HEK293 cells transiently transfected with EK cDNA expressed Na⁺ currents similar in amplitude and time course to WT channels (FIGURE 5.3A). Mean peak current density was not different in cells expressing WT or EK channels: 254±21 pA/pF (n=13) and 259±31 pA/pF (n=10), respectively. FIGURE 5.3B shows that, in contrast to most of the previously reported LQT-3 mutations, we did not measure any mutation-induced increase in sustained current in response to voltage pulses applied near the expected peak of the I/V relationship (-10 mV). The measured fractional tetrodotoxin (TTX)-sensitive current after 50 ms was 0.29±0.09% (n=9) of peak current with WT channels and 0.24±0.07% (n=5) with mutant channels.

We next fitted the time course of the onset of current inactivation with a monoexponential decay function, because it is possible that changes in inactivation kinetics may contribute to control of APD. In some cells, this fit could be slightly improved

FIGURE 5-3

A, Representative Na^+ currents in HEK293 cells transiently transfected with WT and EK cDNAs. The currents were evoked by 25 ms pulses to voltages ranging from -80 to +70 mV (5 mV steps) with a 30 mmol/L Na^+ extracellular solution.

B, TTX-sensitive current (30 $\mu\text{mol/L}$) evoked by a test pulse to -10 mV (traces are average of 10 sweeps). Traces were normalized for comparison (peak WT=5.5 nA and EK=7.1 nA). Insets, same recordings but with expanded scale.



when a biexponential function was used, but in these fits, the slower component of inactivation never exceeded 10% of the total weight (data not shown). Therefore, we used a monoexponential model for simplicity. The effect of the EK mutation on kinetics was restricted to the voltage range between -35 and -20 mV where it significantly slowed the onset of inactivation (FIGURE 5.4A). We then measured the time course of recovery from inactivation (RFI) (after a 100 ms conditioning pulse to -10 mV) and observed a mutation-induced speeding of this process (FIGURE 5.4B). Time constants and relative weights on the averaged data are as follows: WT (○): $\tau_{\text{fast}}=20.1$ ms, $a_{\text{fast}}=0.87$, $\tau_{\text{slow}}=446$ ms, $a_{\text{slow}}=0.13$; EK (●): $\tau_{\text{fast}}=11.6$ ms, $a_{\text{fast}}=0.90$, $\tau_{\text{slow}}=464$ ms, $a_{\text{slow}}=0.10$. Time of half-recovery ($T_{1/2}$) from inactivation was significantly faster with EK channels than with WT channels when this parameter was determined for each individual cell: WT $T_{1/2}=18.2\pm4.0$ ms ($n=6$) and EK $T_{1/2}=9.6\pm1.6$ ms ($n=8$); $P<0.05$.

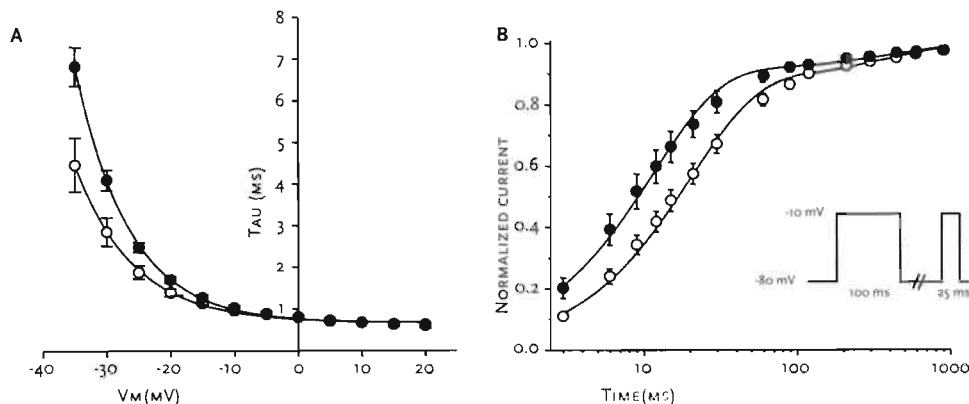


FIGURE 5.4
A, Time constant of onset of inactivation of WT and EK channels fitted with a monoexponential decay versus command membrane voltage ($n=6$ for WT and $n=7$ for EK).
B, Recovery from inactivation was fitted with a biexponential function (see results).

We next evaluated the effects of the EK mutation on the voltage dependence of steady-state activation and inactivation. Activation was determined from I/V relationships by normalizing peak current to driving force and maximal current and plotting normalized conductance versus voltage (FIGURE 5.5). This analysis showed small but consistent positive shifts in activation. We detected a larger mutation-induced positive shift in the voltage dependence of inactivation that is also illustrated in FIGURE 5.5. Boltzmann relationships were fitted to steady-state activation and inactivation data, and we obtained the following results. Slope factors of inactivation and activation were not different. For inactivation, $V_{1/2}$: -65.2 ± 0.2 , -60.0 ± 0.2 ; k : 6.1 ± 0.2 , 6.1 ± 0.1 ($n=13$ for WT and $n=10$ for EK); for activation: $V_{1/2}$: -21.5 ± 0.3 , -18.6 ± 0.3 ; k : 6.9 ± 0.3 , 6.7 ± 0.2 ($n=6$ for WT and $n=7$ for EK). All differences between inactivation and activation $V_{1/2}$ are statistically significant at $P < 0.01$.

Mutation-induced Shift in Window Current

Are these effects on the voltage dependence of activation and inactivation related to the cellular phenotype: APD prolongation? Close inspection of the effects of the EK curves in FIGURE 5.5 suggests that the mutation changes the window of voltages where these two curves overlap. To test for this, we used a slow-voltage ramp protocol

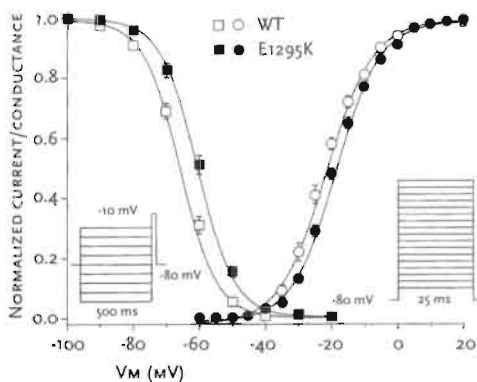


FIGURE 5.5
Steady-state activation and inactivation relationships were measured with protocols presented in the insets. For activation measurements, peak currents were normalized to driving force to determine conductance. Fits to experimental data yielded the resulting Boltzmann parameters (see results).

to measure window currents. Such slowly rising voltage ramps promote inactivation of transient currents and have proven useful in the measurement of the voltage dependence of noninactivating Na^+ current for other LQT-3 mutations (35). We applied this protocol before and after the application of 30 $\mu\text{mol/L}$ TTX to first measure and then subtract background currents. As illustrated in FIGURE 5.6, we measured small Na^+ channel window current for WT and EK channels. Current density of the window current was not modified by the mutation (WT= 0.54 ± 0.21 pA/pF ($n=8$); EK= 0.40 ± 0.12 pA/pF ($n=10$); NS). However, the peak of the window current is shifted. The average voltage of the peak was shifted by

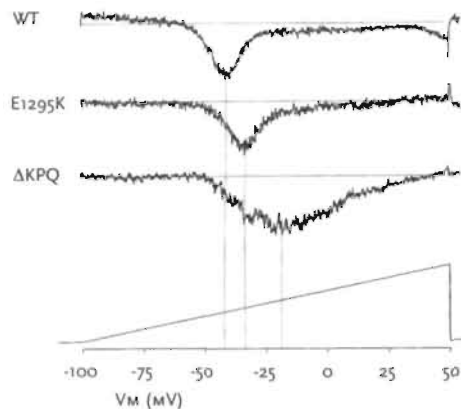


FIGURE 5.6

Currents with WT, EK, and ΔKPQ channels elicited with a ramp protocol ranging from -100 to +50 mV in 2 seconds. Recordings shown are scaled for comparison and are TTX-subtracted (30 $\mu\text{mol/L}$).

about +10 mV by the EK mutation: WT = -44.5 ± 1.3 mV ($n=8$) and EK = -35.5 ± 1.0 mV ($n=10$); $P < 0.001$. The I/V relationship obtained from this protocol indicates a very restricted range of voltages over which noninactivating Na^+ current is expressed for the EK channel, a range of voltages that coincides only with the window of overlap between the two gating curves (FIGURE 5.5). Furthermore, this voltage dependence distinguishes the activity of EK mutant channels from other LQT-3 mutant channels that conduct sustained channel activity over

a broader voltage range and have a fundamentally distinct response to voltage-ramp protocols as illustrated by the ΔKPQ mutation (16,35,36) in FIGURE 5.6. Moreover, note that peak ΔKPQ channel currents evoked with this protocol were on average 6 to 8 times larger than window currents (3.44 ± 0.84 pA/pF; peak voltage -15.0 ± 0.6 mV; $n=4$), again pointing to a fundamental different mechanism underlying mutation-induced gating changes.

Discussion

Novel Mechanism of APD Prolongation Linked to the LQT-3 Syndrome

The main findings of this study are that a novel *SCN5A* mutation, which is linked to a clinical phenotype of LQT-3 (33), changes the biophysical properties of expressed

channels in a manner that is distinct from previously reported LQT-3 mutations. In contrast with other previously investigated LQT-3 mutations such as the Δ KPQ mutation, the EK mutation promotes sustained channel activity only over a very narrow window of voltages that differs from WT channels only in the voltage range of the window. To significantly alter net membrane current, the mutation-induced window current must flow when currents through repolarizing channels are small.

Heterogeneity in the Pathological Mechanisms in LQT-3

Thus far, seven mutations linked with LQT-3 have been functionally studied (18,20,35,37-40). Most of these mutations alter the fast inactivation properties of the channel-inducing sustained Na^+ current on prolonged membrane depolarization over a wide range of plateau voltages. Such a defect is consistent with an increase in inward current during the entire plateau phase of the AP, which consequently prolongs the APD. This is not the only mechanism by which LQT-3-linked Na^+ channel mutations are able to prolong cellular APD. Recent studies (17,18) showed that an LQT-3 mutation in the carboxy-terminus region of the channel (D1790G), which does not produce persistent current different from WT channels, prolongs APD indirectly through effects on other ion channels. In the present work, we report yet a third mechanism by which an LQT-3 mutation is likely to prolong the cellular AP.

Roles of K^+ Channel Rectification in EK Channel Cellular Phenotype

It has been known for almost 50 years that the plateau phase of the cardiac AP is a period in which the cellular input impedance is maximal (3). Consequently, during this plateau, small changes in net ionic current will cause large changes in membrane potential. Repolarization of the AP normally begins when outward current through delayed rectifier (I_{Ks} and I_{Kr}) channels is sufficient to just balance and eventually exceed the total flow of inward current across the membrane. As repolarization begins, the cellular membrane potential reenters the voltage range for which WT Na^+ channels may again open to contribute as window current. This voltage range, however, coincides with voltages at which rectification of inward rectifier (I_{K1}) and *HERG* channels (32,41,42) is relieved. Consequently, the effect of WT Na^+ channel window current is minimal. In the case of cells expressing EK channels, the range of voltages over which window current can flow is more positive, and the contribution of these channels is more pronounced because window current through them is activated over a voltage range in which rectification of I_{K1} and I_{Kr} channels minimizes their contribution to total membrane current.

Note that because the functional effects of this mutation are most pronounced when background K^+ channel currents are minimized, it is likely that the cellular (and hence systemic) effects of the mutation may be more pronounced in cells with smaller outward repolarizing current such as M cells (43). If one assumes heterogeneity of repolarizing current across the ventricular wall (44), then it is likely that the effect of the EK mutation will be blunted in cells with higher density of outward currents. A difference between repolarization in different cell types might therefore exacerbate heterogeneity in APD within the myocardial wall and increase the likelihood of an arrhythmic event (45).

Structure-function Relationship

Glutamic acid (E1295), mutated into a positively charged lysine in this patient, is found in a 4-amino acid extracellular loop connecting DIIIS3 with DIIIS4. E1295 is the amino acid closest to DIIIS4, which is one of the voltage sensors for activation gating process of the channel (46). The presence of a negative residue just external to the DIIIS4 segment is not only conserved among cardiac channels of different species but also among all different isoforms of the Na^+ channel. We postulate that this mutation-induced change in charge alters the voltage dependence of activation and/or inactivation gating sensor and that this is reflected by the recorded shifts in steady-state activation and inactivation curves. Window currents are found at voltages where there is overlap of the activation and inactivation curves, and as there is a concomitant shift of both, window currents are shifted accordingly (FIGURE 5.6). The EK mutation hastens the RFI after a 100 ms inactivating pulse. This observation is consistent with recent observations (47,48) showing that movement of DIIIS4 and DIVS4 is coupled to fast inactivation. These changes in channel kinetics may also have to be taken into account when considering the basis of frequency-dependent changes in cellular electrical activity induced by the EK mutation.

Clinical and Therapeutic Implications

This study provides a further illustration that the LQT-3 type of LQTS is aggravated by bradycardia (FIGURE 5.2). Beta-blockers are the mainstay in the management of the LQTS; however, the efficacy of this treatment in LQT-3 patients has been questioned (49) mainly because the decrease in heart rate that accompanies this treatment can enhance QT prolongation in LQT-3 carriers. Because the present study provides evidence that bradycardia markedly aggravates the phenotype (prolonged QT) in the case of the EK mutation, our results predict that beta-blockers may worsen the phenotype carriers of this

mutation by slowing heart rate. Clearly, our results emphasize the importance of identifying the genotype of LQTS patients in general and LQT-3 patients in particular, before an optimum therapeutic regimen can be planned. For example, in the case of the EK mutation, alternative strategies such as pacing (which prevents bradycardia) or administration of mexiletine (which by shifting the inactivation curve to more negative voltages may normalize the voltage dependence of the window current) might prove to be more effective in preventing arrhythmias.

Implications for Drug-induced LQTS

Our investigation into the functional consequence of the EK mutation on Na^+ activity provides one more example of the delicate interplay of small inward and outward currents that control the plateau phase of the cardiac AP. In the case of the EK mutation, there is no net increase in the magnitude of inward current flowing through Na^+ channels; instead, there is a shift in the voltages over which channels can reopen. Such small changes in the voltage-dependent properties of inward Na^+ channel current can have marked effects on APD only if they occur in the presence of a highly nonlinear background of outward K^+ channel currents (50). By inference, these results suggest that alteration in background K^+ channel activity against different patterns of Na^+ channel activity would be expected to have distinct effects on APD. It is interesting to speculate that subtle changes in Na^+ channel gating caused by coding changes in the α -subunit, insufficient to cause substantial changes in cellular APD by themselves, may lead to excessive changes in APD in the face of inhibition of one of these key K^+ channels and thus contribute to some forms of drug-induced LQTS. Experiments are underway to test for this possibility.

Acknowledgments

This work was supported by United States Public Health Service Grant R01-HL-56810-04 (to R.S.K.). H.A. was supported by the Swiss National Foundation for Fellowships in Medicine and Biology.

References

1. Kass RS. Ionic basis of electrical activity in the heart. In: Sperelakis N (ed). Physiology and pathophysiology of the heart. Norwell, Mass: Kluwer Academic 1984:83-96.
2. Antzelevitch C, Shimizu W, Yan GX, Sicouri S, Weissenburger J, Nesterenko VV, Burashnikov A, Di Diego J, Saffitz J, Thomas GP. The M cell: its contribution to the ECG and to normal and abnormal electrical function of the heart. *J Cardiovasc Electrophysiol* 1999;10:1124-52.
3. Weidmann S. Effect of current flow on the membrane potential of cardiac muscle. *J Physiol* 1951;115:227-36.
4. Sanguinetti MC, Zou A. Molecular physiology of cardiac delayed rectifier K⁺ channels. *Heart Vessels* 1997;Suppl 12:170-72.
5. Kass RS. Delayed potassium channels in the heart: regulatory and molecular properties. In: Morad M, Ebashi S, Trautwein W, Kurachi Y (eds). Molecular physiology and pharmacology of cardiac ion channels and transporters. Boston, Mass: Kluwer Academic Publishers 1994:74-82.
6. Moss AJ, Robinson JL. The long-QT syndrome: genetic considerations. *Trends Cardiovasc Med* 1993;2:81-83.
7. Moss AJ, Robinson J. Clinical features of the idiopathic long-QT syndrome. *Circulation* 1992;85(Suppl 1):140-44.
8. Priori SG, Barhanin J, Hauer RN, Haverkamp W, Jongsma HJ, Kleber AG, McKenna WJ, Roden DM, Rudy Y, Schwartz K, Schwartz PJ, Towbin JA, Wilde AA. Genetic and molecular basis of cardiac arrhythmias; impact on clinical management. Study group on molecular basis of arrhythmias of the working group on arrhythmias of the European Society of Cardiology. *Eur Heart J* 1999;20:174-95.
9. Schwartz PJ, Locati EH, Napolitano C, Priori SG. The long-QT syndrome. In: Zipes DP, Jalife J (eds.) Cardiac electrophysiology: from cell to bedside. New York, NY: WB Saunders; 1994:597-615.
10. Keating MT, Sanguinetti MC. Pathophysiology of ion channel mutations. *Curr Opin Genet Dev* 1996;6:326-33.
11. Sanguinetti MC, Spector PS. Potassium channelopathies. *Neuropharmacology* 1997;36:755-62.
12. Kameyama M, Kakei M, Sato R, Shibasaki T, Matsuda H, Irisawa H. Intracellular Na⁺ activates a K⁺ channel in mammalian cardiac cells. *Nature (Lond)* 1984;309:354-56.
13. Roden DM, Kupersmidt S. From genes to channels: normal mechanisms. *Cardiovasc Res* 1999;42:318-26.
14. An RH, Bangalore R, Rosero SZ, Kass RS. Lidocaine block of LQT-3 mutant human Na⁺ channels. *Circ Res* 1996;79:103-08.
15. Wang DW, Yazawa K, Makita N, George AL, Bennett PB. Pharmacological targeting of long-QT mutant sodium channels. *J Clin Invest* 1997;99:1714-20.
16. Bennett PB, Yazawa K, Makita N, George AL. Molecular mechanism for an inherited cardiac arrhythmia. *Nature (Lond)* 1995;376:683-85.
17. Wehrens XHT, Abriel H, Cabo C, Benhorin J, Kass RS. Arrhythmogenic mechanism of an LQT-3 mutation of the human heart Na⁺ channel α -subunit: a computational analysis. *Circulation* 2000;102:584-90.
18. An RH, Wang XL, Kerem B, Benhorin J, Medina A, Goldmit M, Kass RS. Novel LQT-3 mutation affects Na⁺ channel activity through interactions between α - and β 1-subunits. *Circ Res* 1998;83:141-46.
19. Abriel H, Wehrens XHT, Benhorin J, Kerem B, Kass RS. Molecular pharmacology of the sodium channel mutation D1790G linked to the long-QT syndrome. *Circulation* 2000;102:921-25.

20. Makita N, Shirai N, Nagashima M, Matsuoka R, Yamada Y, Tohse N, Kitabatake A. A *de novo* missense mutation of human cardiac Na⁺ channel exhibiting novel molecular mechanisms of long-QT syndrome. *FEBS Lett* 1998;423:5-9.
21. Clancy CE, Rudy Y. Linking a genetic defect to its cellular phenotype in a cardiac arrhythmia. *Nature (Lond)* 1999;400:566-69.
22. Attwell D, Cohen I, Eisner D, Ohba M, Ojeda C. The steady state TTX-sensitive ("window") sodium current in cardiac Purkinje fibres. *Pflugers Arch* 1979;379:137-42.
23. Hirano Y, Moscucci A, January CT. Direct measurement of L-type Ca²⁺ window current in heart cells. *Circ Res* 1992;70:445-55.
24. Wasserstrom JA, Salata JJ. Basis for tetrodotoxin and lidocaine effects on action potentials in dog ventricular myocytes. *Am J Physiol* 1988;254:H1157-66.
25. Sakmann B, Trube G. Conductance properties of single inwardly rectifying potassium channels in ventricular cells from guinea-pig heart. *J Physiol (Lond)* 1984;347:641-57.
26. Backx PH, Marban E. Background potassium current active during the plateau of the action potential in guinea pig ventricular myocytes. *Circ Res* 1993;72:890-900.
27. Kass RS. Genesis of cardiac arrhythmias: roles of calcium and delayed potassium channels in the heart. In: Andreoli T, Fambrough D, Hoffman J, Welsh M, Schultz S, Brown AM (eds). *Molecular biology of membrane transport disorders*. New York, NY: Plenum 1994:595-604.
28. Barry DM, Nerbonne JM. Myocardial potassium channels: electrophysiological and molecular diversity. *Annu Rev Physiol* 1996;58:363-94.
29. Schonherr R, Heinemann SH. Molecular determinants for activation and inactivation of *HERG*, a human inward rectifier potassium channel. *J Physiol (Lond)* 1996;493:635-42.
30. Smith PL, Baukrowitz T, Yellen G. The inward rectification mechanism of the *HERG* cardiac potassium channel. *Nature (Lond)* 1996;379:833-36.
31. Sanguinetti MC, Jurkiewicz NK. Two components of cardiac delayed rectifier K⁺ current: differential sensitivity to block by class III antiarrhythmic agents. *J Gen Physiol* 1990;96:195-215.
32. Sanguinetti MC, Jiang C, Curran ME, Keating MT. A mechanistic link between an inherited and an acquired cardiac arrhythmia: *HERG* encodes the I_{Kr} potassium channel. *Cell* 1995;81:299-307.
33. Schwartz PJ, Priori SG, Locati EH, Napolitano C, Cantu F, Towbin JA, Keating MT, Hammoude H, Brown AM, Chen LSK, Colatsky TJ. Long-QT syndrome patients with mutations of the *SCN5A* and *HERG* genes have differential responses to Na⁺ channel blockade and to increases in heart rate: implications for gene-specific therapy. *Circulation* 1995;92:3381-86.
34. Swan H, Viitasalo M, Piippo K, Laitinen P, Kontula K, Toivonen L. Sinus node function and ventricular repolarization during exercise stress test in long-QT syndrome patients with *KvLQT1* and *HERG* potassium channel defects. *J Am Coll Cardiol* 1999;34:823-29.
35. Wang DW, Yazawa K, George AL Jr, Bennett PB. Characterization of human cardiac Na⁺ channel mutations in the congenital long-QT syndrome. *Proc Natl Acad Sci U S A* 1996;93:13200-05.
36. Wang Q, Shen J, Splawski I, Atkinson D, Li Z, Robinson JL, Moss AJ, Towbin JA, Keating MT. *SCN5A* mutations associated with an inherited cardiac arrhythmia, long-QT syndrome. *Cell* 1995;80:805-11.
37. Dumaine R, Wang Q, Keating MT, Hartmann HA, Schwartz PJ, Brown AM, Kirsch GE. Multiple mechanisms of Na⁺ channel linked long-QT syndrome. *Circ Res* 1996;78:916-24.
38. Kambouris NG, Nuss HB, Johns DC, Tomaselli GF, Marban E, Balser JR. Phenotypic characterization of a novel long-QT syndrome mutation (R1623Q) in the cardiac sodium channel. *Circulation* 1998;97:640-44.

39. Bezzina C, Veldkamp MW, Van Den Berg MP, Postma AV, Rook MB, Viersma JW, Van Langen IM, Tan-Sindhunata G, Bink-Boelkens MT, Der Hout AH, Mannens MM, Wilde AA. A single Na⁺ channel mutation causing both long-QT and Brugada syndromes. *Circ Res* 1999;85:1206-13.
40. Wei J, Wang DW, Alings M, Fish F, Wathen M, Roden DM, George AL Jr. Congenital long-QT syndrome caused by a novel mutation in a conserved acidic domain of the cardiac Na⁺ channel. *Circulation* 1999;99:3165-71.
41. Spector PS, Curran ME, Zou A, Keating MT, Sanguinetti MC. Fast inactivation causes rectification of the I_{Kr} channel. *J Gen Physiol* 1996;107:611-19.
42. Kass RS, Sanguinetti MC. Calcium channel inactivation in the cardiac Purkinje fiber: evidence for voltage- and calcium-mediated mechanisms. *J Gen Physiol* 1984;84:705-26.
43. Liu DW, Antzelevitch C. Characteristics of the delayed rectifier current (I_{Kr} and I_{Ks}) in canine ventricular epicardial, midmyocardial, and endocardial myocytes: a weaker I_{Ks} contributes to the longer action potential of the M cell. *Circ Res* 1995;76:351-65.
44. Antzelevitch C. The M cell. *J Cardiovasc Pharmacol Ther* 1997;2:73-76.
45. Antzelevitch C. Electrical heterogeneity, cardiac arrhythmias, and the sodium channel. *Circ Res* 2000;87:964-65.
46. Catterall WA. From ionic currents to molecular mechanisms: the structure and function of voltage-gated sodium channels. *Neuron* 2000;26:13-25.
47. Cha A, Ruben PC, George AL Jr, Fujimoto E, Bezanilla F. Voltage sensors in domains III and IV, but not I and II, are immobilized by Na⁺ channel fast inactivation. *Neuron* 1999;22:73-87.
48. Sheets MF, Kyle JW, Hanck DA. The role of the putative inactivation lid in sodium channel gating current immobilization. *J Gen Physiol* 2000;115:609-20.
49. Moss AJ, Zareba W, Hall WJ, Schwartz PJ, Crampton RS, Benhorin J, Vincent GM, Locati EH, Priori SG, Napolitano C, Medina A, Zhang L, Robinson JL, Timothy K, Towbin JA, Andrews ML. Effectiveness and limitations of beta-blocker therapy in congenital long-QT syndrome. *Circulation* 2000;101:616-23.
50. Noble D. Ionic mechanisms in normal cardiac activity. In: Jalife J, Zipes DP (eds). *Cardiac Electrophysiology*. Philadelphia, Pa: WB Saunders 1990.

Chapter 6

Chapter 6

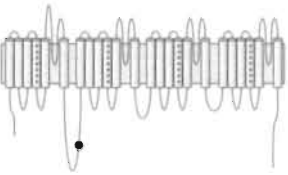
Heterozygous *SCN5A* Mutation in the Domain I-II Linker causes Long-QT Syndrome with 2:1 Atrioventricular Block



●
Based on:

WEHRENS XHT, Rossenbacker T, Jongbloed RJ, Gewillig M, Heidbüchel H, Doevendans PA, Vos MA, Wellens HJJ, Kass RS. *Submitted*.

Abstract



BACKGROUND. Congenital long-QT syndrome type 3 (LQT-3) is caused by mutations in the gene encoding the α -subunit of the cardiac Na^+ channel (*SCN5A*). Previous studies have linked homozygous mutations in *SCN5A* and the K^+ channel gene *KCNH2* (*HERG*) to congenital long-QT syndrome with functional 2:1 atrioventricular block (AVB), a severe phenotype with a particularly bad prognosis.

METHODS AND RESULTS. In an infant with 2:1 AVB and major QTc prolongation ($657 \text{ ms}^{1/2}$), mutational analysis identified a heterozygous missense mutation (L619F) in the domain I-II linker of the cardiac Na^+ channel. Whole-cell patch-clamp analysis of recombinant L619F mutant channels expressed in HEK293 cells showed a mutation-induced increase in persistent TTX-sensitive inward sodium current (WT: 0.26 ± 0.06 ; L619F: $0.79 \pm 0.17 \text{ pA/pF}$; $P < 0.01$). In addition, a 5.8 mV positive shift in the voltage-dependence of inactivation caused a shift in the peak voltage (WT: -44.3 ± 0.7 ; L619F: $-40.7 \pm 0.9 \text{ mV}$; $P < 0.05$), and an increase in the amplitude of Na^+ channel 'window-current' (WT: 0.58 ± 0.12 ; L619F: $1.07 \pm 0.17 \text{ pA/pF}$; $P < 0.05$).

DISCUSSION. This study provides the first evidence that a heterozygous missense mutation in *SCN5A* may cause LQT-3 with functional 2:1 AVB in an infant. The L619F mutation promotes an increase in sustained (non-inactivating) current as well as an increase in Na^+ channel window-current, two mechanisms which are expected to delay ventricular repolarization. The defective inactivation imposed by the L619F mutation implicates a novel role for the domain I-II linker in the Na^+ channel inactivation process.

Introduction

Congenital long-QT syndrome (LQTS) is an inherited disorder characterized by prolonged ventricular repolarization and a propensity to sudden cardiac death caused by polymorphous ventricular tachycardia (torsades de pointes; TdP). LQTS is considered a pure 'electrical disease', and is usually not associated with congenital heart disease or acquired cardiac disabilities (1,2). The symptoms of LQTS may surface at any age as episodic dizziness, syncope, epileptic seizures, and sudden cardiac death. LQTS may also be involved in some cases of sudden infant death syndrome (3).

Long-QT syndrome in association with two-to-one atrioventricular block (AVB) typically occurs in fetuses, neonates and young infants, and is probably the result of a severely prolonged action potential duration in association with a relatively long effective refractory period of the His-Purkinje system and/or the ventricular myocardium (4,5). It has been suggested that LQTS resulting in AVB in the neonatal period has a particularly poor prognosis (6,7). Despite traditional management with beta-adrenergic blockade and/or cardiac pacing, a large proportion of infants may not survive childhood (6).

Recently, three reports described the association of homozygous mutations in the *KCNH2* (*HERG*) (8,9) and *SCN5A* genes (10) with a severe cardiac phenotype involving marked prolongation of the QT-interval and 2:1 AVB. In contrast, heterozygous carriers were free of symptoms, and had normal or marginally prolonged QTc intervals. In the present study, we describe the first case of an LQTS patient with functional 2:1 AVB due to a *heterozygous* mutation of the *SCN5A* gene. Biophysical characterization of the *SCN5A* mutation L619F revealed a novel combination of enhanced non-inactivating Na⁺ channel activity during prolonged depolarization with increased Na⁺ channel window current, two channel properties that, by themselves, would be expected to delay repolarization and prolong the QT-interval (11). Moreover, the location of the L619F mutation in the domain I-II linker suggests a novel role of this region in Na⁺ channel inactivation.

Materials and Methods

Clinical Data

The study was performed according to a protocol approved by the Leuven University ethics committee and informed consent was obtained. The patient studied was the second child of asymptomatic, non-consanguineous Western European parents.

Mutation Analysis

Genomic DNA was extracted from peripheral blood lymphocytes using standard techniques. The entire coding regions of the known LQTS genes were amplified using PCR. Denaturing high performance liquid chromatography (D-HPLC; Wave Transgenomics) was performed to analyze the *KCNQ1*, *KCNH2* and *KCNE2* genes. The *KCNE1* and *SCN5A* gene were analyzed by sequence analysis of the complete coding region by the Big-Dye terminator ready reaction kit (PE Applied Biosystems) on an ABI-3100 genetic analyzer (PE Applied Biosystems). The mutation L619F was excluded in a control panel of 150 (300 alleles) healthy individuals.

Construction and Expression of Recombinant Na⁺ Channels

The mutant *hH1/C1855T* was engineered using the QuikChange-XL™ site-directed mutagenesis kit (Stratagene, La Jolla, CA) using the following mutagenic sense and antisense primers: 5'-CC.CCA.GGA.AGC.CAC.CTC.TTC.CGC.CCT.GTG.ATG.CTA.G-3' 5'-C.TAG.CAT.CAC.AGG.GCG.GAA.GAG.GTG.GCT.TCC.TGG.GG-3'

Na⁺ channels were expressed in HEK293 cells. Transient transfections of wild-type (WT) and L619F mutant Na⁺ channels were carried out with equal amounts of Na⁺ channel α -subunit, β 1-subunit, and CD-8 antigen cDNA subcloned individually into the pcDNA3.1 (Invitrogen) vector (total cDNA 2.5 mg) using a previously-described procedure (12). Transfected cells were identified by light microscopy and the use of anti-CD8-coated beads (Dynabeads M450 CD8).

Electrophysiology

Membrane currents were measured using whole-cell patch-clamp procedures, with Axopatch 200B amplifiers (Axon Instruments, Foster City, CA). Recordings were made at room temperature (22°C) using an internal solution containing (mmol/L) CsCl 60, cesium aspartate 80, EGTA 11, MgCl₂ 1, CaCl₂ 1 (effective free calcium 100 nmol/L), HEPES 10,

and Na₂ATP 5, pH adjusted to 7.2 with CsOH. In experiments recording I/V curves, external Na⁺ was reduced to 30 mmol/L using n-methyl-glucamine as a Na⁺ substitute. The use of these solutions in our experiments allowed us to make very stable recordings with minimal time-dependent changes in voltage-parameters of activation and inactivation (13). Protocols to analyze mutant channel gating have been described previously (13,14).

Statistical Analysis

Data were collected and analyzed with pClamp8 (Axon Instruments, Foster City, CA); Excel (Microsoft, Seattle, WA); and Origin (Microcal Software, Northampton, MA). Data are represented as mean ± SEM. Two-tailed Student t-test was used to compare means; P<0.05 was considered statistically significant.

Results

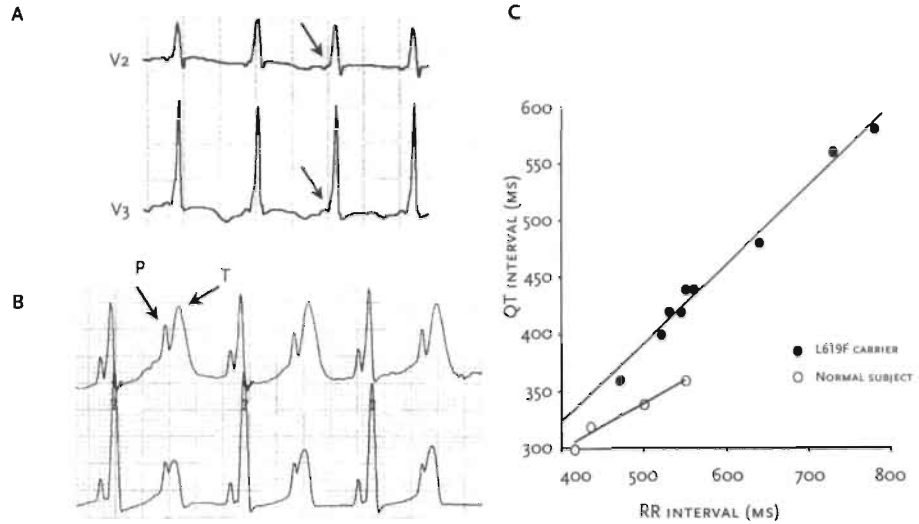
Clinical Characteristics

The mother of the index patient was referred at a gestational age of 27 weeks for ultrasound evaluation because of fetal bradycardia and a large perimembraneous ventricular septal defect. Echography at 35 weeks revealed AVB with ventricular bradycardia of 72 bpm. Maternal serum was negative for anti-SSA/Ro antibodies.

A female baby, weighing 2840 gram, was born prematurely at 36 weeks of gestation by uneventful vaginal delivery. Initial ECG after birth showed sinus rhythm of 139 bpm, normal atrioventricular conduction, signs of pre-excitation, and a prolonged QTc interval of 538 ms^{1/2} (FIGURE 6.1A). Serum levels of potassium, magnesium, and calcium were within normal limits. No evidence of impaired hearing was found. In the second week after birth, symptomatic 2:1 AVB developed when sinus rate exceeded 140 bpm. Treatment with propranolol was instituted (3x3 mg/day) in order to slow the sinus rhythm to allow 1:1 AV conduction. Continuous ECG recording (Holter) performed on day 10 after birth confirmed frequency-dependent conduction anomalies with episodes of 2:1 AVB (FIGURE 6.1B), and intermittent pre-excitation without documented episodes of supraventricular tachycardias. A clinical challenge with mexiletine had no effect on the QTc interval. Digoxin therapy was initiated in order to prevent development of cardiac failure in anticipation of the closure of the ventricular septal defect. Patient was discharged on beta-blocker and

FIGURE 6.1

(A) Leads V2 and V3 of a 12-lead electrocardiogram at day one after birth showing 1-to-1 atrioventricular conduction, delta-waves (arrow) indicative of pre-excitation, and QT-interval prolongation. (B) Two lead electrocardiogram from 24-hour recording at 10 days of age, showing 2:1 atrioventricular conduction. (C) Analysis of the QT versus R-R interval relationship in the L619F carrier (lead II during Holter recording at different heart rates) revealed QT/R-R slopes of 0.703 and 0.407 for the proband and an age-matched control subject, respectively.



digoxin therapy in combination with cardiac home monitoring. Two weeks later, while temporarily disconnected from the monitor for breast feeding, patient underwent a period of paleness and hypotonia, which could be rapidly reversed by mouth-to-mouth resuscitation by the father. Evaluation in hospital showed sinus rhythm, prolonged QT-intervals, and intermittent episodes of 2:1 AVB, which were clinically well tolerated. Breast feeding was discontinued and propranolol increased to 4x3 mg/day. Subsequent follow-up until 11 months of age is uneventful, with QTc values ranging between 481 and 657 ms^{1/2}. Despite several weeks of continuous monitoring, and multiple Holter and ECG recordings, no ventricular ectopy has ever been observed in the first year of life. At the age of 5 months, digoxin therapy was discontinued and the ventricular septal defect was surgically closed.

FIGURE 6.1C, which compares the relationship between QT and R-R intervals for the proband and an age-matched non-carrier indicates almost a doubling of the QT/R-R slope for the proband. These data show an increased propensity to excessive QT prolongation at slow heart rate for the carrier of the L619F mutation and suggest increased risk of arrhythmia during bradycardia. This abnormal adaptation of the QT-interval has been reported in carriers of LQT-3 mutations (13,15), but not in carriers of LQT-1 or LQT-2 mutations or in control subjects (15). Thus, the clinical phenotype suggests the possibility of an LQT-3 lesion.

None of the family members had experienced any symptoms related to LQTS. The father has normal QTc intervals, the mother has a borderline positively prolonged QTc interval of 450 ms^{1/2}, and information for the older sibling is lacking.

Identification of the *SCN5A* Mutation

Bidirectional sequencing analysis of the *SCN5A* gene revealed a single nucleotide transition (C-T) at position 1855, which is expected to cause a change from a leucine (L) to a phenylalanine (F) at codon 619 within the cytoplasmic linker between domains I and II (FIGURE 6.2). In addition, D-HPLC analysis of the proband revealed a heteroduplex fragment with abnormal elution profile in the *KCNE2* gene, and subsequent sequence analysis revealed the common polymorphism T8A-*MiRP1* in the *KCNE2* gene (16). The L619F mutation in *SCN5A* and polymorphism in *KCNE2* were also present in the mother, but not in the father. No mutations were identified within the *KCNQ1*, *KCNH2*, and *KCNE1* genes.

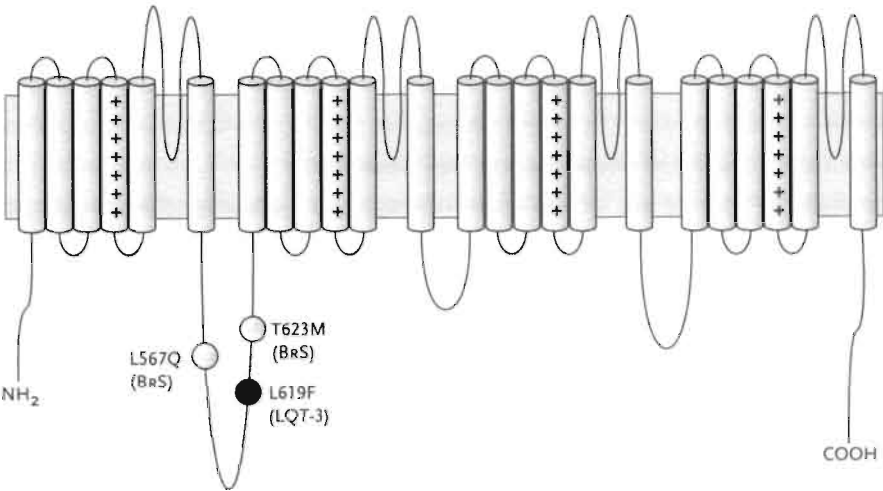
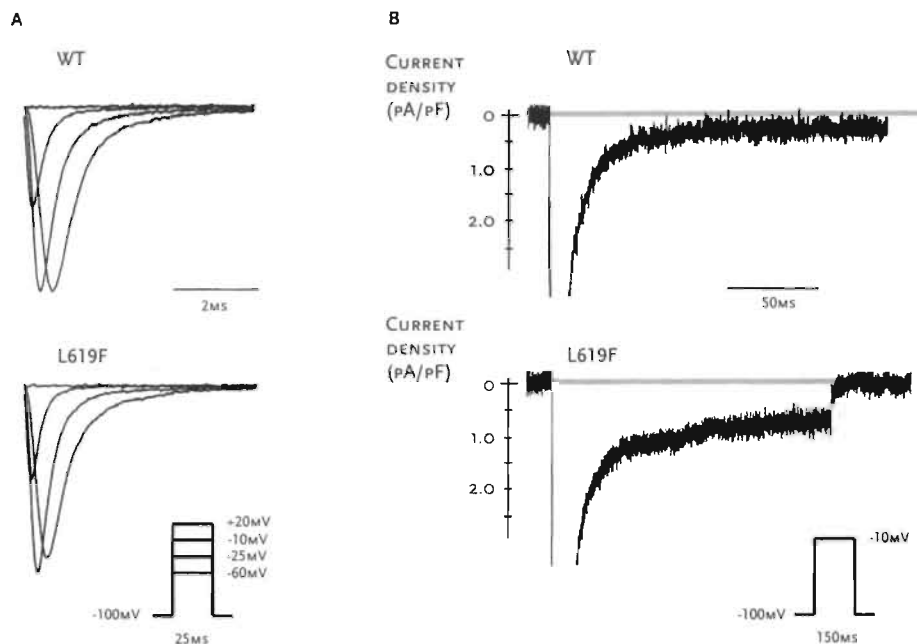


FIGURE 6.2
Arrhythmogenic *SCN5A* mutations in the domain I-II linker of the cardiac sodium channel protein. Topological model of the channel is illustrated with location of 2 Brugada syndrome mutations (L567Q, T632M), and the LQT-3 mutation L619F of the present study.

FIGURE 6.3

(A) Representative Na^+ currents in HEK293 cells transiently transfected with WT or L619F cDNA. Currents in 30 mmol/L Na^+ extracellular solution were evoked by 25 ms pulses from a holding potential of -100 mV to -60, -25, -10, and +20 mV, respectively. (B) TTX-sensitive current (30 $\mu\text{mol/L}$) in 130 mmol/L Na^+ extracellular solution evoked by a test pulse from -100 mV to -10 mV (traces are average of 10 sweeps).



Biophysical Properties of L619F Mutant Na^+ Channels

Macroscopic Na^+ current was recorded from HEK 293 cells expressing wild-type ($hH1/\text{WT}$) and mutant channels ($hH1/\text{L619F}$). Peak current density was not affected by the L619F mutation (WT: 362 ± 40 pA/pF ($n=12$); L619F: 301 ± 33 pA/pF ($n=10$); $P=\text{NS}$). At low recording gain, there is no marked difference between the waveforms of WT and L619F channels (FIGURE 6.3A), but at higher gain, recordings reveal a mutation-induced increase in sustained channel activity (FIGURE 6.3B). Assayed as the tetrodotoxin (TTX)-sensitive current at -10 mV and 150 ms, this mutation-induced increase in sustained current is significant (WT: 0.26 ± 0.06 pA/pF ($n=9$); L619F 0.79 ± 0.17 pA/pF ($n=9$); $P < 0.01$).

The L619F mutation does not affect the kinetics of the onset of inactivation (FIGURE 6.4A), but almost halves the time for recovery from inactivation (RFI) (FIGURE 6.4B). $T_{1/2}$ (time to half recovery from inactivation) was 2.78 ± 0.19 ms for WT ($n=12$); 1.45 ± 0.12 ms for L619F ($n=10$); $P < 0.001$. Similar speeding of the RFI for L619F was measured when the holding potential was -60 mV, -80 mV, or -120 mV (data not shown).

L619F also results in a +5.8 mV shift in the voltage-dependence of channel availability (WT: -64.0 ± 0.8 mV ($n=8$); L619F: -58.2 ± 1.1 mV ($n=10$); $P < 0.05$) (FIGURE 6.5A).

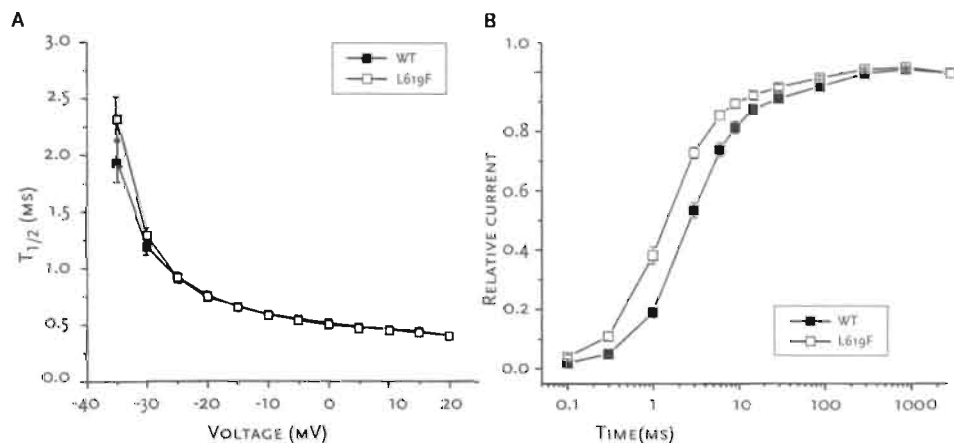


FIGURE 6.4
(A) The L619F mutation does not affect the onset of inactivation kinetics. Time to 50% inactivation was similar for WT and L619F channels. **(B)** The L619F mutation speeds recovery from inactivation (RFI). RFI was fitted with a bi-exponential function for each individual experiment: the time constants and relative weights on the averaged data are: WT: $\tau_{fast}=3.21$ ms, $a_{fast}=0.87$, $\tau_{slow}=79.2$ ms, $a_{slow}=0.13$; and for L619F: $\tau_{fast}=1.75$ ms, $a_{fast}=0.88$, $\tau_{slow}=42.5$ ms, $a_{slow}=0.12$.

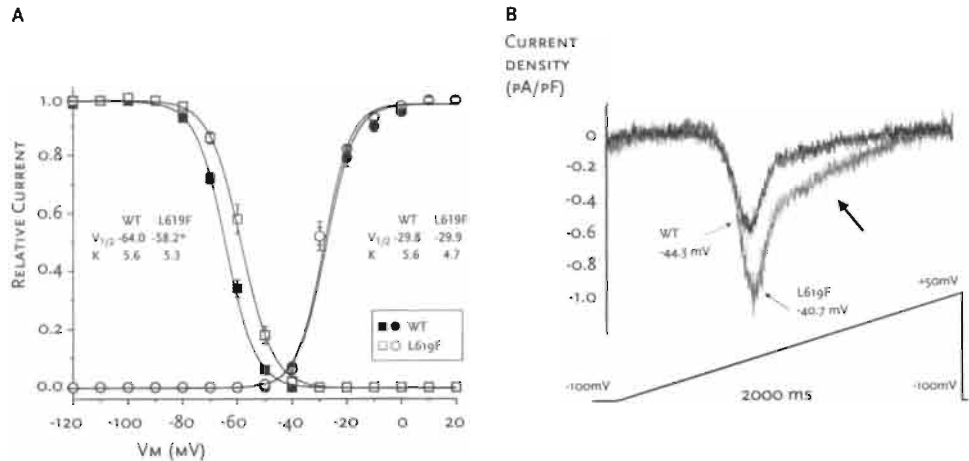
A positive shift in the voltage-dependence of channel availability, in the absence of a change in the voltage-dependence of activation, would be expected to change the window of voltages where non-inactivating (window) current can be measured (17). In combination with the mutation-induced increase in sustained current at voltages outside of this window of activation/inactivation overlap (FIGURE 6.3B), the data predict that the L619F mutation should cause marked changes in the voltage-dependence of steady-state (non-inactivating) Na⁺ channel current. We used a ramp voltage protocol for which voltage-changes are imposed at a sufficiently slow rate to reveal steady-state Na⁺ channel currents as a function of membrane potential (13). The L619F mutation increases the current density of the peak window current (WT: 0.58 ± 0.12 pA/pF ($n=7$); L619F: 1.09 ± 0.17 pA/pF ($n=7$); $P < 0.05$), and shifts the voltage at which the maximum window current occurs by +3.6 mV (WT: -44.3 ± 0.7 mV ($n=7$); L619F: -40.7 ± 0.9 mV ($n=7$); $P < 0.01$) (FIGURE 6.5B), consistent with the effects of the mutation on the voltage-dependence of activation and inactivation. In addition, the window current waveform also indicates the presence of non-inactivating channels over a broad voltage-range as evidenced by the 'shoulder' in the curve (see the arrow in FIGURE 6.5B). Thus, the voltage-dependence of the non-inactivating component of L619F channel activity is due to both the overlap in steady-state activation and channel availability (FIGURE 6.5A) as well as to mutation-induced sustained Na⁺ current (FIGURE 6.3B).

FIGURE 6.5

(A) Voltage-dependence of inactivation but not activation is modified by the L619F mutation.

For activation measurements, peak currents were normalized to driving force to determine conductance. * $P < 0.001$. (B) Currents with WT and L619F channels elicited with a ramp protocol ranging from -100 mV to +50 mV in 2 s. The presented recordings are normalized to capacitance, and are TTX-subtracted (30 mmol/L). Averaged L619F window current was larger.

The arrow indicates non-inactivating channels over a broad voltage-range as evidenced by the 'shoulder' in the curve.



Discussion

Previous studies have reported the association of homozygous mutations in the *SCN5A* and *KCNH2* genes with congenital long-QT syndrome and 2:1 atrioventricular block (8-10). In the present study, we describe a novel heterozygous LQT-3 missense mutation, L619F, identified in a neonate with prolonged QT-intervals and episodes of 2:1 AVB.

Long-QT Syndrome and 2:1 Atrioventricular Block

Long-QT syndrome with 2:1 AVB is rare, with an incidence of 4% reported in pediatric series of long-QT syndrome patients (6), and to the best of our knowledge 64 cases reported so far in the world literature (1,4-10,18-30). Electrophysiological studies have revealed that during 2:1 atrioventricular conduction, AVB may occur within the His bundle (24,28), or more distal in the Purkinje system and/or ventricular myocardium (4,7,23). In 95% of the reported cases of LQTS with 2:1 AVB, QTc prolongation exceeded 500 ms^{1/2}, and despite the usual treatment regime of beta-blockers with or without a pacemaker, infant mortality approximated 50%.

In only three previous cases, the genotype of the patient with LQTS and 2:1 AVB was assessed (8-10). Two separate cases of homozygous mutations in *HERG* (8,9), and one case of a homozygous mutation in *SCN5A* were responsible for this severe phenotype. Our case is unique, as it represents the first case of a heterozygous Na⁺ channel mutation

associated with LQTS and 2:1 AVB. In addition to the *SCN5A* mutation, our patient was carrier of the amino acid polymorphism T8A-*MiRP1* in the β -ancillary subunit accessory of the I_{Kr} channel (31), which is a relatively common polymorphism with an allelic frequency of 1.6% in the general population. We believe that this polymorphism probably did not contribute to the clinical phenotype, as T8A-*MiRP1* does not significantly affect I_{Kr} channel properties in the absence of QT prolonging drugs (16). Interestingly, the mother of the index patient, who also carried both the *SCN5A* mutation and the *MiRP1* polymorphism, displayed only borderline QTc interval prolongation, and did not experience any long-QT syndrome-related symptoms.

Association long-QT syndrome, 2:1 AVB, and VSD

The complex cardiac phenotype of long-QT syndrome with functional 2:1 AVB, in combination with a ventricular septal defect has been reported in 6 cases so far (TABLE 6.1). Most cases were identified prenatally because of fetal bradycardia or (supra)ventricular tachycardia. Neonatal QTc intervals were usually very long

TABLE 6.1
Characteristics of long-QT syndrome patients with 2:1 atrioventricular conduction, and a ventricular septal defect.

Gender	Presentation	Family history	Neonatal QTc (sec)	Symptoms	TWA/TdP	Treatment	Dead	Reference
F	n.a.	n.a.	n.a.	n.a.	TWA	-	18 d.	(22)
n.a.	fetal SVT	-	0.693	-	TWA/TdP	BB	<1 mo	(24)
n.a.	fetal brady	-	0.666	-	TWA	BB,mexil.	2 mo	(6)
M	brady	-	0.633	+	TdP	BB,PP	26 mo	(27)
F	fetal brady fetal VT	+	0.636	+	TdP	BB,PP	10 mo	(30)
F	fetal brady	+	0.860	-	TdP	TP	4 d.	(30)
F	fetal brady	+	0.538	+	-	BB	-	This study

Legend: F= female; M= male; n.a. = not assessed; brady= bradycardia; TWA= T wave alternans; TdP= torsades de pointes; (S) VT= (supra-)ventricular tachycardia; BB= beta-blocker; mexil.= mexiletine; TP = temporarily pacemaker, PP = permanent pacemaker.

(538-860 ms^{1/2}), and all 6 previously reported infants died before the age of 2 years (6,22,24,27,30,31), despite treatment with beta-blockers (n=4) or pacemakers (n=3).

It is possible that the presence of long-QT syndrome and VSD in our patient occurred by chance, but the recognition of seven patients with an association of two uncommon disorders may suggest otherwise (TABLE 6.1). Although it is attractive to assume that the association is not random, and that a genetic mechanism may be responsible, our data suggest that this may not be the case. Importantly, the proband and mother carry the same *SCN5A* mutation and *MiRP1* polymorphism, but only the infant had a VSD and experienced severe QT-interval prolongation. Since proband and mother are of the same sex, the distinction in clinical presentation strongly suggests that other factors likely contribute both to the structural and electrical dysfunction. In terms of the electrical problem, it is possible that the developmentally distinct modifier gene activity may, in combination with the detected Na⁺ channel defect, produce severe changes in QT prolongation seen in the proband.

Novel Biophysical Phenotype of the L619F Mutation

Functional analysis shows that the biophysical phenotype of the L619F mutation is novel, as it combines increased non-inactivating sodium current as reported previously for several other LQT-3 mutations (33,34), with an increase in the magnitude of window current as first reported by Abriel et al. (13,35). Using a single channel based model of the ventricular action potential, Clancy and Rudy (11) showed that an increased sustained sodium current can prolong ventricular repolarization, which may cause arrhythmogenic early afterdepolarization (11). The increase in Na⁺ channel window current is most likely sufficient to cause prolongation of the QT-interval by itself, as two previous studies (13,35) reported such channel defect in *SCN5A* mutants associated with the long-QT syndrome. Neither of these mutations, however, caused non-inactivating sodium current as well. An increase in Na⁺ channel window current is expected to offset the delicate balance between inward and outward membrane currents during the final phase of repolarization (13), which may lead to prolongation of the ventricular action potential. Thus, the biophysical changes caused by the L619F mutation are consistent with the expected cellular phenotype: action potential prolongation.

We also observed a speeding of the recovery from inactivation kinetics in L619F mutant Na⁺ channels. Although faster recovery kinetics are observed in the majority of LQT-3 mutants (13,14,34,35), it is currently not fully understood whether or not this change in gating contributes to action potential prolongation, but this change in recovery kinetics

will certainly shorten refractory periods in the ventricle and predispose the heart to premature excitation. Interestingly, the mother of the index patient, who also carried the *SCN5A* mutation, displayed only borderline QTc interval prolongation, and did not experience any long-QT syndrome-related symptoms. This suggests that other (genetic) factors, in combination with the channel defect, may be necessary to induce the long-QT syndrome phenotype.

First LQTS Mutation in the Cytoplasmic Linker Between Domain I and II of *SCN5A*

The L619F mutation is the first LQTS mutation in *SCN5A* to occur in the cytoplasmic loop, connecting domains I and II. This mutation causes the substitution from an evolutionary conserved leucine to phenylalanine, which is likely to change the protein secondary structure. Previously, two *SCN5A* mutations linked to Brugada syndrome have been reported in the same domain of the Na⁺ channel. Gulcheney et al. (36) reported the missense mutation T632M, and Priori et al. (37) reported the L567Q mutation in a 14-month old girl that died of ventricular fibrillation due to Brugada syndrome. Wan et al. (38) studied the biophysical properties of L567Q Na⁺ channels in HEK cells, and demonstrated that L567Q channels accelerate fast inactivation, and enhance closed-state inactivation. The resulting decrease in Na⁺ channel availability is believed to be responsible for idiopathic ventricular fibrillation (38).

Together with our results, the data of Wan et al. (38) implicate a role of the intracellular I-II linker in the control of Na⁺ channel inactivation. The L619F mutation speeds the recovery from inactivation, which suggests that the fast inactivated state of mutant Na⁺ channels is destabilized. Whether the L619F mutation directly interferes with the fast inactivation particle (39), or its docking sites (40,41), or whether this phenomenon is due to allosteric interactions, remains to be determined.

Summary

In summary, we have identified a novel heterozygous mutation in the *SCN5A* gene in an infant with congenital long-QT syndrome and 2:1 atrioventricular block. The clinical presentation and the electrophysiological findings make this mutation very likely to be the cause of the disease. The L619F mutation causes a unique biophysical phenotype, as it combines increased non-inactivating Na^+ current with a larger window current. The defective inactivation imposed by the L619F mutation implicates a novel role for the domain I-II linker in the Na^+ channel inactivation process.

Acknowledgments

X.H.T.W. was a recipient of a Hein Wellens Fund travel grant; T.R. is a research assistant of the Fund for Scientific Research- Flanders (FWO Belgium); M.G. was supported in part by the Belgium Foundation for Research in Pediatric Cardiology. This work was supported in part by grant HL-56810 awarded to RSK from the USPHS. We thank Drs. Colleen Clancy and Michihiro Tateyama for helpful discussion.

References

1. Mache CJ, Beitzke A, Haidvogel M Jr, Gamillscheg A, Suppan C, Stein JI. Perinatal manifestations of idiopathic long-QT syndrome. *Pediatr Cardiol* 1996;17:118-21.
2. Schwartz PJ. Idiopathic long-QT syndrome: progress and questions. *Am Heart J* 1985;109:399-411.
3. Schwartz PJ, Priori SG, Dumaine R, Napolitano C, Antzelevitch C, Stramba-Badiale M, Richard TA, Berti MR, Bloise R. A molecular link between the sudden infant death syndrome and the long-QT syndrome. *N Engl J Med* 2000;343:262-67.
4. Van Hare GF, Franz MR, Roge C, Scheinman MM. Persistent functional atrioventricular block in two patients with prolonged QT-intervals: elucidation of the mechanism of block. *Pacing Clin Electrophysiol* 1990;13:608-18.
5. Pruvot E, De Torrente A, De Ferrari GM, Schwartz PJ, Goy JJ. Two-to-one AV block associated with the congenital long-QT syndrome. *J Cardiovasc Electrophysiol* 1999;10:108-13.
6. Trippel DL, Parsons MK, Gillette PC. Infants with long-QT syndrome and 2:1 atrioventricular block. *Am Heart J* 1995;130:1130-34.
7. Gorgels AP, Al Fadley F, Zaman L, Kantoch MJ, Al Halees Z. The long-QT syndrome with impaired atrioventricular conduction: a malignant variant in infants. *J Cardiovasc Electrophysiol* 1998;9:1225-32.
8. Hoorntje T, Alders M, Van Tintelen P, Van der Lip K, Sreeram N, Van der Wal A, Mannens M, Wilde A. Homozygous premature truncation of the *HERG* protein: the human *HERG* knockout. *Circulation* 1999;100:1264-67.
9. Piippo K, Laitinen P, Swan H, Toivonen L, Viitasalo M, Pasternack M, Paavonen K, Chapman H, Wann KT, Hirvela E, Sajantila A, Kontula K. Homozygosity for a *HERG* potassium channel mutation causes a severe form of long-QT syndrome: identification of an apparent founder mutation in the Finns. *J Am Coll Cardiol* 2000;35:1919-25.
10. Lupoglazoff JM, Cheav T, Baroudi G, Berthet M, Denjoy I, Cauchemez B, Extramiana F, Chahine M, Guicheney P. Homozygous *SCN5A* mutation in long-QT syndrome with functional two-to-one atrioventricular block. *Circ Res* 2001;89:E16-21.
11. Clancy CE, Rudy Y. Linking a genetic defect to its cellular phenotype in a cardiac arrhythmia. *Nature* 1999;400:566-69.
12. An RH, Wang XL, Kerem B, Benhorin J, Medina A, Goldmit M, Kass RS. Novel LQT-3 mutation affects Na^+ channel activity through interactions between α - and β 1-subunits. *Circ Res* 1998;83:141-46.
13. Abriel H, Cabo C, Wehrens XHT, Rivolta I, Motoike HK, Memmi M, Napolitano C, Priori SG, Kass RS. Novel arrhythmogenic mechanism revealed by a long-QT syndrome mutation in the cardiac Na^+ channel. *Circ Res* 2001;88:740-45.
14. Wehrens XHT, Abriel H, Cabo C, Benhorin J, Kass RS. Arrhythmogenic mechanism of an LQT-3 mutation of the human heart Na^+ channel α -subunit: A computational analysis. *Circulation* 2000;102:584-90.
15. Schwartz PJ, Priori SG, Locati EH, Napolitano C, Cantu F, Towbin JA, Keating MT, Hammoude H, Brown AM, Chen LS. Long-QT syndrome patients with mutations of the *SCN5A* and *HERG* genes have differential responses to Na^+ channel blockade and to increases in heart rate. Implications for gene-specific therapy. *Circulation* 1995;92:3381-86.
16. Sesti F, Abbott GW, Wei J, Murray KT, Saksena S, Schwartz PJ, Priori SG, Roden DM, George AL, Goldstein SA. A common polymorphism associated with antibiotic-induced cardiac arrhythmia. *Proc Natl Acad Sci U S A* 2000;97:10613-18.

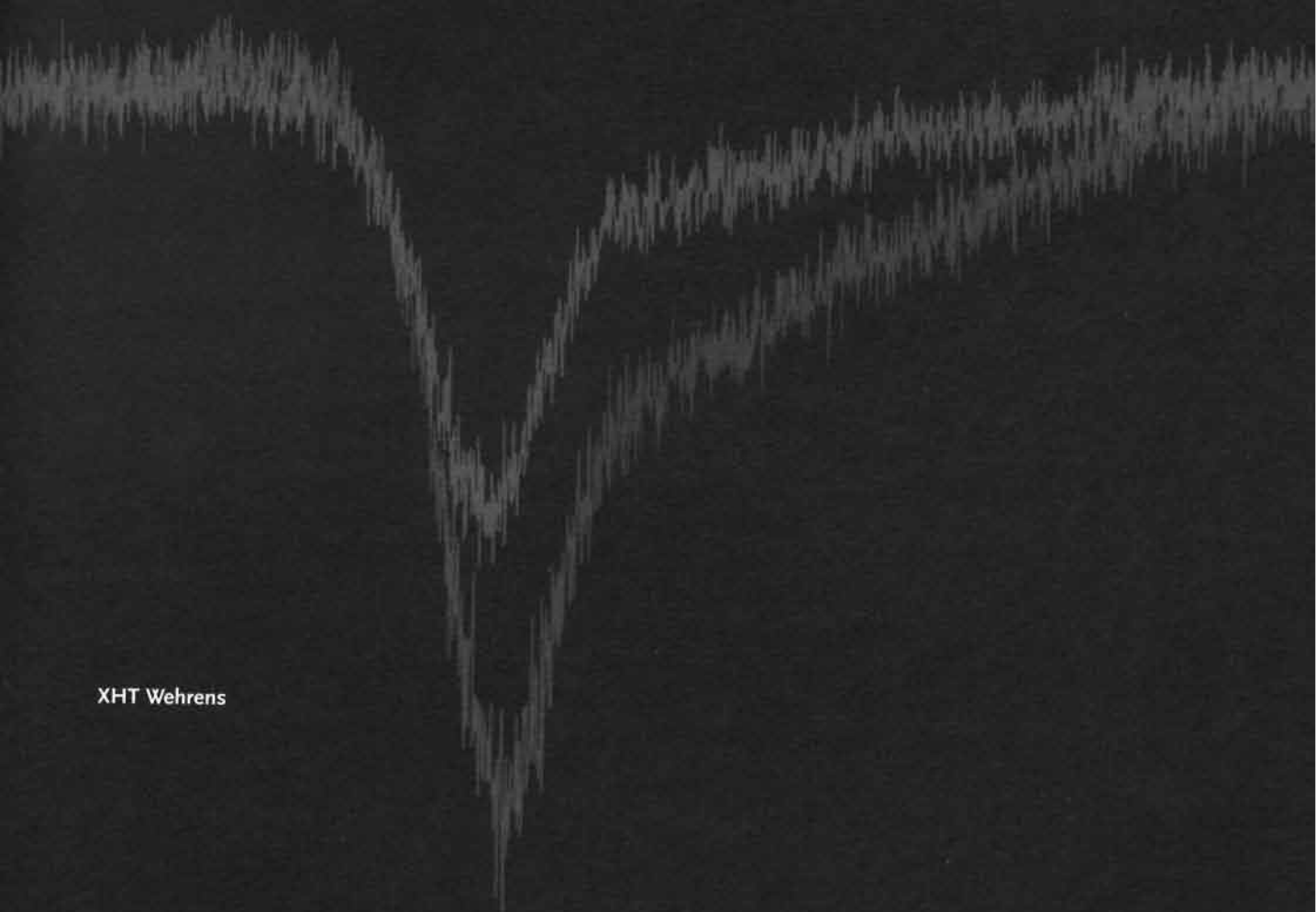
17. Attwell D, Cohen I, Eisner D, Ohba M, Ojeda C. The steady state TTX-sensitive ("window") sodium current in cardiac Purkinje fibres. *Pflügers Arch* 1979;379:137-42.
18. Kernohan RJ, Froggatt P. Atrioventricular dissociation with prolonged QT-interval and syncopal attacks in a 10-year old boy. *Br Heart J* 1974;36:516-19.
19. Di Segni E, David D, Katzenstein M, Klein HO, Kaplinsky E, Levy MJ. Permanent overdrive pacing for the suppression of recurrent ventricular tachycardia in a newborn with long-QT syndrome. *J Electrocardiol* 1980;13:189-92.
20. Batisse A, Belloy C, Fermon L, Piechaud JF, Kachaner J. Allongement de l'espace QT avec bloc auriculo-ventriculaire fonctionnel chez le nouveau-né et le jeune nourrisson. *Arch Fr Pédiatr* 1981;38:657-62.
21. Morville P, Mauran P, Motte J, Digeon B, Coffin R. Torsades de pointe fœtales et syndrome du QT long. *Arch Mal Coeur Vaiss* 1985;78:781-84.
22. Pellegrino A, Ho SY, Anderson RH, Hegerty A, Godman MJ, Michaelsson M. Prolonged QT-interval and the cardiac conduction tissues. *Am J Cardiol* 1986;58:1112-13.
23. Case CL, Gillette PC. Conduction system disease in a child with long-QT syndrome. *Am Heart J* 1990;120:984-86.
24. Saoudi N, Bozio A, Kirkorian G, Atallah G, Normand J, Touboul P. Prolonged QT, atrioventricular block, and sudden death in the newborn: an electrophysiologic evaluation. *Eur Heart J* 1991;12:838-41.
25. Garson A Jr, Dick M, Fournier A, Gillette PC, Hamilton R, Kugler JD, van Hare GF 3rd, Vetter V, Vick GW 3rd. The long-QT syndrome in children. An international study of 287 patients. *Circulation* 1993;87:1866-72.
26. Perticone F, Canepa SA, Ceravolo R, Cloro C, Mattioli PL. A case of torsades de pointes occurring in a newborn with persistent 2:1 atrioventricular block. *Cardiology* 1993;83:134-40.
27. Marks ML, Whisler SL, Clericuzio C, Keating M. A new form of long-QT syndrome associated with syndactyly. *J Am Coll Cardiol* 1995;25:59-64.
28. Tanel RE, Friedman JK, Walsh EP, Epstein MR, DeLucca JM, Mayer JE Jr, Fishberger SB, Saul JP. High-rate atrial pacing as an innovative bridging therapy in a neonate with congenital long-QT syndrome. *J Cardiovasc Electrophysiol* 1997;8:812-17.
29. Donofrio MT, Gullquist SD, O'Connell NG, Redwine FO. Fetal presentation of congenital long-QT syndrome. *Pediatr Cardiol* 1999;20:441-44.
30. Wu MH, Hsieh FC, Wang JK, Kau ML. A variant of long-QT syndrome manifested as fetal tachycardia and associated with ventricular septal defect. *Heart* 1999;82:386-88.
31. Abbott GW, Sesti F, Splawski I, Buck ME, Lehmann MH, Timothy KW, Keating MT, Goldstein SA. *MiRP1* forms I_{Kr} potassium channels with *HERG* and is associated with cardiac arrhythmia. *Cell* 1999;97:175-87.
32. Lin MT, Wu MH, Hsieh FJ, Wang JK, Teng RJ, Tsou KI, Lue HC. Long-QT syndrome manifested as fetal ventricular tachycardia and intermittent AV block. *Am J Perinatol* 1998;15:145-47.
33. Bennett PB, Yazawa K, Makita N, George AL Jr. Molecular mechanism for an inherited cardiac arrhythmia. *Nature* 1995;376:683-85.
34. Wang DW, Yazawa K, George AL Jr, Bennett PB. Characterization of human cardiac Na^+ channel mutations in the congenital long-QT syndrome. *Proc Natl Acad Sci U S A* 1996;93:13200-05.
35. Wedekind H, Smits JP, Schulze-Bahr E, Arnold R, Veldkamp MW, Bajanowski T, Borggrefe M, Brinkmann B, Warnecke I, Funke H, Bhuiyan ZA, Wilde AA, Breithardt G, Haverkamp W. *De novo* mutation in the *SCN5A* gene associated with early onset of sudden infant death. *Circulation* 2001;104:1158-64.

36. Guicheney P, Descheres I, Nicolas L, Berthet M, Chalvidan T, Davy JM, Leenhardt A, Coumel P, Denjoy I, Chahine M. Novel mutation in the cardiac Na⁺ channel α -subunit gene (SCN5A) in patients with Brugada syndrome. *Eur Heart J* 1999;20:465 (abstract).
37. Priori SG, Napolitano C, Giordano U, Collisani G, Memmi M. Brugada syndrome and sudden cardiac death in children. *Lancet* 2000;355:808-09 (letter).
38. Wan X, Chen S, Sadeghpour A, Wang Q, Kirsch GE. Accelerated inactivation in a mutant Na⁺ channel associated with idiopathic ventricular fibrillation. *Am J Physiol Heart Circ Physiol* 2001;280:H354-60.
39. West JW, Patton DE, Scheuer T, Wang Y, Goldin AL, Catterall WA. A cluster of hydrophobic amino acid residues required for fast Na⁺ channel inactivation. *Proc Natl Acad Sci U S A* 1992;89:10910-14.
40. Tang L, Kallen RG, Horn R. Role of an S4-S5 linker in sodium channel inactivation probed by mutagenesis and a peptide blocker. *J Gen Physiol* 1996;108:89-104.
41. McPhee JC, Ragsdale DS, Scheuer T, Catterall WA. A critical role for the S4-S5 intracellular loop in domain IV of the sodium channel α -subunit in fast inactivation. *J Biol Chem* 1998;273:1121-29.

Chapter 7

General Discussion

XHT Wehrens



Overview of Cardiac Ion Channelopathies

In 1995, it became clear that the congenital long-QT syndrome resulted from mutations in cardiac ion channels (1). Mutations in cardiac potassium channels, followed by the cardiac sodium channel, and auxiliary β -subunits of potassium channels have all been linked to the long-QT syndrome (1-7) . At present time, a molecular genetic diagnosis can be made in about 80-90% of all patients with familial long-QT syndrome (P. Doevendans, *personal communication*), implicating that mutations in proteins not yet identified may also underlie this disease. It is in the line of expectation that other ion channels, as well as auxiliary subunits, and proteins involved in the regulation of cardiac ion channels, will be linked to

TABLE 7.1
Overview of genes causing
cardiac ion channelopathies.

Syndrome	Gene	Ion channel	Reference
LQT-1	KCNQ1	I _{Ks}	(3)
LQT-2	KCNH2	I _{Kr}	(2)
LQT-3	SCN5A	I _{Na}	(1)
LQT-4	-	-	(4)
LQT-5	KCNE1	I _{Ks}	(5)
LQT-6	KCNE2	I _{Kr}	(6)
BrS	SCN5A	I _{Na}	(11)
PCCD	SCN5A	I _{Na}	(12)
ICCD	SCN5A	I _{Na}	(13)
Andersen's syndrome	KCNJ2	I _{Kir2.1}	(14)
CPVT	RYR2	Ryanodine receptor	(15)
ARVD2	RYR2	Ryanodine receptor	(16)

BrS= Brugada syndrome; PCCD= progressive cardiac conduction disease; ICCD= isolated cardiac conduction disease; CPVT= catecholaminergic polymorphic ventricular tachycardia; ARVD2= arrhythmogenic right ventricular dysplasia type 2.

the long-QT syndrome in the near future (8). Alterations of any of these components may interfere with normal function of ion channels, and thus lengthen ventricular repolarization.

The congenital long-QT syndrome was the first cardiac ion “channelopathy” to be identified. Since then, a whole spectrum of inherited arrhythmias based on cardiac ion channel mutations has emerged (TABLE 7.1). Although familial arrhythmic syndromes are relatively uncommon, they can provide significant insight into the mechanisms underlying more general conduction and repolarization abnormalities (9). The understanding of the genetic basis, or the molecular origin, of inherited cardiac arrhythmias is likely to have major impact on the diagnostic approach, prevention and treatment of these disorders (10).

Biophysical Phenotypes of Congenital Long-QT Syndrome Na⁺ Channel Mutations

As reviewed in CHAPTERS 1 and 2 of this thesis, congenital long-QT syndrome type 3 (LQT-3) is caused by mutations in the *SCN5A* gene, which encodes the cardiac sodium channel. After the first mutations were discovered in 1995 (1), the function of recombinant sodium channels encoded by mutated *SCN5A* genes were studied in heterologous expression systems, in particular *Xenopus laevis* oocytes and human embryonic kidney (HEK) cells (17-19). From these early studies, it became clear that most of the LQT-3 mutant sodium channels failed to completely inactivate, which leads to so-called ‘noninactivating current’ visible during prolonged depolarizing pulses (17,19). In addition to ‘destabilizing’ the inactivated state of the sodium channel (i.e. allowing reopenings of inactivated channels) (17,19-22), an allied mechanism has been described for R1623Q mutant channels, which exhibit a slowed rate of entry into the fast-inactivated state, causing a net ‘gain of function’ by prolonging Na⁺ current decay (23,24).

In 1998, An et al. (25) reported the D1790G mutation, located in the early C-terminal part of the sodium channel, which does not lead to incomplete inactivation of the sodium channel. In CHAPTER 3 of this thesis, we have extended the finding that noninactivating current is absent (26), and used the Luo-Rudy computer model of the ventricular action potential to get a better idea how this mutation might evoke action

potential prolongation (26). In short, the changes in D1790G Na⁺ channel kinetics reduce Na⁺ current during the action potential upstroke, which is predicted to produce a less positive overshoot of the action potential (CHAPTER 3). The computational model predicts an increased Ca²⁺ entry via L-type Ca²⁺ channels, leading to an augmented subsequent Ca²⁺ transient. Two important ionic pathways, the Na⁺/Ca²⁺ exchanger (27) and slowly activating delayed K⁺ channel current I_{Ks} (28), are affected, which is predicted to cause a net increase of inward plateau current and corresponding increase in action potential duration. Because the Luo-Rudy computer model may oversimplify intracellular calcium handling, future studies using transgenic mice harboring the D1790G mutation are needed to confirm that action potential prolongation is indeed dependent on Ca²⁺-sensitive ionic pathways. Recently, Baroudi et al. (98) measured noninactivating Na⁺ current in HEK cells expressing D1790G channels. Other parameters also differed from those measured in our study (26), in particular V_{1/2} values for steady-state activation and inactivation, which might reflect differences in experimental conditions. Additional studies are required to further investigate these interesting observations.

The E1295K mutation, described in CHAPTER 5, is another example of an LQT-3 mutation that does not promote sustained sodium channel activity during prolonged depolarizations (29). This mutation prolongs the ventricular action potential in a distinctly different way. The mutation-induced gating changes shift the window of voltages over which Na⁺ channels do not completely inactivate, and this causes marked changes in action potential duration because of the unique voltage-dependent rectifying properties of cardiac K⁺ channels that underlie the plateau and terminal repolarization phases of the action potential. Because the peak of the E1295K Na⁺ channel window current occurs at more positive potentials, it is likely to have a greater effect on net membrane current because total K⁺ channel conductance is lower at these more positive potentials (29). The same biophysical phenotype has been reported for LQT-3 mutation A1330P (30).

Interestingly, the novel L619F mutation, described in CHAPTER 6, is the first LQT-3 mutation that combines both noninactivating sodium current and an increase in window current. These data clearly demonstrate that there are at least four different mutation-induced gating changes in LQT-3 sodium channels. Although distinctly different, and not always associated with noninactivating sodium current during sustained depolarization, all of these biophysical phenotypes seem to result from mutation-induced defects in the inactivated conformational state of the sodium channel. The first combination of such gating changes has been described for the L619F mutation, and it is likely that in the near future even more variations in biophysical phenotypes will be described.

Correlating Na⁺ Channel Structure and Gating Function in LQT-3 Mutations

The functional characterization of sodium channels containing LQT-3 mutations revealed the biophysical mechanisms causing aberrant conduction of sodium current. Based on the knowledge that has been obtained from mutagenesis experiments over the past decade, a picture of the structure-function relationship of the different domains in the sodium channel has emerged (for review, see CHAPTER 2, and (31,32)). In the following paragraphs, we try to integrate the LQT-3 mutations into the latest insights in the structure of the sodium channel (FIGURE 7.1).

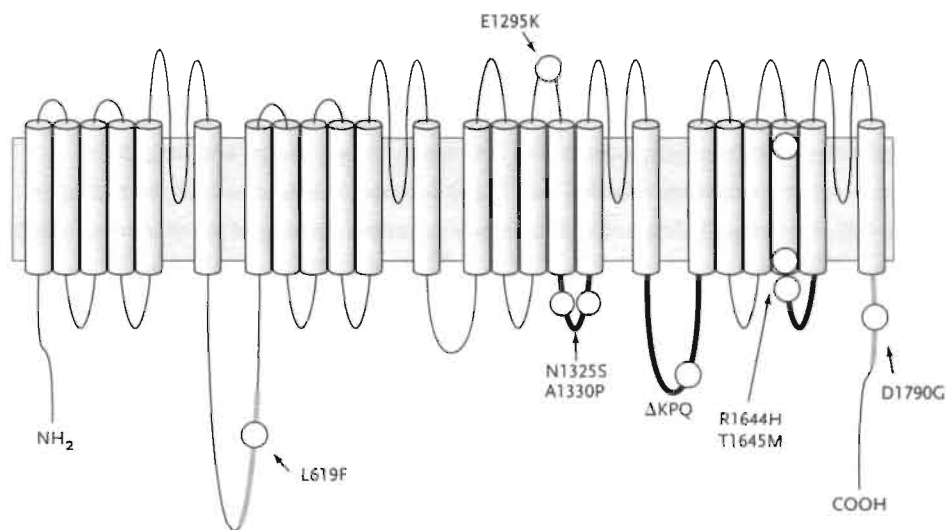


FIGURE 7.1

Structure of the cardiac Na⁺ channel α -subunit. Indicated with the circles are long-QT syndrome mutations with the respective amino-acid substitutions. The domain III-IV linker, as well as the S4-S5 loops of domain III and IV (thick black lines) are known to be involved in fast inactivation. Data presented in this thesis implicate that the domain I-II linker and C-terminus might be involved in this process as well (thick grey lines).

Fast Inactivation Particle: Domain III-IV Linker

The finding that the Δ KPQ deletion in the loop between domain III and IV reduces fast inactivation of Na⁺ currents was not unexpected (17). It was already recognized that this region serves as the inactivation particle of the Na⁺ channel (33,34). A cluster of three hydrophobic amino acids (I1485, F1486, M1487) is thought to bind to a receptor region on the cytoplasmic surface of the channel protein. It is therefore likely that the Δ KPQ deletion due to its close proximity to the IFM motif may disrupt the inactivation particle, hereby interfering with fast inactivation.

Rohl et al. (35) determined the three-dimensional structure of the central portion of the inactivation gate as a peptide in a phosphate buffer using multidimensional NMR methods. The experiments revealed a rigid α -helix flanked on its N-terminal side by two turns, the second of which contains the IFM motif. They found that M1487 (residue number in the cardiac isoform) of the IFM motif hydrophobically interacts with Y1494 and Y1495, consistent with a three-dimensional structure of the IFM motif itself. The structure of the inactivation gate peptide in solution suggests that the rigid helix serves as a scaffold to present the IFM motif and the adjacent T1488 to a receptor in the mouth of the pore as the gate closes (hinged lid model).

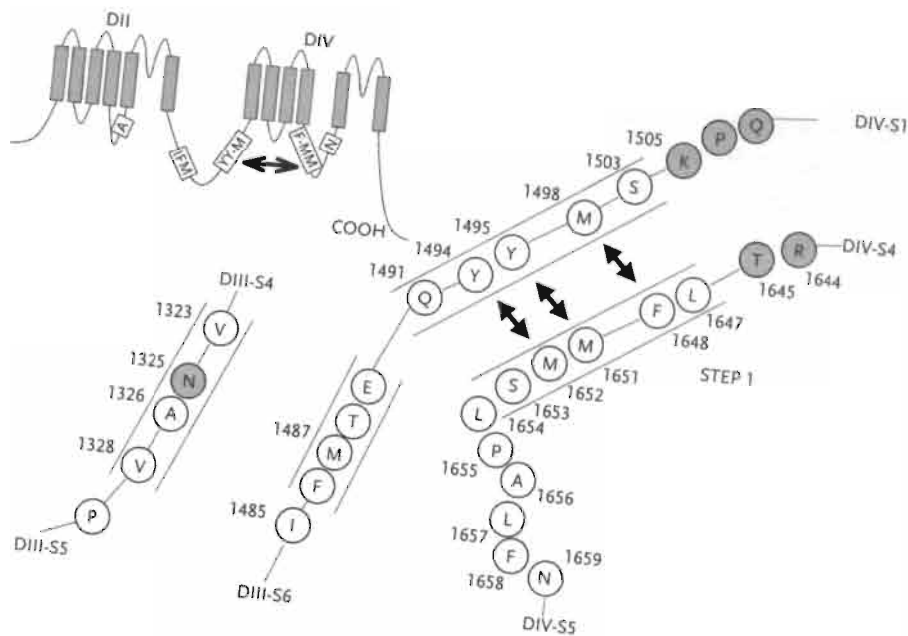
Since the interaction of the inactivation particle with its receptor is considered to be mediated by the hydrophobic forces (36), the conformation Rohl et al. (35) determined in phosphate buffer seems to represent the IFM motif at a resting or open state of the channels, but not in an inactivated state. Miyamoto et al. (37) determined the solution structure of the III-IV linker in sodium dodecyl sulfate (SDS) micelles (a relevant environment at the inactivated state of the channels), and confirmed the presence of a large hydrophobic cluster composed of the IFM motif, Y1494, Y1495, and M1498. In addition, a subsequent study revealed that T1488 probably is bound to I1485 by hydrogen bonds (38). This large hydrophobic cluster may assist the docking of the IFM motif within its receptor regions.

Docking Stations for the Inactivation Particle: Domain III-S4/S5 and Domain IV-S4/S5

The S4-S5 linkers of domain III and IV are thought to form the docking stations for the inactivation particle (39-42). Recent data from Miyamoto et al. (43) extended these electrophysiological data, and it now seems reasonable to assume that after initial depolarization, two hydrophobic clusters in DIV-S4/S5 interact with the III-IV linker. This hydrophobic interaction would then reduce polarity around the IFM motif, allowing I1485-F1486 to meet the hydrophobic cluster as a result of a conformational change (37,44). The inactivation gate then closes by interacting with A1326 in domain III-S4/S5 and/or with N1659 in DIV-S4/S5 (43) (FIGURE 7.2).

Several naturally occurring long-QT syndrome mutation occur in the DIII-S4/S5 (N1325S, A1330P), and DIV-S4/S5 loops (R1644H, T1645M), and it seems tempting to reconcile them with the discussed structural picture of fast inactivation (FIGURE 7.1 and 7.2). Whereas the N1325S and R1644H mutations show persistent inward current consistent with disrupted fast inactivation, the A1330P (30) and T1645M (Wehrens et al.,

A



B

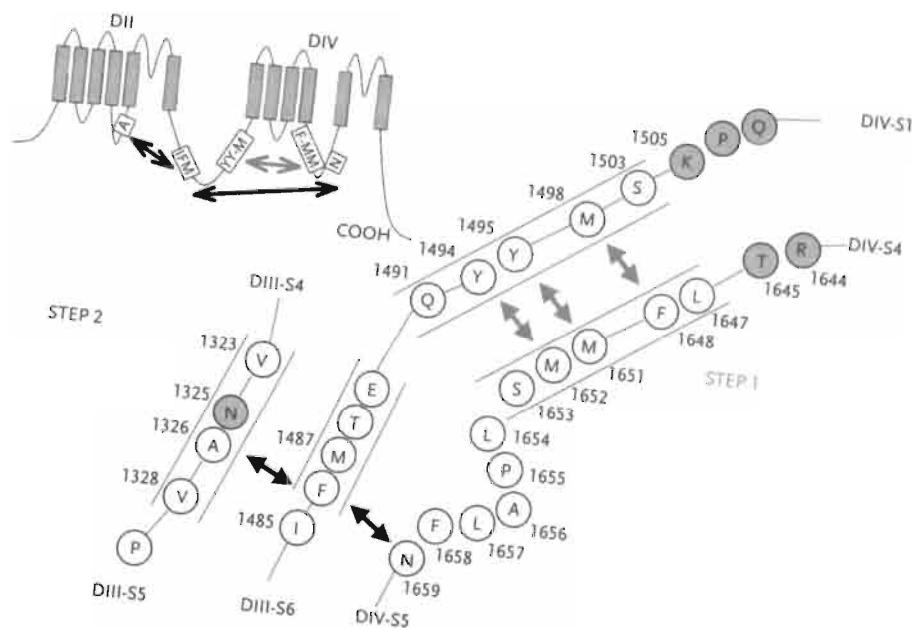


FIGURE 7.2

Schematic representation of the interaction of the III-IV linker with the D3-S4/S5 and D4-S4/S5 domains during sodium channel inactivation. After depolarization, two hydrophobic clusters in domain IV-S4/S5 interact with the III-IV linker (panel A). This hydrophobic interaction reduces polarity around the IFM motif, allowing F1486 to interact with A1326 in domain III-S4/S5 and N1659 in domain IV-S4/S5, hereby closing the inactivation gate (panel B). Please note that residue V1328 is an L in the brain type IIA isoform of the sodium channel. The cylinders represent α -helical structural parts. Mutations of the residues in the grey circles have been linked to the congenital long-QT syndrome. Figure modified from Miyamoto et al. (*J Pept Res* 2001;58:193-203).

unpublished data) do not show these electrophysiological properties. The N1325 residue is directly adjacent to A1326, which is believed to interact with the phenylalanine of the IFM motif (40,43). For now, it remains unclear how the other long-QT syndrome mutations cause structural changes directly affecting channel gating, and it is more likely that allosteric changes are responsible for impaired channel inactivation.

Role of the C-Terminus in Channel Inactivation

Little is known about the function of the C-terminal region of the voltage-gated sodium channels. Recently, the study of long-QT syndrome mutations in the C-terminus of the human cardiac sodium channel implicated a role possible of this channel region in fast inactivation (see also CHAPTER 3) (20,22,26,45). Using chimeric channels between the human heart isoform (*hH1*) (46) and the human skeletal muscle isoform (*hSkM1*) (47), Deschenes et al. (48) showed that the first 100 amino acids of the C-terminal region of the α -subunit of the sodium channel are responsible for differences in current decay kinetics between heart and skeletal muscle channels. These results together with the modeling study by Sato et al. (49) link the C-terminus to fast inactivation, along with the inactivation gate.

Considerable heterogeneity consists in the biophysical properties of the four long-QT syndrome mutations reported so far in the first 23 amino acids of the C-terminus (20,22,25,45). All but one, D1790G, promote non-inactivating Na^+ current during prolonged depolarizations. On the other hand, whereas three mutations cause a large negative shift in the steady-state inactivation curve, consistent with increased close-state inactivation, the Y1795C mutation does not alter this parameter (TABLE 7.2). Based on computer model predictions of the sodium channel structure, it is believed that the negatively charged proximal C-terminus might interact with the positively charged III-IV, and possibly also the II-III cytoplasmic linker regions of the Na^+ channel (49). More comprehensive structural analysis of the carboxy-terminus will be essential to better comprehend the biophysical changes imposed by long-QT syndrome mutations in this region of the channel.

A Role for the Domain I-II Linker in Channel Inactivation?

In CHAPTER 6, we reported that the L619F mutation in the cytoplasmic loop connecting domain I and II speeds recovery from inactivation, and is thus likely to destabilize the inactivated state of the sodium channel. The intracellular domain between domain I and II is relatively unconserved between sodium channel isoforms (50,51). In the cardiac isoform,

TABLE 7.2
Biophysical characteristics
of long-QT syndrome-
associated Na⁺ channel
mutations.

Mutation	Maintained current (% peak)	Current decay	Activation shift V _{1/2} (mV)	Inactivation shift V _{1/2} (mV)	Recovery from inact. (x fold)	Reference
L619F	0.3%	n.s.	n.s.	+5.8	τ_f 0.55	Wehrens, this thesis*
S941N	0.25-0.4%	n.a.	n.a.	n.a.	n.a.	(21)
E1295K	n.s.	n.s.	+3.4	+5.2	τ_f 0.58	(29)*
N1325S	1.0% 2.5-5.0%	n.s. $\tau_f/\tau_s <$	n.a. -6.4	n.a. n.s.	τ_s 1.25 $\tau >$	(19) (18)*
A1330P	n.s.	τ 0.64	n.s.	+8.3	τ_f 0.58	(30)*
Δ KPQ (1505-1507)	<5% 2-5% 1.0% 0.8%	τ_f 0.7, τ_s 0.6 $\tau_f/\tau_s <$ τ 0.21-0.34 $\tau_f <$, τ_s n.s.	n.a. +6.0 n.s. +6.6	-5.8 -3.6 -6.3 n.s.	n.s. $\tau <$ τ_f 0.6 $\tau <$	(17) (18)* (95)* (96)*
R1623Q	<5.0% <3.0% n.a.	τ_f 3.2, τ_s 1.9 τ 3.4 τ 3.7	n.s. n.a. n.a.	n.s. n.a. -5.8	τ 0.77 (n.s.) n.a. τ_f 0.29, τ_s 0.53	(23) (24)* (79)
R1644H	0.5% 0.8%	n.s. $\tau_f/\tau_s <$	n.a. n.s.	n.a. n.s.	n.s. $\tau_f/\tau_s <$	(19) (18)*
V1777M	4.0%	n.a.	-9.0	-12.0	n.a.	(45)*
E1784K	2.0-4.0% 1.5%	$\tau <$ n.s.	n.a. +8.8	-12.1 -14.0	τ_f 0.83, τ_s 0.53 τ 0.5	(20) (97)*
D1790G	n.s. n.s.	n.s. τ 0.5	n.s. +6	-16.2 -15	n.a. τ_f 0.73	(25)* (26)*
Y1795C	2.0%	$\tau >$	n.s.	+2.8	n.s.	(22)*

* Sodium channels expressed in HEK cells. N.a. = not assessed; n.s. = not significant.

two mutations in this region have been linked to the Brugada syndrome. Wan et al. (52) studied the biophysical properties of one of these, the L567Q mutation, in HEK cells and demonstrated that L567Q channels accelerate fast inactivation, but at the same time enhance closed-state inactivation which decreases Na⁺ channel availability, which is believed to cause idiopathic ventricular fibrillation (52).

Our data from CHAPTER 6 along with the data from Wan et al. (52), suggest that the I-II linker region is involved in Na⁺ channel inactivation (FIGURE 7.1). However, it is impossible to conclude whether these mutations in the I-II linker directly interfere with the fast inactivation particle (17,36), or its docking sites (39,42,53,54), or whether this phenomenon is due to allosteric interactions.

Conclusions Regarding LQT-3 Biophysical Phenotypes

In the last couple of years, it has become apparent that LQT-3 mutations over a fairly wide range of the sodium channel α -subunit can destabilize the inactivated state of the channel, directly or through possible allosteric effects. This suggests that the structural requirements for normal inactivation are fairly precise, and depend upon complex ensemble interactions among many structural domains (31).

Some biophysical properties occur commonly in LQT-3 mutations, most notably a speeding of the onset of inactivation, and a faster recovery from inactivation (TABLE 7.2). Whereas some features such as increased bursting (noninactivating current) and increased window current are easily correlated to a cellular phenotype (29,55), other kinetic properties may also contribute to action potential prolongation in subtle, as yet unexplored, ways.

Molecular Pharmacology of LQT-3 Mutations

Local Anesthetic Action is Gating-dependent

In CHAPTER 2, we described that local anesthetic/ class I antiarrhythmic drug activity is gating-dependent (the ‘modulated receptor theory’) (56-59). Indeed, mutagenesis experiments have revealed that amino acid residues critical to drug binding and channel gating overlap to some degree. For example, alanine substitution of residues F1760 and Y1767 (in SCN5A) in D4S6 increase the IC₅₀ for depolarization-dependent block by lidocaine up to two orders of magnitude (60,61). In addition, mutations in D1S6

(N406 and L409 in the cardiac isoform) also reduce drug affinity (62,63). Interestingly, channels with the mutation F1760A show impaired fast inactivation (64,65), and substitution of the residue N406 alters both fast and slow inactivation (62). Current conceptualization predicts that the channel inactivation process may alter the orientation of amino acid side chains in S6 domains in a manner that facilitates drug binding (62,66).

Proximity of the Local Anesthetic Receptor Site and the Pore Segments

A pore-plugging motif for LA molecules is well supported by evidence that permanently charged lidocaine derivatives (i.e. QX-314) move deeply (50-70%) into the pore from the cytoplasmic site (67-69). This implies that the putative LA binding residues in S6 lie intracellular to the selectivity filter, which is formed by the 'DEKA' ring contributed by the

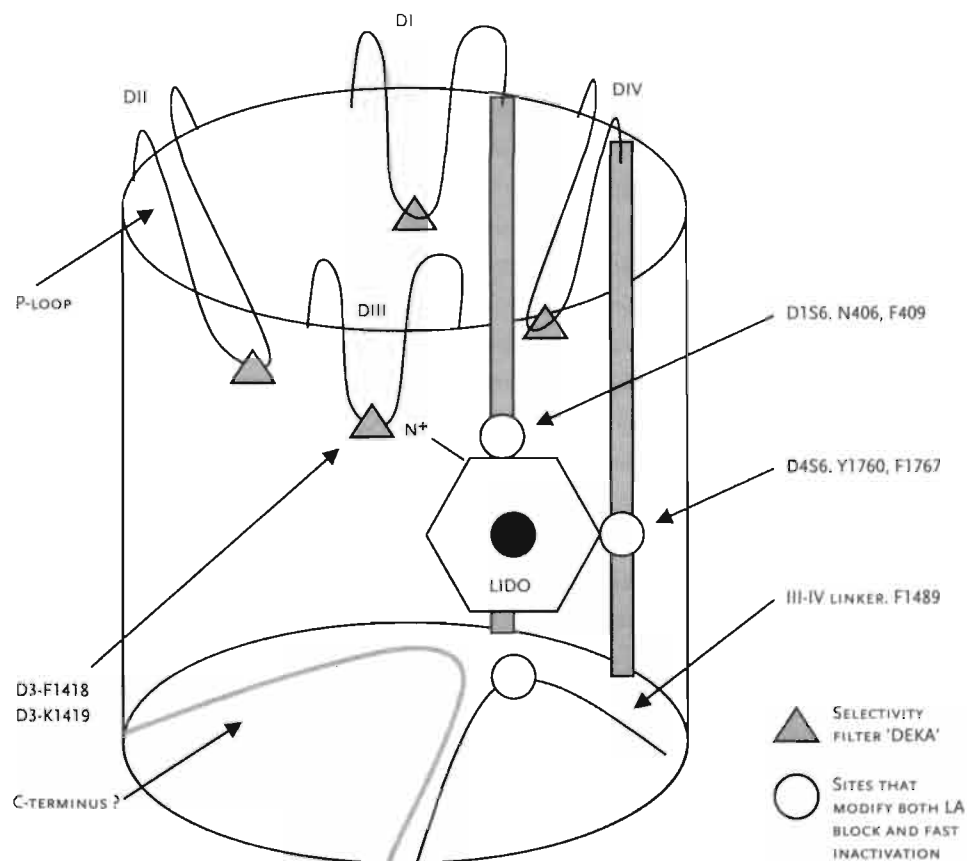


FIGURE 7-3
Schematic view of the Na⁺ channel pore (cylinder), with a lidocaine residing in the pore (LIDO). The outer pore region is formed by the pore-loops of the four homologous domains (I-IV), while the S6 segments line the inner pore. The P-segment selectivity filter residues bridge the outer and inner pore regions. As described in the text, residues in the selectivity filter (i.e. K1419) and the domains I and IV, S6 segments interact with local anesthetics. Residue numbers correspond to the human cardiac isoform (46). Adapted from Balser, *J Mol Cell Cardiol* 2001;33:599-613.

P-loops of each domain (CHAPTER 2). P-loop residues in domains I, II, and IV limit external access (and escape) of hydrophilic LAs, and the domain III lysine residue repels the LA through an electrostatic interaction with the ionizable amino group (70,71). These findings suggest proximity between the S6 segments of domains I and IV and the P-loop selectivity filter regions (70,71), which could provide a rationale for LA induced conformational changes involving the outer P-loops (FIGURE 7.3).

Tonic Block of Sodium Channels: Interaction of Local Anesthetics with the Fast-inactivated State

The earliest modulated-receptor schemes for LA and class I antiarrhythmic drug action assigned a high affinity for the drugs to the open channel state (57). However, experiments that disabled the inactivation gate by replacing the hydrophobic triplet IFM by QQQ in the cytoplasmic III-IV linker suggested an interaction between Na⁺ channel blockers and the inactivated conformational state (69,72). However, more recent studies suggest that LA block can occur without affecting the inactivation gate directly (73). Although lidocaine accelerates depolarization-dependent binding of the inactivation particle to its receptors, it does not 'trap' the fast-inactivation gate as proposed in earlier studies (73), and therefore seems to function as an allosteric effector.

Studies by Hanck et al. (74,75) examined the S₄ voltage sensors during lidocaine block, and revealed that the maximum gating charge (I_g) associated with channel depolarization is reduced by lidocaine. Moreover, site-3 toxins (that specifically inhibit movement of the voltage-sensor associated with inactivation) have an additional effect with lidocaine to suppress the maximum gating charge, further suggesting that lidocaine does not 'stabilize' the Na⁺ channel in the fast-inactivated state (75). These studies suggest that lidocaine may alter closed-state inactivation by influencing the voltage sensors coupled to inactivation gating.

Differential Pharmacological Effects of Na⁺ Channel Blockers in LQT-3 Patients

From clinical studies, it became clear that Na⁺ channel blockers may be particularly useful in managing patients with LQT-3 mutations (76,77). The noninactivating inward current conducted by certain LQT-3 mutations is potentially inhibited by lidocaine and its analogous (19,78). The selective blockade of the late current probably accounts for the QT-interval shortening without QRS prolongation in these patients (76).

However, the class IB antiarrhythmics lidocaine and mexiletine may not have beneficial effects on all LQT-3 mutations. Enhanced sensitivity of the R1623Q peak sodium

current to lidocaine raised concerns regarding the pro-arrhythmic potential of Na⁺ channel blockade in these patients (79). The pro-arrhythmic consequences of Na⁺ channel blockade are well known from the CAST trial (80). In addition, lidocaine did not correct repolarization abnormalities in carriers of the D1790G mutation (77), a mutation that does not enhance late Na⁺ current (25,26). Interestingly, the class IC antiarrhythmic drug flecainide did correct QT-intervals in D1790G mutation carriers (77). Furthermore, there are now clinical data that flecainide might also be effective in carriers of the ΔKPQ mutation (81).

Molecular Pharmacology of Sodium Channel Blockers and LQT-3 Mutations

Certain LQT-3 mutations reduce stability of the inactivated state, inducing a small noninactivating plateau of inward current during depolarization (17,19). When exposed to very low concentrations of the class IB antiarrhythmic agents lidocaine or mexiletine, ΔKPQ channels exhibit gating behavior that approaches the wild-type phenotype (78,82). At the single channel level, lidocaine suppresses the bursting mode (82) and isolated late channel openings (83) of ΔKPQ mutant channels.

Studies of the R1623Q sodium channel mutation exposed an alternative mechanism for lidocaine action on sustained current (79). This study revealed that not only the sustained current component, but also the peak sodium current was unusually sensitive to lidocaine. Further studies revealed that 'closed-state inactivation' (as evidenced by a hyperpolarizing shift in the steady-state inactivation curve) in drug-free conditions was increased (79), in contrast to the more obvious mutation-induced disruption in open-state inactivation (as evidenced by a slowed onset of inactivation) (23). Using a quantitative Markovian model, it was demonstrated that state-dependent lidocaine affinity could further augment closed-state inactivation through an allosteric effector mechanism (79). The same model was also sufficient to reproduce observed effects of lidocaine on sustained current induced by the ΔKPQ mutation, suggesting that an allosteric interaction between lidocaine and the closed-state inactivation state may be more generally applicable. Although the complete picture is still emerging, it is increasingly clear that interactions among multiple mutation-induced gating processes influence local anesthetic action, thereby affording tremendous pharmacologic diversity.

Use-dependent Sodium Channel Block

The previous paragraphs discussed the sensitivity of Na⁺ channels to blockade that ensues immediately upon depolarization ('first-pulse' or 'tonic' block), which correlates primarily

to block that develops during a stimulus delivered after a long diastolic pause. Additional mechanisms may be involved in modulating drug activity that develops during repetitive depolarizations ('use-dependent' block) (84,85). A recent study (70,86) revealed that slow recovery of drug-bound channels between depolarizing stimuli may involve an interaction between local anesthetics and slow-inactivated conformational states. Ong et al. (86) showed that an electrostatic interaction between the domain III P-loop residue K1419/F1418 and the lidocaine amino terminus might induce structural rearrangements associated with slow inactivation that move Na⁺ channel P-loops into positions that stabilize the interaction between lidocaine and the pore (FIGURE 7.3). Therefore, 'use-dependent' block may occur when lidocaine induces sodium channels to occupy a slow inactivating state (86). However, further evidence is required before definite conclusions may be drawn regarding the role of slow inactivation in use-dependent local anesthetic block.

LQT-3 Mutations that Alter Use-dependent Block of Sodium Channels

Flecainide, which is thought to preferentially block open but not inactivated channels, is effective in correcting DG-induced QT prolongation in patients carrying the DG gene defect, while lidocaine has no effect (77). Using heterologously expressed D1790G channels, we showed that this disparity is based on markedly increased use-dependent block sensitivity to flecainide (compared to wild-type channels), but not to lidocaine (87). It was already known that flecainide, as other type IC agents, dissociates relatively slowly after it binds primarily to activated sodium channels (88), and is capable of producing strong use-dependent block of sodium channels (89). From our study (CHAPTER 4), however, it is not clear how a mutation in the C-terminal part of the sodium channel may selectively alter channel sensitivity to use-dependent flecainide block.

Interestingly, the specific alteration of the sensitivity to use-dependent block by flecainide is not a general property of all LQT-3 mutant channels. Recently, Nagatomo et al. (90) found that LQT-3 Δ KPQ mutant channels have an intrinsically higher affinity than wild-type channels to flecainide, but in the case of Δ KPQ, sensitivity to both TB and UDB is increased (90,91). These results implicate that Δ KPQ channels are susceptible to enhanced tonic flecainide block as a result of increased closed-state inactivation gating (91). Thus, our data indicate that the D1790G point mutation causes a unique pharmacological response, which is distinct not only from wild-type but also from Δ KPQ mutant channels.

Conclusions Regarding Mutation-specific Pharmacotherapy for LQT-3 Patients

Present knowledge suggests that fast and slow inactivation gating play important roles in sodium channel blockade. Inherited LQT-3 mutations can alter these gating processes, which may substantially influence the response to antiarrhythmic drugs. On the basis of molecular pharmacological studies in combination with current concepts regarding the interactions of local anesthetic with the sodium channel, the clinical usefulness of particular antiarrhythmic drugs may be predicted.

Carriers of the Δ KPQ mutation, and other mutations that cause late Na^+ current during the action potential plateau phase, may benefit from treatment with lidocaine/mexiletine (76,78,82,83,92), or flecainide/pilsicainide (81,83,90). In contrast, patients with the R1623Q mutations may experience pro-arrhythmic consequences of lidocaine treatment (79,80). Finally, our studies revealed that LQT-3 patients with the D1790G mutation benefit from treatment with flecainide, but not from lidocaine (77,87).

Novel Developments in Mutation-specific Pharmacotherapy and Tailor-made Drugs

A critical aspect of the development of gene- or mutation-specific therapeutic approaches is the functional study of disease-related mutations. Whereas in the past, cardiovascular drug discovery often depended on serendipity, more recently, drugs have arise from more logical scientific approaches. Comprehensive understanding of the biophysical mechanisms underlying ion channel dysfunction, ideally in combination with a detailed picture of the protein structure and channel gating, will enable tailor-made design of drugs that may prevent cardiac arrhythmias in a subset of patients with a particular genetic susceptibility (93,94).

References

1. Wang Q, Shen J, Splawski I, Atkinson D, Li Z, Robinson JL, Moss AJ, Towbin JA, Keating MT. *SCN5A* mutations associated with an inherited cardiac arrhythmia, long-QT syndrome. *Cell* 1995;80:805-11.
2. Curran ME, Splawski I, Timothy KW, Vincent GM, Green ED, Keating MT. A molecular basis for cardiac arrhythmia: *HERG* mutations cause long-QT syndrome. *Cell* 1995;80:795-803.
3. Wang Q, Curran ME, Splawski I, Burn TC, Millholland JM, VanRaay TJ, Shen J, Timothy KW, Vincent GM, de Jager T, Schwartz PJ, Toubin JA, Moss AJ, Atkinson DL, Landes GM, Connors TD, Keating MT. Positional cloning of a novel potassium channel gene: *KVLQT1* mutations cause cardiac arrhythmias. *Nat Genet* 1996;12:17-23.
4. Schott JJ, Charpentier F, Peltier S, Foley P, Drouin E, Bouhour JB, Donnelly P, Vergnaud G, Bachner L, Moisan JP. Mapping of a gene for long-QT syndrome to chromosome 4q25-27. *Am J Hum Genet* 1995;57:1114-22.
5. Splawski I, Tristani-Firouzi M, Lehmann MH, Sanguinetti MC, Keating MT. Mutations in the *hminK* gene cause long-QT syndrome and suppress I_{Ks} function. *Nat Genet* 1997;17:338-40.
6. Abbott GW, Sesti F, Splawski I, Buck ME, Lehmann MH, Timothy KW, Keating MT, Goldstein SA. *MiRP1* forms I_{Kr} potassium channels with *HERG* and is associated with cardiac arrhythmia. *Cell* 1999;97:175-87.
7. Geelen JL, Doevendans PA, Jongbloed RJ, Wellens HJ, Geraedts JP. Molecular genetics of inherited long-QT syndromes. *Eur Heart J* 1998;19:1427-33.
8. Kuo HC, Cheng CF, Clark RB, Lin JJ, Lin JL, Hoshijima M, Nguyen-Tran VT, Gu Y, Ross J, Giles WR, Chien KR. A defect in the Kv channel-interacting protein 2 (*KChIP2*) gene leads to a complete loss of transient outward potassium current (I_{TO}) and confers genetic susceptibility to ventricular tachycardia. *Cell* 2001;107:801-13.
9. Cardiovascular Genetics. Doevendans PA, Wilde AAM (eds). *Dordrecht, Netherlands: Kluwer Academic Publisher, 2001.*
10. Wehrens XH, Vos MA, Doevendans PA, Wellens HJ. Novel insights in the congenital long-QT syndrome. *Ann Intern Med* 2002;in press.
11. Chen Q, Kirsch GE, Zhang D, Brugada R, Brugada J, Brugada P, Potenza D, Moya A, Borggrefe M, Breithardt G, Ortiz-Lopez R, Wang Z, Antzelevitch C, O'Brien RE, Schulze-Bahr E, Keating MT, Towbin JA, Wang Q. Genetic basis and molecular mechanism for idiopathic ventricular fibrillation. *Nature* 1998;392:293-96.
12. Schott JJ, Alshinawi C, Kyndt F, Probst V, Hoorntje TM, Hulsbeek M, Wilde AA, Escande D, Mannens MM, Le Marec H. Cardiac conduction defects associate with mutations in *SCN5A*. *Nat Genet* 1999;23:20-21.
13. Tan HL, Bink-Boelkens MT, Bezzina CR, Viswanathan PC, Beaufort-Krol GC, Van Tintelen PJ, Van den Berg MP, Wilde AA, Balser JR. A sodium-channel mutation causes isolated cardiac conduction disease. *Nature* 2001;409:1043-47.
14. Plaster NM, Tawil R, Tristani-Firouzi M, Canun S, Bendahhou S, Tsunoda A, Donaldson MR, Iannaccone ST, Brunt E, Barohn R, Clark J, Deymeer F, George AL Jr., Fish FA, Hahn A, Nitu A, Ozdemir C, Serdaroglu P, Subramony SH, Wolfe G, Fu YH, Ptacek LJ. Mutations in *Kir2.1* cause the developmental and episodic electrical phenotypes of Andersen's syndrome. *Cell* 2001;105:511-19.

15. Priori SG, Napolitano C, Tiso N, Memmi M, Vignati G, Bloise R, Sorrentino V, Danieli GA. Mutations in the cardiac ryanodine receptor gene (*hRyR2*) underlie catecholaminergic polymorphic ventricular tachycardia. *Circulation* 2001;103:196-200.
16. Tiso N, Stephan DA, Nava A, Bagattin A, Devaney JM, Stanchi F, Larderet G, Brahmabhatt B, Brown K, Bauce B, Muriago M, Basso C, Thiene G, Danieli GA, Rampazzo A. Identification of mutations in the cardiac ryanodine receptor gene in families affected with arrhythmogenic right ventricular cardiomyopathy type 2 (ARVD2). *Hum Mol Genet* 2001;10:189-94.
17. Bennett PB, Yazawa K, Makita N, George AL Jr. Molecular mechanism for an inherited cardiac arrhythmia. *Nature* 1995; 376:683-85.
18. Wang DW, Yazawa K, George AL Jr, Bennett PB. Characterization of human cardiac Na⁺ channel mutations in the congenital long-QT syndrome. *Proc Natl Acad Sci U S A* 1996;93:13200-05.
19. Dumaine R, Wang Q, Keating MT, Hartmann HA, Schwartz PJ, Brown AM, Kirsch GE. Multiple mechanisms of Na⁺ channel-linked long-QT syndrome. *Circ Res* 1996;78:916-24.
20. Wei J, Wang DW, Alings M, Fish F, Wathen M, Roden DM, George AL Jr. Congenital long-QT syndrome caused by a novel mutation in a conserved acidic domain of the cardiac Na⁺ channel. *Circulation* 1999;99:3165-71.
21. Schwartz PJ, Priori SG, Dumaine R, Napolitano C, Antzelevitch C, Stramba-Badiale M, Richard TA, Berti MR, Bloise R. A molecular link between the sudden infant death syndrome and the long-QT syndrome. *N Engl J Med* 2000;343:262-67.
22. Rivolta I, Abriel H, Tateyama M, Liu H, Memmi M, Vardas P, Napolitano C, Priori SG, Kass RS. Inherited Brugada and LQT-3 syndrome mutations of a single residue of the cardiac sodium channel confer distinct channel and clinical phenotypes. *J Biol Chem* 2001;276:30623-30.
23. Makita N, Shirai N, Nagashima M, Matsuoka R, Yamada Y, Tohse N, Kitabatake A. A *de novo* missense mutation of human cardiac Na⁺ channel exhibiting novel molecular mechanisms of long-QT syndrome. *FEBS Lett* 1998;423:5-9.
24. Kambouris NG, Nuss HB, Johns DC, Tomaselli GF, Marban E, Balser JR. Phenotypic characterization of a novel long-QT syndrome mutation (R1623Q) in the cardiac sodium channel. *Circulation* 1998;97:640-44.
25. An RH, Wang XL, Kerem B, Benhorin J, Medina A, Goldmit M, Kass RS. Novel LQT-3 mutation affects Na⁺ channel activity through interactions between alpha- and beta1-subunits. *Circ Res* 1998;83:141-46.
26. Wehrens XH, Abriel H, Cabo C, Benhorin J, Kass RS. Arrhythmogenic mechanism of an LQT-3 mutation of the human heart Na⁺ channel alpha-subunit: A computational analysis. *Circulation* 2000;102:584-90.
27. Blaustein MP, Lederer WJ. Sodium/calcium exchange: its physiological implications. *Physiol Rev* 1999;79:763-854.
28. Tohse N. Calcium-sensitive delayed rectifier potassium current in guinea pig ventricular cells. *Am J Physiol* 1990;258:H1200-07.
29. Abriel H, Cabo C, Wehrens XH, Rivolta I, Motoike HK, Memmi M, Napolitano C, Priori SG, Kass RS. Novel arrhythmogenic mechanism revealed by a long-QT syndrome mutation in the cardiac Na⁺ channel. *Circ Res* 2001;88:740-45.
30. Wedekind H, Smits JP, Schulze-Bahr E, Arnold R, Veldkamp MW, Bajanowski T, Borggrefe M, Brinkmann B, Warnecke I, Funke H, Bhuiyan ZA, Wilde AA, Breithardt G, Haverkamp W. *De novo* mutation in the *SCN5A* gene associated with early onset of sudden infant death. *Circulation* 2001;104:1158-64.
31. Balser JR. Structure and function of the cardiac sodium channels. *Cardiovasc Res* 1999;42:327-38.

32. Bezzina CR, Rook MB, Wilde AA. Cardiac sodium channel and inherited arrhythmia syndromes. *Cardiovasc Res* 2001;49:257-71.
33. Vassilev P, Scheuer T, Catterall WA. Inhibition of inactivation of single sodium channels by a site-directed antibody. *Proc Natl Acad Sci U S A* 1989;86:8147-51.
34. Patton DE, West JW, Catterall WA, Goldin AL. Amino acid residues required for fast Na⁺ channel inactivation: charge neutralizations and deletions in the III-IV linker. *Proc Natl Acad Sci U S A* 1992;89:10905-09.
35. Rohl CA, Boeckman FA, Baker C, Scheuer T, Catterall WA, Klevit RE. Solution structure of the sodium channel inactivation gate. *Biochemistry* 1999;38:855-61.
36. West JW, Patton DE, Scheuer T, Wang Y, Goldin AL, Catterall WA. A cluster of hydrophobic amino acid residues required for fast Na⁺ channel inactivation. *Proc Natl Acad Sci U S A* 1992;89:10910-14.
37. Miyamoto K, Nakagawa T, Kuroda Y. Solution structure of the cytoplasmic linker between domain III-S6 and domain IV-S1 (III-IV linker) of the rat brain sodium channel in SDS micelles. *Biopolymers* 2001;59:380-93.
38. Miyamoto K, Kanaori K, Nakagawa T, Kuroda Y. Solution structures of the inactivation gate particle peptides of rat brain type-IIA and human heart sodium channels in SDS micelles. *J Pept Res* 2001;57:203-14.
39. Tang L, Kallen RG, Horn R. Role of an S4-S5 linker in sodium channel inactivation probed by mutagenesis and a peptide blocker. *J Gen Physiol* 1996;108:89-104.
40. Smith MR, Goldin AL. Interaction between the sodium channel inactivation linker and domain III S4-S5. *Biophys J* 1997;73:1885-95.
41. Filatov GN, Nguyen TP, Kraner SD, Barchi RL. Inactivation and secondary structure in the D4/S4-5 region of the SkM1 sodium channel. *J Gen Physiol* 1998;111:703-15.
42. McPhee JC, Ragsdale DS, Scheuer T, Catterall WA. A critical role for the S4-S5 intracellular loop in domain IV of the sodium channel α -subunit in fast inactivation. *J Biol Chem* 1998;273:1121-29.
43. Miyamoto K, Nakagawa T, Kuroda Y. Solution structures of the cytoplasmic linkers between segments S4 and S5 (S4-S5) in domains III and IV of human brain sodium channels in SDS micelles. *J Pept Res* 2001;58:193-203.
44. Kellenberger S, Scheuer T, Catterall WA. Movement of the Na⁺ channel inactivation gate during inactivation. *J Biol Chem* 1996;271:30971-79.
45. Lupoglazoff JM, Cheav T, Baroudi G, Berthet M, Denjoy I, Cauchemez B, Extramiana F, Chahine M, Guicheney P. Homozygous SCN5A mutation in long-QT syndrome with functional two-to-one atrioventricular block. *Circ Res* 2001;89:E16-21.
46. Gellens ME, George AL Jr, Chen LQ, Chahine M, Horn R, Barchi RL, Kallen RG. Primary structure and functional expression of the human cardiac tetrodotoxin-insensitive voltage-dependent sodium channel. *Proc Natl Acad Sci U S A* 1992;89:554-58.
47. George AL, Komisarof J, Kallen RG, Barchi RL. Primary structure of the adult human skeletal muscle voltage-dependent sodium channel. *Ann Neurol* 1992;31:131-37.
48. Deschenes I, Trottier E, Chahine M. Implication of the C-terminal region of the α -subunit of voltage-gated sodium channels in fast inactivation. *J Membr Biol* 2001;183:103-14.
49. Sato C, Matsumoto G. Sodium channel functioning based on an octagonal structure model. *J Membr Biol* 1995;147:45-70.
50. Wang Q, Li Z, Shen J, Keating MT. Genomic organization of the human SCN5A gene encoding the cardiac sodium channel. *Genomics* 1996;34:9-16.
51. Goldin AL. Diversity of mammalian voltage-gated sodium channels. *Ann N Y Acad Sci* 1999; 868:38-50.

52. Wan X, Chen S, Sadeghpour A, Wang Q, Kirsch GE. Accelerated inactivation in a mutant Na⁺ channel associated with idiopathic ventricular fibrillation. *Am J Physiol Heart Circ Physiol* 2001;280:H354-60.
53. Lerche H, Peter W, Fleischhauer R, Pika-Hartlaub U, Malina T, Mitrovic N, Lehmann-Horn F. Role in fast inactivation of the IV/S4-S5 loop of the human muscle Na⁺ channel probed by cysteine mutagenesis. *J Physiol* 1997;505:345-52.
54. Tang L, Chehab N, Wieland SJ, Kallen RG. Glutamine substitution at alanine 1649 in the S4-S5 cytoplasmic loop of domain 4 removes the voltage sensitivity of fast inactivation in the human heart sodium channel. *J Gen Physiol* 1998;111:639-52.
55. Clancy CE, Rudy Y. Linking a genetic defect to its cellular phenotype in a cardiac arrhythmia. *Nature* 1999;400:566-69.
56. Hille B. Local anesthetics: hydrophilic and hydrophobic pathways for the drug-receptor reaction. *J Gen Physiol* 1977;69:497-515.
57. Hondeghem LM, Katzung BG. Time- and voltage-dependent interactions of antiarrhythmic drugs with cardiac sodium channels. *Biochim Biophys Acta* 1977;472:373-98.
58. Bean BP, Cohen CJ, Tsien RW. Lidocaine block of cardiac sodium channels. *J Gen Physiol* 1983;81:613-42.
59. Starmer CF, Grant AO, Strauss HC. Mechanisms of use-dependent block of sodium channels in excitable membranes by local anesthetics. *Biophys J* 1984;46:15-27.
60. Ragsdale DS, McPhee JC, Scheuer T, Catterall WA. Molecular determinants of state-dependent block of Na⁺ channels by local anesthetics. *Science* 1994;265:1724-28.
61. Ragsdale DS, McPhee JC, Scheuer T, Catterall WA. Common molecular determinants of local anesthetic, antiarrhythmic, and anticonvulsant block of voltage-gated Na⁺ channels. *Proc Natl Acad Sci U S A* 1996;93:9270-75.
62. Nau C, Wang SY, Strichartz GR, Wang GK. Point mutations at N434 in D1-S6 of mu1 Na⁺ channels modulate binding affinity and stereoselectivity of local anesthetic enantiomers. *Mol Pharmacol* 1999;56:404-13.
63. Wang GK, Quan C, Wang SY. Local anesthetic block of batrachotoxin-resistant muscle Na⁺ channels. *Mol Pharmacol* 1998;54:389-96.
64. McPhee JC, Ragsdale DS, Scheuer T, Catterall WA. A mutation in segment IVS6 disrupts fast inactivation of sodium channels. *Proc Natl Acad Sci U S A* 1994;91:12346-50.
65. McPhee JC, Ragsdale DS, Scheuer T, Catterall WA. A critical role for transmembrane segment IVS6 of the sodium channel α -subunit in fast inactivation. *J Biol Chem* 1995;270:12025-34.
66. Li HL, Galve A, Meadows L, Ragsdale DS. A molecular basis for the different local anesthetic affinities of resting versus open and inactivated states of the sodium channel. *Mol Pharmacol* 1999;55:134-41.
67. Strichartz GR. The inhibition of sodium currents in myelinated nerve by quaternary derivatives of lidocaine. *J Gen Physiol* 1973;62:37-57.
68. Gingrich KJ, Beardsley D, Yue DT. Ultra-deep blockade of Na⁺ channels by a quaternary ammonium ion: catalysis by a transition-intermediate state? *J Physiol* 1993;471:319-41.
69. Balser JR, Nuss HB, Orias DW, Johns DC, Marban E, Tomaselli GF, Lawrence JH. Local anesthetics as effectors of allosteric gating. Lidocaine effects on inactivation-deficient rat skeletal muscle Na⁺ channels. *J Clin Invest* 1996;98:2874-86.
70. Sunami A, Dudley SCJ, Fozzard HA. Sodium channel selectivity filter regulates antiarrhythmic drug binding. *Proc Natl Acad Sci U S A* 1997;94:14126-31.

71. Sunami A, Glaaser IW, Fozzard HA. A critical residue for isoform difference in tetrodotoxin affinity is a molecular determinant of the external access path for local anesthetics in the cardiac sodium channel. *Proc Natl Acad Sci U S A* 2000;97:2326-31.
72. Bennett PB, Valenzuela C, Chen LQ, Kallen RG. On the molecular nature of the lidocaine receptor of cardiac Na⁺ channels. Modification of block by alterations in the alpha-subunit III-IV interdomain. *Circ Res* 1995;77:584-92.
73. Vedantham V, Cannori SC. The position of the fast-inactivation gate during lidocaine block of voltage-gated Na⁺ channels. *J Gen Physiol* 1999;113:7-16.
74. Hanck DA, Makielski JC, Sheets MF. Kinetic effects of quaternary lidocaine block of cardiac sodium channels: a gating current study. *J Gen Physiol* 1994;103:19-43.
75. Hanck DA, Makielski JC, Sheets MF. Lidocaine alters activation gating of cardiac Na⁺ channels. *Pflugers Arch* 2000;439:814-21.
76. Schwartz PJ, Priori SG, Locati EH, Napolitano C, Cantu F, Towbin JA, Keating MT, Hammoude H, Brown AM, Chen LS. Long-QT syndrome patients with mutations of the SCN5A and HERG genes have differential responses to Na⁺ channel blockade and to increases in heart rate. Implications for gene-specific therapy. *Circulation* 1995;92:3381-86.
77. Benhorin J, Taub R, Goldmit M, Kerem B, Kass RS, Windman I, Medina A. Effects of flecainide in patients with new SCN5A mutation: mutation-specific therapy for long-QT syndrome? *Circulation* 2000;101:1698-706.
78. An RH, Bangalore R, Rosero SZ, Kass RS. Lidocaine block of LQT-3 mutant human Na⁺ channels. *Circ Res* 1996;79:103-08.
79. Kambouris NG, Nuss HB, Johns DC, Marban E, Tomaselli GF, Balser JR. A revised view of cardiac sodium channel "blockade" in the long-QT syndrome. *J Clin Invest* 2000;105:1133-40.
80. Echt DS, Liebson PR, Mitchell LB, Peters RW, Obias-Manno D, Barker AH, Arensberg D, Baker A, Friedman L, Greene HL. Mortality and morbidity in patients receiving encainide, flecainide, or placebo. The Cardiac Arrhythmia Suppression Trial. *N Engl J Med* 1991;324:781-88.
81. Windle JR, Geletka RC, Moss AJ, Zareba W, Atkins DL. Normalization of ventricular repolarization with flecainide in long-QT syndrome patients with SCN5A-ΔKPQ mutation. *Ann Noninvasive Electrocardiol* 2001;6:153-58.
82. Dumaine R, Kirsch GE. Mechanism of lidocaine block of late current in long-QT mutant Na⁺ channels. *Am J Physiol* 1998;274:H477-87.
83. Ono K, Kaku T, Makita N, Kitabatake A, Arita M. Selective block of late currents in the ΔKPQ Na⁺ channel mutant by pilsicainide and lidocaine with distinct mechanisms. *Mol Pharmacol* 2000;57:392-400.
84. Courtney KR. Mechanism of frequency-dependent inhibition of sodium currents in frog myelinated nerve by the lidocaine derivative GEA. *J Pharmacol Exp Ther* 1975;195:225-36.
85. Kambouris NG, Hastings LA, Stepanovic S, Marban E, Tomaselli GF, Balser JR. Mechanistic link between lidocaine block and inactivation probed by outer pore mutations in the rat μ1 skeletal muscle sodium channel. *J Physiol* 1998;512:693-705.
86. Ong BH, Tomaselli G, Balser JR. A structural rearrangement in the sodium channel pore linked to slow inactivation and use dependence. *J Gen Physiol* 2000;116:653-61.
87. Abriel H, Wehrens XH, Benhorin J, Kerem B, Kass RS. Molecular pharmacology of the sodium channel mutation D1790G linked to the congenital long-QT syndrome. *Circulation* 2000;102:921-25.
88. Anno T, Hondeghem LM. Interactions of flecainide with guinea pig cardiac sodium channels. Importance of activation unblocking to the voltage dependence of recovery. *Circ Res* 1990;66:789-803.

89. Campbell TJ, Vaughan Williams EM. Voltage- and time-dependent depression of maximum rate of depolarization of guinea pig ventricular action potentials by 2 new antiarrhythmic drugs, flecainide and lorainide. *Cardiovasc Res* 1983;17:251-58.
90. Nagatomo T, January CT, Makielski JC. Preferential block of late sodium current in the LQT-3 Δ KPQ mutant by the class IC antiarrhythmic flecainide. *Mol Pharmacol* 2000;57:101-07.
91. Viswanathan PC, Bezzina CR, George AL, Roden DM, Wilde AA, Balser JR. Gating-dependent mechanisms for flecainide action in *SCN5A*-linked arrhythmia syndromes. *Circulation* 2001;104:1200-05.
92. Wang DW, Yazawa K, Makita N, George AL Jr, Bennett PB. Pharmacological targeting of long-QT mutant sodium channels. *J Clin Invest* 1997;99:1714-20.
93. Li RA, Tsushima RG, Himmeldirk K, Dime DS, Backx PH. Local anesthetic anchoring to cardiac sodium channels. Implications into tissue-selective drug targeting. *Circ Res* 1999;85:88-98.
94. De Luca A, Natuzzi F, Desaphy JF, Loni G, Lentini G, Franchini C, Tortorella V, Camerino DC. Molecular determinants of mexiletine structure for potent and use-dependent block of skeletal muscle sodium channels. *Mol Pharmacol* 2000;57:268-77.
95. Chandra R, Starmer CF, Grant AO. Multiple effects of Δ KPQ deletion mutation on gating of human cardiac Na^+ channels expressed in mammalian cells. *Am J Physiol* 1998 May;274:H1643-54.
96. Nagatomo T, Fan Z, Ye B, Tonkovich GS, January CT, Kyle JW, Makielski JC. Temperature dependence of early and late currents in human cardiac wild-type and long-QT Δ KPQ Na^+ channels. *Am J Physiol* 1998;275:H2016-24.
97. Deschenes I, Baroudi G, Berthet M, Barde I, Chalvidan T, Denjoy I, Guicheney P, Chahine M. Electrophysiological characterization of *SCN5A* mutations causing long-QT (E1784K) and Brugada (R1512W and R1432G) syndromes. *Cardiovasc Res* 2000;46:55-65.
98. Baroudi G, Chahine M. Biophysical phenotype of *SCN5A* mutations causing long-QT and Brugada syndrome. *FEBS Lett* 2000;487:224-28.



Summary

Samenvatting

Summarium

Dankwoord

Curriculum Vitae

Index

Summary

In recent years, important breakthroughs in the understanding of the congenital long-QT syndrome have followed the linkage to mutations in genes encoding cardiac ion channels. It became clear that what had been classified under the name 'congenital long-QT syndrome' actually represents a variety of different conditions caused by ion channel mutations, most of which produce alterations in ionic currents, leading to the same end result: prolonged ventricular repolarization. From both clinical and biophysical studies, it gradually became evident that heterogeneity exists, even among ion channel mutation in the same gene, which has important implications for both the comprehension of the pathophysiologic mechanisms, and perhaps even more promising, for mutation-specific therapeutic approaches.

In CHAPTER 1, the background of the present thesis is provided. Manifestations of the congenital long-QT syndrome include prolonged ventricular repolarization (QT-interval on the ECG), a propensity for life-threatening ventricular tachyarrhythmias, syncope, and sudden cardiac death. Current estimates suggest that this condition causes 3000-4000 sudden deaths in children and young adults each year in the US only. On the basis of the genetic transmission pattern, two major clinical syndromes are recognized: the autosomal-dominant form (Romano-Ward syndrome) with a pure cardiac phenotype, and the rarer autosomal-recessive form (Jervell and Lange-Nielsen syndrome) characterized by the association with congenital neuronal deafness. Strategies to identify individuals with the congenital long-QT syndrome, with particular attention for the genotype-specific manifestations, and treatment options for different categories of these patients, are discussed in depth.

In CHAPTER 2, the physiology, molecular biology, biophysics, pharmacology, modulation, and regulation of the cardiac sodium channel are reviewed. This review focuses particularly on *SCN5A* mutations that cause congenital long-QT syndrome. Some sodium channel mutations may cause action potential prolongation by inducing sustained sodium channel activity during the action potential plateau phase. However, for several other mutations the arrhythmogenic mechanisms have not been elucidated.

In order to investigate the biophysical phenotypes of Na^+ channel mutations linked to the congenital long-QT syndrome, we expressed recombinant cardiac Na^+ channels in human embryonic kidney (HEK 293) cells. Properties of the voltage-gated

Na⁺ channels were measured using whole-cell patch-clamp analysis. In CHAPTER 3, the biophysical phenotype of the D1790G mutation was investigated. This mutation in the carboxy-terminus of the Na⁺ channel can prolong the ventricular action potential despite the absence of mutation-induced sustained Na⁺ channel current. Using the Luo-Rudy model, computations of the ventricular action potential predicted that D1790G-induced changes in Na⁺ channel activity prolong action potentials in a steeply heart rate-dependent manner. This lengthening is not directly due to changes in Na⁺ entry through bursting mutant channels but instead to alterations in the balance of net plateau currents by modulation of calcium-sensitive exchange and ion channel currents.

A clinical study in carriers of the D1790G mutation revealed that the class IB antiarrhythmic drug lidocaine was ineffective, whereas flecainide, a class IC sodium channel blocker, corrected repolarization parameters in these patients. In CHAPTER 4, we investigated the molecular basis of this divergence. The results of this study demonstrate that the D1790G mutation confers a unique pharmacological response on expressed channels. The therapeutic effect in carriers of this mutation is probably the result of enhanced flecainide use-dependent block of D1790G channels. Furthermore, these data suggest a role of the Na⁺ channel α -subunit C-terminus in the flecainide/channel interaction.

In CHAPTER 5, the functional consequences of the novel E1295K mutation were described. Biophysical analysis of the mutant channels indicated that the E1295K mutation changes channel activity in a manner distinct from previously investigated LQT-3 mutations. The changes in gating shift the window of voltages at which Na⁺ channels do not completely inactivate. The altered window current is likely to affect net membrane current during terminal repolarization, which is most likely the mechanism for action potential prolongation.

In CHAPTER 6, we describe the first case of a congenital long-QT syndrome patient with functional 2:1 atrioventricular block due to a heterozygous mutation of the SCN5A gene. The L619F mutation promotes an increase in sustained (non-inactivating) current as well as an increase in Na⁺ channel window-current, two mechanisms which are expected to delay ventricular repolarization. Importantly, the defective inactivation imposed by the L619F mutation implicates a novel role for the domain I-II linker in the Na⁺ channel inactivation process.

In the final CHAPTER of this thesis (CHAPTER 7), the major findings are discussed in the perspective of biophysical mechanisms underlying congenital long-QT syndrome caused by SCN5A mutations. In addition, new insights in the complex interrelationship

between channel gating, antiarrhythmic block, and long-QT syndrome Na^+ channel mutations are discussed. Finally, the implications for the development of mutation-specific therapy for the long-QT syndrome are discussed.

In short, this thesis deals with the complex functional changes that occur in cardiac sodium channels in patients afflicted by the congenital long-QT syndrome. The data presented contribute to the comprehension that multiple, distinct gating defects in sodium channels may cause long-QT syndrome through discrete arrhythmogenic mechanisms. This notion is likely to increasingly contribute to the design of mutation-specific pharmacotherapy based on unique gating features of long-QT syndrome-associated sodium channels.

Samenvatting

Het aangeboren lange QT-tijd syndroom is de meest voorkomende oorzaak van plotse hartdood in mensen zonder structureel hartlijden. De elektrische stroomvoorziening van het hart regelt de synchrone samentrekking van de hartspier. Als gevolg van deze samentrekking wordt het bloed door het lichaam rondgepompt. Bij het lange QT-tijd syndroom is er sprake van een normaal hart, maar de stroomvoorziening van het hart kan ineens verstoord raken. De naam van de ziekte verwijst naar het tijdsinterval tussen de Q- en T-golf op het electrocardiogram (ECG). In deze QT-tijd herstelt het hart zich van een samentrekking, om zo een volgende hartslag mogelijk te maken. Een afwijking in deze herstelperiode kan een ontsporing van het hartritme veroorzaken. Hierdoor gaat het hart chaotisch en ongecontroleerd kloppen, en kan daardoor geen bloed meer rondpompen, waardoor mensen bewusteloos kunnen raken of snel kunnen overlijden.

Recentelijk is ontdekt dat het aangeboren lange QT-tijd syndroom wordt veroorzaakt door een verandering in het erfelijk materiaal. Dergelijke DNA afwijkingen (mutaties) treden op in genen, die de informatie bevatten voor ionkanalen in het hart. Een goede functie van deze ionkanalen is essentieel voor een nauwkeurige aansturing van de elektrische activiteit in het hart.

In HOOFDSTUK 1 worden de klinische kenmerken van het lange QT-tijd syndroom beschreven. Symptomen zijn onder andere een verlengd QT-interval op het ECG, een verhoogde kans op haritmestoeornissen, en plotselinge dood. Op basis van het overervingspatroon worden twee klinische syndromen onderscheiden: de autosomaal dominant-overervende vorm, Romano-Ward syndroom genaamd, en het autosomaal recessief-overervende Jervell-Lange Nielsen syndroom, hetgeen vaak met doofheid gepaard gaat. In dit hoofdstuk worden de strategieën besproken hoe deze patiënten opgespoord kunnen worden en wat de beste behandeling is voor elke subgroep van lange QT-tijd syndroom patiënten.

Het proefschrift biedt specifiek aandacht aan het lange QT-tijd syndroom type 3, hetgeen veroorzaakt wordt door mutaties in het natriumkanal. In HOOFDSTUK 2 wordt derhalve de fysiologie, moleculaire biologie, biofysica, farmacologie, modulatie en regulatie van het cardiale natriumkanal besproken. In het bijzonder worden mutaties in het natriumkanalgen besproken, die het lange QT-tijd syndroom veroorzaken. Voor een aantal mutaties is aangetoond dat ze het QT-interval kunnen verlengen door een soort lekstroom

te veroorzaken in de zieke natriumkanalen. Echter, er wordt ook geconcludeerd dat voor een aantal mutaties nog niet duidelijk is hoe ze het lange QT-tijd syndroom veroorzaken.

Om de biofysische eigenschappen van natriumkanalmutaties te kunnen onderzoeken, werd een celsysteem gebruikt waarin mutante kanalen tot expressie gebracht werden. Middels de 'whole-cell patch-clamp' techniek konden de biofysische eigenschappen van het voltage-afhankelijke natriumkanal in detail onderzocht worden. In HOOFDSTUK 3 werd de D1790G mutatie onderzocht. Deze mutatie bevindt zich in het carboxy-terminale uiteinde van het natriumkanal en kan de duur van het QT-interval verlengen zonder de prototypische lekstroom te veroorzaken. Door gebruik te maken van het Luo-Rudy computer model van de hartspiercel, werd aangetoond dat de D1790G-geïnduceerde veranderingen in de natriumkanalactiviteit verlenging van het QT-interval kunnen veroorzaken. Deze verlenging is waarschijnlijk het gevolg van indirecte veranderingen die optreden in de functie van andere ionkanalen in het hart, hetgeen het hart gevoeliger maakt voor hartritmestoornissen.

In een klinische studie in patiënten met de D1790G mutatie is aangetoond dat het klasse IB antiaritmicum lidocaine geen effect heeft, terwijl flecainide, een klasse IC natriumkanalblokker, juist wel het QT-interval effectief kan verkorten. In HOOFDSTUK 4 werd de oorzaak van deze verrassende bevinding nader onderzocht. De resultaten van deze studie tonen aan dat de D1790G mutatie unieke farmacologische eigenschappen geeft aan de natriumkanalen. Het therapeutische effect in de mutatiedragers is waarschijnlijk het gevolg van een versterkte 'gebruiks-afhankelijke' blokkade van D1790G kanalen door flecainide. Tevens suggereren deze data dat het carboxy-terminale uiteinde van het natriumkanal een rol kan hebben in de interactie met flecainide.

In HOOFDSTUK 5 worden de functionele eigenschappen beschreven van de E1295K mutatie. Een biofysische analyse toonde aan dat de E1295K mutatie de activiteit van de natriumkanalen op een unieke manier verandert. Deze veranderingen in de natriumkanalgeleiding veranderen het gebied van voltages waarin het natriumkanal niet volledig sluit. Deze veranderde zgn. 'window' natriumstroom verandert waarschijnlijk de totale hoeveelheid stroom in de hartspiercel aan het einde van de elektrische herstelfase na een hartslag, hetgeen de totale duur van het QT-interval kan verlengen.

In HOOFDSTUK 6 beschreven we voor het eerst een pasgeboren patiënt met het aangeboren lange QT-tijd syndroom en 2:1 boezem-naar-kamer geleiding ten gevolge van een heterozygote mutatie in het natriumkanalgen. Biofysische analyse van de L619F mutatie toonde aan dat er sprake was van natriumkanal lekstroom, in combinatie met een toegenomen 'window' natriumstroom. De functionele veranderingen ten gevolge van de

L619F mutatie duiden waarschijnlijk op een niet eerder onderkende rol van het gebied tussen domein I en II in de sluiting van het natriumkanal.

In het laatste hoofdstuk van dit proefschrift (HOOFDSTUK 7) worden de belangrijkste bevindingen bediscussieerd in de context van de biofysische mechanismen die het lange QT-tijd syndroom kunnen veroorzaken. Tevens worden de nieuwste inzichten op het gebied van de natriumkanal functie en farmacologie samengevat. Tenslotte worden de implicaties voor de ontwikkeling van een mutatie-specifieke behandeling van lange QT-tijd patiënten besproken.

Concluderend kan worden gesteld dat de resultaten van de studies beschreven in dit proefschrift hebben geleid tot meer inzicht in de ontstaanswijze van het lange QT-tijd syndroom. Zo werd onder andere duidelijk dat hele subtiele veranderingen in de functie van het natriumkanal verantwoordelijk kunnen zijn voor potentieel dodelijke hartritme-stoornissen. Deze kennis kan bijdragen aan het totstandkomen van een mutatie-specifieke behandeling van patiënten met deze ziekte. Zo zullen sommige mensen meer profijt hebben van een pacemaker om een trage hartslag te voorkomen, terwijl andere mensen (met andere natriumkanal mutaties) beter beschermd worden tegen ritmestoornissen met behulp van bepaalde medicijnen. Door een adequate behandeling van deze patiënten kan de incidentie van hartritmestoornissen, flauwvallen, en plotselinge dood worden teruggedrongen.

LONGO QT CONGENITA SYNDROMA MAIOR CAUSA EST MORTIS SUBITAE CARDIACAE ALIOQUI SANORUM HOMINUM. AESTIMATIONES HODIERNAE CENSENT ISTAM CONDITIONEM QUOTANNIS CAUSAM ESSE MORTIS SUBITAE CARDIACAE MMM-MMMM PUERORUM ET IUVENUM SOLUM IN CIVITATIBUS AMERICAЕ UNITIS. AEGROTI AFFECTI ESSE POSSUNT PROLONGATIONE QT-INTERVALLI, SYNCOPA, VEL MORTE SUBITA CARDIACA. HIS TEMPORIBUS, NOVISSIMA REPERTA IN ARTE GENETICA COMPREHENSIONEM MELIORAVERUNT LONGO QT CONGENITAE SYNDROMAE. MANIFESTUM EST MUTATIONES IN GENIS DEPOSITORIIS INFORMATIONUM DE CANALIBUS IONICIS CARDIACIS CAUSAS ESSE HUIUS MORBI. RECTA FUNCTIO HORUM CANALIUM IONICORUM ESSENTIALIS EST AD NORMALEM RECTIONEM CONTRATIONUM CORDIS.

HAC THESIS DISSERAT DE LONGO QT SYNDROMA TYPO III (LQT-III), A MUTATIONIBUS CANALIS CARDIACI SODII CAUSATA. UTENDO SYSTEMATE CELLULARI EMBRYONIS RENIS HUMANI (HEK- CCXCIII), DIVERSAE LQT-III MUTATIONES EXHIBITA SUNT. DIVERSAE MUTATIONES CAUSANT DIVERSOS DEFECTOS IN FUNCTIONE CANALIS SODII. ETIAM MANIFESTUM EST, INTER ALIA, TARDOS RHYTHMOS CARDIACOS MAGNA PERICULA ESSE ARRHYTHMIAE CORDIS IN AEGROTIS LQT-III AFFECTIS. PHARMACOLOGICA STUDIA INDICANT QUOD SINGULAE MUTATIONES EXHIBENT SENSIBILITATEM SINGULAREM DIVERSORUM MEDICAMENTORUM.

REPERTA DESCRIPTA IN HAC THESI PRAEBENT NOVAS COGNITIONES CIRCA DIVERSITATEM INTER LQT-III CANALIS SODII MUTATIONES. PLURI MECHANISMI CANALIS SODII DISFUNCTIONIS DESCRIPTI SUNT, ET APPARENS EST QUOD PARVI DEFECTI FUNCTIONALES PROVOCARE POSSUNT RHYTHMOS IRREGULARES ATQUE MORTEM SUBITAM CARDIACAM. NOVAE COGNITIONUM ACQUISITIONES CIRCA EXACTOS DEFECTOS A MUTATIONIBUS CANALIS SODII CAUSATOS, ETIAMQUE CIRCA EARUM SENSIBILITATEM PECULIARUM MEDICAMENTORUM, MELIUS DIRIGENT THERAPIAM LONGO QT-III SYNDROMA AFFLICTORUM.

Acknowledgments

LABOR VOLUPTASQUE, DISSIMILLIMA NATURA, SOCIETATE QUADAM INTER SE NATURALI SUNT IUNCTA. The research leading to my thesis was initiated by Dr. P.A. Doevendans, who asked me to become his first PhD student in 1997. We had actually first met 4 years before, when I was in the second year of medical school. Pieter and I carried out two clinical studies together, and he managed to convince me that cardiology is more interesting than surgery. Now, 7 years later, Pieter has been an excellent mentor over all these years, allowing a lot of freedom for own initiative, but also providing guidance at important moments. SUPERFLUA NON NOCENT! His incredible zest for work has been a great inspiration.

Much of the experimental work described in this thesis has been performed under the guidance of Prof. R.S. Kass at Columbia University (New York). Rocky managed to transform an illiterate student into a patch-clamp fanatic: EXERCITIO ARTUM PARAT. His hospitality has been unlimited, his scientific mentorship exemplary. Rocky always managed to transform some crude observations into novel scientific concepts, and deserves great credit for the fast pace at which this thesis could be completed.

Dr. M.A. Vos is greatly acknowledged for his guidance and motivation for thorough reflection of my experimental data. DOLORES CAPITIS NON FERRO, EOS DO. My passionate style of working may have intimidated you at first, but I believe working together was a great learning experience for both of us. Now that I will change focus from congenital to acquired cardiac disease, I will benefit a lot from your lessons in the past.

When I was in medical school, few of my fellow students at the time were aware that one of the 'godfathers' of cardiology, Prof. H.J.J. Wellens, taught at our university. Being a young doctor, it was a dream coming true when I got the opportunity to work for this eminent clinician, scientist, and teacher. RATIO ET CONCILIUM PROPRIAE DUCIS ARTIS. His knowledge of the cardiology field is incredible, and his clear vision on the future of cardiology helped to make choices for my future career.

The members of the thesis assessment committee, Professors H.A.J. Struijker Boudier, E. Carmeliet, H.J. Crijns, J.P. Geraedts, and A.A.M. Wilde, are gratefully acknowledged for critically reading this thesis. I am also indebted to the following mentors from the past: Drs. J.P.M. Offermans, G.J.J.M. van Eys, F.R.C. Ramaekers, J.V. Small (Austrian Academy of Sciences), M.G.A. oude Egbrink, D.W. Slaaf, and G. Ramsay. Also, I would like to thank the following collaborators who contributed importantly to this

thesis: Drs. R. Jongbloed, and H. Smeets (Dept of Genetics, Maastricht); Dr. J. Benhorin (Jerusalem, Israel); Drs. C. Cabo, H. Abriel, I. Rivolta, and H. Motoike (Columbia University, New York); Drs. C. Napolitano, and S.G. Priori (Pavia, Italy); Drs. T. Rossenbacker, M. Gewillig, and H. Heidbuchel (Leuven, Belgium).

I would like to express my gratitude to the Departments of Physiology and Cardiology (Maastricht University), in particular the members of the molecular cardiology group (Leon, Alexandra, Bianca, Chiel, Daan, Denny, Els, Eva, Ewald, Fawzi, Jordie, Meindert, Reinier, Roger, Sara, Sigmund, Vanessa, Victor), and the cardiac electrophysiology group (Cora, Chris, Dirk, Elke, Jérôme, Jet, Jurren, Marieke, Milan, Morten, Paul, Roel), Drs. de Muinck, Gorgels, and Hofstra, the secretaries (in particular Nicolle and Vivian), and the research nurses (Suzanne, Aimee, Margaret, Moniek, and Mireille). I am also very grateful to the members of the Kass lab (Columbia University): Allan, Badru, Colleen, Huajun, Jay, Jenny, Jing, Josh, Junko, Levi, Mary, Michihiro, and Tsedan. A very special thanks goes out to my friends Ellen, Esther, Ronald, and Ruben, for lots of motivation and encouragement. My sister Kim Wehrens and Luciano Nardonne are acknowledged for their help with the translation of the Latin summary. Oscar Toebosch, Romain Groenen, and in particular Paul Maas and Suzanne van den Homberg were essential to transform this text into a wonderful book.

I am grateful to my friends Dr. H. Schulten en Dr. T. Leiner, who will provide moral support during my thesis defense as 'paranymphs'. Tim, best friend since medical school, I hope that we will continue to develop novel ideas on research and medical education being on the other continent. *IN TERRA INCOGNATA VINCEMUS!* Finally, I am forever indebted to my parents and sister for their understanding, endless patience and encouragement when it was most required.

TEMPUS EST ETIAM MAIORA CONARI.

Curriculum Vitae

The author of this thesis was born February 4, 1975 in Heerlen, the Netherlands. He attended the Bernardinus College in Heerlen, where he obtained two first-prize awards in the National Mathematics team Olympiads. In 1993, he graduated valedictorian (*summa cum laude*), with several distinctions for academic excellence.

The same year, he started his medical training at the Faculty of Medicine, Maastricht University. During the pre-clinical years, he served as a research assistant in the departments of Molecular Cell Biology, Physiology, and Surgery. With an E. Dekker-grant from the Netherlands Heart Foundation, he spent three months at the Austrian Academy of Sciences, Institute of Molecular Biology. He was the founding president of the 'Maastricht Medical Students Research Conference Foundation', and served as chairman on its First Annual Conference. In 1997, he graduated *cum laude*, after receiving the Maastricht University 'Student Research Prize 1997' for his MSc thesis.

His clinical training commenced with an internship at the department of General Surgery at the Royal Infirmary of Edinburgh (UK). After completion of the first year of clinical internships, he enrolled in the MD/PhD program at the Cardiovascular Research Institute Maastricht, Department of Cardiology. The year 1999 was spent at the department of Pharmacology, College of Physicians and Surgeons of Columbia University in New York City, with a stipend from 'De Drie Lichten Foundation'. Back in the Netherlands, he graduated as a Medical Doctor (*cum laude*), after receiving the National 'Hippocrates Award' for the best research project performed by a Dutch medical student (CHAPTERS 3 and 4 of this thesis). During his PhD training, he served as secretary of the PhD student Association of Maastricht University (ProVUM).

Dr. Wehrens has accepted a position as postdoctoral research scientist at the department of Cardiology of the Columbia Presbyterian Medical Center in New York City.

Papers

1. WEHRENS XHT, Doevedans PA, Dantzig van JM, Snoep G, Wellens HJJ. Infected sternal fracture hematoma after cardiopulmonary resuscitation presenting as pericarditis. *Am Heart J* 1996;132:685-86.
2. WEHRENS XHT, Mies B, Gimona M, Ramaekers FCS, Eys van GJJM, Small JV. Localization of smoothelin in avian smooth muscle and identification of a vascular-specific isoform. *FEBS Lett* 1997;405:315-20.
3. Eys van GJJM, Völler MCW, Timmer EDJ, WEHRENS XHT, Small JV, Schalken JA, Ramaekers FCS, Van der Loop FTL. Smoothelin expression characteristics: development of a smooth muscle cell *in vitro* system and identification of a vascular variant. *Cell Struct Funct* 1997;22:65-72.
4. WEHRENS XHT, Leiner T, Dammers R. Research performed by medical students [Interesse voor wetenschappelijk onderzoek bij medisch studenten]. *Ned Tijdschr Geneesk* 1998; 1(2):1-2.
5. WEHRENS XHT, Leiner T, Dammers R, Stockbrügger RW. Participation of students in medical research at Maastricht University Medical School [Participatie in wetenschappelijk onderzoek door studenten. Een inventarisatie aan de medische faculteit Maastricht]. *Bull Med Onderw* 1998;17:13-17.
6. WEHRENS XHT, Kirchhoff S, Doevedans PA. Mouse electrocardiography: an interval of thirty years [review]. *Cardiovasc Res* 2000;45:231-37.
7. WEHRENS XHT, Doevedans PA, Oude Ophuis TJ, Wellens HJJ. A comparison of electrocardiographic changes during reperfusion of acute myocardial infarction by thrombolysis or PTCA. *Am Heart J* 2000;139:430-36.
8. WEHRENS XHT, Abriel H, Cabo C, Benhorin J, Kass RS. Arrhythmogenic mechanism of an LQT-3 mutation of the human heart Na⁺ channel α -subunit: a computational analysis. *Circulation* 2000;102:584-90.
9. Abriel H*, WEHRENS XHT*, Benhorin J, Kass RS. Molecular pharmacology of the sodium channel mutation D1790G linked to the long-QT syndrome. *Circulation* 2000;102:921-25. [* contributed equally].
10. WEHRENS XHT, Breda van E, Velzen van JS, oude Egbrink MGA, Slaaf DW. Use of an intact mouse skeletal muscle preparation for endocrine vascular studies: evaluation of the model. *Horm Metab Res* 2000;32:378-80.

11. Abriel H, Cabo C, WEHRENS XHT, Rivolta I, Motoike HK, Memmi M, Napolitano C, Priori SG, Kass RS. Novel arrhythmogenic mechanism revealed by a long-QT syndrome mutation in the cardiac Na⁺ channel. *Circ Res* 2001;88:740-45.
12. WEHRENS XHT, Doevendans PA. Primary osteomyelitis of the sternum. [Primaire osteomyelitis van het sternum] [letter]. *Ned Tijdschr Geneesk* 2001;145:245-46.
13. Dammers R, WEHRENS XHT, oude Egbrink MGA, Slaaf DW, Kurvers HAJM, Ramsay G. Microcirculatory effects of experimental acute limb ischaemia-reperfusion. *Br J Surg* 2001;88:816-24.
14. WEHRENS XHT, Doevendans PA, Widdershoven JWMG, Dassen WRM, Prenger K, Wellens HJJ, Gorgels APM. Usefulness of sinus tachycardia and ST-segment elevation in V₅ to identify impending left ventricular wall rupture in inferior wall myocardial infarction. *Am J Cardiol* 2001;88:414-17.
15. WEHRENS XHT, Leiner T. Publications from extracurricular research [letter]. *Lancet* 2001;358:846.
16. WEHRENS XHT, Offermans JPM, Snijders M, Peeters LHH. Fetal cardiovascular response to large cardiovascular chorioangiomas. *Obstet Gynaecol Comm* 2002, in press.
17. oude Egbrink MGA, Janssen GHGW, Ookawa K, Reneman RS, WEHRENS XHT, Maaijwee C, Ohshima N, Struijker Boudier HAJ, Tangelder GJ. Especially polymorphonuclear, but also monomorphonuclear leukocytes roll spontaneously in venules of intact rat skin: involvement of E-selectin. *J Invest Dermatol* 2002, in press.
18. WEHRENS XHT, Rouwet EV, oude Egbrink MGA, Slaaf DW, Ramsay G. The effect of lower limb ischaemia-reperfusion injury on mesenteric microcirculation. *Br J Surg* 2002, in press.
19. WEHRENS XHT, Doevendans PA, Vos MA, Wellens HJ. Novel insights in the congenital long-QT syndrome [review]. *Ann Intern Med* 2002, in press.

Index

- Acquired long-QT syndrome, 11
- Andersen's syndrome, 140
- Ankyrin, 51
- Antiarrhythmic drug, 47, 100, 148
- Arrhythmogenic mechanism, 14, 58
- Arrhythmogenic right ventricular dysplasia, 140
- Asymptomatic patient, 21
- Atrioventricular block, 20, 60, 123
- Autosomal-dominant, 11
- Autosomal-recessive, 11
- Ball-and-chain model, 46
- Beta-blocker, 16, 116, 125
- Beta-subunit, 13, 49
- Bradycardia, 20, 86, 110, 125
- Brugada syndrome, 21, 40, 101, 133
- Bursting channels, 55
- Calcium channel, 76
- Calcium transient, 75
- Catecholaminergic polymorphic ventricular tachycardia, 140
- Channel gating, 45, 106, 125, 146
- Channel modulation, 93
- Channelopathy, 140
- Chromosome, 13, 41, 75
- Closed-state inactivation, 47, 133, 148
- Compound heterozygosity, 13
- Computational model, 58, 76, 142
- Congenital deafness, 12
- C-terminus, 57, 93, 146
- D1790G mutation, 57, 75, 93, 141
- DEKA ring, 149
- Diagnostic criteria, 15
- Digoxin, 125
- Dominant-negative effect, 14
- E1295K mutation, 107, 142
- Early after-depolarization, 81, 132
- Effective refractory period, 123
- Epileptic seizure, 16, 123
- EP study, 23
- Exercise test, 23
- Fast inactivation, 46, 115, 133, 143
- Flecainide, 21, 47, 93, 150
- Genotype, 11, 130
- Glycosylation, 52
- Guarded receptor model, 48
- Hinged-lid, 46
- Hodgkin-Huxley model, 43, 76
- Holter, 25, 110, 125
- Human embryonic kidney cell, 55, 141
- Idiopathic ventricular fibrillation, 21, 133
- IFM motif, 46, 143
- Implantable cardioverter defibrillator, 20
- Jervell Lange-Nielsen syndrome, 12
- L619F, 54, 123, 142
- Lev-Lenegr syndrome, 60
- Lidocaine, 21, 47, 93, 148
- Local anesthetic, 47, 148
- Luo-Rudy model, 61, 76, 141
- Markov model, 58, 151
- Mexiletine, 17, 52, 117, 125, 150
- Modulated receptor model, 48, 148
- Molecular pharmacology, 58, 101, 148
- Nicorandil, 21
- Noise, 17
- Pacemaker, 10, 117, 130
- Permeation, 43
- Penetrance, 26
- Pharmacotherapy, 18, 58, 152
- Plateau current, 40, 75, 142
- P-loop, 43, 150
- Polymorphism, 11, 127

- Post-translational modification, 52
- Pre-excitation, 125
- Pregnancy, 16
- Progressive cardiac conduction defect, 60, 140
- Protein kinase A, 52
- Protein kinase C, 52

- QT-interval dispersion, 22, 101
- QT-interval prolongation, 11, 59, 107, 132
- Quinidine, 26, 47

- Recombinant DNA, 77, 94, 108, 124, 141
- Recovery from inactivation, 55, 77, 112, 128, 146
- Romano-Ward syndrome, 11
- Ryanodine receptor, 140

- Saxitoxin (STX), 44
- Sinus pause, 23
- Slip-mode conductance, 54
- Slow inactivation, 46, 77, 147
- Stellate ganglionectomy, 20
- ST-segment elevation, 21
- Sudden cardiac death, 11, 60, 123
- Sudden infant death syndrome, 56, 123
- Syncope, 11, 60, 75, 93, 107, 123

- Tetrodotoxin (TTX), 41, 111, 128
- Tocainide, 21, 58
- Tonic block, 48, 94, 150
- Torsades de pointes, 14, 75, 93, 123
- Transcriptional regulation, 51
- Transgenic mice, 61, 142
- Transient outward current, 87
- Triggers, 16
- T wave alternans, 14, 131
- T wave dispersion, 22, 87
- T wave morphology, 22, 110

- Use-dependent block, 48, 92, 152
- Ventricular fibrillation, 14, 56, 133
- Ventricular repolarization, 11, 75, 93, 108, 123
- Ventricular septal defect (VSD), 125
- Voltage-dependent activation, 45
- Voltage-dependent inactivation, 46
- Voltage-sensor, 45, 150

- Whole-cell patch-clamp, 55, 76, 94, 109, 124
- Window current, 41, 108, 123, 142

- Xenopus* oocytes, 13, 50



Picture of Cocomama, the Incan goddess of health and happiness. Originally a promiscuous woman cut in half by jealous lovers; her body grew into the first coca bush.

